



POLITECNICO DI TORINO
Repository ISTITUZIONALE

ADVANCES IN RELIABILITY METHODS FOR REINFORCED CONCRETE STRUCTURES

Original

ADVANCES IN RELIABILITY METHODS FOR REINFORCED CONCRETE STRUCTURES / Gino, Diego. - (2019 Sep 19), pp. 1-199.

Availability:

This version is available at: 11583/2754713 since: 2019-09-25T09:51:17Z

Publisher:

Politecnico di Torino

Published

DOI:

Terms of use:

openAccess

This article is made available under terms and conditions as specified in the corresponding bibliographic description in the repository

Publisher copyright

(Article begins on next page)



ScuDo

Scuola di Dottorato ~ Doctoral School
WHAT YOU ARE, TAKES YOU FAR



Doctoral Dissertation
Doctoral Program in Civil and Environmental Engineering (31th Cycle)

Advances in reliability methods for reinforced concrete structures

Diego Gino

* * * * *

Supervisors

Prof. V.I. Carbone

Dr. G. Bertagnoli, Co-Supervisor

Dr. P. Castaldo, Co-Supervisor

Doctoral Examination Committee:

Prof. P. Foraboschi, Università IUAV di Venezia


Prof. A. Prota, Università degli studi di Napoli

Politecnico di Torino

February 10, 2019

This thesis is licensed under a Creative Commons License, Attribution - Noncommercial - NoDerivative Works 4.0 International: see www.creativecommons.org. The text may be reproduced for non-commercial purposes, provided that credit is given to the original author.

I hereby declare that, the contents and organisation of this dissertation constitute my own original work and does not compromise in any way the rights of third parties, including those relating to the security of personal data.


.....
Diego Gino

Turin, February 10, 2019

Summary

The reliability analysis of reinforced concrete structures requires methodologies able to fulfill the safety requirements expected by the society. These requirements, as defined by international codes, are represented by limits on the likelihood that structural collapse may occur in a given reference period. These limits are dependent from the typology, the destination of use and the lifetime for which a structure should carry out its serviceability.

In this context, approaches and methodologies aimed to the design and the assessment of reinforced concrete structures in compliance to "target" reliability levels are provided. In this way, engineers and designers can handle efficient tools, which, however, are affected by uncertainties of both *aleatory* and *epistemic* nature. The dissertation for obtaining the title of Ph.D. in Civil and Environmental Engineering is part of the described above context.

In the first part, the general framework for the probabilistic calibration of empirical or semi-empirical resistance models has been proposed. This methodology has been applied to the probabilistic calibration of the semi-empirical resistance model reported by the *fib Model Code 2010* for the evaluation of laps and anchorages tensile strength in reinforced concrete structures.

In the second part, the topic related to the use of non-linear finite element analysis for design and assessment purposes has been analyzed. In the details,

international codes allow to use advanced tools for non-linear analysis within the design and assessment processes.

In order to account for the different sources of uncertainty, several safety formats for non-linear analysis of reinforced concrete structures has been proposed by the literature and codes. After a detailed comparison of the mentioned above safety formats, two advances are proposed: the reliability-based calibration of partial safety factor related to resistance model uncertainties using plane stress non-linear finite element analysis; a methodology to account for the influence of failure mode variation within the predictions obtained by different safety formats.

Finally, a code format framework based on the levels of approximation approach for structural design and assessment of reinforced concrete structures by means of non-linear finite elements analysis is proposed and discussed.

Acknowledgment

Il Dottorato di ricerca è costituito, oltre che da conoscenza, anche da viaggi, esperienze ed emozioni rese uniche dalle persone. Ringrazio tutte le persone che ho avuto modo di incontrare, con cui ho avuto modo di discutere e quindi, di crescere.

Ringrazio la mia Famiglia, mia Madre, mio Padre e mio Fratello Alessandro per il supporto dato ogni giorno. Ringrazio la mia cara Elena, compagna di un viaggio che è appena cominciato e la Sua Famiglia, Franca ed Antonio. Ringrazio tutti i colleghi, compagni di lavoro e Costanza per la Sua presenza, leggerezza ed amicizia.

Ringrazio Fabio e Luca per la Loro ironia, competenza ed entusiasmo nel vivere l'ingegneria strutturale. Ringrazio Gabriele per avermi accolto, supportato ed esser stato di riferimento e chiaritore ogni volta che si fosse presentato un problema che nessun altro poteva risolvere. Ringrazio Paolo per credere in me ogni giorno, per spingermi a migliorare e per avermi insegnato che cosa significhi ricoprire un ruolo e lavorare duramente.

Ringrazio il Professor Giuseppe Mancini, per la fiducia riposta fin dal primo giorno e per le enormi opportunità a cui mi ha dato accesso.

Il Dottorato di ricerca è stato Vita, ma anche morte. Ringrazio la mia cara Nonna Angela per avermi insegnato a stare a posto ed in silenzio, a lavorare ed a parlare con i fatti. Ringrazio il Professor Vincenzo Ilario Carbone per la Sua genuinità, accoglienza, amicizia, per le Sue preziose ramanzine, per le risate infinite e per ogni istante passato insieme. Il ricordo non potrà mai colmare il vuoto.

*Dedicato al caro
Ilario
ed alla mia cara
Nonna Angela.*

Contents

Preface.....	1
1 Basics of reliability methods.....	4
1.1 Introduction.....	4
1.2 Limit states design, basic principles and uncertainties.....	5
1.2.1 Uncertainties and their classification.....	6
1.2.3 General formulation of the structural reliability problem.....	11
1.3 Reliability methods and theory background.....	13
1.3.1 Level III methods.....	13
1.3.2 Level II methods.....	19
1.3.3 Level I methods.....	22
1.3.4 Level 0 methods.....	23
1.3.5 Reliability of structural systems.....	23
1.3.6 Target reliability and reliability differentiation for new and existing structures.....	26
1.4 Safety formats for design and assessment of reinforced concrete structures.....	29
1.4.1 The levels of approximation approach.....	29
1.4.2 Probabilistic safety format.....	31
1.4.3 Partial factor format.....	31
1.4.4 Global resistance format.....	33
2 Non-linear finite elements analysis of reinforced concrete structures..	36
2.1 Introduction.....	36
2.1.1 Practical applications of NLFEAs.....	37

2.2	Modelling hypotheses for NLFEA.....	38
2.2.1	Solution methods.....	39
2.2.2	Non-linear modelling of concrete.....	42
2.2.3	Non-linear modelling of reinforcements.....	47
2.3	Safety formats for non-linear analysis of reinforced concrete structures.....	49
3	Probabilistic calibration of empirical and semi-empirical resistance models.....	53
3.1	Introduction.....	53
3.2	Proposed general framework.....	54
3.2.1	Characterization of the empirical or semi-empirical resistance model.....	54
3.2.2	Selection of the probabilistic model.....	55
3.2.3	Definition of the resistance and the auxiliary random variables.....	57
3.2.4	Definition of the reliability-based expressions.....	58
3.3	Probabilistic calibration of <i>fib</i> Model Code 2010 semi-empirical model for laps and anchorages strength evaluation.....	61
3.3.1	General aspects concerning bond of embedded reinforcements.....	61
3.3.2	Estimation of laps and anchorages tensile strength according to <i>fib</i> Bulletin N°72 and <i>fib</i> Model Code 2010.....	65
3.3.3	Estimation of the resistance model uncertainty.....	67
3.3.4	Probabilistic calibration.....	76
3.3.5	Expression for ultimate bond strength.....	86
3.3.6	Validation of the proposed framework and final comments.....	94
4	Advances in safety formats for NLFEAs of reinforced concrete structures.....	101
4.1	Introduction.....	101
4.2	Reliability-based evaluation of the resistance model uncertainty safety factor for NLFEAs.....	102
4.2.1	Literature review related to resistance model uncertainties for NLFEA.....	102
4.2.2	Proposed methodology for calibration of the model uncertainty safety factor γ_{Rd}	104

4.2.3 Benchmark experimental tests	106
4.2.4 NLFEAs: modelling hypotheses and results	113
4.2.5 Evaluation of the resistance model uncertainty safety factor for 2D NLFEAs of reinforced concrete structures	127
4.3 Comparison between safety formats for NLFEAs	137
4.3.1 Case studies and NLFE modelling	138
4.3.2 Results from NLFEAs	144
4.3.3 Comparison between outcomes of safety formats	154
4.3.4 Discussion and proposals	158
4.4 Levels of approximation format for design and assessments of reinforced concrete structures by means NLFEA	166
4.4.1 General	166
4.4.2 Level of approximation I (LoA I)	168
4.4.3 Level of approximation II (LoA II)	170
4.4.4 Level of approximation III (LoA III)	171
5 Conclusions	174
References	177

List of Tables

Table 1.1: Suggested range of target reliability from <i>fib Model Code 2010</i> for <i>new</i> and <i>existing</i> structures.	28
Table 3.1: Definition of the probabilistic model.	56
Table 3.2: Some possible choices of the representative values of relevant random variables within the final reliability-based equation.	58
Table 3.3: Values of the probabilistic coefficients.	59
Table 3.4: Reliability-based expressions according to probability of under-exceedance equal to p	59
Table 3.5: Detail of the literature references collecting the experimental database on lap splices and anchorages.	68
Table 3.6: Filters applied to the experimental database differentiating between <i>new</i> and <i>existing</i> structures.	71
Table 3.7: Verification of null hypothesis H_0 for normality in the case on <i>new/existing</i> structures consider the random variable \mathcal{G} and $\ln\mathcal{G}$. Comparison between p-value and the significance level $\alpha=0.05$	76
Table 3.8: Probabilistic distribution and parameters estimated for resistance model uncertainty random variable \mathcal{G} both for <i>new</i> and <i>existing</i> structures.	76
Table 3.9: Probabilistic model for the random variables.	77
Table 3.10: Values of the probabilistic coefficients $\zeta_p(f_{c,rep})$ in the function of representative value selected for concrete compressive strength for the case of <i>new</i> structures.	83
Table 3.11: Values of the probabilistic coefficients $\zeta_p(f_{c,rep})$ in the function of representative value selected for concrete compressive strength for the case of <i>existing</i> structures.	83
Table 3.12: Example of calculation - <i>new</i> structures.	85
Table 3.13: Values of the probabilistic coefficients $C_p(f_{ck})$ in the function of representative value selected for concrete compressive strength for the case of <i>new</i> and <i>existing</i> structures.	89
Table 3.14: Experimental samples and validation of the calibrated equations.	96

Table 3.15: Comparison between the values of the probabilistic coefficients $\zeta_p(f_{ck})$ for the general framework of Sub-section 3.3.4 and the methodology of <i>Taerwe, 1993</i> for the case of <i>new</i> and <i>existing</i> structures.	99
Table 3.16: Comparison between the coefficient of variation for resistance random variable R with general framework of Sub-section 3.3.4 and the methodology of <i>Taerwe, 1993</i> for the case of <i>new</i> and <i>existing</i> structures.	99
Table 4.1: Assumptions related to the basic <i>modelling hypotheses</i> devoted to the definition of the non-linear FE numerical models.	114
Table 4. 2: Results in terms of resistance from the experimental tests $R_{EXP,i}$ (<i>Filho, 1995</i>) and NLFEAs $R_{NLFEA,i}$ for the different structural models.	119
Table 4.3. Results in terms of resistance from the experimental tests <i>Foster and Gilbert, 1998</i> and NLFEAs $R_{NLFEA,i}$ for the different structural models.	121
Table 4.4: Results in terms of resistance from the experimental tests $R_{EXP,i}$ of <i>Lefas and Kotsovos, 1990</i> and NLFEAs $R_{NLFEA,i}$ for the different structural models.	121
Table 4.5: Results in terms of resistance from the experimental tests $R_{EXP,i}$ by <i>Leonhardt and Walther, 1966</i> and NLFEAs $R_{NLFEA,i}$ for the different structural models.	123
Table 4. 6 Results in terms of resistance from the experimental tests $R_{EXP,i}$ of <i>Vecchio and Collins, 1982</i> and <i>Pang and Hsu, 2000</i> and NLFEAs $R_{NLFEA,i}$ for the different structural models.	126
Table 4.7: Results of the investigation: ratios $\vartheta_i = R_{EXP,i}/R_{NLFEA,i}$ for the different <i>modelling hypotheses</i> (Mo.1-9).	128
Table 4.8: Mean values and coefficients of variation of the prior/posterior and new information distribution functions (all results) with the statistical uncertainty.	132
Table 4.9: Mean values and coefficients of variation of the prior/posterior and new information distribution functions (excluding <i>Pang and Hsu, 2000</i> results) with the inherent statistical uncertainty.	133
Table 4.10: Values of the partial safety factor γ_{Rd} for the model uncertainties in 2D NLFEAs of reinforced concrete structures according to <i>fib Model Code 2010</i> (hypothesis of <i>non-dominant</i> resistance variable).	135
Table 4.11: Values of the partial safety factor γ_{Rd} for the model uncertainties in 2D NLFEAs of reinforced concrete structures according to <i>fib Model Code 2010</i> (hypothesis of <i>dominant</i> resistance variable).	135
Table 4.12: Beams selected with the geometric details of longitudinal reinforcements and with properties of concrete.	138

Table 4. 13: Properties of the reinforcements.	139
Table 4.14: Basic <i>modelling hypotheses</i> assumed in the definition of NLFE numerical models.	142
Table 4.15: Comparison between the NLFEAs results and the experimental outcomes.	142
Table 4. 16: Probabilistic models (<i>JCSS Probabilistic Model Code, 2001</i>) for the main independent random variables affecting the structural behaviour.	148
Table 4.17: Results from the LH sampling and ML estimates of the parameters.	154
Table 4.18: Results in terms of design ultimate load from different safety formats.	155
Table 4.19: Results from the <i>preliminary analyses</i>	161
Table 4.20: Summary of the global resistance factors γ_R , of the failure mode factors γ_{FM} and of the model uncertainty factor γ_{Rd} for the different safety formats.	162
Table 4.21: Partial factors involved by the different safety formats according to ordinary structures of new construction having moderate consequences of failure with 50 years of service life (i.e. $\beta = 3.8$, $\alpha_R = 0.8$).	168
Table 4.22: Simplified probabilistic model for SPM.	171

List of Figures

Figure 1.1: Probabilistic modelling of concrete compressive strength (a) and reinforcement yielding strength (b).	9
Figure 1.2: Relationship between the probability of failure P_f and reliability index β	12
Figure 1.3: General representation of the <i>limit state domain</i> with 2 random variables X_1 and X_2	12
Figure 1.4: Stratified sampling according to LHS: example of LHS sampling from basic variable.....	18
Figure 1.5: Definition of <i>reliability index</i> β according to (Cornell, 1969).	19
Figure 1.6: Definition of design point and reliability index (Hasofer and Lindt, 1974).	20
Figure 1.7: Differences in cost optimization for the design of <i>new</i> structures versus upgrading of <i>existing</i> structures (<i>fib Bulletin 80</i>).	27
Figure 1.8: Levels of approximation approach as defined by <i>Muttoni and Ruiz, 2012</i> and <i>fib Model Code 2010</i>	30
Figure 1.9: Comparison between local structural analysis and global structural analysis.....	33
Figure 2.1: Scheme representing the Newton-Rapson method.	40
Figure 2.2: Scheme representing the Modified Newton-Rapson method.	41
Figure 2.3: Quadrilateral iso-parametric finite element (plane stress).	43
Figure 2.4: Mono-axial constitutive model for concrete in compression by <i>EN1992-1-1</i>	44
Figure 2.5: Mono-axial constitutive model for concrete in compression by <i>fib Model Code 1990</i>	45
Figure 2.6: Linear tension softening model for concrete tensile behavior.	46
Figure 2.7: Bi-axial failure domain proposed by <i>Kupfer and Gerstle, 1973</i> . .46	
Figure 2.8: Fixed smeared crack model (a) and rotated smeared crack model (b).	47
Figure 2.9: Constitutive model for reinforcement.....	48

Figure 3.1: Summary of the framework for probabilistic calibration of empirical and semi-empirical models.	60
Figure 3.2: Actual bond stress developing and average bond stress idealization (a); actual force within the lap or anchorage length compared to the one reached in the hypothesis of constant bond stress idealization (b).....	61
Figure 3.3: The bond mechanism in reinforced concrete elements (representation by <i>Jakubovskis and Juknys, 2016</i>).	63
Figure 3.4: Differentiation between failure modes (representation by <i>Lemmitzer et al, 2009</i>).	64
Figure 3.5: Equilibrium of forces in <i>splitting</i> failure mode modelling (<i>fib Bulletin 72</i>).	65
Figure 3.6: Definition of concrete cover in Eq.(3.10) (a) and of the effectiveness of shear links related to Eq.(3.11) (b).	66
Figure 3.7: Detail of results of Eq.(3.10) for the <i>fib TG 4.5 bond database</i> ...	69
Figure 3.8: Trend of variation of model uncertainty in function of main parameters involved by Eq.(3.10) related to the experimental sets reported by <i>fib TG 4.5 bond database</i>	70
Figure 3.9: Detail of results of Eq.(3.10) for the filtered database related to <i>new</i> structures.	71
Figure 3.10: Detail of results of Eq.(3.10) for the filtered database related to <i>existing</i> structures.	71
Figure 3.11: Trend of variation of model uncertainty in function of main parameters involved by Eq.(3.10) related to the filtered database concerning <i>new structures</i>	72
Figure 3.12: Variation of model uncertainty in function of main parameters involved by Eq.(3.10) related to the filtered database concerning <i>existing structures</i>	73
Figure 3.13: <i>New</i> structures: frequency histogram and probabilistic distribution fit (a); lognormal probability plot (b) and normal probability plot (c) with associate p-values after <i>Chi-square</i> goodness of fit test ($\alpha=0.05$).	74
Figure 3.14: <i>Existing</i> structures: frequency histogram and probabilistic distribution fit (a); lognormal probability plot (b) and normal probability plot (c) with associate p-values after <i>Chi-square</i> goodness of fit test ($\alpha=0.05$).	75
Figure 3.15: Relative frequency histogram for the Monte Carlo simulation of then random variable $Z(f_c, \mathcal{G}; f_{ck})$ in the hypothesis of 10^4 , 10^6 and 10^8 samples. The case is relative to <i>new</i> structures.	79

Figure 3.16: Relative frequency histogram for the Monte Carlo simulation of the <i>auxiliary random variables</i> $Z(f_c, \Theta; f_{cm})$, $Z(f_c, \Theta; f_{ck})$ and $Z(f_c, \Theta; f_{cd})$ in the hypothesis of 10^6 samples; <i>New</i> structures (a); <i>Existing</i> structures (b).	80
Figure 3.17: Lognormal distribution (PDF (a) and CDF (b)) for the <i>auxiliary random variables</i> Z : $Z(f_c, \vartheta; f_{cm})$, $Z(f_c, \vartheta; f_{ck})$ and $Z(f_c, \vartheta; f_{cd})$ concerning <i>new</i> structures.	81
Figure 3.18: Lognormal distribution (PDF (a) and CDF (b)) for the <i>auxiliary random variables</i> Z : $Z(f_c, \vartheta; f_{cm})$, $Z(f_c, \vartheta; f_{ck})$ and $Z(f_c, \vartheta; f_{cd})$ concerning <i>existing</i> structures.	82
Figure 3.19: Variation of the design probabilistic coefficients $\zeta_d(f_{c,rep})$ and associated curve fitting differentiating between <i>new</i> and <i>existing</i> structures in function of the reliability index β ($\alpha_R=0.8$).	84
Figure 3.20: Comparison in terms of laps strength f_{st} between experimental results and Eq.(3.10) predictions in function of the ratio between lap length l_b and bar diameter Φ (entire database) (a); comparison in terms of bond strength f_b between experimental results and Eq.(3.10) predictions in function of the ratio between lap length l_b and bar diameter Φ (entire database) (b).	86
Figure 3.21: Variation of the design probabilistic coefficients $C_d(f_{ck})$ for <i>average bond strength</i> and associated curve fitting differentiating between <i>new</i> and <i>existing</i> structures in function of the reliability index β ($\alpha_R=0.8$).	89
Figure 3.22: Bond strength $f_{b,d,0}$ evaluated according to EN1992-1-1, <i>fib</i> Model Code 2010 and proposed models. $\Phi=12mm$ (a), $\Phi=16 mm$ (b), $\Phi=20 mm$ (c), $f_{ck}=25 MPa$ and steel <i>Grade 500</i>	92
Figure 3.23: Required anchorage length $l_{b,req}/\Phi$ evaluated according to EN1992-1-1, <i>fib</i> Model Code 2010 and proposed models. $\Phi=12mm$ (a), $\Phi=16 mm$ (b), $\Phi=20 mm$ (c), $f_{ck}=25 MPa$ and steel <i>Grade 500</i>	93
Figure 3.24: Experimental validation of the mean ($p=0.5$ (m)) (a) and of the characteristic ($p=0.05$ (k)) (b) expressions reported by Eq.(3.18a-b-c) concerning the sample for <i>new</i> structures.	95
Figure 3.25: Experimental validation of the mean ($p=0.5$ (m)) (a) and of the characteristic ($p=0.05$ (k)) (b) expressions reported by Eq.(3.18a-b-c) concerning the sample for <i>existing</i> structures.	96

Figure 4. 1: Detail of the walls tested by <i>Filho, 1999 (a-e)</i>	108
Figure 4.2: Detail of the deep beams tested by <i>Foster and Gilbert, 1998 (a-b)</i>	109
.....	
Figure 4. 3: Detail of the wall tested by <i>Lefas and Kotsovos, 1990</i>	110
Figure 4. 4: Detail of the walls tested by <i>Leonhardt and Walther, 1966 (a-d)</i>	111
.....	
Figure 4.5: Detail of the panels tested by <i>Vecchio and Collins, 1982 (a)</i> and by <i>Pang and Hsu, 1995 (b)</i>	112
Figure 4.6: Different constitutive laws for concrete tensile behaviour.	115
Figure 4.7: Distinction between the 9 <i>modelling hypotheses</i> (Mo.1-9) adopted for the resistance model uncertainty investigation and summary of the benchmark NLFEMs.	116
Figure 4.8: Load vs displacement diagrams from experimental tests of <i>Filho, 1995</i> and NLFEM results (a-e); numerical model schematization (f); crack patterns and σ_2 principal stress flow at first yielding (g) and principal strain ϵ_2 at failure (h) for MB11AA.....	119
Figure 4.9: Load vs displacement diagrams from experimental tests of <i>Foster and Gilbert, 1998</i> and NLFEM results (a-e); numerical model schematization (f); crack patterns and principal strain ϵ_2 at failure for B3.01/ B2.0A-4 (g-h).....	121
Figure 4.10: Load vs displacement diagrams from experimental tests of <i>Lefas and Kotsovos, 1990</i> and NLFEM results (a); numerical model schematization (b); crack patterns and σ_2 principal stress flow at first yielding (c) and principal strain ϵ_2 at failure for SW11 (d).....	122
Figure 4.11: Load vs displacement diagrams from experimental tests of <i>Leonhardt and Walther, 1966</i> and NLFEM results (a-e); numerical model schematization (f); crack patterns and principal strain ϵ_2 at failure for WT2/WT6 (g-h).	124
Figure 4.12: Shear stress τ vs angular distortion γ diagrams from experimental tests of <i>Vecchio and Collins, 1982</i> and <i>Pang and Hsu, 2000</i> and NLFEM results (a-i); numerical model schematization (l).	126
Figure 4.13: Histogram and lognormal probability density function of the ratio \mathcal{G}_i for the Model 6 (a); Probability plot of $\ln(\mathcal{G}_i)$ for the Model 6 (b); excluding <i>Pang and Hsu, 2000</i> results.....	129
Figure 4.14: Histogram and lognormal probability density function of the ratio \mathcal{G}_i for all the models excluding <i>Pang and Hsu [6]</i> results (a); Probability plot of $\ln(\mathcal{G}_i)$ for all the models excluding <i>Pang and Hsu, 2000</i> results (b).....	130

Figure 4.15: Framework for the Bayesian updating and assessment of the partial safety factor for resistance model uncertainty in 2D NLFEAs of reinforced concrete structures; in the present investigation $m=9$ and $n=20-25$	131
Figure 4.16: Prior and posterior and new information PDFs (a) and CDFs (b); (all results).	132
Figure 4.17: Prior and posterior and new information PDFs (a) and CDFs (b); (excluding <i>Pang and Hsu, 2000</i> results.	133
Figure 4.18: Reinforcements arrangement for beams with square openings SL, SM, SH (a) and CLX (c); representation of the tests set and loading configuration (b) and (d) (modified from <i>Aykac et al., 2013</i>). (Dimensions in [mm])......	139
Figure 4.19: Reinforcements arrangement for the T-Beam (a) and representation of the static scheme and loading configuration (b). (Dimensions in [mm]).	140
Figure 4.20: Failure modes recognised from NLFEAs with numerical and experimental load-displacement curves.....	143
Figure 4.21: Beam SL <i>Aykac et al, 2013</i> : Failure mode recognised for simulations performed with NLFEAs (a); results in terms of ultimate global resistance R for the NLFE simulations in agreement with the PFM, ECOV and GRF methods (b).	145
Figure 4. 22: Beam SM <i>Aykac et al, 2013</i> : Failure mode recognised for simulations performed with NLFEAs (a); results in terms of ultimate global resistance R for the NLFE simulations in agreement with the PFM, ECOV and GRF methods (b).	145
Figure 4.23: Beam SH <i>Aykac et al, 2013</i> : Failure mode recognised for simulations performed with NLFEAs (a); results in terms of ultimate global resistance R for the NLFE simulations in agreement with the PFM, ECOV and GRF methods (b).	146
Figure 4.24: Beam CLX <i>Aykac et al, 2013</i> : Failure mode recognised for simulations performed with NLFEAs (a); results in terms of ultimate global resistance R for the NLFE simulations in agreement with the PFM, ECOV and GRF methods (b).	146
Figure 4.25: T-Beam: Failure mode recognised for simulations performed with NLFEAs (a); results in terms of ultimate global resistance R for the NLFE simulations in agreement with the PFM, ECOV and GRF methods (b).....	146
Figure 4.26: Beam SL (<i>Aykac et al., 2013</i>): sampled values of the relevant random variables of the 30 NLFE models.	147

Figure 4.27: Beam SL (<i>Aykac et al., 2013</i>): Failure mode recognised for simulations performed with NLFEAs (a); results in terms of ultimate global resistance R for the NLFE simulations coming from n=30 LHS samples (b); lognormal probabilistic distribution for the global resistance R (c).	149
Figure 4.28: Beam SM (<i>Aykac et al., 2013</i>): Failure modes recognised for simulations performed with NLFEAs (a)-(b); results in terms of ultimate global resistance R for the NLFE simulations coming from n=30 LHS samples (c); lognormal probabilistic distribution for the global resistance R (d).	150
Figure 4.29: Beam SH (<i>Aykac et al., 2013</i>): Failure mode recognised for simulations performed with NLFEAs (a); results in terms of ultimate global resistance R for the NLFE simulations coming from n=30 LHS samples (b); lognormal probabilistic distribution for the global resistance R (c).	151
Figure 4.30: Beam CLX (<i>Aykac et al., 2013</i>): Failure mode recognised for simulations performed with NLFEAs (a); results in terms of ultimate global resistance R for the NLFE simulations coming from n=30 LHS samples (b); lognormal probabilistic distribution for the global resistance R (c).	152
Figure 4.31: Beam designed according to <i>fib</i> Model Code 2010 and to EC2 (T-Beam): Failure modes recognised for simulations performed with NLFEAs (a)-(b); results in terms of ultimate global resistance R for the NLFE simulations coming from n=30 LHS samples (c); lognormal probabilistic distribution for the global resistance R (d).	153
Figure 4.32: Probability plot of the design ultimate loads related to the different <i>safety formats</i> : Beam SL(a); Beam SM(b); Beam SH(c); Bema CLX(d); T-Beam (e). ($\gamma_{Rd}=1.00$; $\beta=3.8$; $\alpha_R=0.8$).....	157
Figure 4.33: Graphical representation of the two preliminary NLFE analyses assuming as variables the reinforcement yielding strength f_y and the concrete compressive strength f_c	158
Figure 4.34: Beam SM (<i>Aykac et al., 2013</i>): <i>failure modes</i> recognised for the two <i>preliminary</i> simulations (a)-(b); load-displacement curves (c).	159
Figure 4.35: Beam designed according to <i>fib</i> Model Code 2010 and to EN 1992-1-1 (T-Beam): <i>failure modes</i> recognised for the two <i>preliminary</i> simulations (a)-(b); load-displacement curves (c).	160
Figure 4. 36: Flowchart of the proposed methodology for the assessment of design global resistance R_d by means of NLFEAs.	162
Figure 4.37: Bounds for coefficient of variation showed by global resistance.	163

Figure 4.38: Ratio between the design resistances obtained with the different safety formats (i.e. PFM, ECOV, GRF, GSF and SMVM) and the PM for the beams SL (<i>Aykac et al., 2013</i>) and T-Beam.	164
Figure 4.39: Summary of the proposed code format based on the levels of approximation approach.	173

Preface

The present dissertation concerns the reliability analysis of *new* and *existing* reinforced concrete structures. As for other fields of engineering and physics, the influence of uncertainties is relevant and strongly affects the procedures for design and assessment. In particular, scientific literature and codes provides refined methodologies able to account for uncertainties (both *aleatory* and *epistemic*) in case of high levels probabilistic analyses and for the activity of practitioners. However, advances in reliability methods are needed for different fields, as for the emergent use of non-linear finite elements software for design and assessment of reinforced concrete structures.

The *Chapter 1* deals with the basic notions related to structural reliability analysis. The limit states approach and measure of the structural reliability are described together to the main sources of uncertainty. Then, the basic assumptions for probabilistic modelling of reinforced concrete structures are proposed and the methodology to assess resistance model uncertainty is reported. Successively, the fundamentals of Level III, Level II, Level I and Level 0 methods for reliability analysis of structural components and systems are described. The target reliability for *new* and *existing* reinforced concrete structures are commented accounting for the reliability differentiation. The levels of approximation approach introduced by *fib Model Code 2010* for structural design and assessment is described and the most common safety formats implemented in structural codes are outlined.

The *Chapter 2* concerns the non-linear finite elements analysis (NLFEA) of reinforced concrete structures. The main applications of NLFEA to design and assessment of *new* and *existing* reinforced concrete structures are listed and commented. After that, the most common modelling hypotheses adopted in order to perform non-linear analysis of reinforced concrete structures are reported focusing mainly on plane stress models. Finally, different safety formats proposed by scientific literature for assessment of the structural safety by means NLFEA are described.

In *Chapter 3* the methodology for probabilistic calibration of empirical and semi-empirical resistance models is proposed. The framework, which is based on the Monte Carlo's method, allows to take into account both *aleatory* and *epistemic* sources of uncertainty. The methodology has been applied to the probabilistic calibration of the semi-empirical model for laps and anchorages tensile strength evaluation proposed by *fib Model Code 2010*. After the description of fundamentals of bond behaviour in reinforced concrete members, the reliability-based expressions for laps and anchorages tensile strength are derived distinguishing

between *new* and *existing* structures. Subsequently, the reliability-based expression for ultimate average bond strength along the lap or anchorage length has been derived according to equilibrium hypothesis. Finally, the possible implications for design and assessment are commented and the derived equations validated.

Chapter 4, deals with advances related to the use of NLFEA for design and assessment of reinforced concrete structures.

The first part concerns the evaluation of the model uncertainty safety factor for global analysis related to plane stress non-linear finite element models. Several structural members tested in laboratory with outcomes known from the literature are considered. Different non-linear structural models are defined for each experimental test to investigate the influence of model uncertainty on the 2D NLFEAs of reinforced concrete structures in terms of global resistance, considering different modelling hypotheses to describe the mechanical behaviour of reinforced concrete members (i.e. *epistemic* uncertainties). Subsequently, the numerical results are compared to the experimental outcomes. Then, a consistent treatment of the resistance model uncertainties is proposed following a Bayesian approach. Then, the probabilistic distribution, the mean value and the coefficient of variation characterizing the resistance model uncertainty random variable are identified. Finally, in agreement with the safety formats for NLFEAs of reinforced concrete structures, the partial safety factor for global analysis related to the resistance model uncertainties is evaluated.

The second part, relates to the comparison of different safety formats within the approach of the global resistance format for the estimation of the design strength of different reinforced concrete structures. Specifically, non-linear finite element models are properly defined to reproduce different experimental tests. Successively, several non-linear finite element analyses have been carried out in compliance to the different safety formats for each one of the reinforced concrete structures experimentally tested. The results are critically discussed and compared in terms of resistance and failure mode. Then, a methodology based on a specific preliminary evaluation, composed of two non-linear finite element analyses, is proposed to verify the applicability of the different simplified safety formats depending on the possible modifications that can occur to the failure mode. Contextually, a new safety factor denoted as “failure mode-based safety factor” accounting for inherent simplification within the definition of different safety formats is defined. Finally, a comprehensive code format framework based on the levels of approximation approach is proposed.

The *Chapter 5* summarize the main conclusions about the different topics highlighting the possible future developments.

The achievements reported in the present dissertation led to the following scientific publications on international technical journals and conferences:

- *Journal papers:*

1. G. Mancini, V.I. Carbone, G. Bertagnoli, D. Gino (2018): *Reliability-based evaluation of bond strength for tensed lapped joints and anchorages in new and existing reinforced concrete structures*, **Structural Concrete** 19, 904-917, 2018 <https://doi.org/10.1002/suco.201700082>.
2. P. Castaldo, D. Gino, V.I. Carbone, G. Mancini (2018): *Framework for definition of design formulations from empirical and semi-empirical resistance models*, **Structural Concrete**, 19(4), 980-987, 2018. <https://doi.org/10.1002/suco.201800083>.
3. P. Castaldo, D. Gino, G. Bertagnoli, G. Mancini (2018): *Partial safety factor for resistance model uncertainties in 2D non-linear analysis of reinforced concrete structures*, **Engineering Structures**, 176, 746-762. <https://doi.org/10.1016/j.engstruct.2018.09.041>
4. P. Castaldo, D. Gino, G. Mancini (2019): *Safety formats for non-linear analysis of reinforced concrete structures: discussion, comparison and proposals* **Engineering Structures**, 193, 136-153, <https://doi.org/10.1016/j.engstruct.2018.09.041>

- *Conference papers:*

1. P. Castaldo, D. Gino, D. La Mazza, G. Bertagnoli, V.I. Carbone, G. Mancini (2018): *Assessment of the partial safety factor related to resisting model uncertainties in 2D NLFEA of R.C. structures*, Il calcestruzzo strutturale oggi, Italian Concrete Days 2018, 13-15 Giugno, Milano-Lecco, Italy, 2018.
2. D. Gino, P. Castaldo, G. Bertagnoli, G. Mancini (2018): *Probabilistic assessment of laps and anchorages strength in reinforced concrete structures*, Proceedings of WMCAUS 2018, June 18-22, Prague, Czech Republic.
3. D. Gino, P. Castaldo, G. Bertagnoli, G. Mancini (2018): *Design equations from empirical and semi-empirical resisting models: a reliability-based approach*, Proceedings of 12th International fib Symposium in Civil Engineering, August 28-31, Prague, Czech Republic.
4. P. Castaldo, D. Gino, G. Bertagnoli, G. Mancini (2018): *Toward fib Model Code 2020: partial safety factor for resistance model uncertainties in plane stress NLFE analyses of R.C. systems*, Proceedings of 5th International fib Congress, October 07-11, Melbourne, Australia.

Chapter 1

Basics of reliability methods

1.1 Introduction

The physical phenomena in nature (and then, also in structural engineering) contains, inevitably, a certain amount of uncertainty. It means that these phenomena, in principle, cannot be predicted with complete certainty. It is possible to consider the following simple example: several "identical" specimens of concrete cubes are loaded in laboratory until they reach failure. The failure load in compression would be different for each one of the specimens. Hence, the compressive resistance of these concrete cubes is a random quantity (i.e. random variable). In general, in structural engineering, all the parameters of interest for design and assessment of *new* and *existing* structures can be considered as uncertain and then, assumed to be random variables. Dealing with uncertainties, the term *reliability* is often used very vaguely and deserves some clarifications. The fundamental concept of reliability is commonly perceived as an absolute property of the structure. Then, if the structure can be considered as reliable it never fails and, conversely, if the structure results to be not reliable its failure is certain. Moreover, for most of the people, the positive statement "the structure is reliable" is understood in the sense that "a failure of the structure will never occur". This interpretation is unfortunately a strong and un-correct simplification. Although it may be unpleasant (or unacceptable) for "non-expert" people, the hypothetical "absolute *reliability*" for structures simply does not exist. In general, any structure may fail (although with a small probability) even when it is declared as "reliable". The correct statement to be adopted and that should be disclosed also to "non-expert" people is the following: "*failures of structures are accepted as they are part of the real world and the probability or frequency of failures occurrence is quantified and limited by means of economic, human safety and structural considerations*". Inevitably, in structural engineering it is necessary to admit a certain small probability that failure may occur within the intended service life of the structure. Otherwise, the design of *new* civil structures (and infrastructures) and assessment of *existing* ones simply would not be possible.

In the present Chapter, the basic notions of *structural reliability* according to the *limit states* approach are outlined, highlighting the different sources of uncertainty. The distinction between the design of *new* structures and the assessment of *existing* ones is defined. Moreover, the fundamental methodologies for the evaluation of *structural reliability* are described differentiating between

Level III, II, I, 0 methods. Finally, the most used *safety formats* adopted from current structural codes and standards are described and commented.

1.2 Limit states design, basic principles and uncertainties

The basic principles of *structural reliability* are reported by the international codes as *ISO 2394*, *EN 1990* and *fib Model Code 2010*.

According to the mentioned above codes, the fundamental performance requirements for structures should be related to *reliability* and *economy* concepts. In particular, a structure should be designed and executed to sustain all the actions that may occur during its working life maintaining its functionality. These requirements should be fulfilled with appropriate levels of reliability and economic sustainability.

The *structural reliability* can be defined as the ability of the structure to comply with given requirements under specific loading conditions during its service life. Quantitatively, the term *reliability* may be considered as the complement to one of the probability of structural failure. The *service life* (i.e., design working life for *new* structures, residual service life for *existing* structures) is intended as the interval for which the structure should accomplish its functionality. The main performance requirements for structural design are represented by *safety* (i.e. *structural resistance and ductility*), *serviceability*, *durability* and *robustness*.

In order to verify these requirements related to specific design situations, the so-called *limit states* are identified. In literature and structural codes (e.g. *EN 1990*; *fib Model Code 2010*) the generic *limit state* is defined as: “*the condition beyond which the structure, or a part of it, does no longer satisfy one of its performance requirements*”.

Related to the mentioned above performance requirements, several *limit states* can be distinguished between:

- *ultimate limit states (ULS)*, that refers directly to the structural safety, the safety of people and/or protection of the content of a structure. Beyond *ultimate limit state* the bearing or deformation capacity of the structure is overpassed and the overall structure or part of it fails inevitably. Commonly, different *ULS* can be defined as, for example: loss of static equilibrium of the structural system or part of it; arising of mechanisms of a structural system or part of it (i.e. structural collapse); fracture or excessive deformation in crucial sections of the structural system or within connections; fatigue and time dependent phenomena; instability, divergence of equilibrium (e.g. buckling, lateral buckling, aero-elastic instability).
- *serviceability limit states (SLS)*, that refers to the functionality, comfort and visual aspect of the structure during the normal use. The requirements related to serviceability of the structures can be related to *deformations*, *vibrations* and *damages* that may influence durability. In general, *SLS* can

be distinguished in *irreversible SLS* and *reversible SLS*. The former can be identified within the cases where the critical value of limit state indicator remains permanently crossed also after removal of the load caused the first passage (e.g. permanent deflection). The latter can represent the cases where the critical value of the limit state indicator is no longer crossed after removal of the load that caused the first passage (e.g. excessive vibrations, temporary deflections, cracking in prestressed concrete members).

These *limit states* should be addressed for different structures according to different levels of reliability depending from the intended service life.

In order to deal with the *limit states* approach and to perform *reliability analysis*, the following distinction (not merely terminological) between *new* and *existing* structures should be outlined. In fact, according to *fib Model Code 2010* and *fib Bulletin 80*, the *design* process can be recognized as a series of activities devoted to warranty the structural reliability in the design service life of the *new* structural realization, whereas, the *assessment* process represents the set of activities performed in order to verify the actual reliability of an *existing* structural system or component accounting for its residual service life.

Then, in the following, *assessment* and *design* will be maintained as separate aspects belonging to the field of *structural reliability* analysis.

1.2.1 Uncertainties and their classification

The process aimed to the evaluation of the *structural reliability* of *new* or *existing* structures should account for several sources of uncertainties. These uncertainties may be of different nature and, mainly, can be represented by:

- *randomness* (or *inherent variability*): it represents the natural variability that can be considered as intrinsic to physical process or property (e.g. material property and external actions). The randomness can not be affected or reduced by external (i.e. human) intervention as it is an intrinsic characteristic of the physical process or property itself;
- *model uncertainty*: it is the uncertainty related to the idealization of mathematical models adopted in order to describe and make predictions related to the physical process or property. Then, the model uncertainty is related to ignorance, inherent simplifications and choices performed in the definition of the mathematical models devoted to describe the real world. It can be reduced by increasing the knowledge and improving the quality of the models;
- *statistical uncertainty*: this type of uncertainty is related to the process that leads to the estimation of the randomness of a physical process or property. It is due to the limited size of sample of observations for statistical analysis

and it can be reduced by increasing the data from experience (e.g. experimental results);

- *measurement error*: is the error performed measuring or observing the data for estimating the randomness (and for statistical analysis) of a physical process or property. Measurements errors may be reduced improving the measurements or observation systems;
- *human errors*: are errors related to the *design* or *assessment* process performed by human beings. This kind of uncertainty is one of the hardest to be analysed and can be reduced increasing controls on the whole process.

All the different sources of uncertainty affect, at different levels, the *reliability analysis* of a structural system.

It can be observed that if the *randomness* (i.e. *inherent variability*) of a physical process or property can be considered as not reducible, the other sources of uncertainty may be reduced by improving, for example, testing, measurements procedures and predictive models. Commonly, in the scientific literature, this observation leads to perform the distinction between two different macro-families of uncertainty: *aleatory* and *epistemic*.

Specifically, concerning structural reliability analysis, the *aleatory* uncertainties concerns the intrinsic randomness of the variables that governs a specific structural problem, whereas the *epistemic* uncertainties are mainly related to the “lack of knowledge” in the definition of the structural model and may be also represented by auxiliary non-physical variables or choices. For example, in order to simulate the response of a structural system, different models or modelling hypotheses may be adopted. These choices, inevitably, influences the global level of uncertainty within reliability analysis. However, it does not mean that simplified models are necessarily more uncertain if compared to refined ones. Specifically, it may happen that very refined and complex non-linear structural models leads to higher levels of *epistemic* uncertainty if compared to simplified ones. In fact, the availability of several plausible modelling hypothesis may lead to diverse solutions for the same problem. This, sometimes, makes simplified models more efficient, even if they are often conservative.

One can deserve that all the sources of uncertainty can be considered as *epistemic* in a predetermined model universe. In fact, *Der Kiureghian and Dietlevsen, 2009* makes a very clever example of this way of thinking: concerning the mentioned above distinction between *new* and *existing* structures, the concrete compressive strength may be considered as *aleatory* in the former case and as *epistemic* in the latter case. In fact, focusing the problem of a *new* structure, the concrete compressive strength is affected by an *aleatory* uncertainty, as there is not the possibility to perform measurements on something that still does not exist at the design stage. Conversely, in an *existing* structure, concrete has been already casted and its compressive strength is the actual realization of a random variable. In this case, the problem is just related to perform an adequate number of tests and

inspections in order to increase the knowledge about the structure. Nevertheless, by definition, this is an *epistemic* type of uncertainty. Another example can be related to the definition of *model uncertainty*. In fact, inherent simplifications can be related also to the fact that some variables may not be included in the definition of a specific model. It implies that their possible random variability (i.e. *aleatory*) can affect the level of model uncertainty. However, in the most of applications, the model uncertainty is classified as *epistemic*. These simple examples clarify that the distinction between *aleatory* and *epistemic* uncertainties is just a classification of convenience for practical applications, since a delineated distinction can not be made.

Then, in the present dissertation the inherent variability of material properties and actions are considered as *aleatory* sources of uncertainty while, the measurement errors, the statistical uncertainty, the human errors and model uncertainty are considered as the *epistemic* ones.

The evaluation of the aleatory uncertainties for resistance models

The inherent randomness of material properties, geometrical parameters and environmental actions are well described by common methods. In fact, codes as *EN 1990* and *JCSS Probabilistic Model Code, 2001* and scientific literature provides efficient methodologies and information in order to define probabilistic models for these variables in reinforced concrete structures. However, in particular when the *assessment* of *existing* structures should be performed, the lack of data may cause significant problems in order to define the probabilistic model for basic random variables.

In the following, the most common (and simplified) assumptions adopted for probabilistic modelling of main *aleatory* uncertainties affecting resistance models in reinforced concrete structures are reported. Nevertheless, more refined probabilistic models accounting for correlation between dependent variables may be acknowledged by *JCSS Probabilistic Model Code, 2001*.

a) Probabilistic model for concrete properties

In general, according to *JCSS Probabilistic Model Code 2001*, *EN 1990* and *fib Model Code 2010* the cylinder concrete compressive strength random variable f_c may be represented by a *lognormal* distribution having:

- *expected value* equal to the *mean value* f_{cm} obtained by testing results or by codes prescription (e.g. *EN 1992-1-1*, *fib Model Code 2010*);
- *coefficient of variation* V_c equal to 0.15; this result shows to be very conservative, in particular, in presence of growing magnitude of the concrete compressive strength (*JCSS Probabilistic Model Code 2001*). However, it can be considered as a safe assumption if experimental or inspection results are not available.

The other parameters as concrete tensile strength f_{ct} , Young modulus E_c , fracture energy G_f , peak strain at concrete compressive strength and ultimate deformation may be evaluated depending from cylinder concrete compressive strength according to expressions reported by *EN1992-1-1* and *fib Model Code 2010* or probabilistically modelled according to *JCSS Probabilistic Model Code, 2001*.

b) *Probabilistic model for reinforcement properties*

According to *JCSS Probabilistic Model Code 2001*, *EN 1990* and *fib Model Code 2010* the probabilistic model for the yielding strength of ordinary reinforcements may be defined adopting a lognormal distribution with the following parameters:

- *expected value* equal to the *mean value* f_{ym} obtained by testing results or by codes prescription (e.g. *EN 1992-1-1*; *fib Model Code 2010*);
- *coefficient of variation* V_y equal to 0.05 in absence of test results (*JCSS Probabilistic Model Code 2001*; *fib Model Code 2010*).

Other properties as ultimate strain and elastic modulus may be assumed according to *fib Model Code 2010* or probabilistically modelled according to *JCSS Probabilistic Model Code 2001* accounting for correlation between the different properties.

In particular, the elastic modulus E_s can be modelled as a *lognormal* distribution having mean value equal to 210000 MPa and coefficient of variation equal to 0.03.

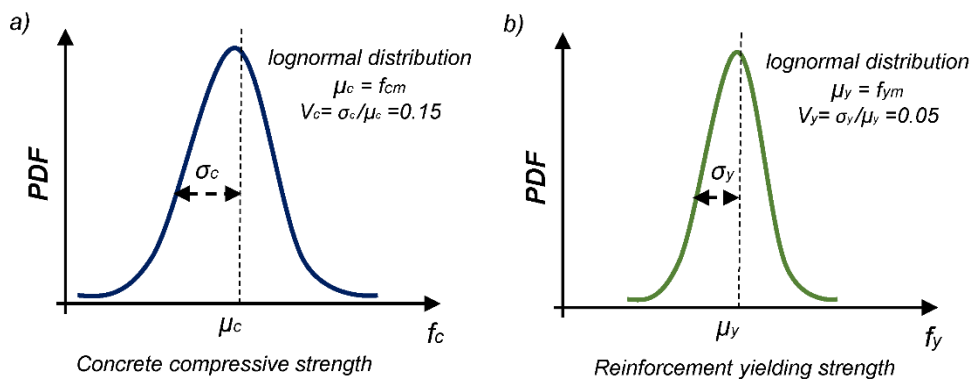


Figure 1.1: Probabilistic modelling of concrete compressive strength (a) and reinforcement yielding strength (b).

The evaluation of the resistance model uncertainty (epistemic)

The evaluation of the resistance of reinforced concrete structural members is performed adopting appropriate assumptions regarding physical-mechanical properties of materials and geometrical parameters. As already discussed, these

variables are usually well known and assessed, but they are not enough to provide a comprehensive evaluation of the actual resistance of a structural component.

In fact, the latter is usually evaluated by means of a model (i.e. reality simplification), which allows to make predictions more or less accurate and realistic. Such physical, semi-empirical or empirical models show an intrinsic uncertainty due to simplified assumptions in their definition and because they disregard some parameters that may have influence on the resistance mechanism. Therefore, a good description of resistance model uncertainty (i.e. *epistemic* uncertainty) is significant as an accurate assessment of the *aleatory* variability of material properties.

A methodology useful to quantify model uncertainties related to resistance models is proposed by *JCSS Probabilistic Model Code, 2001*. A clear and comprehensive treatment of the main issues related to resistance model uncertainties identification is discussed by *Holický et al., 2016*.

The following aspects have to be considered in order to quantify resistance model uncertainty:

- the *database* of experimental observations should provide all the parameters for the reproduction of the tests and the calculation of the resistance using the model under consideration;
- the *range* of parameters that composes the set of experimental results defines the limits of applicability of the analysis and, consequently, the limits of the resistance model after model uncertainty incorporation;
- *statistical inference* for the observed sample of the model uncertainty needs to be carried out in order to define the most likely probabilistic distribution and its parameters.

In general, the model uncertainty may be estimated by means of an additive or a multiplicative relationship. In this dissertation, the latter is adopted.

Defining \mathcal{G} as the *model uncertainty random variable* due to factors affecting test and model results, the following expression may be written:

$$R(X, Y) \approx \mathcal{G} \cdot R_{Model}(X) \quad (1.1)$$

Where:

- $R(X, Y)$ is the actual response of a structure in general (e.g. the experimental one);
- $R_{Model}(X)$ is the response (or the resistance) estimated by the model;
- X is a vector of basic variables included into the resistance model;
- Y is a vector of variables that may affect the resistance mechanism but are neglected in the definition of the model (e.g. variables for which their influence is

still not completely clear or widely assessed). The unknown effect of Y variables, if present, is then covered indirectly by the variable \mathcal{G} .

Specifically, the assessment of the model uncertainty random variable can be performed identifying a vector $R_{Experimental,j}$ of observations and an associated vector of estimated response $R_{Model,i}$. Then, the ratio:

$$\mathcal{G}_j = \frac{R_j(X, Y)}{R_{Model,j}(X)} \quad (1.2)$$

represents the i^{th} outcome of the *model uncertainty random variable* estimated from the selected experimental database. Finally, by means of inferential analysis, the parameters of the most likely probabilistic distribution able to represent the *model uncertainty random variable* \mathcal{G} can be identified. According to *JCSS Probabilistic Model Code, 2001*, in general, the most appropriate probabilistic distribution able to represents the *model uncertainty random variable* \mathcal{G} is the *lognormal* one.

1.2.3 General formulation of the structural reliability problem

The procedure to estimate the reliability of a structural system requires to define the “measure” able to quantify the available level of reliability and to provide the mathematical idealization of the *limit states* conditions. In this Sub-section these two aspects are clarified.

The measure of structural reliability

In reliability analysis, the structural behaviour can be described by means of a set of N *basic random variables* X_i :

$$X_i = (X_1, X_2, \dots, X_i, \dots, X_N) \quad i = 1, 2, \dots, N \quad (1.3)$$

where the variable X_i may be represented by *material properties*, *actions* (loads), *geometrical properties* and *model uncertainties* (both for actions and resistances). Concerning all basic variables, an appropriate probabilistic model should be adopted (*JCSS Probabilistic Model Code, 2001*). The most common measure of the structural reliability is represented by the *probability of failure* P_f . An alternative measure of the structural reliability is represented by the *reliability index* β , which formally can be defined as the negative value of the inverse of the standard normal variable corresponding to the *probability of failure* P_f :

$$\beta = -\Phi(P_f)^{-1} \quad (1.4)$$

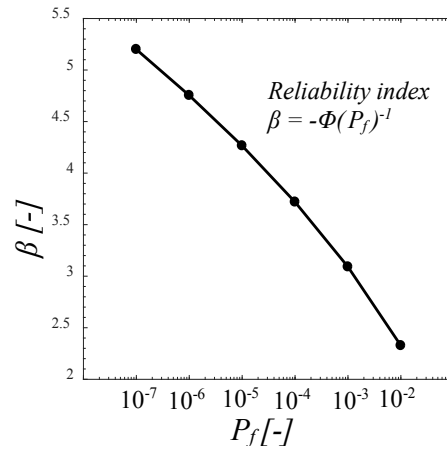


Figure 1.2: Relationship between the probability of failure P_f and reliability index β .

where the Φ represents the cumulative standard normal distribution. The *reliability index* β is used very often by international codes (*ISO 2394*; *EN 1990*; *fib Model Code 2010*) in order to quantify structural reliability. The bigger is the *reliability index* β , the more reliable is the structure (i.e. lower P_f).

The numerical correspondence between *reliability index* β and *probability of failure* P_f is reported in Figure 1.2. The meaning of *probability of failure* P_f can be associated to the probability of exceed a specified *limit state* (i.e. *ULS*, *SLS*).

The limit state function

The *limit state* for a structure or a part of it (i.e. *ULS*, *SLS*) can be outlined by the *limit state function* Z (also denoted as *performance function*) which, in general, is defined in the following form as a function of main random variables X_i :

$$Z = g(X_i) = 0 \quad (1.5)$$

The *limit state function* Z is defined, according to Figure 1.3, so that:

$$\begin{cases} Z \geq 0 \rightarrow \text{safe region} \\ Z < 0 \rightarrow \text{failure region} \end{cases} \quad (1.6)$$

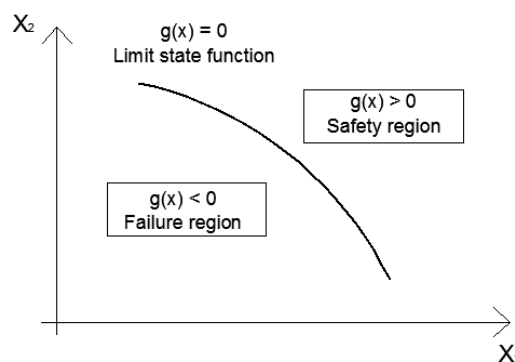


Figure 1.3: General representation of the *limit state domain* with 2 random variables X_1 and X_2 .

Then, the *limit state function* Z is defined in such a way that for a favourable configuration (i.e. safe region) of the structure the function is positive $Z \geq 0$, and for an unfavourable configuration (i.e. failure region) the function is negative $Z < 0$. Based to this definition, the *probability of failure* P_f can be calculated as:

$$P_f = P[Z < 0] \quad (1.7)$$

In the details, defining as $f_{X_i}(x_i)$ the N-dimensional probability density function of the N basic variables X_i , the *probability of failure* P_f can be expressed in the following integral form:

$$P_f = \int_{Z < 0} f_{X_i}(x_i) dx_i \quad i = 1, 2, \dots, N \quad (1.8)$$

Conversely, the *probability of survival* (i.e. *structural reliability*) P_s can be valuated as:

$$P_s = 1 - P_f \quad (1.9)$$

The *probability of failure* P_f have to be estimated considering a specific reference period t_{ref} that commonly, but not necessarily, corresponds to the design or residual service life.

1.3 Reliability methods and theory background

The quantification of the structural reliability can be performed by means the refined estimation of the *probability of failure* P_f or by means of simplified approaches. The latter are devoted to reduce the computational effort and to enhance the applicability of reliability concepts in engineering practice.

In general, the *reliability methods* can be classified in four different levels:

- *level III methods* (probabilistic);
- *level II methods* (probabilistic);
- *level I methods* (semi-probabilistic);
- *level 0 methods* (deterministic).

Progressively, starting from the *level III methods* to the *level 0 methods* the level of implementation of probability theory and the computational effort for estimation of the structural reliability decreases significantly.

1.3.1 Level III methods

The adoption of *level III methods* for the evaluation of structural reliability implies the exact calculation of the probability of failure P_f (or reliability index β) by using the integral expression reported by Eq.(1.8).

In order to solve the problem, analytical solutions, numerical integration and Monte Carlo's simulation may be adopted.

The use of analytical solutions is possible in a limited number of simple cases and the numerical integration results to be convenient only when a small number of variables are involved in the reliability analysis. Then, for complex systems, simulations techniques as the Monte Carlo's method are very efficient tools in order to solve the integral expressed by Eq.(1.8).

In the following, a simple reliability problem is described as a basic example able to be solved by means analytical solutions. Subsequently, the Monte Carlo's method is described together some reduced sampling techniques (i.e. importance sampling and Latin Hypercube sampling).

Reliability analysis with two independent random variables and linear limit state function

In the present simple example, the case of two random independent random variables R (i.e. resistance, having density function $f_R(r)$) and E (i.e. action, having density function $f_E(e)$) with linear *limit state function* is considered. The *limit state function* may be expressed as:

$$Z = g(R, E) = R - E \quad (1.9)$$

Then, the *probability of failure* P_f is defined as:

$$P_f = \int_{Z < 0} f_{R,E}(r, e) dr de = \int_{Z < 0} f_R(r) \cdot f_E(e) dr de \quad (1.10)$$

In order to solve the Eq.(1.10), two different ways can be followed:

$$\begin{aligned} P_f &= \int_{-\infty}^{+\infty} P[(R < e) \cap (e \leq E \leq e + de)] de = \\ &= \int_{-\infty}^{+\infty} F_R(e) \cdot f_E(e) de = \end{aligned} \quad (1.11a)$$

$$\begin{aligned} P_f &= \int_{-\infty}^{+\infty} P[(r \leq R \leq r + dr) \cap (E > r)] dr = \\ &= \int_{-\infty}^{+\infty} f_R(r) \cdot [1 - F_E(r)] dr = \end{aligned} \quad (1.11b)$$

In general, both R and E can be function of other random variables, so that $R = g_R(R_1, R_2, \dots, R_N)$ and $E = g_E(E_1, E_2, \dots, E_M)$. Then, the simple integrals expressed by Eq.(1.11a-b) becomes multiple integrals difficult, if not impossible, to be solved analytically and requires the adoption of numerical integration or Monte Carlo's techniques.

The analytical solution may be found easily if both the random variable R and E are *normally* or *lognormally* distributed.

In fact, if R and E are normally distributed with mean values μ_R , μ_E and variance σ_R^2 , σ_E^2 , respectively, the variable Z (Eq.1.9) is normally distributed too with mean value $\mu_Z = \mu_R - \mu_E$ and variance $\sigma_Z^2 = \sigma_R^2 + \sigma_E^2$.

Then, the *probability of failure* P_f can be expressed according to:

$$P_f = P[Z < 0] = \Phi\left[-\frac{\mu_Z}{\sigma_Z}\right] = \Phi[-\beta] \quad (1.12)$$

where Φ is the cumulative standard normal distribution and β is the *reliability index*. In case R and E are lognormally distributed the solution is similar, having care to take into account that the variables $R'=\ln R$ and $E'=\ln E$ are normally distributed.

However, in most part of the cases, the simulations techniques as Monte Carlo's method are necessary in order to perform reliability analysis.

The Monte Carlo's method and sampling techniques

The Monte Carlo method ((Haldar and Mahadevan, 2000) is a simulation technique used to directly estimate the *probability of failure* P_f of a structural system or component by its application for the evaluation of the integral proposed by Eq.(1.8).

This probability can be written as:

$$P_f = \int_{g(X_i) < 0} f_{X_i}(x_i) dx_i = \int_{-\infty}^{+\infty} I[g(X_i)] f_{X_i}(x_i) dx_i \quad i = 1, 2, \dots, N \quad (1.13)$$

Where $I[g(X_i)]$ is the *indicator function* is defined as:

$$I[g(X_i)] = \begin{cases} 0 & \text{if } g(X_i) \geq 0 \\ 1 & \text{if } g(X_i) < 0 \end{cases} \quad i = 1, 2, \dots, N \quad (1.14)$$

The Monte Carlo's simulation is based on the generation of a large number of samples of the random variables X_i and on the evaluation of the *limit state function* to check if the single realization belongs to the safe, to the failure region or to the limit state bound. The relative number of samples that gives structural failure (i.e. $g(X_i) < 0$) are considered as an estimation of the probability of failure.

The estimated *probability of failure* P_f with n samples can be written as:

$$P_f \approx P_f^n = \frac{1}{n} \sum_{j=1}^n I[g(X_i)] \quad i = 1, 2, \dots, N; j = 1, 2, \dots, n \quad (1.15)$$

where n_{sim} is the total number of simulations.

The accuracy of the probabilities estimated by Monte Carlo's technique may be assessed by defining the coefficient of variation of the solution in function of the number of samples.

The *coefficient of variation* of P_f may be estimated by assuming each simulation cycle to constitute a "Bernoulli trial", and the number of failures in n_{sim} trials can be considered to follow a binomial distribution. Then the coefficient of variation of P_f at the j^{th} sample may be calculated as:

$$V_{P_f}^j = \frac{\sqrt{\frac{(1-P_f^j)P_f^j}{j}}}{P_f^j} \quad j = 1, 2, \dots, n \quad (1.16)$$

The number of samples to be used for the simulation is proportional to the inverse of the target probability of failure to be estimated. Consequently, the number of simulations required for the *reliability analysis* is extremely high (commonly around $10^5 - 10^6$ simulations). It implies that the computational effort may be demanding, in particular when complex non-linear resistance models have to be adopted.

In order to reduce the number of simulations and then the computational effort, several *sampling techniques* has been developed and reported by scientific literature. The following methods are herein described:

- the *importance sampling method*;
- the *latin hypercube sampling method* (i.e. LHS).

a) *Importance sampling method*

This variance reduction method uses prior information about the region of the domain of basic variables that have contribution to the probability integral in order to concentrate the sampling in the area of the *standard normal space* U which has the largest contribution to the *probability of failure* P_f .

The *probability of failure* can be written as:

$$\begin{aligned} P_f &= \int_{-\infty}^{+\infty} I[g(U_i)] f_{U_i}(u_i) dU_i = \\ &= \int_{-\infty}^{+\infty} I[g(U_i)] \frac{f_{U_i}(u_i)}{f_{Z_i}(u_i)} f_{Z_i}(u_i) dU_i \quad i = 1, 2, \dots, N \end{aligned} \quad (1.17)$$

Where $f_{U_i}(u_i)$ the *jointed probability density function* expressed in the *standard normal space*; $f_{Z_i}(u_i)$ is the *sampling density function*.

In order to reduce the error in prediction of the probability of failure, and then reduce the required numbers of sampling, is necessary to select properly the

sampling density function. The best choice that it possible to do is to adopt a *sampling density function* $f_{Z_i}(u_i)$ proportional to the *jointed probability density function* $f_{U_i}(u_i)$ expressed the standard normal space: $f_{Z_i}(u_i) \propto |f_{U_i}(u_i)|$.

The following procedure can be adopted:

- 1) generate a vector z_i' of random numbers having standard normal distribution;
- 2) define the *design point* u_i^* as the point on the limit state surface into the standard normal space that have the lower distance from the origin, is possible to write: $u_i = u_i^* + \Sigma_{ij}$. In general, Σ_{ij} is represented by the *unit matrix*.
- 3) calculate $f_{U_i}(u_i)$ and $f_{Z_i}(u_i)$ according to:

$$f_{U_i}(u_i) = \frac{1}{(2\pi)^{\frac{n}{2}}} \exp\left[-\frac{1}{2} u_i^T \cdot u_i\right] \quad i = 1, 2, \dots, N \quad (1.18)$$

$$f_{Z_i}(u_i) = \frac{1}{(2\pi)^{\frac{n}{2}} \cdot \det \Sigma_{ij}} \exp\left[-\frac{1}{2} (u_i - u_i^*)^T \cdot \Sigma_{ij}^{-1} \cdot (u_i - u_i^*)\right] \quad i = 1, 2, \dots, N \quad (1.19)$$

- 4) Transform in the original space of basic variables and evaluate the *limit state function* for the correspondent realization x_i in order to determine the value of $I[g(u_i)]$.

Finally, the estimation of *probability of failure* P_f with n samples can be written as:

$$P_f \approx P_f^n = \frac{1}{n} \sum_{j=1}^n I[g(U_i)] \frac{f_{U_i}(u_i)}{f_{Z_i}(u_i)} \quad i = 1, 2, \dots, N; j = 1, 2, \dots, n_{sim} \quad (1.20)$$

b) *Latin hypercube sampling (LHS)*

The *latin hypercube sampling– LHS* – (Mckey, 1979), is a stratified sampling method able to reduce the computational effort required for Monte Carlo's simulation. The basic concept behind LHS method is the following: the variables are sampled by their probabilistic distribution and, successively, randomly combined. The sampling algorithm ensures that each distribution function is sampled uniformly between the interval of probabilities (0,1). The Figure 1.4 reports the difference between theoretical cumulative distribution for the generic variable X_i and the stratified sampling of a lognormal distribution.

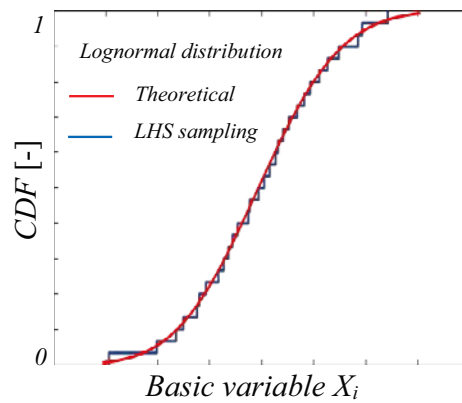


Figure 1.4: Stratified sampling according to LHS: example of LHS sampling from basic variable.

The sampling from the probabilistic distribution of basic variables X_i can be performed according to the following steps:

- 1) for each variable X_i the probability interval $(0,1)$ is subdivided in n non-overlapping equiprobable sub-intervals (h_{inf}, h_{sup}) ;
- 2) in each one of the n sub-intervals, one value between (h_{inf}, h_{sup}) is sampled randomly from a uniform distribution and the corresponding value of the basic variable X_i is evaluated;
- 3) a random permutation between the n values sampled for each variable X_i is performed in order to randomly combine the outcomes. In this way, the n input sets of basic variables to perform the simulations is defined.

As discussed in next Chapters, the LHS method can be very efficient in case *reliability analysis* is performed by means of non-linear finite element method. In this way, the number of numerical simulations required in order to characterize the probabilistic distribution of the structural resistance can be strongly reduced. In fact, it can be demonstrated that when the coefficient of variation of basic variables is lower or equal to 0.2, a number of 30-40 samples are sufficient in order to determine mean, variance and probabilistic distribution of the investigated structural resistance. Then, LHS sampling can be adopted efficiently in order to characterize probabilistic distribution of structural resistance by means of a reduced number of samples.

1.3.2 Level II methods

The Level II methods allows to perform *reliability analysis* by using moments of basic variables only. Specifically, the first and the second order moments (i.e. covariance matrix) are adopted in most of the cases.

Furthermore, the limit state function $Z=g(X_i)$ is linearized (i.e. first order approximation) around predefined points represented, commonly, by the mean value (Cornell, 1969) of the joint probabilistic distribution of basic variables and by the *design point* (Hasofer and Lindt, 1974). Because of these two approximations, the mentioned above methods are called “First Order Second Moment – FOSM” or “First Order Reliability Methods – FORM”.

Within Level II methods, the measure of structural reliability is performed by means the *reliability index* β that, according to (Cornell, 1969) can be defined as:

$$\beta = \frac{\mu_Z}{\sigma_Z} \quad (1.21)$$

where μ_Z and σ_Z are the mean value and the standard deviation, respectively, of the limit state function Z . The relationship between *reliability index* β and the *probability of failure* P_f is defined in Sub-section 1.2.3 . Then, the *reliability index* β is defined as the distance between the mean value μ_Z from the failure condition (i.e. $Z=0$) expressed in number of standard deviation of the limit state function σ_Z (Figure 1.5).

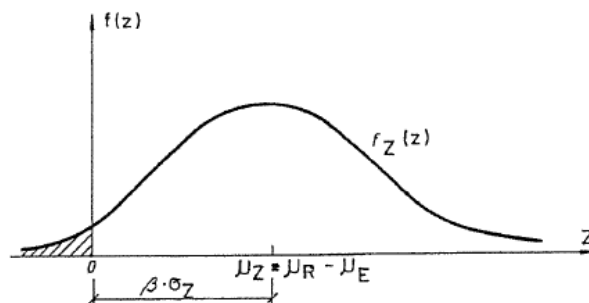


Figure 1.5: Definition of *reliability index* β according to (Cornell, 1969).

A more general and geometric definition of *reliability index* β as been defined by Hasofer and Lindt, 1974. Specifically, the *reliability index* β is defined as the closest distance between the mean value of the joint probabilistic distribution of basic variables in the standard normal space and the multidimensional limit state surface. The explanation is reported in Figure 1.6 in the case of two random variable R and E with *linear limit state function*.

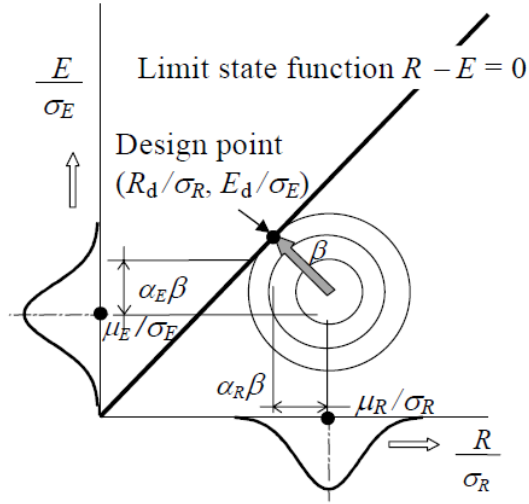


Figure 1.6: Definition of design point and reliability index (Hasofer and Lindt, 1974).

In verification of structural reliability any point of the failure surface $Z=R-E=0$ (i.e. limit state function) can be considered as a critical structural configuration. However, it has been proved by *Konig and Hosser, 1982* that the best solution with level II methods is achieved performing the linearization of the limit state function in the so called “*design point*”. The *design point* represents the point pertaining to the limit state surface having the highest probability density. In the details, is the point having coordinates (R_d, E_d) closest to the mean point of coordinates (μ_R, μ_E) . In literature is denoted also as the “most probable failure point”. Accepting the present hypothesis, the coordinates of the *design point* may be written in function of the *reliability index* β as:

$$R_d = \mu_R - \alpha_R \beta \sigma_R \quad (1.22a)$$

$$E_d = \mu_E - \alpha_E \beta \sigma_E \quad (1.22b)$$

where α_R and α_S denotes the First Order Reliability Method - FORM – sensitivity factors of the random variables R and E . From the Figure 1.5 that the sensitivity factors α_R and α_S may be evaluated as the direction cosines of the *design point*:

$$\alpha_R = \frac{\sigma_R}{\sqrt{\sigma_E^2 + \sigma_R^2}} \quad (1.23b)$$

$$\alpha_E = -\frac{\sigma_E}{\sqrt{\sigma_E^2 + \sigma_R^2}} \quad (1.23b)$$

with:

$$\alpha_E^2 + \alpha_R^2 = 1 \quad (1.24)$$

In the *EN 1990* and *fib Model Code 2010*, an approximation of these values according to *Konig and Hosser, 1982* is performed. Specifically, the value of α_R is set equal to 0.8 and the value of α_S is set equal to -0.7. The validity on this approximation is bounded by the following limits of validity: $0.16 < \sigma_R/\sigma_E < 7.6$.

Since these approximations are extremely on the safe side, the condition expresses by Eq.(1.24) is not satisfied. When limits of validity (i.e. $0.16 < \sigma_R/\sigma_E < 7.6$) are not fulfilled, the values of α_R and α_S can be set equal to +1 and -1, respectively.

The mentioned above values for α_R and α_S are defined for dominant random variables. In case of accompanying or non-dominant random variables (as, according to *fib Model Code 2010*, is the case of model uncertainty) the value of FORM sensitivity factors can be pre-multiplied for 0.4.

In the case R and E are *normal* distributed random variables, the *design point* coordinates can be evaluated according to the following probabilities (in case of dominant random variables):

$$P[E > E_d] = \Phi(\alpha_E \beta) = \Phi(-0.7\beta) \quad (1.25a)$$

$$E_d = \mu_E + 0.7\beta\sigma_E$$

$$P[R \leq R_d] = \Phi(\alpha_R \beta) = \Phi(0.8\beta) \quad (1.25b)$$

$$R_d = \mu_R - 0.8\beta\sigma_R$$

Similarly, in case of R and E are *lognormal* distributed random variables the mentioned above equations become:

$$P[\ln E > \ln E_d] = \Phi(\alpha_E \beta) = \Phi(-0.7\beta) \quad (1.26a)$$

$$E_d = \mu_E \exp\left(0.7\beta \frac{\sigma_E}{\mu_E}\right)$$

$$P[\ln R \leq \ln R_d] = \Phi(\alpha_R \beta) = \Phi(0.8\beta) \quad (1.26b)$$

$$R_d = \mu_R \exp\left(-0.8\beta \frac{\sigma_R}{\mu_R}\right)$$

The level II methods, are the base for calibration of Levels I methods according to the semi-probabilistic approach.

1.3.3 Level I methods

The Level I method allows to take into accounts the probabilistic distribution of basic variables with a simplified approach. In fact, the basic variables are represented by their *characteristic value*, that corresponds to a low quantile in case of strength distributions or to a high quantile in case of distributions related to actions. Furthermore, *partial safety factors* are introduced with values that are based on Level II calculations.

The basic verification format, introduced by *EN 1990*, consist of verifying whether the limit state is not exceeded when all basic variables in the limit state equation are replaced by so called design values (identified by “d”). In case of a simple limit state function, as the case of Eq.(1.9), one has to verify whether the design resistance R_d is at least equal to the design value of the load effect E_d :

$$R_d \geq E_d \quad (1.27)$$

$$E_d = E(F_{d,1}, F_{d,1}, \dots; a_{d,1}, a_{d,2}, \dots; \vartheta_{d,1}, \vartheta_{d,1}) \quad (1.28)$$

$$R_d = R(X_{d,1}, X_{d,1}, \dots; a_{d,1}, a_{d,2}, \dots; \vartheta_{d,1}, \vartheta_{d,1}) \quad (1.29)$$

Where F represents an external action; X represents a material property; a is a geometrical property; ϑ is the model uncertainty.

The partial safety factors for material properties (i.e. γ_m) and actions (i.e. γ_f), in general, are derived from their *characteristic values* according to:

$$\gamma_m = \frac{R_k}{R_d} \quad \text{for resistances} \quad (1.30)$$

$$\gamma_f = \frac{E_d}{E_k} \quad \text{for load effects} \quad (1.31)$$

The design values R_d and E_d may be evaluated according to Eq.(1.25a-b) or Eq.(1.26a-b) deriving from Level II methods. In general, the *characteristic value* is considered as be the 5% quantile of the probabilistic distribution of the resistances, the 50% quantile of the probabilistic distribution of permanent actions and the 95-98% quantile in case of variable actions.

The *semi-probabilistic limit states approach* proposed by *EN1990* and *fib Model Code 2010* are based on a Level I methodology, accounting for deterministically the geometrical parameters. These methods are the used in practice for *design* and *assessment* of structures.

1.3.4 Level 0 methods

The Level 0 methods are conceived as pure determinist methods. In general, the deterministic or nominal values of variables are used accounting for one global safety factor (having empirical nature). The basic verification is performed basing of the following equation:

$$R_{Nom} \geq \gamma E_{Nom} \quad (1.32)$$

These method does not allow to quantify the level of reliability within assessment or design and may leads to underestimate the structural safety without any control about it.

The introduction of probability-based methods made obsolete these deterministic methods that, in current structural codes, are no longer implemented.

1.3.5 Reliability of structural systems

In general, real structures are realised collecting a large number of structural components (e.g. beams and columns) and may be considered as structural systems. The reliability of the system depends from the reliability of each component. Moreover, structural components may be interested by different *failure modes* (e.g. bending and shear) described, each one, by a specific *limit state function* according to previous Sections.

Furthermore, different *failure modes* may result to be brittle, ductile or brittle with residual strength. In particular, concerning reinforced concrete structures, the clear distinction between ductile or brittle failure modes is not always possible in cases of particularly complex geometries and reinforcements arrangements. Then, the exact analysis of reliability of complex structural systems is almost impossible for most of cases and some simplifications are required.

Generally, two systems of structural components can be identified:

- *series systems*;
- *parallel systems*.

In the following, the general approaches to the calculation of the probability of failure of structural systems are outlined in their fundamentals.

Structural system with series components

Let consider a structure represented by n components collected in series. Denoting with F_i the failure event of the i^{th} component that occur with probability $P[F_i]$, the *probability of failure of the series structural system* $P_{f,s}$ can be expressed by the following general summation law:

$$\begin{aligned} P_{f,s} &= P[F_1 \cup F_2 \cup \dots \cup F_n] = \\ &= \sum_{i=1}^n P[F_i] - \sum_{i<j} P[F_i \cap F_j] + \sum_{i<j<k} P[F_i \cap F_j \cap F_k] + \\ &\dots + (-1)^{n-1} P\left[\bigcap_{i=1}^n F_i\right] \end{aligned} \quad (1.33)$$

The simple case of three structural components leads to the following expression:

$$\begin{aligned} P_{f,s} &= P[F_1 \cup F_2 \cup F_3] = \\ &= P[F_1] + P[F_2] + P[F_3] - P[F_1 \cap F_2] - P[F_1 \cap F_3] + \\ &- P[F_2 \cap F_3] + P[F_1 \cap F_2 \cap F_3] \end{aligned} \quad (1.34)$$

The Eq.(1.33) may be elaborated by applying the following law related to conditional probabilities:

$$P[F_1 \cap F_2 \cap \dots \cap F_n] = P[F_1] \cdot P[F_2|F_1] \cdot \dots \cdot P[F_n|F_1 \cap F_2 \cap \dots \cap F_{n-1}] \quad (1.35)$$

Then, for the case of three components:

$$P[F_1 \cap F_2 \cap F_3] = P[F_1] \cdot P[F_2|F_1] \cdot P[F_3|F_1 \cap F_2] \quad (1.36)$$

The *probability of failure of the series structural system* $P_{f,s}$ may be estimated according to upper and lower bound.

In fact, in case of *mutually exclusive failure events* F_i , Eq.(1.33) become:

$$P_{f,s} = \sum_{i=1}^n P[F_i] \quad (1.37)$$

Let consider now the case with three structural components with *perfectly correlated failure vents*. The following hypothesis is performed: $P[F_1] \geq P[F_2] \geq P[F_3]$.

According to Eq.(1.34) and Eq.(1.36):

$$\begin{aligned} P_{f,s} &= P[F_1] + P[F_2] + P[F_3] - P[F_2] \cdot P[F_1|F_2] + \\ &- P[F_3] \cdot P[F_1|F_3] - P[F_3] \cdot P[F_2|F_3] \cdot P[F_1|F_2 \cap F_3] = P[F_1] \end{aligned} \quad (1.38)$$

The Eq.(1.37) and Eq.(1.38) represents the expression of upper and lower bound for the failure probability of the series system. The general expression for boundaries of failure probability for series structural systems has been provided by *Cornell, 1967*:

$$\max\{P[F_i]\} \leq P_{f,s} \leq \sum_{i=1}^n P[F_i] \quad (1.39)$$

Successively, narrower upper and lower bound has been proposed by *Ditlevsen, 1979*:

$$P[F_1] + \max\left\{P[F_i] - \sum_{j=1}^{i-1} P[F_i \cap F_j], 0\right\} \leq P_{f,s} \leq \sum_{i=1}^n P[F_i] - \sum_{i=2}^n \max_{j<i} P[F_i \cap F_j] \quad (1.40)$$

In the case the failure probability $P[F_i]$ are strongly different (i.e. $P[F_1] \gg P[F_2] \gg P[F_3] \gg \dots$), the lower and the upper bounds are converging toward the highest component failure probability represented by $P[F_1]$.

Structural system with parallel components

Let now consider a structure represented by n components collected in parallel. Denoting with F_i the failure event of the i^{th} component that occur with probability $P[F_i]$, the *probability of failure of the parallel structural system* $P_{f,p}$ can be expressed by the intersection of the failure events of each component:

$$P_{f,p} = P[F_1 \cap F_2 \cap \dots \cap F_n] \quad (1.41)$$

Also for parallel structural systems, bounds for the failure probability $P_{f,p}$ can be derived. In fact, in case of *mutually exclusive failure events* F_i :

$$P_{f,p} = \prod_{i=1}^n P[F_i] \quad (1.42)$$

Then, the following upper and lower bounds can be derived:

$$0 \leq P_{f,p} \leq \min\{P[F_i]\} \quad (1.43)$$

Concerning both series and parallel structural systems the following observations can be outlined:

- increasing the level of correlation between the failure events F_i , the failure probability decreases for *series* systems and increases for *parallel* systems;
- increasing the number n of structural components, the failure probability increases for *series* systems and decreases for *parallel* systems.

Combined structural systems

Concerning the series and parallel combined structural systems, the probability of failure can be expressed as:

$$P_{f,p} = P \left[\bigcup_{i=1}^k \left(\bigcap_{r=1}^l F_{ir} \right) \right] \quad (1.44)$$

for the case of k parallel sub-systems and:

$$P_{f,p} = P \left[\bigcap_{i=1}^s \left(\bigcup_{r=1}^t F_{ir} \right) \right] \quad (1.45)$$

for the case of s series sub-systems.

In general, real structures are combined systems with structural members collected in series and in parallel. Several design and assessment strategies are based on the theory of systems. For example, redundancy and robustness principles are based on creating parallel system (if an element fails, the others elements connected in parallel have to carry the extra load), while, capacity seismic design is based on concepts related to series systems (some elements are connected in series in order to fail before the others).

1.3.6 Target reliability and reliability differentiation for new and existing structures

Notices about the target reliability levels are reported by codes as *EN 1990*, *fib Model Code 2010*, *ISO 2394* and scientific literature as *fib Bulletin 80*.

The definition of the target levels of reliability have to take into account the possible consequences of structural failure in terms of human casualties or injuries and the potential direct and indirect economic implications. Moreover, the selection of level of reliability also have to consider the expenses required for safety measures able to reduce the probability of structural failure.

Concerning the *limit states* approach, the maximum acceptable failure probability depends on the type of the limit state (i.e. serviceability of ultimate), considered consequences of structural failure, relative costs for safety measures and reference period (that may be different from the service life).

The reliability analysis of *existing* structures differs from *new* structures in several aspects:

- increased target reliability levels implicate greater increment of costs for *existing* structures than for *new* structures;

- the remaining service life of *existing* structures is often smaller than the design service life of 50-100 years assumed for *new* structures;
- information on actual structural conditions should be available for the assessment of an *existing* structure (i.e. inspection reports, tests, measurements).

In general, for both evaluating target reliability for *new* and *existing* structures the following aspect should be analyzed:

- human safety;
- economical implication.

In an extremely simplified model, the total costs C_{tot} of a structure during its working life can be expressed as:

$$C_{tot} = C_i + P_f D \quad (1.45)$$

Where C_i are the initial costs for build the *new* structure (C_{build}) or for up-grade the *existing* one ($C_{upgrade}$) and $P_f D$ is the expected failure costs related to the working life (which is intended as the design service life for *new* structures and the residual service life for *existing* structures). The optimum target reliability index can be identified as the one that meet the principle of minimizing the total cost C_{tot} without be lower to the minimum requirements for human safety. In Figure 1.7 this procedure for both *new* and *existing* structures is represented.

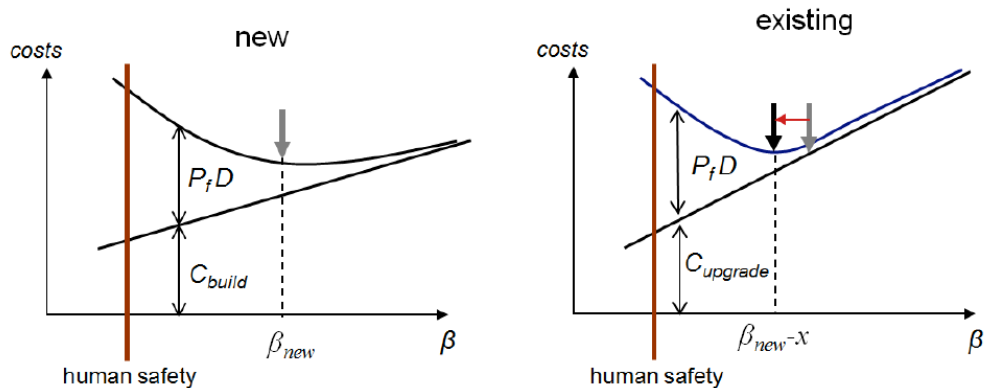


Figure 1.7: Differences in cost optimization for the design of *new* structures versus upgrading of *existing* structures (*fib Bulletin 80*).

Basing on the mentioned above criteria, the target levels of reliability should be differentiated between *new* and *existing* structures. In fact, the cost for upgrading of the *existing* structure are higher than the cost for build the *new* structure with appropriate safety measures. As a result, optimum target reliability indexes for *existing* structures have to be lower if compared to the ones for *new* structures.

Moreover, target reliability of *existing* structures should be based on their residual service life, that is a case dependent property. The methodology to derive target reliability indexes accounting for these aspects related to *existing* structures is outlined in *fib Bulletin 80*.

In Table 1.1, the target reliability indexes for *new* and *existing* structures proposed by *fib Model Code 2010* are reported. However, concerning *existing* structures, the state of the art for determination of target reliability indexes is represented by *fib Bulletin 80*.

Table 1.1: Suggested range of target reliability from *fib Model Code 2010* for *new* and *existing* structures.

Limit states	Target reliability index β	Reference period
New structures <i>(fib Model Code 2010)</i>		
<i>Serviceability (SLE)</i>		
reversible	0.0	Service life
irreversible	1.5	50 years
irreversible	3.0	1 year
<i>Ultimate (SLU)</i>		
Low consequences of failure	3.1	50 years
	4.1	1 year
Medium consequences of failure	3.8	50 years
	4.7	1 year
High consequences of failure	4.3	50 years
	5.1	1 year
Existing structures <i>(fib Model Code 2010)</i>		
<i>Serviceability (SLE)</i>	1.5	Residual service life
<i>Ultimate (SLU)</i>		
	3.1 – 3.8*	50 years
	3.4 – 4.1*	15 years
	4.1 – 4.7*	1 year
*depending from costs for safety measures and upgrading of the structure; more detailed information can be derived from <i>fib Bulletin 80</i> .		

According to *fib Model Code 2010*, the reliability of each component of the structural system should depend on the system characteristics itself. The target reliability indexes given in Table 1.1 are related to the structural systems, to the dominant failure mode of the single component or to the structural component that dominate the failure of whole system. Then, if the structure is in presence of multiple equally important failure modes, it should be designed for a higher level of reliability.

The mentioned above target reliability indexes are also intended for structures for which failure is preceded by a certain level of warning (e.g. ductile failure modes). In this way, preventive measures can be adopted in order to limit the possible consequences of structural failure (at least in term of human casualties).

The failure modes that are not warned by the structure (e.g. brittle failure modes), should be avoided by means design procedure and correct detailing. In general, the brittle failure must not occur. If a structural component or system would fail with brittle failure mode, it should be designed accounting for a higher target reliability.

1.4 Safety formats for design and assessment of reinforced concrete structures

In this Section the basic principles of *safety formats* reported by codes as *EN1990*, *fib Model Code 2010* and *fib Bulletin 80* are described. The *safety format* can be identified as a series of rules and methods defined in order to perform *design* or *assessment* of *new* and *existing* structures according to pre-determined target reliability levels.

Next, the methodology introduced for the first time by *fib Model Code 2010* denoted as “*levels of approximation approach*” is described. Then, the different *safety formats* are commented.

1.4.1 The levels of approximation approach

The structural analysis grounds on representative models that are only an approximation of the reality. Each model, from the simplest to the most refined one, it may represent the reality with different degrees of accuracy.

The *fib Model Code 2010* and *Muttoni and Ruiz, 2012* has introduced the *design* and *assessment* methodology denoted as “*levels of approximation approach*” (*LoAs*). Specifically, a “*level of approximation*” (*LoA*) is a *design* or *assessment* methodology where the accuracy on the estimate of the response of a structural member or system can be refined by improving the knowledge about the involved physical parameters and the complexity of the mathematical model. In general, four *LoAs* are suggested with growing level of refinement and time devoted to perform the structural analysis form the first one to the last one:

- *level of approximation I (LoA I)*: has to provide simple and safe hypotheses for evaluating the physical parameters related to the resistance model. It leads to safe predictions of the structural response of the structural member or systems. This *LoA* requires low time-consuming and is usually sufficient for preliminary design or assessment purposes. The estimate of *LoA I* may be refined in successive *LoAs* by devoting more time to the estimate of the physical parameters and adopting more complex analytical or numerical procedures;

- *level of approximation II and III (LoA II, III)*: in these LoAs the physical parameters and the resistance models are still evaluated through analytical methods accounting for the equilibrium and mechanical parameters. Again, these LoAs are low time-consuming and are usually sufficient to cover most design and assessment cases;
- *level of approximation IV (LoA IV)*: numerical procedures allow typically obtaining the best estimates of the structural response. They are commonly adopted as the the highest LoA. The use of this level of refinement can be very time consuming and is suggested for design of very complex structures or for the assessment of critical existing structures. This LoA is justified in cases where a more accurate estimate of the structural response can lead to significant economical savings.

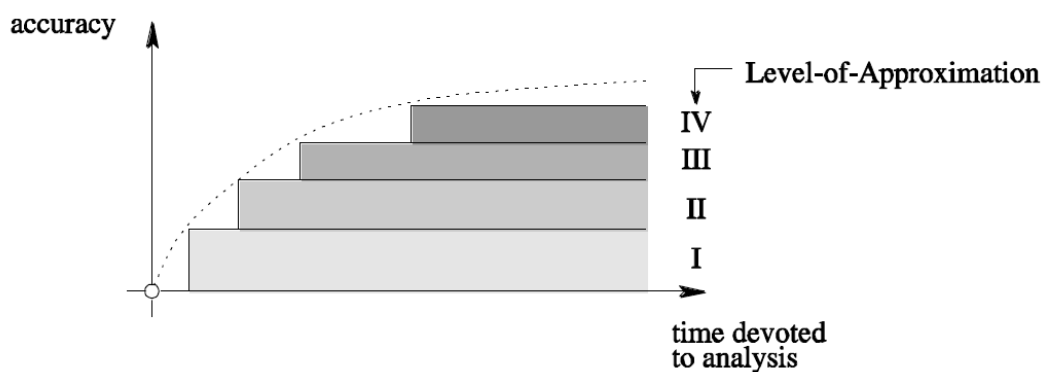


Figure 1.8: Levels of approximation approach as defined by *Muttoni and Ruiz, 2012* and *fib Model Code 2010*.

The choice of a suitable LoA is left to designer and practitioners. It depends on the type of analysis performed, on the stage of the design or assessment process (preliminary or executive) and on the potential savings that can be provided if a higher *LoAs* is adopted. In Figure 1.8 the schematization representing the concept of the *LoAs* is reported.

Once selected the LoA related to the representative model of structural response, the reliability concepts should be introduced by appropriate *safety formats*.

As discussed later in the present dissertation, the basic concept of the LoAs can be extended also to the choice of a specific *safety format* when refined non-linear analyses are adopted.

Next, the basic principles of *safety formats* based on the *limit states* approach proposed by codes (*EN 1990, fib Model Code 2010*) are commented.

1.4.2 Probabilistic safety format

The *fib Model Code 2010* allows to perform full probabilistic analysis in according to the methodologies outlined by the Level III and Level II methods. The probabilistic safety format is suitable also for the assessment of *existing* structures.

The verification of a structure, according to particular *limit state* is carried out by means the estimation of the probability of failure P_f in a specified reference period (i.e. service life for new structures or residual service life for existing structures).

According to Section 1.3.1, the equation for safety verification can be expressed in terms of *probability of failure* P_f as:

$$P_f = P[g(X_i) \leq 0] \leq P_{f,T} \quad i=1,2,\dots,N \quad (1.46)$$

where $P_{f,T}$ are the target probability of failure according to target reliability indexes reported in Section 1.3.6. The relation between the reliability index β and the probability of failure is reported in Subsection 1.2.3. The methodologies described in Subsection 1.3 can be adopted in order to evaluate P_f and define the probabilistic model for basic variables X_i .

1.4.3 Partial factor format

The *partial factor format* is defined according to the Level I methodology and it is implemented by *fib Model Code 2010* and *EN 1990*. The safety measures are applied partially to loads and material resistances by means of partial safety factors.

The partial safety factors can be distinguished as:

- *partial safety factors for material properties:*

$$\gamma_M = \gamma_{Rd1} \cdot \gamma_{Rd2} \cdot \gamma_m \quad (1.47)$$

where γ_{Rd1} is the model uncertainty partial safety factor set equal to 1.05 and 1.025 for concrete and reinforcement, respectively; γ_{Rd2} is the partial factor accounting for geometrical uncertainties set equal to 1.05; γ_m is the partial factor for material uncertainty evaluated according to Eq.(1.30). Assuming normal distribution for material uncertainties, the value of γ_M is equal to 1.5 for concrete cylinder compressive strength assuming a coefficient of variation equal to 0.15 and is equal to 1.15 for bar reinforcements accounting for a coefficient of variation equal to 0.05; the related target of reliability is define by $\beta=3.8$ according to Table 1.1.

- *partial safety factors for permanent actions (G) and variable actions (Q):*

$$\gamma_{G,Q} = \gamma_{sd} \cdot \gamma_{g,q} \quad (1.48)$$

where γ_{sd} is the model uncertainty partial safety factor set equal to 1.05; $\gamma_{G,Q}$ is the partial safety factor for permanent (G) and variable loads (Q) accounting for aleatory variability and reference service life according to Eq.(1.31).

The actions are properly combined for ULS and SLS accounting for appropriate combination coefficients in order to maximize and minimize their effect of the structural response. Specific values for partial safety factors for actions can be acknowledged by *fib Model Code 2010* and *EN 1990*.

Partial factor formats for existing structures

The mentioned above *partial factor format* has been conceived for the realization of *new* structures.

As discussed in Subsection 1.3.6, the assessment *existing* structures significantly differ from the design of *new* ones. For instance, two methodologies for the updating of partial factors for the assessment of *existing* structures has been proposed by *fib Bulletin 80* accounting for:

- possible knowledge about the *existing* structure deriving from testing;
- modified target of reliability accounting for residual service life and costs for upgrading of the *existing* structure.

Specifically, two methodologies has been defined:

- the “*Design Value Method*” (*DVM*), which allow to recalculate the partial factors γ_X from the actual distribution of the variable X under consideration (based on prior information, or results of tests or the combination of both). This method is more refined and it is suggested for structures of particular relevance and may leads to results discordant to ones obtained by *EN1990* and *fib Model Code 2010*;
- the “*Adjusted Partial Factor Method*” (*APFM*), which allow to correct partial factors $\gamma_{X,New}$ for new structures proposed by *EN1990* by means to *adjustment factors* ω_X as follows:

$$\gamma_X = \omega_X \cdot \gamma_{X,New} \quad (1.49)$$

The method is fully consistent with *EN1990* provisions and it is considered as a simplification if compared to the *DVM*.

1.4.4 Global resistance format

The *global resistance format* (i.e. *GRF*) treats the uncertainties associated to structural behavior according to the limit state approach (Section 1.2.3) at the level of overall structural resistance (i.e. global resistance). The sources of uncertainties are integrated in a *design global resistance* R_d and can be accounted for by means *global safety factors*. The *global safety factors* reflect the uncertainty in the determination of the overall structural response depending from *aleatory* variability of basic variables and *epistemic* uncertainties.

The *GRF* has been introduced in order to allow structural *design* and *assessment* by means of non-linear analysis. In fact, refined mechanical and geometrical non-linear models are generally based on a global structural level, and the *GRF* represents an efficient format to perform safety verifications. However, it can be applied also to single members or specific cross sections.

The “global” and the “local” approach for structural design and assessment

In common practice and in Codes the *design/assessment* of *new/existing* structures is performed by means of cross-sectional analysis comparing the design agent (E_d) and resisting (R_d) internal actions (e.g., bending moment, shear and axial forces) according to the inequality $E_d < R_d$. In general, the *limit states* approach in compliance with the *partial factor method* is adopted. In this framework, the internal actions E_d are evaluated by means of linear elastic analysis combining the effects of the external loads (with linear superimposition), while, the sectional internal resistance R_d is evaluated according to the limit analysis. This approach to assess the structural safety is defined as “local”, as it involves only sectional verifications of the structural members disregarding from the global actual behavior and progressive redistribution of internal forces within the reinforced concrete structure.

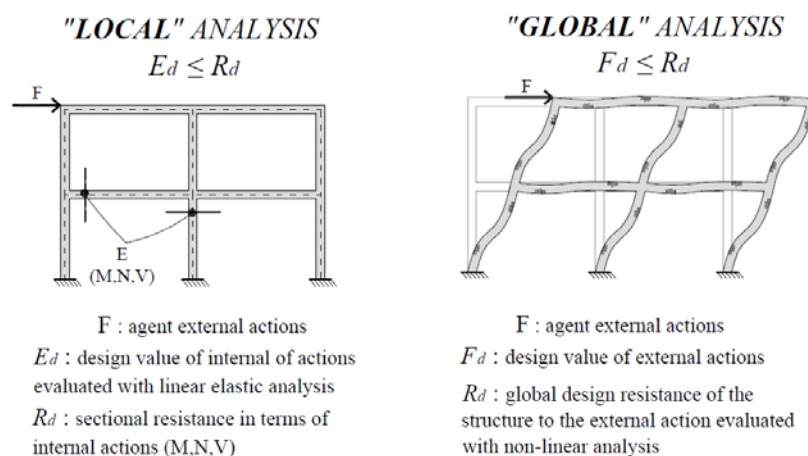


Figure 1.9: Comparison between local structural analysis and global structural analysis.

The local analysis is very efficient when low LoAs are used by performing simplified assumptions for the definition of the structural model, constitutive laws and resistance mechanisms. On the contrary, as introduced in Subsection 1.4.1, when the assessment of structural safety is performed by means of higher LoAs with refined non-linear analysis (e.g., NLFEMs), the global capability of the reinforced concrete structures to redistribute internal forces under a specific loading condition can not be neglected. In this context, the use of non-linear structural models implies the adoption of a “global” approach for the structural assessment, comparing the global external action under a specific loading combination and the global structural resistance. Then, the progressive damaging of the structure and internal forces redistribution are accounted for within the global verification justifying also the adoption of such complex non-linear models. The differences between the two approaches are explained in Figure 1.8.

Definition of the design global resistance

According to the GRF, the representative variable for the global resistance is the structural resistance R . The following representative values of resistance can be derived:

- R_m , mean value of global structural resistance;
- R_k , 5% characteristic value of the global structural resistance;
- R_d , design value of the global structural resistance according to specified target reliability index β .

The safety condition is represented by the following equations:

$$F_d \leq R_d, \quad R_d = \frac{R_m}{\gamma_R \cdot \gamma_{Rd}} \quad (1.50)$$

where F_d is the design external action defined according to the partial factor format; γ_R is denoted as the *global resistance safety factor*, which account for material aleatory uncertainties; γ_{Rd} represents the *resistance model uncertainty safety factor*, which account for the resistance model uncertainty (i.e. epistemic).

The values for the mentioned above safety factors are evaluated depending from the type of the resistance model and from the global structural behaviour. A deeper discussion about their evaluation is reported in following Chapters.

Global safety factors differ from the well-known *partial safety factors* adopted within local analysis by partial factor format. In fact, *global safety factors* refer to the global structural response evaluated by means mean values of material properties, instead, *partial safety factors* refer just to each material property (i.e. concrete compressive strength, reinforcement yielding strength) evaluated with its characteristic value for local verification of structural members.

However, as the term “*partial safety factor*” descend from Level I methods where safety is applied partially to actions and to material resistances, very often global safety factors are denoted also as “*partial safety factors for global response*”. In the present dissertation, the term *global safety factor* is adopted, however, the term *partial safety factor* can be associated also to *global safety factors* within GRF without running into any terminological mistake.

Chapter 2

Non-linear finite elements analysis of reinforced concrete structures

2.1 Introduction

In common practice, *assessment* and *design* of reinforced concrete structures can be performed efficiently by means linear elastic analysis. In fact, for structures as beams, plates, shells and walls the linear finite element analysis (i.e. LFEA) is sufficient in order to get results able to estimate demands (e.g. internal actions, elastic distribution of stresses) and to determine the reinforcement arrangements. To perform *assessment* and *design* adopting linear analysis, in general, provides safe solutions within the *limit states* approach.

However, for some cases, the use of linear analysis may not be sufficient in order to fulfil the safety requirements and deeper investigations may be required, in particular, for economic reasons.

In the last decades, non-linear finite element analyses (NLFEAs) have increasingly become the most common and practical tool able to simulate the actual mechanical behavior of structural systems, such as reinforced concrete members, in any loading condition (i.e., serviceability limit state (SLS) and ultimate limit state (ULS)). In this context, several guidelines for NLFEAs, as *fib Bulletin 45*, have been defined in order to provide efficient methodologies devoted to calibrate NLFE models. However, the results from such complex calculations needs to be properly processed in order to satisfy the reliability targets as discussed in Chapter 1.

In the present Chapter, after a short discussion about usefulness of NLFEA for *assessment* and *design* purposes, the basic principles about the non-linear finite elements (i.e. NLFE) method and the modelling of non-linear behaviour of materials are outlined. Finally, the methodologies able to introduce reliability concepts within safety verifications by using NLFEA are described (i.e. *safety formats* for NLFEA).

2.1.1 Practical applications of NLFEAs

The NLFE method turns out to be an efficient tool when is necessary to perform *assessment/design* of reinforced concrete structures having complex geometry, poorly detailed or locally damaged structural members (e.g. localized cracking or local damaging due to impacts).

In the following, the most common cases where NLFEA may be very efficient are listed and shortly commented:

- a) *Estimation of the reliability of reinforced concrete members having complex geometry or detailing*: in case of particularly complex geometries and reinforcement arrangements (e.g. beams with openings), the structural codes may not provide sufficient information in order to estimate efficiently the structural resistance. In general, the “*struts and ties*” method is the most common approach adopted for complex problems, however, it leads to different solutions that may be more or less efficient as they are just based on equilibrium verification. In the mentioned above cases, the NLFEA can be very useful in order to get to solution that satisfies both equilibrium and kinematic compatibility. Moreover, the NLFE models may be adopted in order to simulate and to predict the progressive cracking development by increasing the load level up to failure of the reinforced concrete member.
- b) *Assessment of the reliability of existing structures*: the choice to upgrade (or not) an existing reinforced concrete structure is a crucial decision within the *assessment* process. In *existing* structures are often built base on old design standards and reinforcements arrangements not consistent with current specifications. In cases where costs for upgrading of the structure are very significant, the NLFEA may be useful in order to estimate the actual safety margin against the failure and, possibly, to avoid expensive interventions.
- c) *Seismic assessment by means push-over analysis*: many design codes allows to perform the seismic assessment by means push-over analysis and, it means that NLFE models can be adopted in order to estimate the structural capacity.
- d) *Analysis of the “D-regions”*: the regions affected by localized stress and deformation fields (as zones affected by prestressing introduction devices) may be efficiently simulated by means NLFEA.
- e) *Explanation of observed crack patterns and local damaging*: in particular cases, the observed crack patterns and/or local damaging of reinforced concrete members may be due unknown causes (e.g. forensic engineering). Then, the possible causes can be identified by means back analysis starting from in-situ observations.

- f) *Estimation of second order effects*: the use of NLFEA allows to take into account geometrical non-linearity in presence of progressive cracking (i.e. decreasing of stiffness) and can be an efficient tool for assessment of very slender concrete members.
- g) *Evaluation of safety in presence of accidental loading situations and for robustness assessment*: the evaluation of safety in case accidental loading situations as explosions, terroristic attacks and extreme earthquakes can benefit by the use of NLFEA. In particular, the evaluation of structural *robustness* by means removal of one of more structural elements can be performed also accounting for the dynamic effects.
- h) *Evaluation of fire resistance*: the effects on complex structures of exposure to high temperature may be investigated by means NLFEA accounting for mechanical non-linearities, progressive damaging and thermal expansion.

The mentioned above applications are just a few of the possible ones. However, the use of such NLFE models for *design* and *assessment* should be always performed by engineers and designers confident with the approach and after an accurate *calibration* and *validation* procedure. In fact, the user can be misled from the apparent precise results obtained by the NLFEA simulations.

Firstly, the *calibration* of a structural model should be performed analysing the sensitivity of results in case the analysis parameter and mesh size are modified.

Secondly, the results of the NLFE simulation should be *validated* on the base of physical assumptions and observations (as for example from similar benchmark tests) in order to be sure that structural model is able to reflect the actual structural behaviour. Finally, *reliability* concepts should be properly addressed in order to get results suitable for design or assessment purposes.

Next, a short description of common *modelling hypothesis* adopted for NLFEA is proposed.

2.2 Modelling hypotheses for NLFEA

In the present Section, the most common and herein adopted hypotheses adopted for NLFE modelling are reported. The term *modelling hypothesis* concerns all the choices performed related to:

- the definition of *constitutive laws* for basic materials;
- the fulfillment of *equilibrium* and *kinematic compatibility* requirements, including solution methods and choice of the type of finite element, respectively.

Subsequently, basic notes about solution methods and modelling of non-linear material properties are reported.

2.2.1 Solution methods

The general structural problem can be solved by means the following system of equilibrium equations:

$$\lambda p - f(q) = 0 \quad (2.1a)$$

$$K(q)q - f(q) = 0 \quad (2.1b)$$

where:

- q is the vector of nodal displacements;
- p is the vector of external loads;
- λ is the multiplier of the vector of external loads;
- $K(q)$ is the stiffness matrix of the system, in general as a function of the vector q ;
- $f(q)$ is the vector of internal forces as a function of the nodal displacements.

The Eq.(2.1a-b) describes the equilibrium of the discretized structure. The solution of the linear system:

$$K q - f = 0 \quad (2.2)$$

can be directly estimated, whereas, the non-linear system of equations expressed by Eq.(2.2b) is possible to be solved only by numerical calculation.

In the following, two common methods adopted by common NLFE software in order to solve Eq.(2.1b) are described: the Newton-Raphson and the Modified Newton Raphson methods. However, other methods are proposed by literature as, for example, the arch-length method (*Riks, 1972 and 1979*).

Finally, a short discussion about the convergence criteria is proposed.

Newton-Raphson method

The Newton-Raphson method is an iterative approach able to solve non-linear systems of equations by means progressive linear approximations. It is one of the most used techniques by NLFE software.

Defining the set $(q_0, \lambda p)$ as the current trial displacement condition and the loads vector, respectively, the solution may be iteratively calculated by adding the change in displacements δq_i to the current displacement state evaluated as:

$$\delta q_i = (K_T^i)^{-1} r(q_i) \quad (2.3)$$

where K_T^i is the tangent stiffness matrix determined for the current state and $r(q_i)$ is the vector of out of balance forces. The explanation of the Newton-Raphson method is depicted in Figure 2.1.

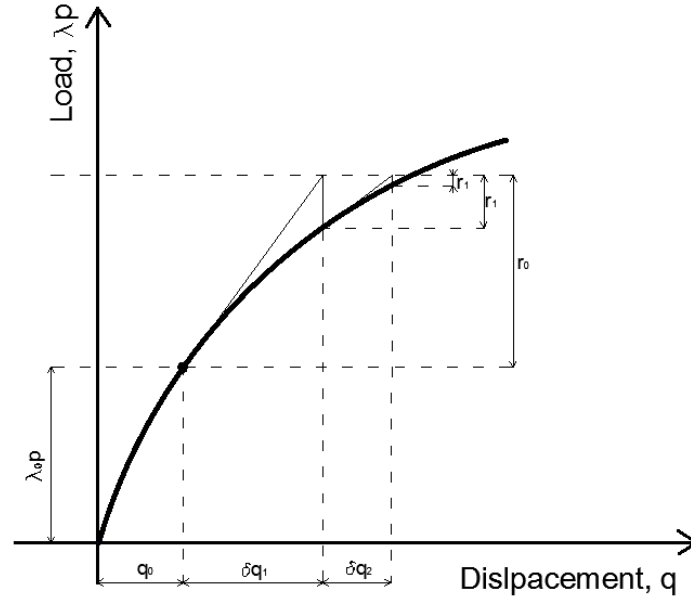


Figure 2.1: Scheme representing the Newton-Raphson method.

In this method, within every iteration step the current stiffness matrix is defined and the linearized equations are solved considering the increment δq_i . For this reason, the method results to be very efficient, even though may require more computational time.

Modified Newton-Raphson method

As previously described, the Newton-Raphson method requires to re-calculate the tangent stiffness matrix for each iteration and may be more time consuming.

In order to overcome to this problem, the approximation to maintain the tangent stiffness matrix constant between the iterations may be performed assuming: $K_T^i = K_T^0$.

Then, the Eq.(2.3) becomes:

$$\delta q_i = (K_T^0)^{-1} r(q_i) \quad (2.4)$$

In this way, the solution for each iteration may be very fast, however, more iterations are needed in order to meet the convergence criteria.

The schematization of the Modified Newton-Raphson method is reported in Figure 2.2.

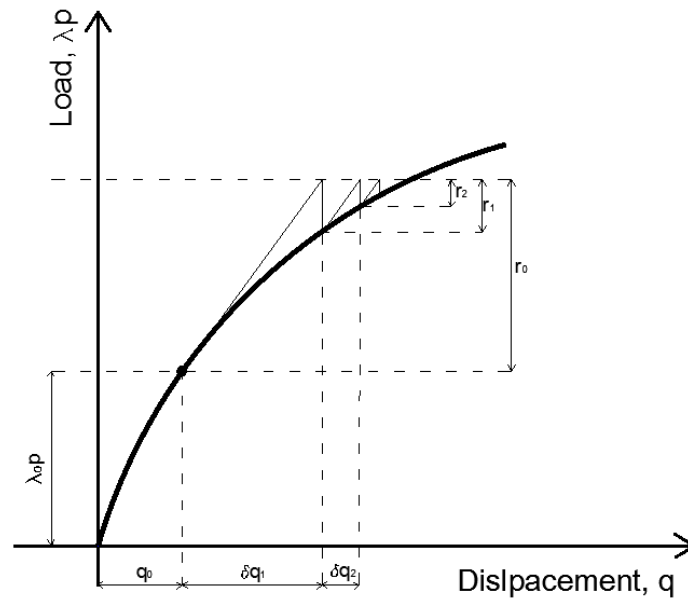


Figure 2.2

Figure 2.2: Scheme representing the Modified Newton-Raphson method.

The choice between Newton-Raphson and Modified Newton-Raphson methods depends from the size and from the complexity of structural problem. If the problem is computationally demanding, the Newton-Raphson method is preferable even if may requires more time.

Convergence criteria

The solution of a structural problem by means of NLFEA leads to solutions which are necessarily an approximation of the exact one. Precisely, the exact solution is the one that corresponds to an out of balance force equal to zero: $r(q_i)=0$.

Then, the solutions obtained by NLFEA are always in presence of a certain amount of out of balance force. For this reason, is necessary to define criteria (i.e. convergence criteria) able to discern if the iterative solution process has reached the required level of accuracy.

In general, the monitored quantities in order to check the progressive convergence of the solution procedure are the differences between two consecutive iterations of: the out of balance force, the displacements and the strain energy.

The generic i^{th} load step may be considered as concluded when:

$$|\psi^i| < \varepsilon \cdot \max |\psi^j| \quad \text{with } j = 1, 2, \dots, i \quad (2.5)$$

where for displacement-based convergence criteria:

$$|\psi^i| = \sqrt{\partial q_i^T \cdot \partial q_i} \quad (2.6)$$

and for force-based convergence criteria:

$$|\psi^i| = \sqrt{r(q_i)^T \cdot r(q_i)} \quad (2.7)$$

Concerning reinforced concrete structures, the displacement-based convergence criteria is commonly adopted.

2.2.2 Non-linear modelling of concrete

In the present Subsection, the hypotheses for non-linear modelling of concrete adopted in the present dissertation are outlined in their fundamentals. Specifically, the most common modelling hypotheses for plane stress models are reported. Deeper information may be acknowledged by literature and original references.

Finite element formulation

The simpler and most common finite element formulation for plane stress NLFEA of reinforced concrete structures is the *quadrilateral iso-parametric plane stress elements*. It is adopted to represent the concrete bodies with constant or variable thickness. This element is implemented by all the main software of common use for NLFEA or reinforced concrete structures.

The nodal displacements are interpolated by means linear model as shown in Eq.(2.8) and 2x2 Gauss integration scheme is used.

$$u(r, s) = a_0 + a_1 \cdot r + a_2 \cdot s + a_3 \cdot r \cdot s \quad (2.8)$$

The schematization of the mentioned above finite element is reported in Figure 2.3.

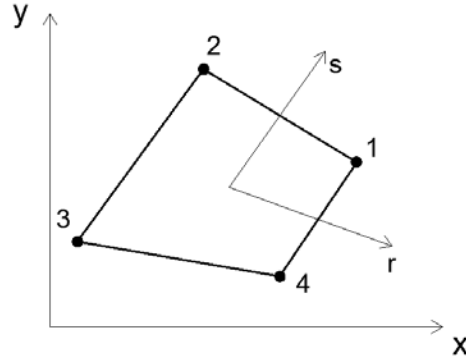


Figure 2.3: Quadrilateral iso-parametric finite element (plane stress).

The mesh refinement should be calibrated case by case limiting the dependence of results from the mesh size.

Behaviour of concrete in compression

In the following, three common models for mono-axial compressive constitutive behavior of concrete are described:

- the *EN1992-1-1* constitutive model;
 - the *fib Model Code 1990* constitutive model;
 - the *Thorenfeldt et al, 1987* constitutive model
- *EN1992-1-1 constitutive model*

The non-linear constitutive law of concrete in compression defined by *EN1992-1-1* is written in Eq.(2.9) and represented in Figure 2.4.

$$\frac{\sigma}{f_c} = \frac{\left(\frac{E_c}{E_s}\right) \cdot \left(\frac{\varepsilon}{\varepsilon_c}\right)}{1 + A\left(\frac{\varepsilon}{\varepsilon_c}\right) + B\left(\frac{\varepsilon}{\varepsilon_c}\right)^2 + C\left(\frac{\varepsilon}{\varepsilon_c}\right)^3} \quad (2.9)$$

$$A = \frac{\left[\frac{E_c}{E_u} + (p^3 - 2p^2)\frac{E_c}{E_s} - (2p^3 + 3p^2 + 1)\right]}{\left[(p^2 - 2p + 1)p\right]} \quad (2.10)$$

$$B = \left[\left(2\frac{E_c}{E_s} - 3\right) - 2A\right]; \quad C = \left[\left(2 - \frac{E_c}{E_s}\right) + A\right] \quad (2.11)$$

$$E_s = \frac{f_c}{\varepsilon_c}; \quad E_u = \frac{f_u}{\varepsilon_u}; \quad p = \frac{\varepsilon_u}{\varepsilon_c} \quad (2.12)$$

where E_0 is the zero-stress tangent Young Modulus; E_s secant Young modulus of concrete corresponding to peak strength; E_u is the secant Young modulus of concrete corresponding to ultimate strength; ε is the concrete strain; ε_u is the ultimate concrete strain; σ is the stress within concrete; f_c is the peak concrete strength; f_u is the ultimate concrete strength; p is the ration between ultimate and peak strain.

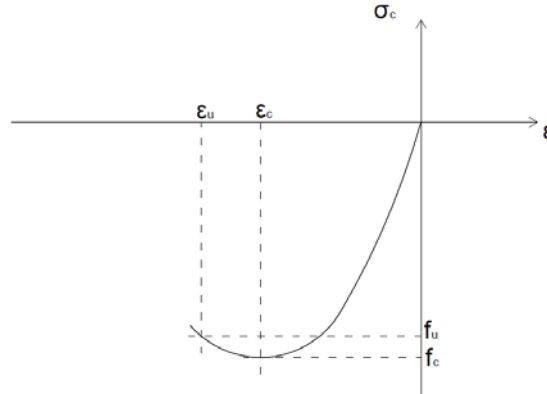


Figure 2.4: Mono-axial constitutive model for concrete in compression by *EN1992-1-1*.

- *fib Model Code 1990 constitutive model*

The constitutive law of concrete in compression defined by fib Model Code 1990, is described by Eq.(2.13) and represented by Figure 2.5.

$$\frac{\sigma}{f_c} = \frac{kx - x^2}{1 + (k-2)x} \quad (2.13)$$

$$x = \frac{\varepsilon}{\varepsilon_c}; \quad k = \frac{E_0}{E_c} \quad (2.14)$$

where σ is the stress within concrete; f_c is the peak concrete strength; x non-dimensional strain; ε is the concrete strain; ε_c is the peak concrete strain; k is the shape parameter; E_0 is the zero-stress tangent Young Modulus; E_c is the secant Young modulus of concrete corresponding to peak strength.

After the peak strength, the constitutive law linearly decreases and can be described by a model based on the energy dissipated or through a model based on the ultimate strain ε_u .

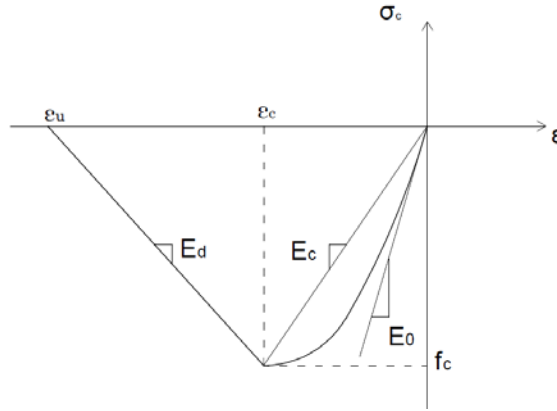


Figure 2.5: Mono-axial constitutive model for concrete in compression by *fib Model Code 1990*.

- *Thorenfeldt et al., 1987 constitutive model*

The constitutive law of concrete in compression defined by *Thorenfeldt et al., 1987*, is described by Eq.(2.15).

$$\frac{\sigma}{f_c} = \frac{\varepsilon}{\varepsilon_c} \left(\frac{n}{n - \left(1 - \left(\frac{\varepsilon}{\varepsilon_c} \right)^{nk} \right)} \right) \quad (2.15)$$

$$n = 0.8 + \frac{R_c}{17}; \quad k = \begin{cases} 1 & \text{if } 0 > \varepsilon > \varepsilon_c \\ 0.67 + \frac{R_c}{62} & \text{if } \varepsilon \leq \varepsilon_c \end{cases} \quad (2.16)$$

where σ is the stress within concrete; f_c is the peak concrete strength; ε is the concrete strain; ε_c is the peak concrete strain; R_c is the mono-axial cubic compressive strength; n and k model parameters.

The input parameters for constitutive models may be derived according to fib Model Code 2010, EN1992-1-1 suggestions or from experimental results when available.

Behaviour of concrete in tension

The tensile behaviour of concrete can be modelled by means elastic-softening laws accounting for fracture energy G_f and influence of “*tension stiffening effect*” due to interaction of cracked concrete and reinforcement.

Typically, a linear tension softening (i.e. LTS) law can be adopted to simulate concrete tensile behaviour. The value of maximum strain ε_{max} can be defined according to experimental results, from literature results or as a percentage of the elastic peak strain ε_{ct} (e.g. 10-15% concerning normal strength concrete). The linear

tension softening law for tensile concrete behaviour modelling is reported in Figure 2.6.

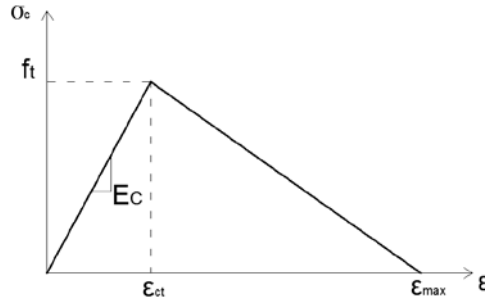


Figure 2.6: Linear tension softening model for concrete tensile behavior.

Biaxial failure domain

The biaxial failure domain can be modelled by means of the *Kupfer and Gerstle, 1973* domain. The equations that define the domain in the regions compression-compression, tension-compression and tension-tension are reported subsequently.

$$f'_{c,eff} = \frac{1+3.65a}{(1+a)^2} f_c; \quad a = \frac{\sigma_{c1}}{\sigma_{c2}} \quad (2.17)$$

$$f'_{c,eff} = f_c \cdot r_{ec}; \quad r_{ec} = \left(1 + 5.3278 \frac{\sigma_{c1}}{f_c} \right) \quad (2.19)$$

$$f'_{c,eff} = f_t \cdot r_{et}; \quad r_{et} = \left(1 - 0.95 \frac{\sigma_{c2}}{f_c} \right) \quad (2.21)$$

Where f_c^{ef} is the compressive strength under biaxial state of stress; σ_{c1} and σ_{c2} are the principal stresses; f_c is the mono-axial cylinder compressive strength; r_{ec} is the reduction factor for compressive strength variable within the interval 0.9-1.0; r_{et} reduction factor for tensile strength variable within the interval 0.9-1.0.

The representation of the bi-axial failure domain is reported in Figure 2.6.

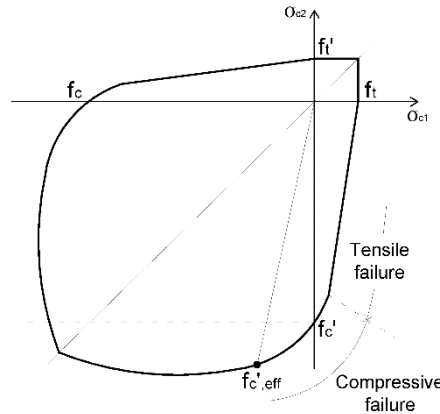


Figure 2.7: Bi-axial failure domain proposed by *Kupfer and Gerstle, 1973*.

Smeared cracking models

In plane stress modelling of reinforced concrete, the following two methods based on smeared crack modelling (*De Borst and P. Nauta, 1985; Riggs and Powell, 1986*) are widely adopted:

- *fixed crack direction model* (*Cervenka, 1985, Darwin, 1974*);
- *rotated crack direction model* (*Vecchio, 1986, Crisfield, 1989*).

In the smeared *fixed crack direction model* the crack direction is defined at first cracking and does not change during the following load steps. Shear stresses can be present on the crack surface by means of reduction of shear stiffness after cracking denoted as *shear retention factor* β (often set equal to 0.2). The directions of principal stresses and principal strains coincide in uncracked field. After cracking the material becomes orthotropic with a strong axis m_2 parallel to the cracks and a weak axis m_1 orthogonal to them. In such condition the directions of principal strains ε_1 and ε_2 do not coincide any more with the orthotropy axis m_1 and m_2 because of shear friction present on cracks as shown in Figure 2.8(a).

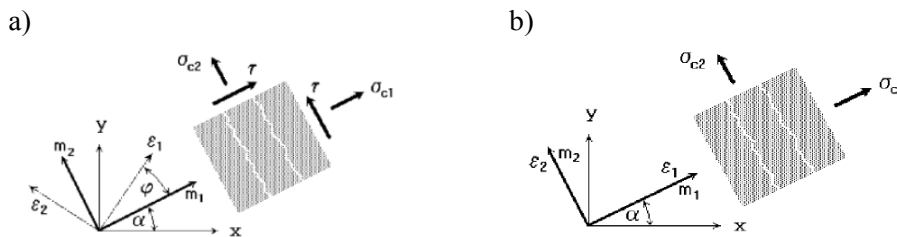


Figure 2.8: Fixed smeared crack model (a) and rotated smeared crack model (b).

In the smeared *rotated crack direction model* the direction of the principal stress coincides with the direction of the principal strain. No shear strain occurs on the crack plane and only two normal stress components must be defined, as shown in Figure 2.8 (b). If the principal strain axes rotate during the loading the direction of the cracks rotate, too. Then, the normal direction to the crack is always assumed to be aligned to the principal strain ε_1 .

2.2.3 Non-linear modelling of reinforcements

The non-linear influence of reinforcement within concrete matrix may be accounted for with two methodologies:

- by *discrete reinforcement model*, where appropriate trusses elements are connected to mesh nodes and rigid conditions are created between trusses nodes and plane stress concrete element;

- by *smearred reinforcement model*, where the stiffness of the bars is smeared homogeneously on a chosen set of plane stress elements and incorporated within stiffness matrix.

The constitutive law can be defined according to elastic with post-yielding hardening law according to material characteristics as shown in Figure 2.9.

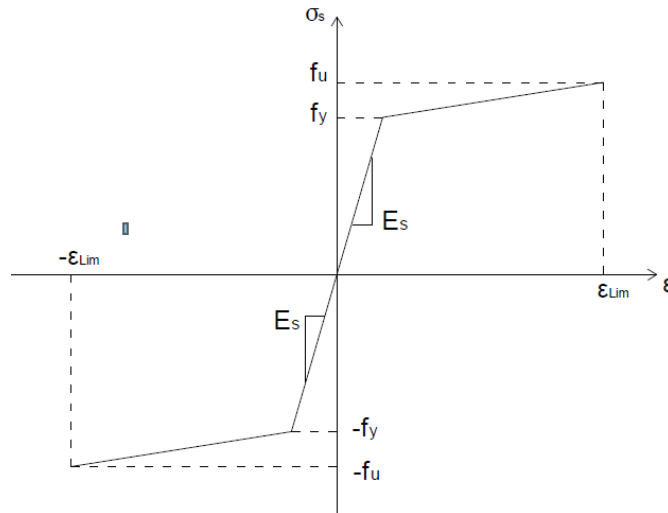


Figure 2.9: Constitutive model for reinforcement.

However, advanced non-linear model can be also adopted to model non-linear behavior of reinforcements, also accounting for hysteretic energy dissipation.

2.3 Safety formats for non-linear analysis of reinforced concrete structures

As discussed in Section 1.4.4 the safety verifications by means of non-linear finite element analysis can be performed according to the *Global Resistance Format* (GRF). In fact, the GRF result to be an efficient tool in order to evaluate structural reliability by using non-linear models, as the case of NLFEA.

In scientific literature and codes, different *safety formats* based on GRF has been proposed. In the present dissertation, the following *safety formats* are considered:

1. Partial Factor Method (PFM) (*fib Model Code 2010*);
2. Global Resistance Methods (GRMs)
 - Method of estimating the coefficient of variation of the structural resistance (ECOV) (*fib Model Code 2010*);
 - Global Resistance Factor (GRF) (*fib Model Code 2010*);
 - Global Safety Format (GSF) (*Allaix et. Al, 2013*);
3. Probabilistic Method (PM) (*fib Model Code 2010*).

In the following, a short description of each one of the abovementioned safety formats is reported.

2.3.1 Partial Factor Method (PFM)

With reference to the *partial factor method* (PFM) proposed by *fib Model Code 2010*, the design resistance R_d is obtained by means of a single NLFEA, which is performed using the design values (evaluated according to the *partial factor format* proposed by *fib Model Code 2010*, *EN 1990* and *fib Bulletin 80*) of the material resistances f_d :

$$R_d = \frac{R_{NLFEA}(f_d)}{\gamma_{Rd}} \quad (2.22)$$

where $R_{NLFEA}(f_d)$ represents the global load bearing capacity of the structure (i.e., the global structural resistance) estimated by means of a non-linear analysis; γ_{Rd} is the NLFE resistance model uncertainty safety factor.

2.3.2 Global Resistance Methods (GRMs)

The *Global Resistance Methods* (GRMs) - *fib Model Code 2010* - are safety formats based on the evaluation of the design global resistance by means global resistance safety factors according to the Global Resistance Format (GRF).

Global resistance factor method (GRF)

As for the *global resistance factor* (GRF) method, according to *fib Model Code 2010* and *EN1992-2*, the global resistance is defined as follows:

$$R_d = \frac{R_{NLFEA}(f_{cmd}, f_{ym})}{\gamma_{GL}} \quad (2.23)$$

adopting a value of the global safety factor γ_{GL} set equal to 1.27 and equal to the global resistance factor γ_R assuming an unitary value for γ_{Rd} . To estimate the representative value of the global resistance, the mean value of the yield stress f_{ym} has to be considered for the reinforcing steel:

$$f_{ym} = 1.1 f_{yk} \quad (2.24)$$

where f_{yk} is the characteristic yield stress. In addition, a reduced value f_{cmd} for the concrete compressive strength has to be used to equalize the partial factor for both steel and concrete failure, as follows:

$$f_{cmd} = 0.85 f_{ck} \quad (2.25)$$

where f_{ck} denotes the characteristic value of the concrete compressive strength.

Estimation of coefficient of variation method (ECOV)

Concerning the *estimation of the coefficient of variation* (ECOV) method, as suggested by *fib Model Code 2010*, the design global resistance is obtained as:

$$R_d = \frac{R_{NLFEA}(f_m)}{\gamma_R \cdot \gamma_{Rd}} \quad (2.26)$$

where R_d is the design value of the structural resistance; $R_{NLFEA}(f_m)$ denotes the structural resistance predicted by a NLFEA performed introducing the mean values of the material properties in the structural model; γ_R is the global resistance safety factor accounting for the uncertainties related to the material properties; γ_{Rd} is the NLFE resistance model uncertainty safety factor.

Assuming a lognormal distribution for the global load bearing capacity of the structure, the global resistance factor γ_R can be written as:

$$\gamma_R = \exp(\alpha_R \cdot \beta \cdot V_R) \quad (2.27)$$

where V_R is the coefficient of variation of the distribution of the global structural resistance. In the ECOV method, the value of V_R can be estimated, with a simplified approach, using a lognormal distribution for represent the variability of global structural resistance:

$$V_R = \frac{1}{1.65} \ln \left(\frac{R_{NLFEA}(f_m)}{R_{NLFEA}(f_k)} \right) \quad (2.28)$$

where $R_{NLFEA}(f_k)$ is the structural resistance predicted by a NLFEA performed using the characteristic values of the material properties to define the structural model.

2.3.4 Global safety format (GSF)

The global safety format (GSF) according to *Allaix et al, 2013* allows to define the design global resistance as:

$$R_d = \frac{R_{NLFEA}(f_m)}{\gamma_R \cdot \gamma_{Rd}} \quad (2.29)$$

where R_d is the design value of the structural resistance; R_m denotes the structural resistance predicted by a NLFEA performed introducing the mean values of the material properties in the structural model; γ_R is the global resistance safety factor accounting for the uncertainties related to the material properties; γ_{Rd} is the NLFE resistance model uncertainty safety factor.

The GSF differs from the ECOV method in assessing the coefficient of variation of the global structural resistance $V_R = \sigma_R / \mu_R$ in the hypothesis of lognormal distribution (with σ_R and μ_R the standard deviation and the mean value of the structural resistance, respectively). Specifically, statistical parameters are estimated by means of a reduced Monte Carlo simulation adopting the Latin Hypercube Sampling method with a reduced number of samples.

The probabilistic model for the random randomness of material properties can be assumed according to *JCSS Probabilistic Model Code* or in simplified manner according to Section 1.2. Finally, the γ_R can be calculated according to Eq.(2.27).

2.3.5 Probabilistic method (PM)

Finally, with reference to the *probabilistic method* (PM) according to *fib Model Code 2010*, the approach consists of running several NLFEMs adopting a sampling technique such as Monte Carlo or Latin Hypercube to define the input data. The numerical results are fitted by an appropriate probabilistic model (that may differ from the lognormal one) estimating the statistical parameters (i.e., mean and dispersion). In addition, from the probabilistic distribution it is possible to directly assess the quantile associated to the design value of the global structural resistance corresponding to a specific reliability index β

$$R_d = \frac{F_R^{-1}[\Phi(\alpha_R \beta)]}{\gamma_{Rd}} \quad (2.30)$$

The PM is different from GSF method because this latter, assuming a lognormal probabilistic model, is based on mean values of material properties performing a first order approximation of the Taylor expansion function of the ultimate global resistance (*Allaix at al., 2013*), whereas, the PM directly refers to a quartile of the appropriate probabilistic distribution (Eq.(2.30)).

Assuming a lognormal model for global structural resistance also for the PM, the design global resistance can be expressed as:

$$R_d = \frac{\mu_R}{\gamma_R \cdot \gamma_{Rd}} \quad (2.31)$$

where μ_R is the mean value of the global structural resistance and γ_R can be calculated according to Eq.(2.27) once defined the coefficient of variation $V_R = \sigma_R / \mu_R$.

The *safety formats* herein introduced with their basic formulation will be compared and discussed in Chapter 4.

Chapter 3

Probabilistic calibration of empirical and semi-empirical resistance models

3.1 Introduction

The resistance models based on physical laws, semi-empirical and empirical formulations are widely employed in structural engineering in order to design/assess new/existing structures.

According to the semi-probabilistic design approach (*EN 1990*), the target safety requirements are fulfilled by means of partial safety factors accounting for material properties, geometrical and model uncertainties. Concerning the resistance models based on physical assumptions (e.g., equilibrium of forces and kinematic compatibility), the direct application of partial factors to materials strength leads to design expressions almost consistent with the prescribed levels of reliability. On the contrary, considering empirical or semi-empirical resistance models (e.g. *Muttoni and Ruiz 2018, Bertagnoli and Mancini 2009*), the direct application of partial safety factors within the formulation does not lead to the same conclusion.

In fact, empirical and semi-empirical resistance models are calibrated basing on the experimental evidences and by means of empirical coefficients involved within the formulation. Such kind of coefficients are calibrated in order to achieve the best agreement between the model predictions and the experimental outcomes. Furthermore, empirical coefficients are calibrated basing on the realization of material properties which are observed during the experiments and that can be likely assumed as be the expected ones (i.e. mean values). Then, empirical coefficients have significance only when mean values of material properties are considered within the formulation. Furthermore, this kind of resistance models are often non-linear in function of the main involved variables. It implies that the direct application of partial safety factors to materials properties, without a straightforward probabilistic calibration of the resistance model accounting for both aleatory and epistemic uncertainties, does not allow to meet the required safety levels. A general methodology devoted to calibrate empirical or semi-empirical formulations in relation to a specific level of reliability is still not available and needs for a clear definition.

In the present Chapter, a framework based on the Monte Carlo method for calibration of empirical and semi-empirical resistance models is proposed. The

procedure is able to account for both stochastic variability of material and geometrical properties (i.e., *aleatory* uncertainties) and the influence of the resistance model uncertainties (i.e., *epistemic* uncertainties). After the detailed description of the methodology, its application to the calibration of the semi-empirical model for laps and anchorages tensile strength evaluation suggested by *Model Code 2010, 2012* and *fib Bulletin 72, 2015* is described. First of all, statistical calibration of model uncertainties is performed on an extensive experimental database (*fib TG 4.5 bond tests database, 2005*) differentiating between new and existing structures. Secondly, the reliability-based expressions are derived and discussed in terms of implication in the design and the assessment of new and existing structures. Finally, the results of the general framework are compared to the ones obtained by means of the analytical procedure proposed by *Taerwe, 1993*.

3.2 Proposed general framework

In the present Section the general framework for the probabilistic calibration of empirical and semi-empirical resistance models is defined and described. The proposed framework, which is based on the Monte Carlo's method, consist of four main steps:

- 1) the characterization of the *empirical or semi-empirical resistance model*;
- 2) the selection of the *probabilistic model* for the relevant random variables;
- 3) the assessment of the *resistance* and the *auxiliary random variables*;
- 4) the definition of the quantiles of the auxiliary random variable and the evaluation of the final *reliability-based expressions*.

3.2.1 Characterization of the empirical or semi-empirical resistance model

As introduced in the previous Section, the resistance models herein considered for the probabilistic calibration are the ones derived from the experimental evidences: empirical or semi-empirical.

Specifically, empirical resistance models are completely derived in order to best fit the experimental results without relying on, even just simplistic, physical and mechanical assumptions. Differently, the semi-empirical resistance models are based on basic physical and mechanical hypotheses and are improved and calibrated in order to agree with the experimental evidences.

Therefore, concerning both empirical and semi-empirical resistance models, it is essential to collect a sufficiently extensive experimental database.

The experimental database should present tests with material properties and geometrical configurations that ranges as much as possible within the interval usually adopted in practice. In particular, this is in order to get to a final formulation with scope and applicability within the limits defined by the Codes.

Once the resistance model has been defined from the experimental results, the parameters involved within the formulation should be distinguished between:

- *relevant random variables*: parameters that may strongly affect the resistance mechanism with their aleatory variability (e.g. material properties);
- *deterministic parameters*: parameters that may be considered as constant values, for example, as their limited variability does not affect significantly the resistance mechanism (e.g. geometrical properties):

The experience related to practice and experimental observations joined to a preliminary sensitivity analysis can be useful to perform this kind of selection.

Finally, the estimated value of the resistance by means of an empirical or semi-empirical model R_{Model} can be generally expressed as:

$$R_{Model} = f(x_{i,exp}; a_j; C_l) \quad i = 1, 2, \dots, N; \quad j = 1, 2, \dots, M; \quad l = 1, 2, \dots, K \quad (3.1)$$

where the generic function f depends on: $x_{i,exp}$, vector containing an experimental realization of a set of N relevant random variables which plays a significant role in the resistance model; a_j is a vector containing all the other M parameters that can be assumed as deterministic in the resistance model; C_l is a vector containing the K best fitting empirical coefficient(s) calibrated on the experimental database.

3.2.2 Selection of the probabilistic model

Once the resistance model has been characterised, the probabilistic model for the main involved random variables should be defined.

The probabilistic calibration can be performed accounting for the distinction between aleatory and epistemic uncertainties.

Concerning to the *aleatory uncertainties*, they are represented by the relevant random variables identified according to Sub-section 3.2.1, and can be collected in the random vector X_i :

$$X_i = (X_1, X_2, \dots, X_i, \dots, X_N) \quad i = 1, 2, \dots, N \quad (3.2)$$

These random variables can be related to:

- *material properties*;
- *geometrical parameters*.

Details for the probabilistic modelling of the relevant random variables may be acknowledged from the scientific literature as, for example, from the *JCSS Probabilistic Model Code, 2001* (Section 1.3.1).

Relating to the *epistemic uncertainties* their inclusion in the probabilistic calibration can be performed by means of the assessment of the *model uncertainty random variable* ϑ . The *model uncertainty random variable* ϑ can be assessed, as described in Section 1.3.1 and according to *JCSS Probabilistic Model Code, 2001*, by means of statistical inferential analysis of the ratio between experimental results and resistance model predictions (Eq.(1.2)).

The source of experimental result for the assessment of the *model uncertainty random variable* ϑ can derive from the database by which the empirical or semi-empirical resistance model has been defined (i.e. in absence of additional experimental tests), from other studies collecting different experimental databanks or from both. At this stage, the range of variation of the involved parameters collected within the experimental database (i.e. material properties, geometrical configurations and test conditions) should be defined according to the limits of applicability expected for the final reliability-based formulation (i.e. required specifications and Code limitations). Concerning the case of biased resistance models with non-constant bias, the assessment of the *model uncertainty random variable* ϑ can be performed in sub-intervals of the required range of variation of parameters. These sub-intervals should be defined so that the value of the bias can be assumed, reasonably, as a constant value within them.

The results of probabilistic calibration are valid only for values of main parameters pertaining to the range of variation adopted for the assessment of the *model uncertainty random variable* ϑ .

The *statistical uncertainties* related to the finite size of sample of ϑ for assessment of model uncertainty can be reduced by enlarging the number of experimental tests collected within the experimental database and adopting efficient statistical inferential techniques (e.g. maximum likelihood estimators - MLE - and Bayesian inference). Moreover, if prior knowledge about the *model uncertainty random variable* ϑ related to the specific resistance model are available, Bayesian updating techniques can be also adopted (*Gelman, 2014*).

Table 3.1: Definition of the probabilistic model.

Type of uncertainty	Symbol	Variables	Probabilistic modelling
<i>Aleatory</i>	$X_i (i=1, \dots, N)$	Relevant random variables: materials and geometrical properties	<i>JCSS Probabilistic Model Code, 2006; fib Model Code 2010</i>
<i>Epistemic</i>	ϑ	Model uncertainty random variable	<i>JCSS Probabilistic Model Code, 2006; statistical inferential analysis; prior information</i>

The *experimental uncertainties* should be carefully evaluated collecting the experimental database, as for example excluding particularly uncertain test cases. For this reason, a deep knowledge of the original scientific references related to each test reported in the experimental database is essential.

In conclusion, both random variables X_i and ϑ have to be modelled by the appropriate probabilistic distribution (i.e., PDFs and/or CDFs). The summary of the hypotheses that have to be performed for probabilistic modelling is reported in Table 3.1.

3.2.3 Definition of the resistance and the auxiliary random variables

In order to perform the probabilistic calibration of an empirical or semi-empirical resistance model it is necessary to define two new random variables.

The first one can be denoted as *resistance random variable* R and can be evaluated as a function of the random vector X_i and model uncertainty ϑ .

According to the definition of model uncertainty random variable (JCSS Probabilistic Model Code, 2006) reported in Eq.(1.1), the generic outcome of the *resistance random variable* $R(X_i, \vartheta)$ can be expressed as the product of the *model uncertainty random variable* ϑ and the function f representing the resistance model expressed depending from the *relevant random variables* X_i , the *deterministic parameters* a_j and the *empirical coefficients* C_l :

$$R(X_i, \vartheta) = \vartheta \cdot f(X_i; a_j; C_l) \quad i = 1, 2, \dots, N; \quad j = 1, 2, \dots, M; \quad l = 1, 2, \dots, K \quad (3.4)$$

Eq.(3.4) is able to represent the random variability of the resistance accounting for aleatory and model uncertainties.

The second random variable that have to be defined depends from *resistance random variable* R and can be denoted as *auxiliary random variable* Z .

In order to define a general procedure the following ratio can be addressed:

$$Z(X_i, \vartheta; x_{i,rep}) = \frac{R(X_i, \vartheta)}{f(x_{i,rep}; a_j; C_l)} \quad i = 1, 2, \dots, N; \quad j = 1, 2, \dots, M; \quad l = 1, 2, \dots, K \quad (3.5)$$

where $Z(X_i, \vartheta; x_{i,rep})$ is the *auxiliary random variable* and $x_{i,rep}$ is a vector containing the representative values selected to represent the random variables X_i in the final design formulation (e.g., design or 5% characteristic or mean value). Commonly, the resisting models proposed by the structural Codes are based on the characteristic values of the involved variables. Then, the definition of the *auxiliary random variable* Z allows, at the end of the probabilistic calibration, to define reliability-based equations expressed as a function of the selected representative value for the main involved variables according to Structural Codes (Table 3.2).

Table 3.2: Some possible choices of the representative values of relevant random variables within the final reliability-based equation.

Auxiliary random variable	Representative values of relevant random variables		
	$x_{i,rep}$		
$Z(X_i, \mathcal{G}; x_{i,rep})$	$x_{i,m}$ mean values	$x_{i,k}$ characteristic values	$x_{i,d}$ design values

The probabilistic characterisation of the *auxiliary random variable* $Z(X_i, \mathcal{G}; x_{i,rep})$ can be performed by means of the Monte Carlo sampling method from the probabilistic distributions of the random variables involved by Eq.(3.5). Also reduced Monte Carlo's techniques may be adopted as, for example, the Latin Hypercube Sampling (see Chapter 1). Once a significant number of samples of the population of the random variable $Z(X_i, \mathcal{G}; x_{i,rep})$ is available, the most appropriate probabilistic distribution able to describe Z can be identified by means of statistical inferential technique.

3.2.4 Definition of the reliability-based expressions

The evaluation of the expressions devoted to design and assessment purposes (i.e. complying with a specific reliability level) can be performed defining quintiles of the *auxiliary random variable* Z . Therefore, the following probabilities can be defined:

$$P[Z(X_i, \mathcal{G}; x_{i,rep}) \leq \zeta_p(x_{i,rep})] = p \quad i = 1, 2, \dots, N \quad (3.6)$$

where $\zeta_p(x_{i,rep})$ represents the quantile related to a specific probability to not be exceeded of the *auxiliary random variable* $Z(X_i, \mathcal{G}; x_{i,rep})$ accounting for the hypothesis for representative values within the final expression $x_{i,rep}$; p represents the probability of under-exceedance related to the quantile $\zeta_p(x_{i,rep})$.

In engineering practice and according to international codes (*ISO 2394, 2015; fib Model Code 2010; EN 1990; EN 1992*) the following quantiles of $Z(X_i, \mathcal{G}; x_{i,rep})$ can be estimated:

- 50% fractile $\zeta_m(x_{i,rep})$, setting $p = 0.5$;
- 5% characteristic value $\zeta_k(x_{i,rep})$, setting $p = 0.05$;
- design value $\zeta_d(x_{i,rep})$, setting $p = \Phi(-\alpha_R \beta)$.

with β denoting the reliability index, α_R the first order reliability method (FORM) sensitivity factor (assumed equal to 0.8 for dominant resistance variables) and $\Phi(\cdot)$ the cumulative standard normal distribution.

Estimated the *probabilistic coefficient* $\zeta_p(x_{i,rep})$, the general formulation for the selected quantile of the resistance random variable R_p can be expressed as follows:

$$R_p = \zeta_p(x_{i,rep}) \cdot f(x_{i,rep}; a_j; C_l) \quad i = 1, 2, \dots, N; \quad j = 1, 2, \dots, M; \quad l = 1, 2, \dots, K \quad (3.7)$$

In Table 3.3 and 3.4 are reported the possible alternative solutions for the *probabilistic coefficients* $\zeta_p(x_{i,rep})$ and for the expressions representing the quantile of the *resistance random variable* R having probability of under-exceedance equal to p .

Table 3.3: Values of the probabilistic coefficients.

Quantile of Z	Auxiliary random variable		
	$Z(X_i, \mathcal{G}; x_{i,m})$	$Z(X_i, \mathcal{G}; x_{i,k})$	$Z(X_i, \mathcal{G}; x_{i,d})$
	Probabilistic coefficients $\zeta_p(x_{i,rep})$		
$p=0.5$	$\zeta_m(x_{i,m})$	$\zeta_m(x_{i,k})$	$\zeta_m(x_{i,d})$
$p=0.05$	$\zeta_k(x_{i,m})$	$\zeta_k(x_{i,k})$	$\zeta_k(x_{i,d})$
$p=\Phi(-\alpha_R \cdot \beta)$	$\zeta_d(x_{i,m})$	$\zeta_d(x_{i,k})$	$\zeta_d(x_{i,d})$

Table 3.4: Reliability-based expressions according to probability of under-exceedance equal to p .

Quantile of R	Auxiliary random variable		
	$Z(X_i, \mathcal{G}; x_{i,m})$	$Z(X_i, \mathcal{G}; x_{i,k})$	$Z(X_i, \mathcal{G}; x_{i,d})$
	Reliability -based expressions $R_p = \zeta_p(x_{i,rep}) \cdot f(x_{i,rep}; a_j; C_l)$		
R_m $p=0.5$	$\zeta_m(x_{i,m}) \cdot f(x_{i,m}; a_j; C_l)$	$\zeta_m(x_{i,k}) \cdot f(x_{i,k}; a_j; C_l)$	$\zeta_m(x_{i,d}) \cdot f(x_{i,d}; a_j; C_l)$
R_k $p=0.05$	$\zeta_k(x_{i,m}) \cdot f(x_{i,m}; a_j; C_l)$	$\zeta_k(x_{i,k}) \cdot f(x_{i,k}; a_j; C_l)$	$\zeta_k(x_{i,d}) \cdot f(x_{i,d}; a_j; C_l)$
R_d $p=\Phi(-\alpha_R \cdot \beta)$	$\zeta_d(x_{i,m}) \cdot f(x_{i,m}; a_j; C_l)$	$\zeta_d(x_{i,k}) \cdot f(x_{i,k}; a_j; C_l)$	$\zeta_d(x_{i,d}) \cdot f(x_{i,d}; a_j; C_l)$

In conclusion, the summary of the four main steps for the probabilistic calibration of empirical and semi-empirical models is reported in Figure 3.1.

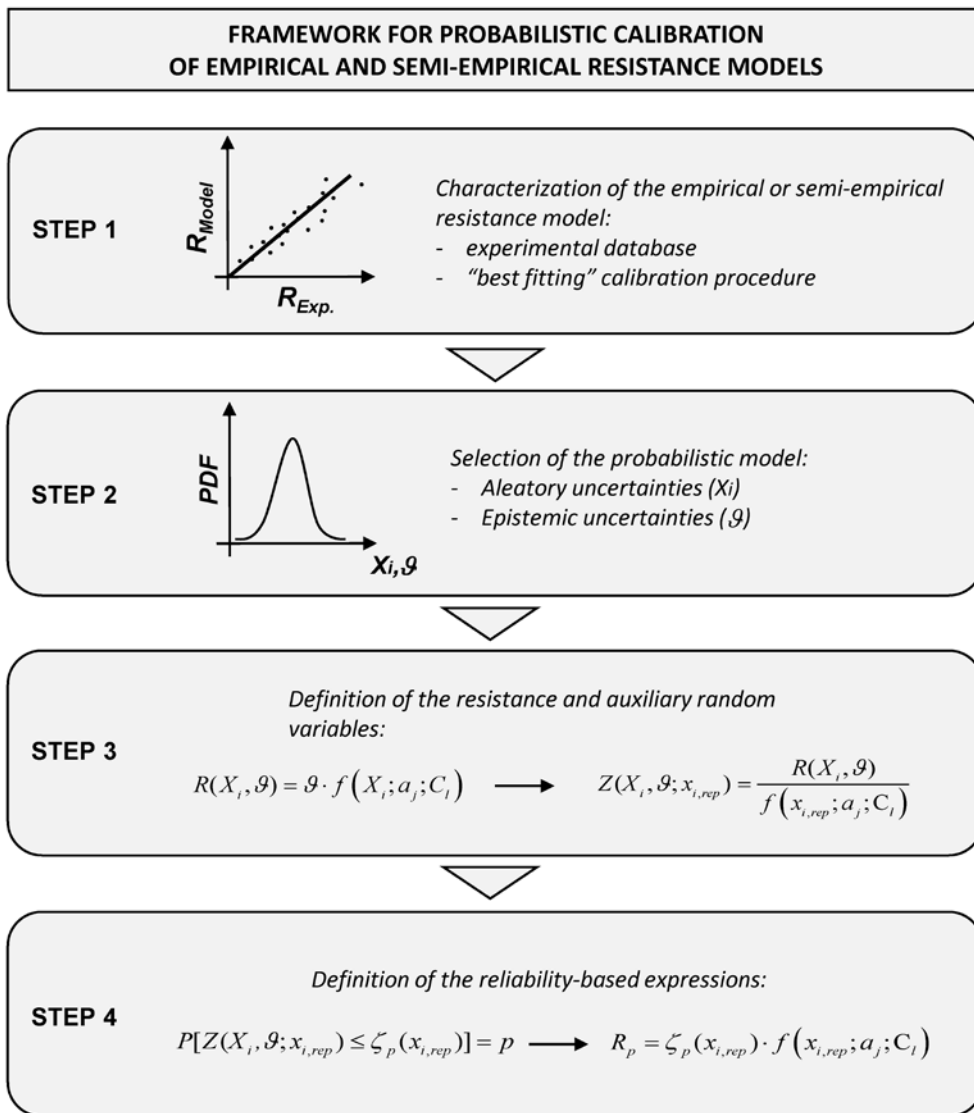


Figure 3.1: Summary of the framework for probabilistic calibration of empirical and semi-empirical models.

3.3 Probabilistic calibration of *fib* Model Code 2010 semi-empirical model for laps and anchorages strength evaluation

The present Section proposes the calibration of the semi-empirical model for ultimate tensile strength f_{st} (i.e. maximum tensile stress transferable inside reinforcing bar before lap or anchorage failure) for tensed lapped joints and anchorages reported by *fib Bulletin N°72* and *fib Model Code 2010*.

3.3.1 General aspects concerning bond of embedded reinforcements

The term “bond” is commonly used to denote the mechanism by which forces are transferred between bars reinforcement and concrete matrix within reinforced concrete members.

The bond stress between bars and concrete is conventionally described as the force within the reinforcement bar divided by the area of bar surface over the lap or anchorage length. This simple model is described by the equilibrium equation reported in Eq.(3.8).

$$A_s \cdot \sigma_s = f_b \cdot \pi \cdot \Phi \cdot l_b \quad \rightarrow \quad f_b = \frac{A_s \cdot \sigma_s}{\pi \cdot \Phi \cdot l_b} \quad \text{Average bond stress} \quad (3.8)$$

where A_s = longitudinal reinforcement area ; l_b lap or anchorage length (also denoted as bond length); σ_s = tensile stress into the re-bar; Φ = nominal bar diameter ; f_b = average bond stress exchanged between reinforcing bar and concrete over the lap or anchorage length l_b .

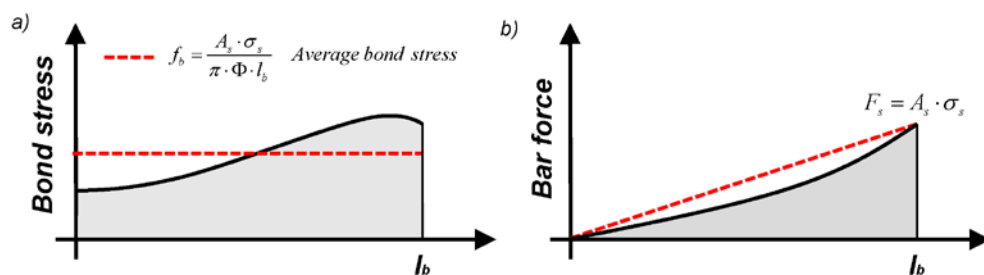


Figure 3.2: Actual bond stress developing and average bond stress idealization (a); actual force within the lap or anchorage length compared to the one reached in the hypothesis of constant bond stress idealization (b).

However, the actual mechanism is more complex: the bond stress is not constant along the lap or anchorage length and to assume an average value for bond stress is a strong simplification (Figure 3.2).

Hence, although the Eq.(3.8) seems to be very simple, the bond strength of laps and anchorages is extremely complex to be investigated. In general, there is agreement concerning the parameters that influence bond resistance. However, the quantification of the magnitude of each one contribution is still debated and investigated.

Recent achievements reported in scientific literature (as *fib Bulletin 10*, *fib Bulletin 72*) had let to agree that bond is not a fundamental property of the bar but is a quantity influenced by bars and concrete section geometries, materials characteristics and stress field.

In fact, a wide number of parameters may influence the bond behavior, as:

- bar geometry (e.g. ribs geometry, relative rib area);
- structural member geometry (e.g. concrete cover);
- stress state within surrounding concrete (e.g. confinement pressure);
- strength and quality of concrete;
- technological aspects related both to reinforcements and concrete (e.g. bar diameter, lap or anchorage length, aggregate size);
- environmental aspects (e.g. initial bar rusting, steel corrosion, high-temperature bond decay, low-temperature bond improvement);

Depending from the degree of interaction between bar reinforcement and concrete, two different failure modes related to bond behavior can be recognized:

- the *pull-out failure mode*, where the bond failure is related to the shearing-off of the concrete keys located between two ribs. In general, it is considered as a *local failure* because it is related mainly related to the interface collapse;
- the *splitting failure mode*, where bond failure is due to the longitudinal splitting of the concrete surrounding the bars. Differently from pull-out failure, *splitting* failure is considered as a *structural failure*, as it involves parameters that related to the structural configuration (e.g. concrete cover) and not only related to the nature of the interface.

The bond mechanism

In order to activate the bond mechanism, it is necessary that relative displacements (i.e. slip) between reinforcement and concrete takes place. The bond interaction is developed by means of mechanical interlocking between reinforcement ribs and concrete matrix. Progressively, the ribs start to penetrate into the mortar matrix by increasing the level of slip between bar and concrete. Then, compressive stresses arise in the concrete and induces perpendicular tensile stresses. This leads to the formation of inclined bond cracks that starts from ribs denoted in literature as Goto-cracks (*Goto, 1971*). The compression struts that arise in concrete are balanced by circumferential tensile stresses in surrounding concrete.

In the case these tensile stresses overpass the tensile strength of the concrete matrix, longitudinal cracks take place along the re-bars direction as described by *Tepfers, 1973*.

In condition of low degree of confinement (mainly related to the concrete cover and/or presence of transverse reinforcements), the longitudinal splitting cracks may reach the external surface of the structural member. Under this circumstance, the bond strength drops dramatically and the *splitting failure* occur.

On the contrary, if sufficient confinement is provided (minimum concrete cover requirements and high transversal reinforcement amount), the uncontrolled developing of splitting crack may be avoided without immediate loss of bond strength. By increasing the slip between concrete and bars, the *pull-out failure* occurs when concrete between ribs is completely shared-off. Figures 3.3 and 3.4 represents the bond mechanism and the different failure modes according to literature results (*Jakubovskis and Juknys, 2016; Lemnitzer et al, 2009*).

These two types of bond failures can be studied separately in laboratory tests (e.g. four points bending test) that, however, does not reflect the actual condition of structures during their service life. In fact, actual laps and anchorages are in general considered as “long” (i.e. $l_b/\Phi > 10-20$) and presents mixed failure modes that can strongly depend from the structural configuration. In particular, in case of high level of transversal confinement (e.g. provided by shear links and stirrups) and/or large concrete cover the *pull-out failure* with very limited concrete splitting (not visible on external surface) is observed. In case of moderate confinement pressure and/or limited concrete cover, the *pull-out failure* occurs with visible splitting cracks on outer surface. Finally, in case of absence or limited confinement pressure and very small concrete cover, the *splitting failure* with spalling-off of cover is recognized.

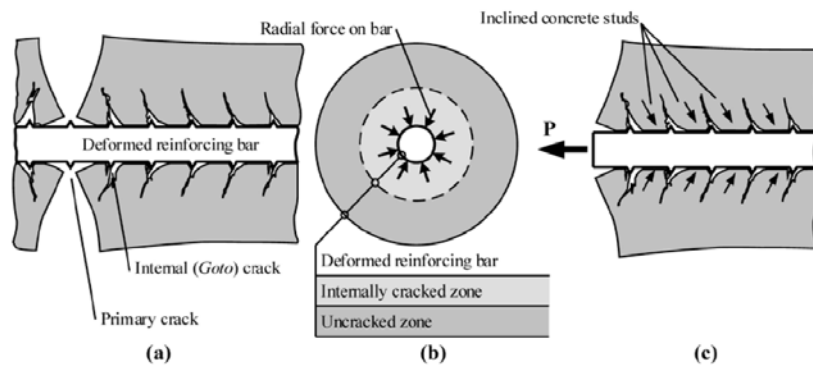


Figure 3.3: The bond mechanism in reinforced concrete elements (representation by *Jakubovskis and Juknys, 2016*).

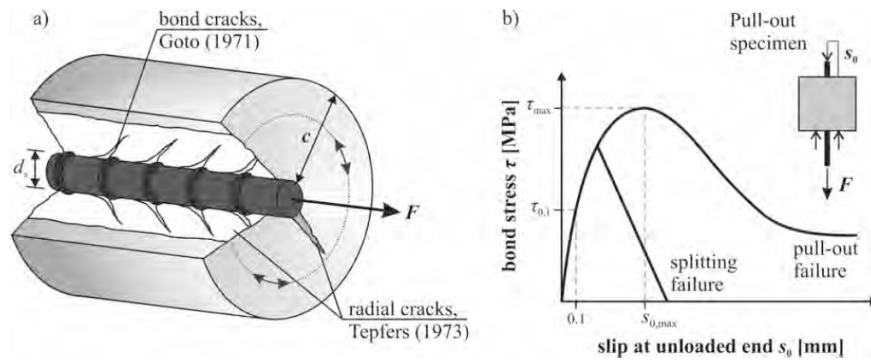


Figure 3.4: Differentiation between failure modes (representation by Lemnitzer *et al*, 2009).

In conclusion, the *pull-out failure* mode allows a sort of internal redistribution of forces during the progressive sharing-off of concrete between ribs and allow to reach higher levels of laps and anchorages strength if compared to *splitting failure* mode.

In fact, *splitting failure* is the weaker failure mode as it happens, generally, in brittle manner due to the quick propagation of longitudinal splitting cracks toward the external surface of the structural member. Very often, this failure mode controls the strength in lapped joints and may control it in some anchorage situations.

Therefore, the design methodologies are developed in order to avoid *splitting failure* as it is the weakest failure mode (e.g. by means the requirement of minimum concrete cover and of minimum amount of transversal reinforcements).

Influence of bond on structural behavior

The tensile forces within concrete are carried by the reinforcement and transferred by bond action. It implies that cracks widths and cracks spacing are significantly influenced by the bond behavior. Then, in the regions of structural members where laps and anchorages are located, the stiffness and the deformation response are directly affected by the bond stresses development.

Based on these observations, an efficient bond between concrete and reinforcements it is necessary in order to achieve adequate levels of safety, to control the structural behavior and also provide adequate level of ductility avoiding brittle failure modes (i.e. splitting failure). Then, bond behavior influences the performance of reinforced concrete structures both for the serviceability and ultimate limit states.

Concerning the *serviceability limit states* (SLS), bond influences width and spacing of transverse cracks, tension stiffening and curvature.

Referring to *ultimate limit states* (ULS), bond behavior is the responsible for resistance of end anchorages and laps of reinforcement. Bond behavior has also influence on rotation capacity within regions of formation of plastic hinges.

3.3.2 Estimation of laps and anchorages tensile strength according to *fib* Bulletin N°72 and *fib* Model Code 2010

In the scientific literature, many empirical or semi-empirical formulations that can provide appropriate predictions on the strength of laps and anchorages, like *Canbay and Frosch, 2005* and *Lettow, 2006*, are available.

In the present work, the semi-empirical model proposed in *fib Model Code 2010* and *fib Bulletin 72* will be subjected to a probabilistic calibration.

Physical assumptions

As discussed Sub-section 3.3.1 bond failure can occur both due to splitting or pull-out failure mechanisms. The *splitting failure* is the weaker and, in general, is considered for the development of design approaches.

The resistance models for *splitting failure* mode can be evaluated assuming that the radial tensile stresses generated by bond interaction does not exceed the splitting resistance provided by the surrounding concrete.

The anchored force F_b is equilibrated by means the arising of compression struts inclined of an angle β generated by bond interaction. The system is balanced in direction orthogonal to the reinforcement by radial tensile forces that should not overpass the overall splitting resistance (Figure 3.5).

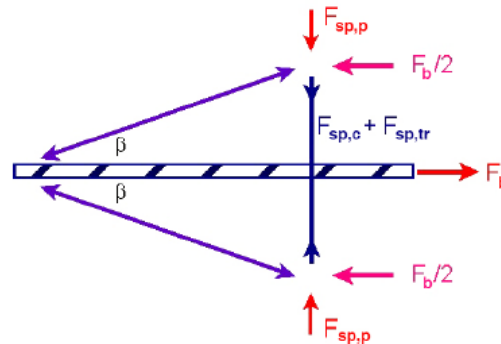


Figure 3.5: Equilibrium of forces in *splitting* failure mode modelling (*fib Bulletin 72*).

Then, the following equilibrium equation may be written:

$$F_b \cdot \tan \beta \leq F_{sp,c} + F_{sp,tr} + F_{sp,p} , \quad \text{with} \quad F_b = \sigma_s \cdot A_s \quad (3.9)$$

where σ_s is the tensile stress developed within the reinforcement; A_s is the transversal area of the reinforcement; β is the angle of inclination of compression struts; $F_{sp,c}$ is the contribution to splitting resistance provided by concrete cover; $F_{sp,tr}$ is the contribution to splitting resistance to provided by transverse reinforcements which crossing the splitting surface; $F_{sp,p}$ is the contribution to splitting resistance provided by transverse confinement pressure.

The three contributes to splitting resistance has been determined by means experimental observations by *Canbay and Frosch, 2005* leading to the semi-empirical resistance model that will be discussed next. The entire derivation procedure is not herein reported because is out of purposes of the present dissertation. Deeper information can be acknowledged by *fib Bulletin N° 72*.

The semi-empirical resistance model

According to *Canbay and Frosch, 2005* the *fib Model Code 2010* and *fib Bulletin N°72* expresses the mean strength of a tensed lapped joint or anchorage f_{stm} as follows:

$$f_{stm} = 54 \text{ MPa} \cdot \left(\frac{f_{cm}}{25 \text{ MPa}} \right)^{0.25} \left(\frac{l_b}{\Phi} \right)^{0.55} \left(\frac{25 \text{ mm}}{\Phi} \right)^{0.2} \left[\left(\frac{c_{min}}{\Phi} \right)^{0.25} \left(\frac{c_{max}}{c_{min}} \right)^{0.1} + k_m K_{tr} \right] \quad (3.10)$$

where f_{cm} is the mean concrete compressive strength; l_b is the lap or anchorage length (or bond length); Φ is the bar diameter; the concrete covers c_{min} , c_{max} and effectiveness coefficient k_m are evaluated according to Figure 3.6(a-b). The coefficient K_{tr} accounts for the effect of confinement provided by shear links and/or stirrups located along the lap or anchorage, and it can be evaluated as follows:

$$K_{tr} = \frac{n_l n_g A_{sv}}{(l_b \Phi n_b)} \quad (3.11)$$

where n_l is the number of legs of a link and/or stirrup; n_g is the number of groups of links and/or stirrups; A_{sv} is the transverse area of each leg of a link and/or stirrup; n_b is the number of individual anchored bars or pairs of lapped bars. All the units are expressed in MPa and mm.

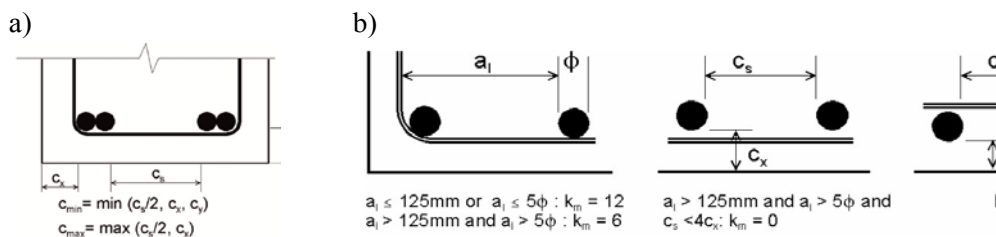


Figure 3.6: Definition of concrete cover in Eq.(3.10) (a) and of the effectiveness of shear links related to Eq.(3.11) (b).

The expression reported by Eq.(3.10) has been derived and calibrated and validated based on an extensive experimental database related to laps and anchorages containing more than 800 tests coming from American (ACI) and European investigations and represents a modification of the resistance model

proposed by *Lettow, 2006* based on *Canbay and Frosch, 2005; Burkhardt, 2000* and *Eligehausen, 1979*.

The *fib Bulletin N°72* sets the following limits for Eq.(3.10) being them also the limits for the parameters involved within the tests reported by the database:

- $15 \text{ MPa} \leq f_{cm} \leq 110 \text{ MPa}$;
- $K_{tr} \leq 0.05$;
- $0.5 \leq c_{min}/\Phi \leq 3.5$ and $c_{max}/c_{min} \leq 5$;
- $l_b \geq 10 \cdot \Phi$;
- $25/\Phi \geq 2$.

The Eq.(3.10) represents the semi-empirical resistance model expressed in function of the relevant parameters that can affect laps and anchorages resistance. The expression takes into account the non-linear influence on lap strength f_{stm} of the involved parameters, as the ratio l_b/Φ and the concrete cylinder compressive strength f_{cm} . From now on, according to *fib Bulletin N°72*, the term lap will be adopted also to represents the term anchorage.

3.3.3 Estimation of the resistance model uncertainty

The first step required in order to perform the probabilistic calibration is the assessment of the uncertainty related to the definition of the resistance model (i.e. resistance model uncertainties).

As described in Section 1.3 and according to Eq.(1.1), the assessment of resistance model uncertainty random variable requires the identification of two different sets of data:

- a vector $R_{Experimental,h}$ of observations of laps strength;
- a vector of estimated strength $R_{Model,h}$.

Specifically, $R_{Experimental,h}$ is the maximum tensile stress measured within the reinforcement bar during the experimental test before bond failure, while $R_{Model,h}$ represents the lap strength f_{stm} estimated by Eq. (3.10) assuming as input parameters the experimental ones.

In the present study case, the X vector includes all the material and geometrical parameters explicitly considered into the model described by Eq. (3.10), while the Y vector collect other parameters that can have influence on lap strength as the relative rib area of the reinforcement bars, the shape of the ribs and other size effects (e.g. beam dimensions). The effect of parameters involved by Y are indirectly accounted for in the probabilistic calibration by the assessment of the resistance model uncertainty random variable.

The experimental database

In the present study, the experimental data adopted for the estimation of resistance model uncertainty derives from the work of *fib Task Group 4.5*. The *fib TG 4.5 database on lap splices and anchorages* collect the results of an extensive series of laboratory tests on laps and anchorages collected mainly by *ACI 408*

(bottom casted beams only – good bond condition), and it is enriched by additional data from European and a few Asian investigations.

Table 3.5: Detail of the literature references collecting the experimental database on lap splices and anchorages.

Source	Year	Authors	N° Tests
ACI	1955	<i>Chinn, Ferguson, and Thompson</i>	32 (32) [0]
	1958	<i>Chamberlin</i>	6 (6) [0]
	1956	<i>Chamberlin</i>	11 (11) [0]
	1965	<i>Ferguson and Breen</i>	35 (26) [9]
	1975	<i>Thompson, Jirsa, Breen, and Meinheit</i>	15 (11) [4]
	1965	<i>Ferguson and Thompson</i>	4 (4) [0]
	1961	<i>Mathey and Watstein</i>	14 (0) [14]
	1991, 1993	<i>Hester, Salamizavaregh, Darwin, and McCabe</i>	17 (7) [10]
	1990, 1991	<i>Choi, Hadje-Ghaffari, Darwin and McCabe</i>	8 (8) [0]
	1991	<i>Rezansoff, Konkankar and Fu</i>	34 (0) [34]
	1981	<i>Zekany, Neumann, Jirsa, and Breen</i>	12 (2) [10]
	1991	<i>DeVries, Moehle, and Hester</i>	10 (0) [10]
	1993	<i>Rezansoff, Akanni, and Sparling</i>	15 (4) [11]
	1996	<i>Hasan, Cleary, and Ramirez</i>	2 (0) [2]
	1996	<i>Darwin, Tholen, Idun, and Zuo</i>	73 (13) [60]
	1998, 2000	<i>Zuo and Darwin</i>	91 (28) [63]
	1994	<i>Kadoriku</i>	34 (0) [34]
	1998	<i>Hamad and Itani</i>	8 (8) [0]
	1999	<i>Azizinamini, Pavel, Hatfield and Ghosh</i>	57 (32) [25]
1993	<i>Azizinamini, Stark, Roller and Ghosh</i>	18 (18) [0]	
European and Asian	1995	<i>Azizinamini, Chisala, Ghosh</i>	7 (0) [7]
	1980	<i>Betzle</i>	5 (0) [5]
	1979	<i>Eligehausen</i>	8 (8) [0]
	1996	<i>Hamad, Mansour</i>	17 (17) [0]
	1998	<i>Hegger, Burkhardt</i>	9 (4) [5]
	1994	<i>Hwang, Lee, Lee</i>	8 (4) [4]
	1996	<i>Hwang, Leu, Hwang</i>	10 (2) [8]
	1990	<i>Olsen</i>	21 (0) [21]
	1977	<i>Rehm, Eligehausen</i>	20 (0) [20]
	1977	<i>Stöckl, Menne, Kupfer</i>	25 (0) [25]
	1973	<i>Tepfers</i>	181 (155) [26]
Total results			807 (400) [407]

The overall number of tests collected is 807 and, in majority, laps splices with a few number of anchorages tests are present. In Table 3.5 the literature references herein adopted, related to *fib TG 4.5 database on lap splices and anchorages*, are reported.

The mentioned above experimental database collects, for each test, the parameters required for evaluation of lap tensile strength with Eq.(3.10) (i.e. vector X). Other information related to relative rib area are reported but not exhaustively for all test cases.

The detail of the experimental results $R_{Experimental}$ and of the model prediction by Eq.(3.10) R_{Model} is reported in Figure 3.7.

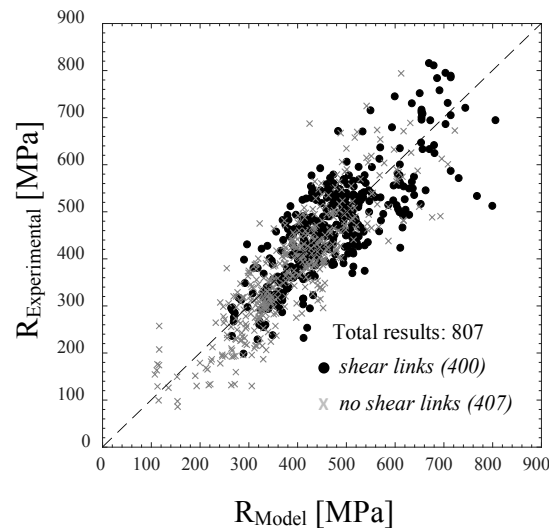


Figure 3.7: Detail of results of Eq.(3.10) for the *fib TG 4.5 bond database*

According to Eq.(3.3), Figure 3.8 reports the variation of model uncertainties ϑ in function of the main parameters involved in Eq. (3.10) considering the whole experimental database. It can be observed that no significant trends of variation may be noted.

According to the provisions of *EN 1992, 2004* and related limits prescribed for concrete cylinder compressive strength and minimum concrete covers, the estimation of resistance model uncertainties for Eq.(3.10) may be performed distinguishing between *new* and *existing* structures by appropriately filtering the experimental database.

In the details, the mentioned above provisions in terms of concrete strength and minimum concrete cover are defined concerning structure of *new* realization. Concerning the case of *existing* structures, very often the minimum provisions of current codes (as *EN 1992, 2004*) may not be complied.

Therefore, defining rules in order to appropriately filter the experimental database, a wider range of parameters should be considered for *existing* structures. This is in order to cover as much as possible the actual variability that can be found in structures built before the application of current codes.

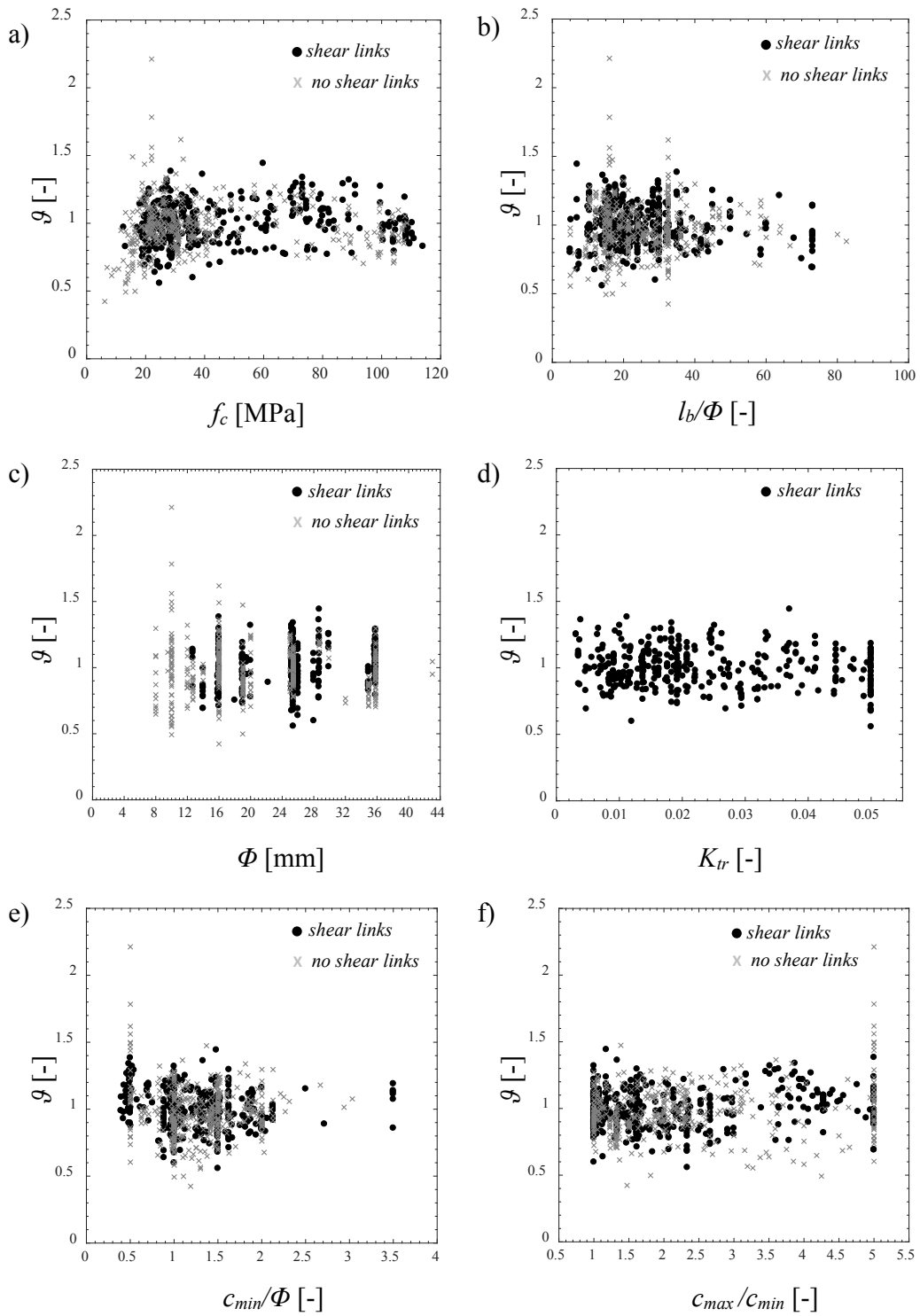


Figure 3.8: Trend of variation of model uncertainty in function of main parameters involved by Eq.(3.10) related to the experimental sets reported by *fib TG 4.5 bond database*.

According to these observations, the ranges for parameter defined in order to filter the experimental database are set distinguishing between *new* and *existing* structures as reported in Table 3.6.

Table 3.6: Filters applied to the experimental database differentiating between *new* and *existing* structures.

Database filters	f_{cm} [MPa]	c_{min}/Φ [-]	l_b/Φ [-]	c_{max}/c_{min} [-]	K_{tr} [-]
<i>New structures</i>	≥ 20 ≤ 110	≥ 0.95 ≤ 3.5	≥ 15	≤ 5	≤ 0.05
<i>Existing structures</i>	≥ 10 ≤ 110	≥ 0.5 ≤ 3.5	≥ 10	≤ 5	≤ 0.05

The range of variation of the ratio between concrete cover and bar diameter is extended to a minimum of 0.5 for existing structures (since this is the minimum value available in the database). This takes into account the influence of higher variability of concrete cover that may be found in *existing* structures built before the drafting of current structural codes.

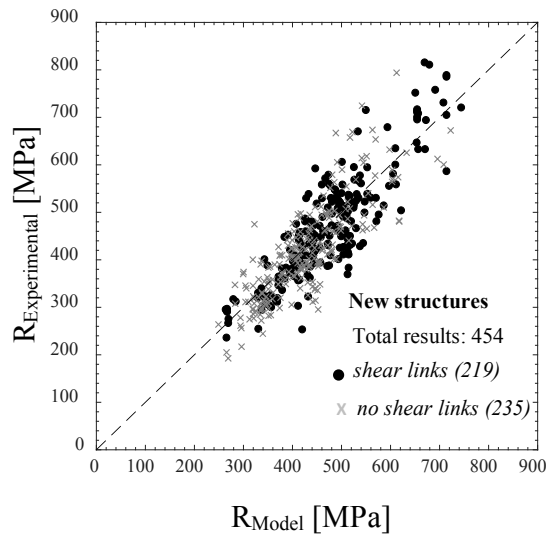


Figure 3.9: Detail of results of Eq.(3.10) for the filtered database related to *new* structures.

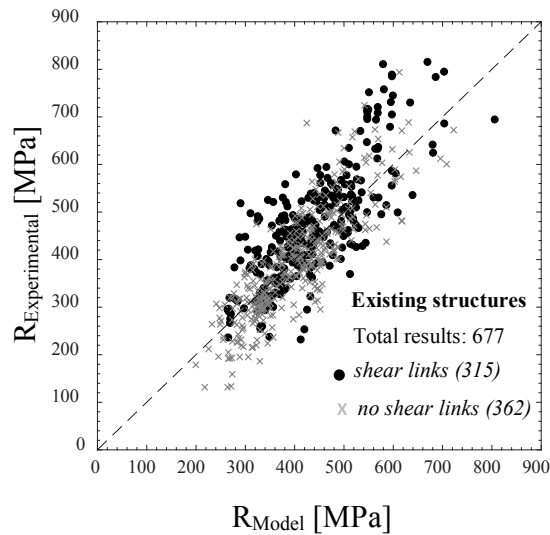


Figure 3.10: Detail of results of Eq.(3.10) for the filtered database related to *existing* structures.

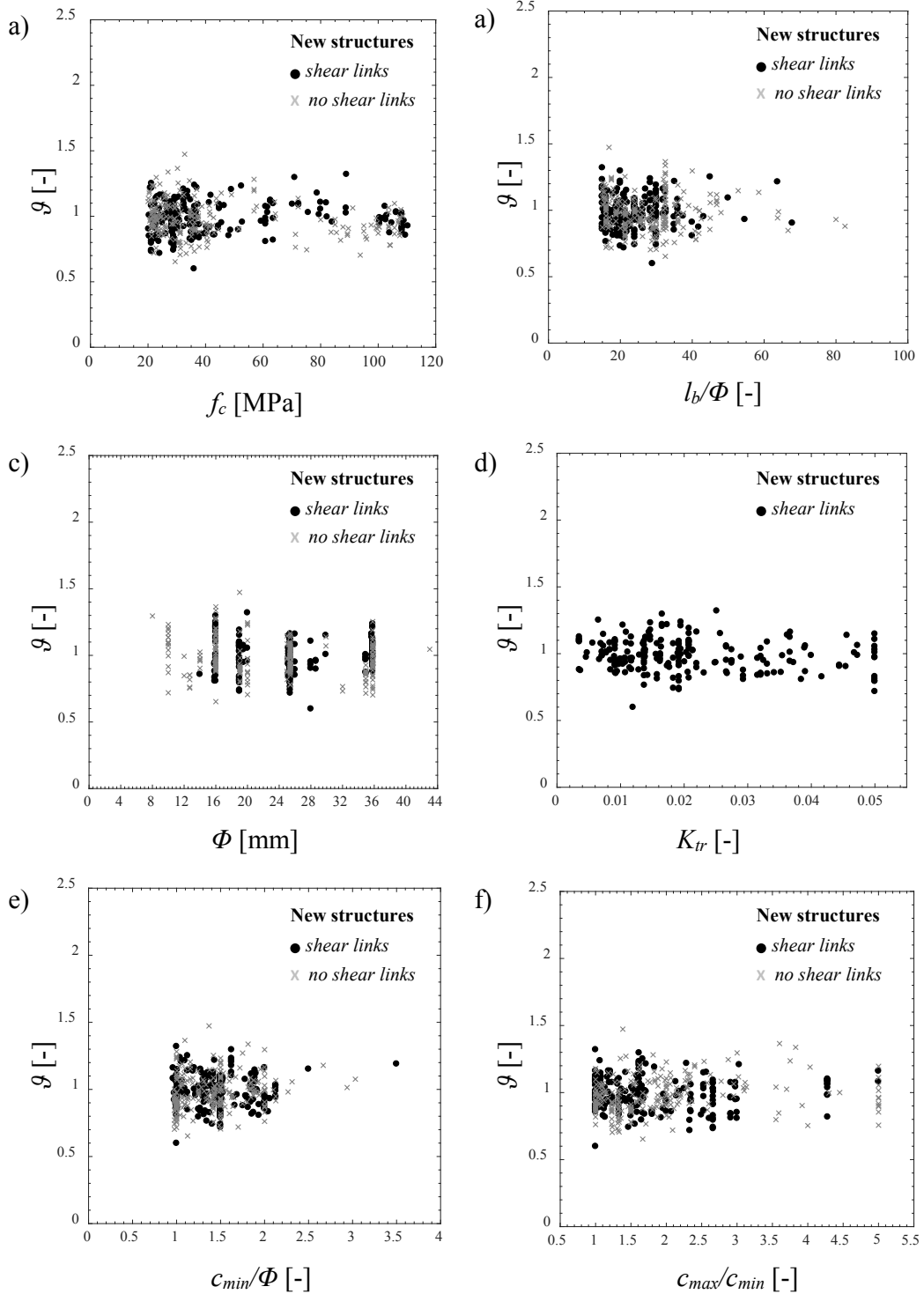


Figure 3.11: Trend of variation of model uncertainty in function of main parameters involved by Eq.(3.10) related to the filtered database concerning *new structures*.

The Figure 3.9 reports the detail of the experimental results $R_{Experimental}$ and of the model prediction by Eq.(3.10) R_{Model} concerning the experimental database related to *new structures*. As for the case of the entire database, Figure 3.11(a-f) shows the variation of the model uncertainties with respect the main involved variables. It can be observed that restricting the number of observed experimental results no trends of variation of g are recognized depending from the main variables.

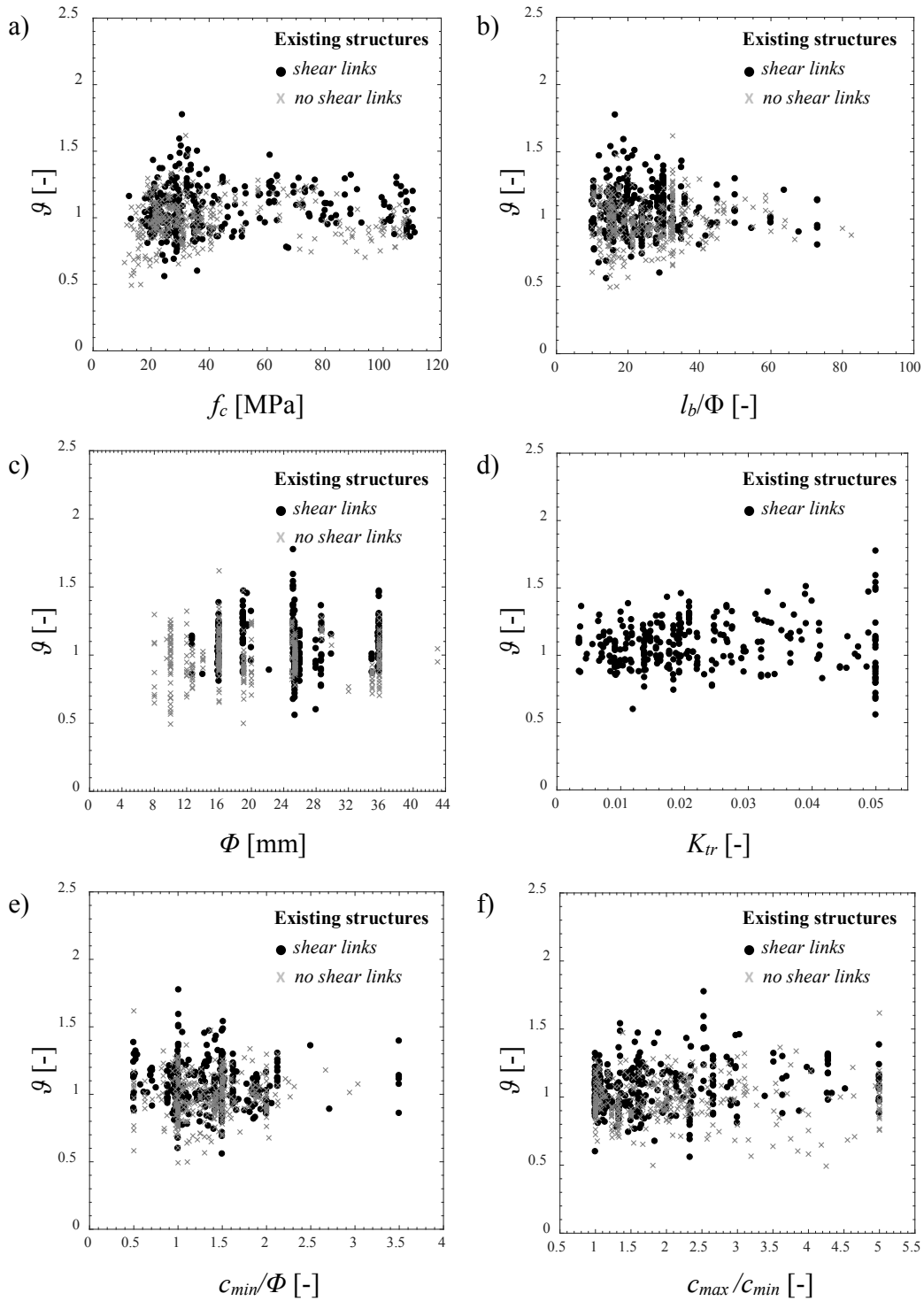


Figure 3.12: Variation of model uncertainty in function of main parameters involved by Eq.(3.10) related to the filtered database concerning *existing structures*.

Similarly, the Figure 3.10 represents the detail of the experimental results $R_{Experimental}$ and of the model prediction by Eq.(3.10) R_{Model} concerning the experimental database related to *existing structures*.

A larger number of experimental results are considered with respect to the case of new structures, however, Figure 3.12(a-f) shows that also in this case no trends of variation of g are recognized depending from the main variables.

The mentioned above ranges for main variables represent also the limit of validity of the final relationships differentiated between *new* and *existing* structures.

Thanks to this observation, it may be concluded that the statistical characterization of model uncertainties may be performed univocally for all the range of variation of parameters.

Furthermore, described in *fib Bulletin 72*, Eq. (3.10) fits well both for lap splices and anchorages laboratory test results with no evidence of distinction between them. All the conclusions on ultimate bond strength evaluation will then be suitable both for laps and anchorages, therefore, the term laps will be used, from now on, meaning also anchorages.

Statistical inference

The selection of the probabilistic distribution and its parameters has to be defined in order to incorporate modelling uncertainties in the probabilistic calibration. This may be assessed by *statistical inference* that allows to associate properties to a certain population, which is only known through a limited number of observations (i.e. experimental sample).

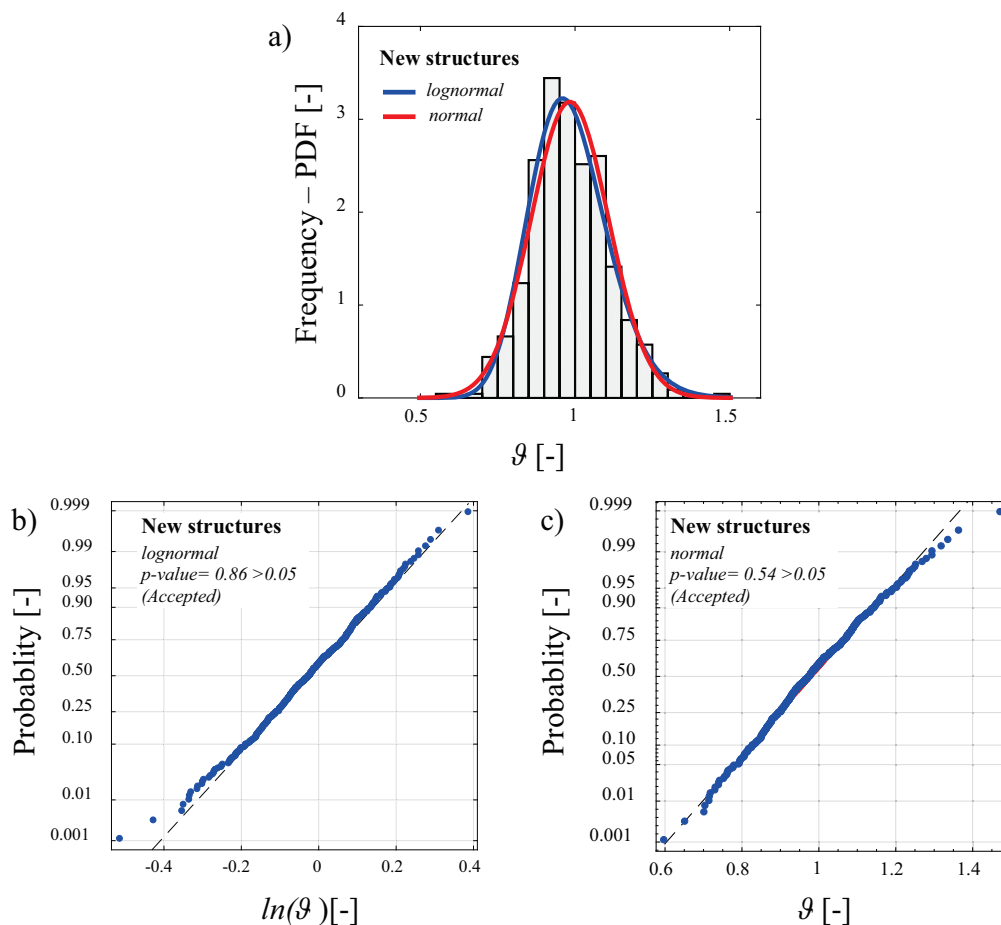


Figure 3.13: *New structures*: frequency histogram and probabilistic distribution fit (a); lognormal probability plot (b) and normal probability plot (c) with associate p-values after *Chi-square* goodness of fit test ($\alpha=0.05$).

Firstly, the null hypothesis H_0 for normality of the population of ϑ and $\ln\vartheta$ (both concerning *new* and *existing* structures) is assessed by means of a *Chi-square goodness-of-fit test* with significance level $\alpha=0.05$.

The frequency histograms with normal and lognormal fitting, the probability plots in Figure 3.13 and 3.14 and the values of Table 3.7 shows that the null hypothesis of normality for $\ln\vartheta$ is not rejected for both *new* and *existing* structures, whereas the hypothesis of normality for ϑ is rejected for *existing* structures.

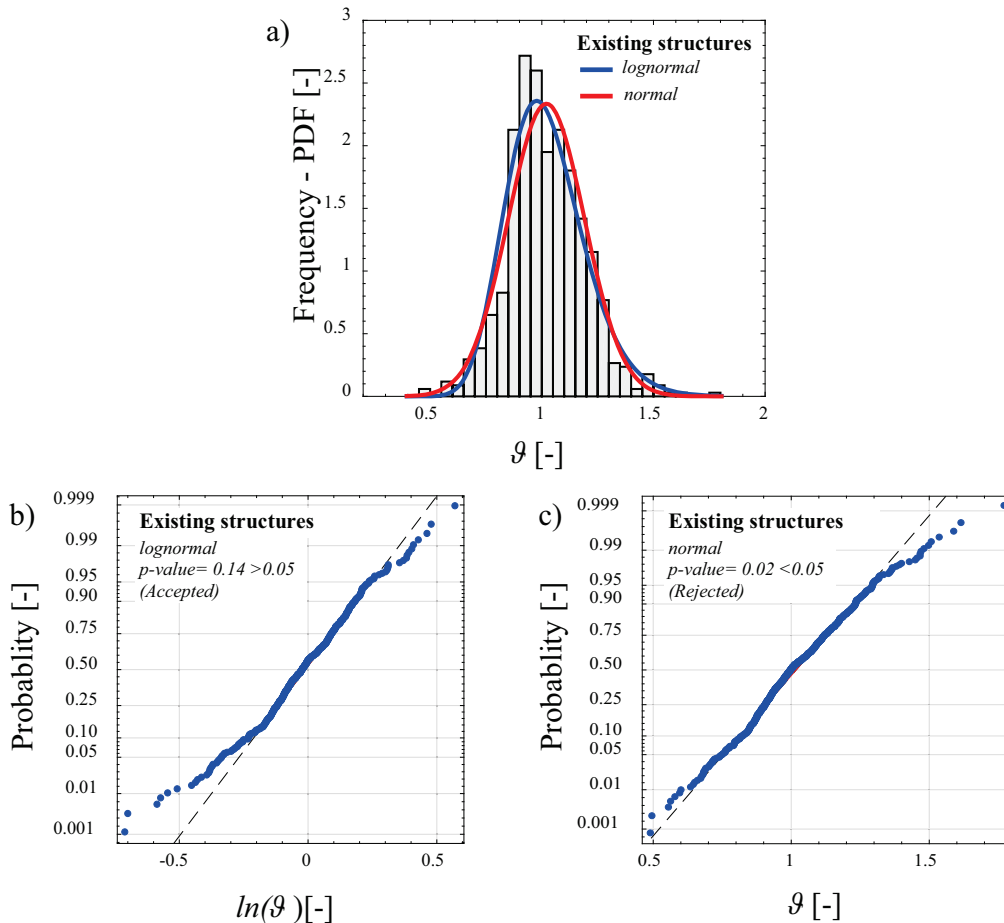


Figure 3.14: *Existing* structures: frequency histogram and probabilistic distribution fit (a); lognormal probability plot (b) and normal probability plot (c) with associate p-values after *Chi-square* goodness of fit test ($\alpha=0.05$).

At the same time, the comparison between p-values shows better results for the normality hypothesis of $\ln\vartheta$ in both cases.

It may be concluded that the most likely probabilistic distribution able to represent the *resistance model uncertainty random variable* ϑ , for both *new* and *existing* structures, is the *lognormal* one. This is in agreement also with suggestions of *JCSS Probabilistic Model Code, 2001*.

The Bayesian inference procedure assuming a non-informative prior distribution is performed and parameters related to lognormal distribution are estimated on the base of the samples represented by the filtered database for *new/existing* structures.

Table 3.7: Verification of null hypothesis H_0 for normality in the case on new/existing structures consider the random variable ϑ and $\ln\vartheta$. Comparison between p-value and the significance level $\alpha=0.05$.

	Variable [-]	p-value [-]	Significance level [-]	Null hypothesis H_0
<i>New structures</i>	ϑ_i	0.54	≥ 0.05	Accepted
	$\ln\vartheta_i$	0.86		Accepted
<i>Existing structures</i>	ϑ_i	0.02	≥ 0.05	Rejected
	$\ln\vartheta_i$	0.14		Accepted

The results in terms of mean value μ_ϑ , variance σ_ϑ^2 and coefficient of variation $V_\vartheta = \sigma_\vartheta / \mu_\vartheta$ for the resistance model uncertainty random variable related to Eq. (3.10) are reported in Table 3.8.

Table 3.8: Probabilistic distribution and parameters estimated for resistance model uncertainty random variable ϑ both for *new* and *existing* structures.

	n^{*1} [-]	μ_ϑ [-]	σ_ϑ^2 [-]	V_ϑ [-]	Type of distribution
<i>New structures</i>	454	0.98	0.016	0.13	<i>Lognormal</i>
<i>Existing structures</i>	677	1.02	0.030	0.17	<i>Lognormal</i>

*1 number of samples after full database filtering according to Table 3.6

Then, the *resistance model uncertainty random variable* ϑ may be represented by a lognormal distribution having mean value equal to 0.98 and coefficient of variation 0.13 and mean value equal to 1.02 and coefficient of variation 0.17 for *new* and *existing* structures, respectively.

3.3.4 Probabilistic calibration

In this Section the probabilistic calibration of the model proposed by Eq.(3.10) is performed adopting the framework proposed in Section 3.2 and summarized in Figure 3.1.

Probabilistic model

A set of relevant random variables has to be defined and characterized by its appropriate probabilistic distribution. These random variables have to represent the parameters that are explicitly considered within the expression of the resistance model.

In this case, the concrete compressive strength can be assumed as the relevant random variable because it strongly affects the resistance mechanism due to its *aleatory* uncertainty. Nevertheless, *JCSS Probabilistic Model Code, 2001* provides information for the probabilistic modelling of concrete cover, in agreement with *EN 1990* geometrical parameters are used for with their nominal value with a given tolerance.

Then, concrete cover will be considered as deterministic parameter in the following. In any case, as showed in Section 3.3.3 the extent of concrete cover affects the resistance model uncertainty. In fact, the differences of the mean and the variance of resistance model uncertainty concerning *new* and *existing* structures is mainly due to the range of variation assumed by the ratio c_{min}/Φ applying the two different filters to the experimental database (see Section 3.3.3). As a consequence, the lower values of c_{min}/Φ , considered for *existing* structures, lead to higher coefficient of variation for the *resistance model uncertainty random variable* ϑ ($V_{\vartheta} = 0.17$ rather than $V_{\vartheta} = 0.13$).

Table 3.9: Probabilistic model for the random variables.

	Ref.	Mean value	C.o.V	Type of distribution	
<i>Concrete compressive strength</i> f_c [MPa]	<i>(fib Model Code 2010; JCSS Probabilistic Model Code, 2001)</i>	f_{cm}	0.15	lognormal	
<i>Resistance model uncertainty</i> ϑ [-]	<i>Section 3.3.3</i>	<i>New structures</i>	0.98	0.13	lognormal
		<i>Existing structures</i>	1.02	0.17	lognormal

At the purpose the present calibration, all the other parameters involved by Eq.(3.10) can be assumed as deterministic. Therefore, in the present application only the concrete compressive strength $X_i=f_c$ ($i=N=1$) will represent the main random variable, according to Eq.(3.4).

As previously discussed, also the *resistance model uncertainty random variable* ϑ have to be accurately addressed and included into the probabilistic model.

According to Table 3.9 the probabilistic model with the following hypotheses is assumed:

- f_c : is the cylinder compressive strength random variable. According to *fib Model Code 2010*, the random variability of f_c can be described by means of a lognormal distribution with coefficient of variation equal to 0.15 and mean value equal to f_{cm} depending by the concrete strength class.
- ϑ : is the *resistance model uncertainty random variable*. It can be described by means of a lognormal distribution with mean value and coefficient of variation as described in Section 3.3.3.

All the other parameters involved by Eq.(3.10) are assumed as deterministic and can be grouped in the vector a_j , which in this example will contain: c_{min} , c_{max} , l_b , Φ , k_m and K_{tr} ($j=1,2,\dots,M=6$).

In this calibration example, only one best fitting empirical coefficient $C=C_l$ ($l=K=1$) is present and is set equal to 54.

Resistance and auxiliary random variables

The semi-empirical expression of Eq.(3.10) can be rewritten according to Eq.(3.4) as follows:

$$f_{st,Model} = R_{Model} = 54 \text{ MPa} \cdot f_{cm}^{0.25} \cdot g(a_j) \quad (3.12)$$

where:

$$g(a_j) = \left(\frac{1 \text{ MPa}}{25 \text{ MPa}} \right)^{0.25} \left(\frac{l_b}{\Phi} \right)^{0.55} \left(\frac{25 \text{ mm}}{\Phi} \right)^{0.2} \left[\left(\frac{c_{\min}}{\Phi} \right)^{0.25} \left(\frac{c_{\max}}{c_{\min}} \right)^{0.1} + k_m K_{tr} \right] \quad (3.12)$$

The *resistance random variable* R , in this case, is represented by the tensile strength of laps or anchorages f_{st} predicted by Eq.(3.10) and can be rewritten as a function of the main random variable f_c and the resistance model uncertainty \mathcal{G} in compliance with to Eq.(3.4), as follows:

$$R(f_c, \mathcal{G}) = \mathcal{G} \cdot C \cdot f_c^{0.25} \cdot g(a_j) \quad (3.14)$$

where $g(a_j)$ is the function of the deterministic parameters and C is the empirical coefficient set equal to 54 MPa.

In the following, as expressed by Eq.(3.5) of Section 3.1, the *auxiliary random variable* Z can be defined selecting as representative value $x_{1,rep}$ ($i=N=1$) the 5% characteristic (f_{ck}) or the mean (f_{cm}) or the design cylinder concrete compressive strength f_{cd} (calculated as f_{ck}/γ_c , with $\gamma_c=1.5$ according to *EN 1992-1-1*), respectively.

Therefore, different *auxiliary random variables* Z can be defined as:

$$Z(f_c, \mathcal{G}; f_{cm}) = \frac{\mathcal{G} \cdot C \cdot f_c^{0.25} \cdot g(a_j)}{C \cdot f_{cm}^{0.25} \cdot g(a_j)} = \frac{\mathcal{G} \cdot f_c^{0.25}}{f_{cm}^{0.25}} \quad (3.15a)$$

$$Z(f_c, \mathcal{G}; f_{ck}) = \frac{\mathcal{G} \cdot C \cdot f_c^{0.25} \cdot g(a_j)}{C \cdot f_{ck}^{0.25} \cdot g(a_j)} = \frac{\mathcal{G} \cdot f_c^{0.25}}{f_{ck}^{0.25}} \quad (3.15b)$$

$$Z(f_c, \mathcal{G}; f_{cd}) = \frac{\mathcal{G} \cdot C \cdot f_c^{0.25} \cdot g(a_j)}{C \cdot f_{cd}^{0.25} \cdot g(a_j)} = \frac{\mathcal{G} \cdot f_c^{0.25}}{f_{cd}^{0.25}} \quad (3.15c)$$

By means of Monte Carlo technique, it is possible to generate three large samples of the populations of the *auxiliary random variables* $Z(f_c, \mathcal{G}; f_{cm})$, $Z(f_c, \mathcal{G}; f_{ck})$ and $Z(f_c, \mathcal{G}; f_{cd})$.

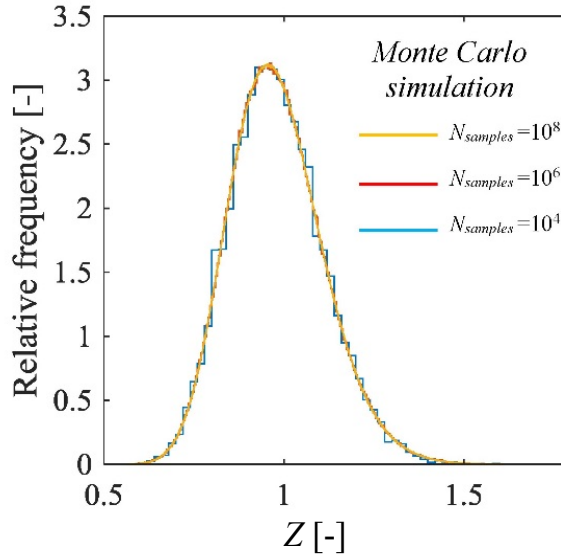


Figure 3.15: Relative frequency histogram for the Monte Carlo simulation of the random variable $Z(f_c, \mathcal{G}; f_{ck})$ in the hypothesis of 10^4 , 10^6 and 10^8 samples. The case is relative to *new* structures.

First of all number of samples N equal to 10^4 , 10^6 and 10^8 has been generated adopting the direct Monte Carlo sampling from the probabilistic distributions of the basic variables listed in Table 3.9. The associated relative frequency histogram is reported in Figure 3.15 concerning the variable $Z(f_c, \mathcal{G}; f_{ck})$ assuming the hypothesis of *new* structures.

As the *resistance random variable* R is a function of two lognormally distributed random variables (i.e. f_c and θ), it is expected that $\zeta(X)$ is lognormally distributed too. As shown by Figure 3.15, the results obtained adopting 10^4 , 10^6 and 10^8 samples give not appreciable difference in the estimation of the distribution parameters for the *auxiliary random variable* Z . Being the total number of samples required for the Monte Carlo simulation inversely proportional to the probability of failure to be estimated, a number of samples set $N=10^6$ can be considered sufficient for the present investigation (as, in the following, the minimum estimated probability is around 10^{-4} , which corresponds to the fractile of the distribution of Z associated to the value of the product $\alpha_R \cdot \beta$ with $\beta = 4.3$ and $\alpha_R = 0.8$).

However, in the case of the estimation of smaller probability of failure, a larger number of samples is recommended in order to represent, within the sample, also lower extreme values of the involved random variables.

Finally, concerning the population with 10^6 samples of the *auxiliary random variable* Z , the *Chi-square* goodness of fit test with 5% level of significance testing the hypothesis of normality of the sample of $\ln(Z)$ have been performed confirming the hypothesis of lognormality of the variable Z . The frequency histograms concerning the three hypotheses for *auxiliary random variable* described by Eq.(3.15 a-b-c) are reported in Figure 3.16(a-b) differentiating between *new* and *existing* structures.

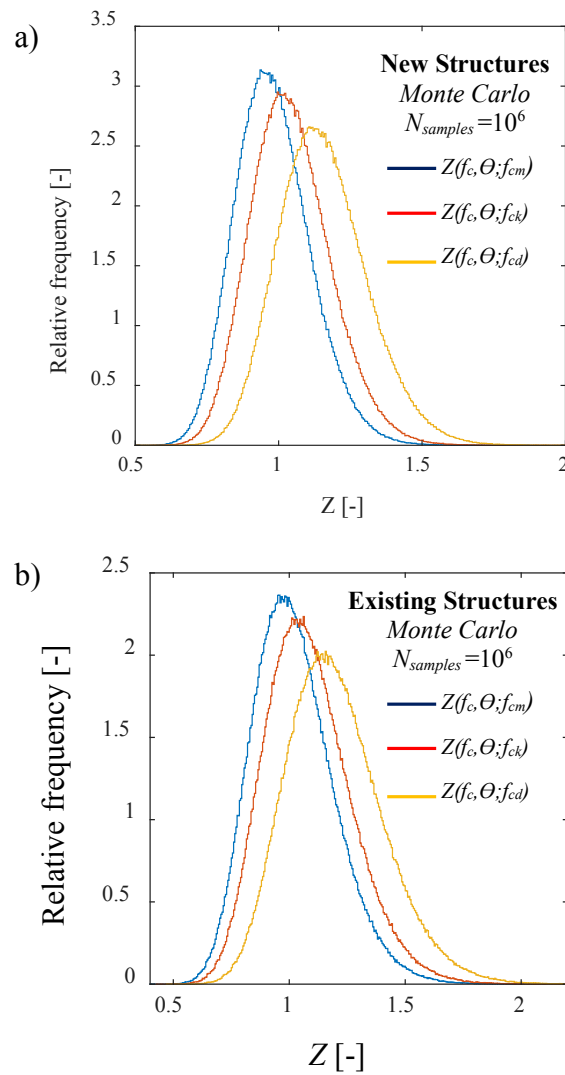


Figure 3.16: Relative frequency histogram for the Monte Carlo simulation of the *auxiliary random variables* $Z(f_c, \Theta; f_{cm})$, $Z(f_c, \Theta; f_{ck})$ and $Z(f_c, \Theta; f_{cd})$ in the hypothesis of 10^6 samples; *New structures* (a); *Existing structures* (b).

Hence, the *auxiliary random variables* $Z(f_c, \vartheta; f_{cm})$, $Z(f_c, \vartheta; f_{ck})$ and $Z(f_c, \vartheta; f_{cd})$ can be described by means of lognormal distributions having: mean value equal to 0.98, 1.04 and 1.15 and coefficient of variation equal to 0.13, 0.14 and 0.15, respectively (Figure 3.17(a-b)), concerning *new structures*; mean value equal to 1.02, 1.08, 1.20 and coefficient of variation equal to 0.17, respectively (Figure 3.18(a-b)), concerning *existing structures*.

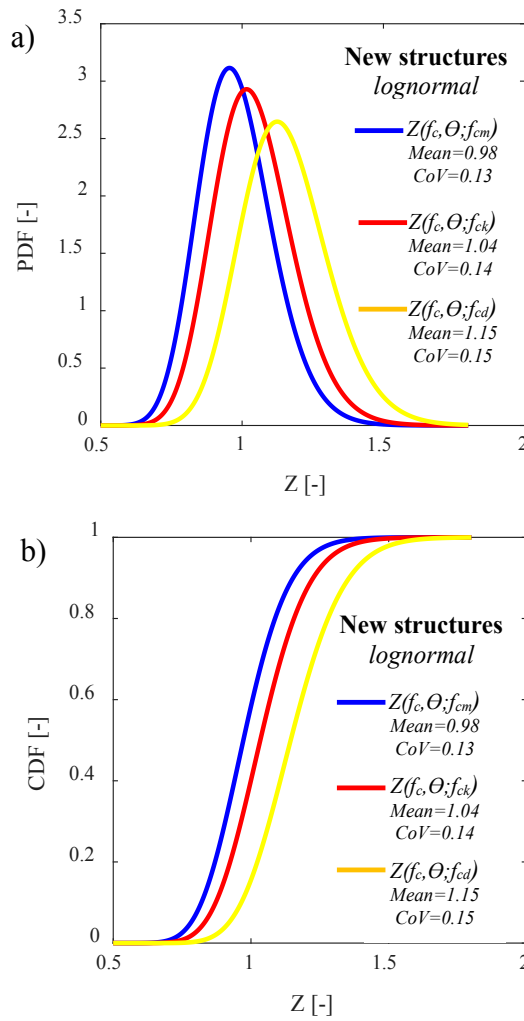


Figure 3.17: Lognormal distribution (PDF (a) and CDF (b)) for the *auxiliary random variables* Z : $Z(f_c, \theta; f_{cm})$, $Z(f_c, \theta; f_{ck})$ and $Z(f_c, \theta; f_{cd})$ concerning *new structures*.

Note that the higher coefficient of variation for resistance model uncertainties (i.e. $V_g = 0.17$) associated to *existing* structures have a strong influence on the coefficient of variation of the auxiliary random variable. In fact, as shown in Figure 3.18, all the hypotheses performed within Eq.(3.15 a-b-c) leads to obtain the same coefficient of variation equal to 0.17 between all the three cases, differently from the case of *new* structures. In fact, in the latter case (i.e. $V_g = 0.13$), the aleatory variability of concrete compressive strength still has influence the variability of the *auxiliary random variable* Z .

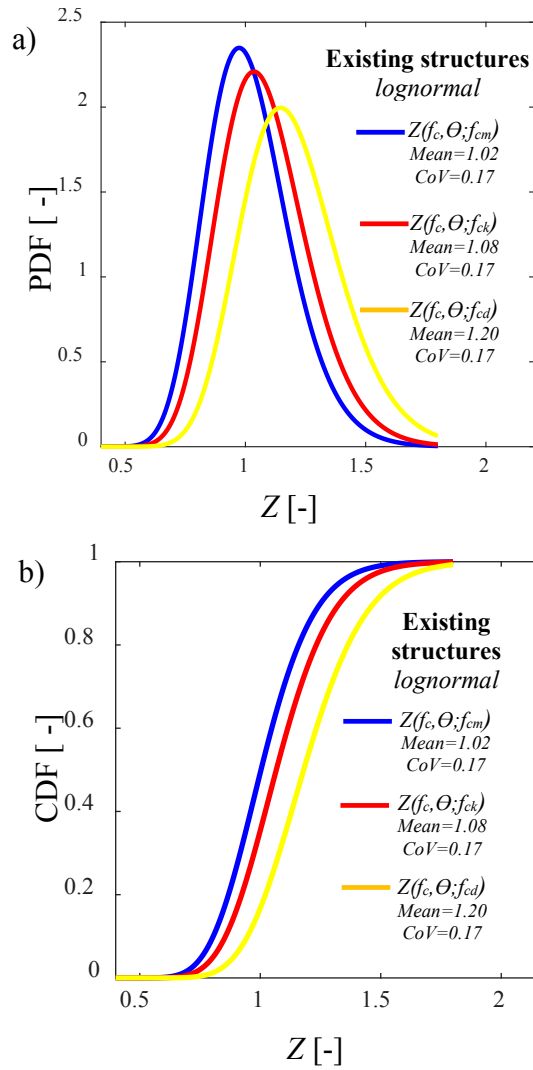


Figure 3.18: Lognormal distribution (PDF (a) and CDF (b)) for the *auxiliary random variables* Z : $Z(f_c, \vartheta; f_{cm})$, $Z(f_c, \vartheta; f_{ck})$ and $Z(f_c, \vartheta; f_{cd})$ concerning *existing structures*.

Finally, the choice of the representative value for concrete compressive strength (i.e. f_{cm} , f_{ck} or f_{cd}) affects the magnitude of the mean value of the *auxiliary random variable* Z (i.e. bias).

Reliability-based expressions

Once characterized the probabilistic distribution for the *auxiliary random variables* $Z(f_c, \vartheta; f_{cm})$, $Z(f_c, \vartheta; f_{ck})$ and $Z(f_c, \vartheta; f_{cd})$, it is possible to calculate their quantiles as described by Eq.(3.6). The quantiles ζ_m , ζ_k and ζ_d of the random variables $Z(f_c, \vartheta; f_{cm})$, $Z(f_c, \vartheta; f_{ck})$ and $Z(f_c, \vartheta; f_{cd})$ with $p=0.5$, 0.05 , $\Phi(-\alpha_R \cdot \beta)$ to not be exceeded, respectively, are reported in Table 3.10 and Table 3.11 differentiating between *new* and *existing* structures.

Note that the described above framework can be easily applied also in the case of probabilistic distributions for main random variables different from the lognormal one.

Table 3.10: Values of the probabilistic coefficients $\zeta_p(f_{c,rep})$ in the function of representative value selected for concrete compressive strength for the case of *new* structures.

Quantile of Z	Auxiliary random variable		
	$Z(f_c, \mathfrak{g}; f_{cm})$	$Z(f_c, \mathfrak{g}; f_{ck})$	$Z(f_c, \mathfrak{g}; f_{cd})$
	Probabilistic coefficients $\zeta_p(f_{c,rep})$		
	$\zeta_p(f_{cm})$ [-]	$\zeta_p(f_{ck})$ [-]	$\zeta_p(f_{cd})$ [-]
$p=0.5$ (<i>m</i>)	0.98	1.03	1.14
$p=0.05$ (<i>k</i>)	0.78	0.83	0.92
$p=\Phi(-\alpha_R \cdot \beta);$ $\alpha_R=0.8, \beta=3.8$ (<i>d</i>)	0.65	0.69	0.77
$p=\Phi(-\alpha_R \cdot \beta);$ $\alpha_R=0.8, \beta=3.8$ (<i>d</i>)	0.62	0.65	0.72

Table 3.11: Values of the probabilistic coefficients $\zeta_p(f_{c,rep})$ in the function of representative value selected for concrete compressive strength for the case of *existing* structures.

Quantile of Z	Auxiliary random variable		
	$Z(f_c, \mathfrak{g}; f_{cm})$	$Z(f_c, \mathfrak{g}; f_{ck})$	$Z(f_c, \mathfrak{g}; f_{cd})$
	Probabilistic coefficients $\zeta_p(f_{c,rep})$		
	$\zeta_p(f_{cm})$ [-]	$\zeta_p(f_{ck})$ [-]	$\zeta_p(f_{cd})$ [-]
$p=0.5$ (<i>m</i>)	1.00	1.07	1.18
$p=0.05$ (<i>k</i>)	0.75	0.80	0.89
$p=\Phi(-\alpha_R \cdot \beta);$ $\alpha_R=0.8, \beta=3.8$ (<i>d</i>)	0.59	0.63	0.67
$p=\Phi(-\alpha_R \cdot \beta);$ $\alpha_R=0.8, \beta=3.8$ (<i>d</i>)	0.55	0.59	0.65

As shown by Figure 3.19, the design probabilistic coefficient $\zeta_d(f_{c,rep})$ decreases when the reliability index β grows.

Then, the calibration of the reliability-based design expressions related to the original semi-empirical model (Eq.(3.10)) can be performed specifically as a function of the target reliability level.

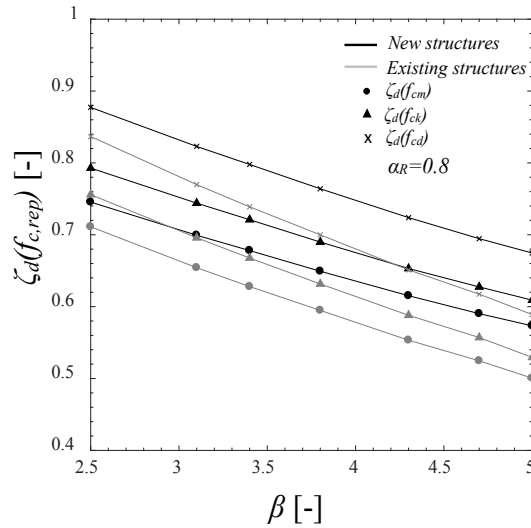


Figure 3.19: Variation of the design probabilistic coefficients $\zeta_d(f_{c,rep})$ and associated curve fitting differentiating between *new* and *existing* structures in function of the reliability index β ($\alpha_R=0.8$).

In Figure 3.19 is also showed the result of curve fitting for design probabilistic coefficients $\zeta_d(f_{c,rep})$ for the different choices of the representative value for concrete compressive strength $f_{c,rep}$ (i.e. f_{cm} , f_{ck} and f_{cd}) and for the differentiation between *new* and *existing* structures. The best fitting has been obtained with an exponential model with R-square equal to 0.99 for all the curves. This result descends clearly from the hypothesis of lognormality for all the main involved variables. The closed-form expressions for the different design probabilistic coefficient $\zeta_d(f_{c,rep})$ are reported in the following Eqs.(3.16a-b-c) and Eqs.(3.17a-b-c):

- *New structures:*

$$\zeta_d(f_{cm}) = 0.98 \cdot \exp(-0.106 \cdot \beta) \quad R^2 = 0.99 \quad (3.16a)$$

$$\zeta_d(f_{ck}) = 1.03 \cdot \exp(-0.106 \cdot \beta) \quad R^2 = 0.99 \quad (3.16b)$$

$$\zeta_d(f_{cd}) = 1.14 \cdot \exp(-0.106 \cdot \beta) \quad R^2 = 0.99 \quad (3.16c)$$

- *Existing structures:*

$$\zeta_d(f_{cm}) = 1.00 \cdot \exp(-0.139 \cdot \beta) \quad R^2 = 0.99 \quad (3.17a)$$

$$\zeta_d(f_{ck}) = 1.07 \cdot \exp(-0.140 \cdot \beta) \quad R^2 = 0.99 \quad (3.17b)$$

$$\zeta_d(f_{cd}) = 1.18 \cdot \exp(-0.139 \cdot \beta) \quad R^2 = 0.99 \quad (3.17c)$$

The 50% quantile $f_{st,m}$, the 5% characteristic $f_{st,k}$ and the reliability-based design $f_{st,d}$ expressions for the semi-empirical model proposed by *fib Model Code 2010* and *fib Bulletin 72* for tensile strength estimation of laps and anchorages can be evaluated according to Eq.(3.18a-b-c) in MPa and to the quantiles values listed in Tables 3.10 and 3.11, considering:

$$f_{st,p} = \zeta_p(f_{cm}) \cdot 54 \text{ MPa} \cdot \left(\frac{f_{cm}}{25 \text{ MPa}} \right)^{0.25} \left(\frac{l_b}{\Phi} \right)^{0.55} \left(\frac{25 \text{ mm}}{\Phi} \right)^{0.2} \left[\left(\frac{c_{\min}}{\Phi} \right)^{0.25} \left(\frac{c_{\max}}{c_{\min}} \right)^{0.1} + k_m K_{tr} \right]$$

[MPa] $p = m, k, d$

(3.18a)

$$f_{st,p} = \zeta_p(f_{ck}) \cdot 54 \text{ MPa} \cdot \left(\frac{f_{ck}}{25 \text{ MPa}} \right)^{0.25} \left(\frac{l_b}{\Phi} \right)^{0.55} \left(\frac{25 \text{ mm}}{\Phi} \right)^{0.2} \left[\left(\frac{c_{\min}}{\Phi} \right)^{0.25} \left(\frac{c_{\max}}{c_{\min}} \right)^{0.1} + k_m K_{tr} \right]$$

[MPa] $p = m, k, d$

(3.18b)

$$f_{st,p} = \zeta_p(f_{cd}) \cdot 54 \text{ MPa} \cdot \left(\frac{f_{cd}}{25 \text{ MPa}} \right)^{0.25} \left(\frac{l_b}{\Phi} \right)^{0.55} \left(\frac{25 \text{ mm}}{\Phi} \right)^{0.2} \left[\left(\frac{c_{\min}}{\Phi} \right)^{0.25} \left(\frac{c_{\max}}{c_{\min}} \right)^{0.1} + k_m K_{tr} \right]$$

[MPa] $p = m, k, d$

(3.18c)

In Table 3.12, an example of calculation using Eqs.(3.18a-b-c) is performed adopting $l_b=50\Phi$, $\Phi=12$ mm, $c_{\min}=\Phi$, $c_{\min}=c_{\max}$, $K_{tr}=0$ (no shear links) as geometric parameters and the following different resistance values:

- $f_{ck}=30 \text{ MPa}$;

- $f_{cm} = f_{ck} \cdot \exp(1.645 \cdot V_f) = 38.4 \text{ MPa}$ (according to the hypothesis of lognormal distribution for the cylinder concrete compressive strength with a coefficient of variation $V_f=0.15$);

- $f_{cd} = f_{ck}/\gamma_C = 20 \text{ MPa}$ ($\gamma_C=1.5$).

Table 3.12: Example of calculation - new structures.

Quantile	Representative values for concrete compressive strength		
	Eq.(3.18a)	Eq.(3.18b)	Eq.(3.18c)
	f_{cm}	f_{ck}	f_{cd}
$f_{st,m}$ [MPa]	582.0	581.6	582.0
$f_{st,k}$ [MPa]	467.8	468.0	467.1
$f_{st,d}$ [MPa] ($\alpha_R=0.8$; $\beta=3.8$)	388.0	388.8	388.0

As Eqs.(3.18a-b-c) are defined dependently from the choice for the representative values of concrete compressive strength, referring to the same probability p of underexceedance, the values of $f_{st,m}$, $f_{st,k}$ and $f_{st,d}$ are almost identical along the rows of Table 3.12 (i.e., the small differences between values are due to unavoidable numerical approximations in the definition of the multiplicative coefficients).

Then, the design relationships expressed by means Eqs.(3.18a-b-c) can be used indifferently for design purposes, as they comply with the target reliability level required by the codes.

In next Subsection, the proposal for an *average bond strength* expression is derived in order to design laps and anchorages length.

3.3.5 Expression for ultimate bond strength

In this Subection, the reliability-based expression for *basic average bond strength* $f_{b,0}$ is derived starting from the results of Section 3.3.4.

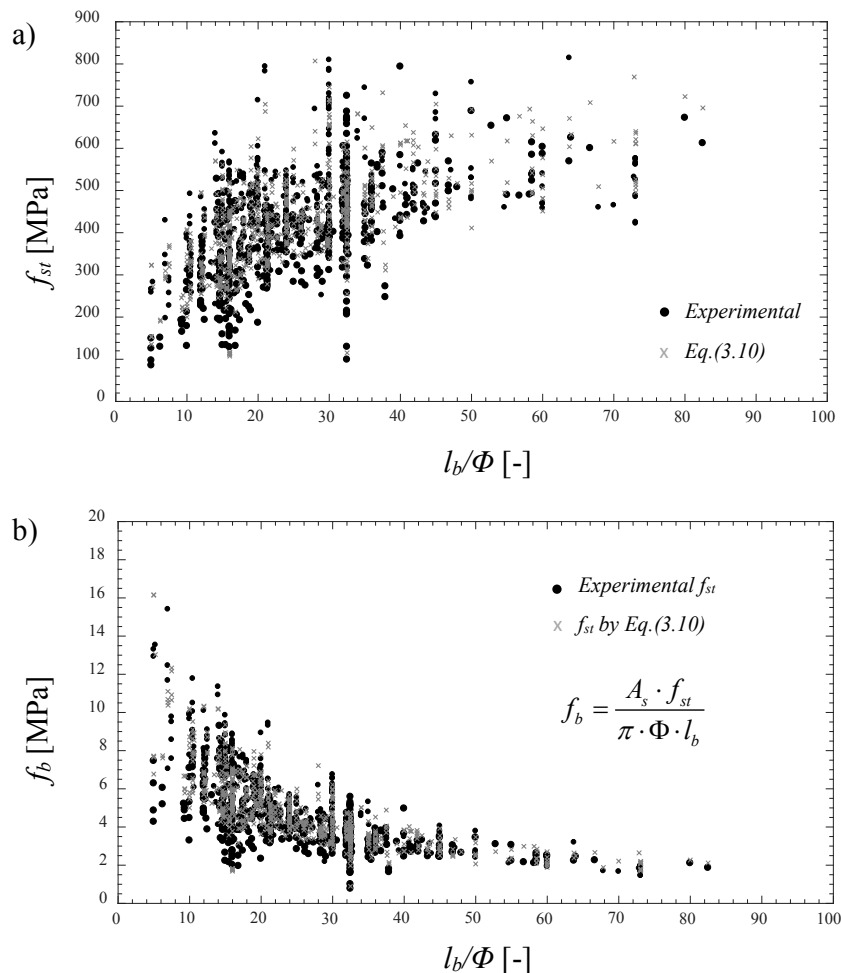


Figure 3.20: Comparison in terms of laps strength f_{st} between experimental results and Eq.(3.10) predictions in function of the ratio between lap length l_b and bar diameter Φ (entire database) (a); comparison in terms of bond strength f_b between experimental results and Eq.(3.10) predictions in function of the ratio between lap length l_b and bar diameter Φ (entire database) (b).

The Figure 3.20(a-b) is obtained on the base of the experimental database collecting all the results (Section 3.3.3). Figure 3.20(a) shows that the lap strength f_{st} versus lap length on bar diameter l_b/Φ increases less than proportionally. It also shows that Eq. (3.10) fits well all the experimental results. F

It is therefore clear that a linear increase of the bar stress σ_s to be transferred at ULS leads to a more than proportional increase of the design lap or anchorage length. In fact, evaluating ultimate bond strength f_b by means equilibrium equation (Eq.(3.8)) for both experimental results and predictions by means Eq.(3.10), Figure 3.20(b) shows a non-linear decrease of bond strength f_b for an increase of the ratio l_b/Φ . As a consequence, a model for *basic average bond strength* $f_{b,0}$ devoted to design laps and anchorages length should consider this relevant non-linearity, contrary to what happens in *EN 1992-1-1* and *fib Model Code 2010*.

In the following the estimation of the reliability-based *basic average bond strength* $f_{b,p,0}$ is performed assuming as representative value for concrete compressive strength ($f_{c,rep}$) the 5% characteristic one (f_{ck}). However, the same procedure can be applied considering the expressions with different representative values $f_{c,rep}$ (i.e. mean value f_{cm} or design value f_{cd}).

First of all, the reliability-based *basic lap strength* $f_{st,p,0}$ in absence of shear reinforcements or effective links and with minimum cover as required in codes ($c_{min} = \Phi$ and $c_{min} = c_{max}$) can be expressed (consistently with Eq.(3.10)) both for *new* and *existing* structures as:

$$f_{st,p,0} = \zeta_p (f_{ck}) \cdot 54 \text{ MPa} \cdot \left(\frac{f_{ck}}{25 \text{ MPa}} \right)^{0.25} \left(\frac{l_b}{\Phi} \right)^{0.55} \left(\frac{25 \text{ mm}}{\Phi} \right)^{0.2} \text{ [MPa]} \quad (3.19)$$

The contribution of cover and shear links to bond strength can be easily re-accounted for after the probabilistic calibration.

The Eq. (3.19) can be rearranged in order to determine the *basic bond length* l_b/Φ in function of the maximum bar stress transferable by the lap according to probability p of under-exceedance $f_{st,p,0}$:

$$\left(\frac{l_b}{\Phi} \right)_p = \left(\frac{f_{st,p,0}}{\zeta_p (f_{ck}) \cdot 54 \text{ MPa}} \right)^{1.82} \left(\frac{f_{ck}}{25 \text{ MPa}} \right)^{-0.45} \left(\frac{25 \text{ mm}}{\Phi} \right)^{-0.36} \text{ [-]} \quad (3.20)$$

Reasonably, the lap strength $f_{st,p,0}$ should be assumed equal to the bar stress σ_s that the lap needs to transfer with probability of under-exceedance p :

$$f_{st,p,0} = \sigma_s \quad (3.21)$$

The introduction of Eq.(3.21) in Eq.(3.20) yields to:

$$\left(\frac{l_b}{\Phi} \right)_p = \left(\frac{\sigma_s}{\zeta_p (f_{ck}) \cdot 54 \text{ MPa}} \right)^{1.82} \left(\frac{f_{ck}}{25 \text{ MPa}} \right)^{-0.45} \left(\frac{25 \text{ mm}}{\Phi} \right)^{-0.36} \text{ [-]} \quad (3.22)$$

In principle, the Eq.(3.22) may be adopted directly for laps and anchorage design purposes (involving also missing terms related to concrete cover and shear links confinement). In fact, the concept of *average bond strength* has very limited physical meaning facing to the complexity of the actual bond mechanism. However, in common practice the concept of *average bond strength* is still strongly ingrained and its derivation procedure is also proposed in the present dissertation.

The *basic average bond strength* $f_{b,p,0}$ related to a bar stress σ_s may be expressed by imposing the equilibrium of each lapped bar and assuming the simplification of uniform distribution of bond stresses along the lap (see Sub-section 3.3.1):

$$f_{b,p,0} = \frac{\pi \cdot \Phi^2}{4 \cdot \pi \cdot \Phi \cdot l_b} \cdot \sigma_s = \frac{\sigma_s}{4 \cdot \left(\frac{l_b}{\Phi}\right)_p} \quad [MPa] \quad (3.23)$$

Then, substituting Eq.(3.21) into Eq.(3.23):

$$f_{b,p,0} = \frac{\sigma_s}{4 \cdot \left(\frac{l_b}{\Phi}\right)_p} = \frac{1 \text{ MPa}}{4 \cdot \left(\frac{1 \text{ MPa}}{\zeta_p(f_{ck}) \cdot 54 \text{ MPa}}\right)^{1.82} \cdot (\sigma_s)^{0.82} \left(\frac{f_{ck}}{25 \text{ MPa}}\right)^{-0.45} \left(\frac{25 \text{ mm}}{\Phi}\right)^{-0.36}} \quad [MPa] \quad (3.24)$$

and calling:

$$C_p(f_{ck}) = \frac{1 \text{ MPa}}{4 \cdot \left(\frac{1 \text{ MPa}}{\zeta_p(f_{ck}) \cdot 54 \text{ MPa}}\right)^{1.82}} \quad [MPa] \quad (3.25)$$

The Eq.(3.23) may be rewritten as

$$f_{b,p,0} = C_p(f_{ck}) \cdot \left(\frac{1 \text{ MPa}}{\sigma_s}\right)^{0.82} \left(\frac{f_{ck}}{25 \text{ MPa}}\right)^{0.45} \left(\frac{25 \text{ mm}}{\Phi}\right)^{0.36} \quad [MPa] \quad (3.26)$$

with $p = m, k, d$.

The probabilistic coefficients $C_p(f_{ck})$ for *average bond strength* are consistent with the probabilistic model and the influence of resistance model uncertainty on laps and anchorages tensile strength evaluation. The coefficient $C_p(f_{ck})$ depends from the coefficient $\zeta_p(f_{ck})$ and relevant values are reported in Table 3.13. Assuming bond strength as a property dependent from the level of stress to be transferred (complying to experimental evidence), from a physical point of view, the coefficients $C_p(f_{ck})$ expressed in [MPa] represents the *basic average bond strength* evaluated in order to transfer 1 MPa with concrete having f_{ck} set equal to 25 MPa and reinforcement bar with diameter equal to 25 mm according to a level of reliability identified by the probability of under-exceedance p .

Table 3.13: Values of the probabilistic coefficients $C_p(f_{ck})$ in the function of representative value selected for concrete compressive strength for the case of *new* and *existing* structures.

Quantile	Probabilistic coefficient for average bond strength $C_p(f_{ck})$ [MPa]	
	New structures	Existing structures
$p=0.5$ (m)	378	400
$p=0.05$ (k)	254	239
$p=\Phi(-\alpha_R \cdot \beta)$; $\alpha_R=0.8, \beta=3.8$ (d)	182	154
$p=\Phi(-\alpha_R \cdot \beta)$; $\alpha_R=0.8, \beta=3.8$ (d)	165	135

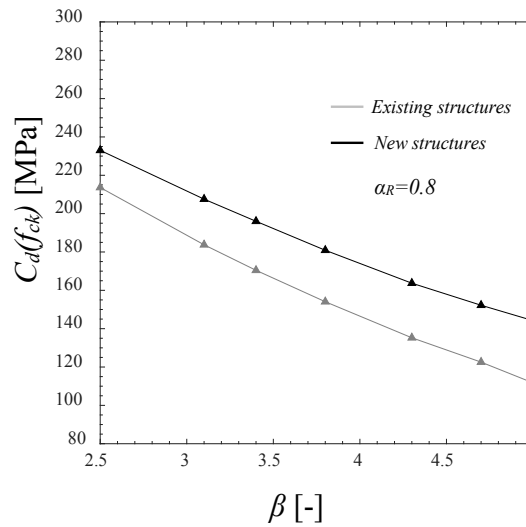


Figure 3.21: Variation of the design probabilistic coefficients $C_d(f_{ck})$ for average bond strength and associated curve fitting differentiating between *new* and *existing* structures in function of the reliability index β ($\alpha_R=0.8$).

The trend of variation of the design probabilistic coefficient for ultimate average bond strength $C_d(f_{ck})$ in the function of the reliability index β is reported in Figure 3.21. As for coefficient $\zeta_p(f_{ck})$, the curve fitting leads to an exponential model for probabilistic coefficient for average bond strength $C_d(f_{ck})$ with R-square equal to 0.99. The expression for the exponential regression are reported by Eq.(3.27) and Eq.(3.28).

- *New structures:*

$$C_d(f_{ck}) = 378 \cdot \exp(-0.193 \cdot \beta) \quad R^2 = 0.99; \text{ [MPa]} \quad (3.27)$$

- *Existing structures:*

$$C_d(f_{ck}) = 404 \cdot \exp(-0.254 \cdot \beta) \quad R^2 = 0.99; \text{ [MPa]} \quad (3.28)$$

Finally, according to *fib Bulletin 72*, the basic formulation for $f_{b,d,0}$ may be completed considering also the effect of confinement due concrete cover different from the minimum and presence of shear links along the lap or anchorage. Then the *average design bond strength* $f_{b,d}$ can be calculated as follows:

$$f_{b,d} = f_{b,d,0} \cdot (\alpha_2 + \alpha_3) \quad (3.29)$$

With:

- $\alpha_2 = [(c_{min}/\Phi)^{0.25} \cdot (c_{max}/c_{min})^{0.1}]^{1.82}$ is the coefficient for concrete cover confinement effect (equal to unit in the case of minimum cover);
- $\alpha_3 = k_d \cdot K_{tr}$ is the coefficient for links confinement effect with $k_d = 20, 10, 0$ instead of $k_m = 12, 6, 0$ evaluated as shown in Figure 3.6 following *fib Bulletin 72* and *fib Model Code 2010*.

Comparison with current codes

In the present section, the comparison between the provisions of EN 1992-1-1, *fib Model Code 2010* and the proposed model for calculation of the *basic average bond strength* $f_{b,d,0}$ and the *required anchorage length* $l_{b,req}$ is reported. The comparison is proposed according to the hypotheses of minimum requirement in terms of concrete cover (i.e., $c_{min} = c_{max}$, $c_{min} = \Phi$) and absence of shear reinforcements (i.e., $K_{tr} = 0$).

First of all, according to the latter hypotheses and Table 3.13, Eq.(3.29) can be rewritten as follows:

- *new* structures ($\beta = 3.8$, 50 years of service life, moderate consequences of failure):

$$f_{b,d,0} = 182 \text{ MPa} \cdot \left(\frac{1 \text{ MPa}}{\sigma_s} \right)^{0.82} \left(\frac{f_{ck}}{25 \text{ MPa}} \right)^{0.45} \left(\frac{25 \text{ mm}}{\Phi} \right)^{0.36} \quad [\text{MPa}] \quad (3.31)$$

- *existing* structures ($\beta = 3.8$, 50 years of service life, moderate consequences of failure):

$$f_{b,d,0} = 154 \text{ MPa} \cdot \left(\frac{1 \text{ MPa}}{\sigma_s} \right)^{0.82} \left(\frac{f_{ck}}{25 \text{ MPa}} \right)^{0.45} \left(\frac{25 \text{ mm}}{\Phi} \right)^{0.36} \quad [\text{MPa}] \quad (3.32)$$

According to the EN 1992-1-1 and *fib Model Code 2010*, $f_{b,d,0}$ can be calculated as reported in Table 3.14.

The *required anchorage length* $l_{b,req}$ can be evaluated according to the following equation:

$$\frac{l_{b,req}}{\Phi} = \frac{\sigma_{sd}}{4 \cdot f_{b,d,0}} \quad (3.33)$$

Table 3.14: Evaluation of bond strength according to EN 1992-1-1 and *fib* Model Code 2010.

Code	Bond strength f_{bd} [MPa]	Other parameters
EN 1992- 1-1	$f_{b,d,0} = 2.25 \cdot \eta_1 \cdot \eta_2 \cdot f_{ctd}$	$f_{ctd} = \frac{0.7 \cdot 0.3 \cdot (f_{ck})^{2/3}}{\gamma_C = 1.5} \leq C50 / 60$ $\eta_1 = 1$ (good bond) $\eta_2 = 1$ ($\Phi \leq 32mm$)
<i>fib</i> Model Code 2010	$f_{b,d,0} = \frac{\eta_1 \cdot \eta_2 \cdot \eta_3 \cdot \eta_4 \cdot \left(\frac{f_{ck}}{25}\right)^{0.5}}{\gamma_C = 1.5}$	$\eta_1 = 1.75$ (ribbed bars) $\eta_2 = 1$ (good bond) $\eta_3 = 1$ ($\Phi \leq 25mm$) $\eta_4 = 1$ (steel grade 500)

The comparison mentioned above is proposed in Figure 4 in function of the stress σ_{sd} according to the expressions reported in Table 3, assuming $\Phi=16$ mm, $f_{ck}=25$ MPa and steel *Grade 500*.

Firstly, it can be noted that according to Eqs.(3.31-3.32) the required anchorage length $l_{b,req}/\Phi$ increases more than proportionally in function of the design stress σ_{sd} to be transferred at ULS.

In fact, the experimental evidence deriving from laboratory tests on laps and anchorages shows that the increment of the lap or anchorage length gives origin to an increment of the lap/anchorage strength that is less than proportional (Figure 3.20(a-b)). This non-linear behaviour is not accounted for by the models proposed by EN 1992-1-1 and *fib Model Code 2010*. In fact, the latter proposes a constant value of bond strength f_{bd} which, according to Eq.(3.33), originates a linear variation as a function of σ_{sd} . Secondly, EN1992-1-1 seems to be unsafe when high level of stresses should be transferred at ULS (i.e., $\sigma_{sd} \geq 250-300$ MPa). This result is in agreement with the observations performed by *Cairns, 2014*. Conversely, *fib Model Code 2010* tends to be too conservative, especially when low level of stress should be carried at ULS.

Finally, concerning the required laps and anchorages length calculated in compliance with EN1992-1-1 and *fib Model Code 2010*, the level of reliability and the associated probability of structural failure are unknown, differently from what happens using Eqs.(3.31-3.32).

The Figures 3.22 and 3.23 reports the comparison of the mentioned above models for bond strength and laps/anchorage length evaluation in case of different combination of the involved parameters.

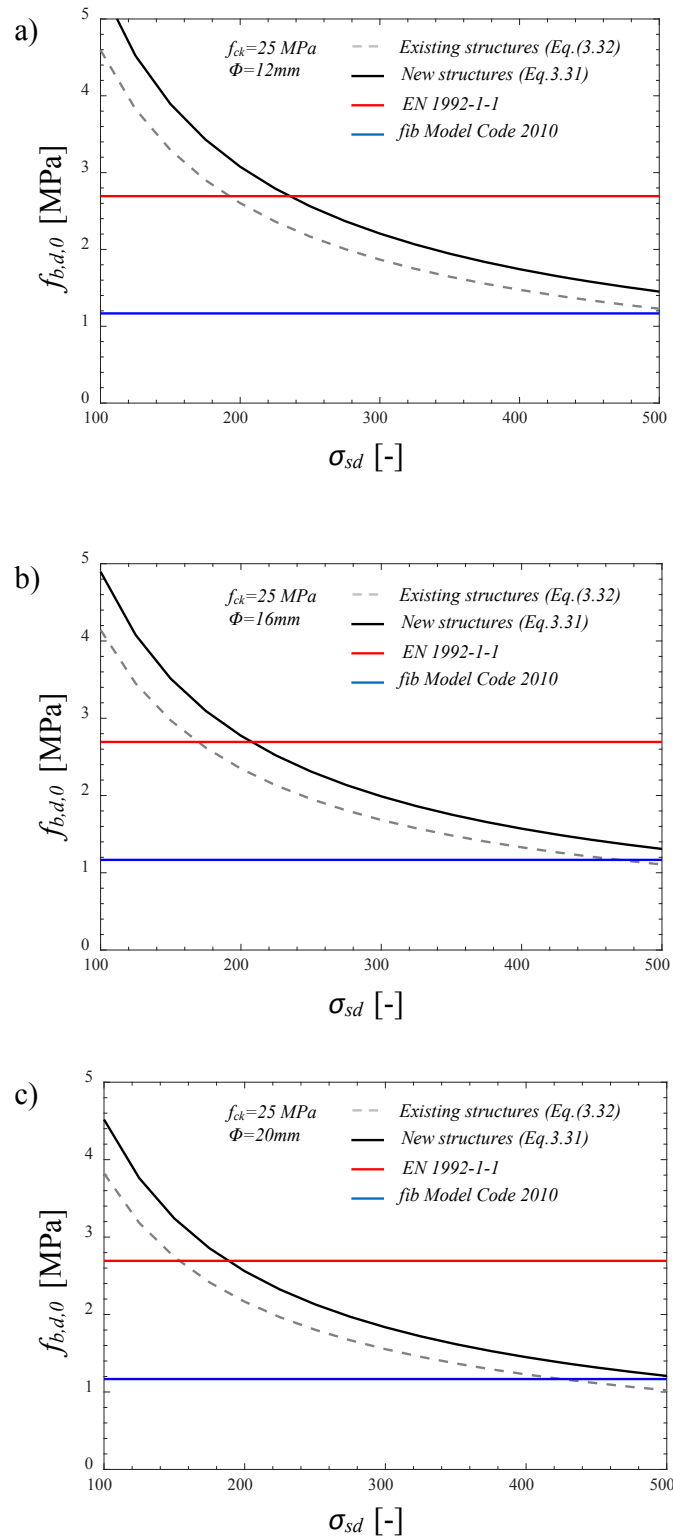


Figure 3.22: Bond strength $f_{b,d,0}$ evaluated according to EN1992-1-1, *fib* Model Code 2010 and proposed models. $\Phi = 12 \text{ mm}$ (a), $\Phi = 16 \text{ mm}$ (b), $\Phi = 20 \text{ mm}$ (c), $f_{ck} = 25 \text{ MPa}$ and steel Grade 500.

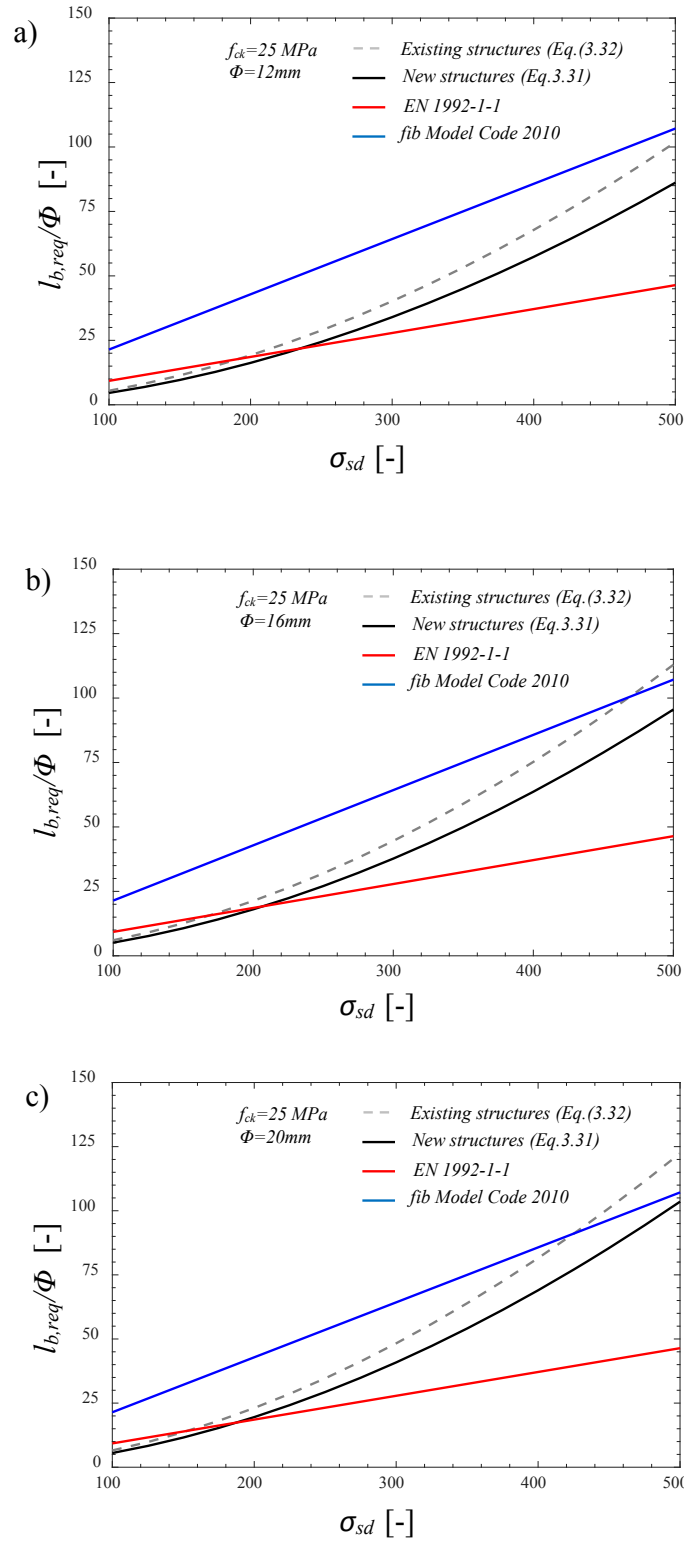


Figure 3.23: Required anchorage length $l_{b,req}/\Phi$ evaluated according to EN1992-1-1, fib Model Code 2010 and proposed models. $\Phi=12\text{mm}$ (a), $\Phi=16\text{mm}$ (b), $\Phi=20\text{mm}$ (c), $f_{ck}=25\text{MPa}$ and steel Grade 500.

3.3.6 Validation of the proposed framework and final comments

In this Subsection two different validation of the general framework applied in Subsection 3.3.4 are reported. First of all the mean and the characteristic expressions are compared and validated on the base of the experimental results for both *new* and *existing* structures.

Subsequently, the results of Subsection 3.3.4 are compared to the ones derived from a theoretical approach proposed by *Taerwe, 1993* valid just for lognormal probabilistic models.

Experimental validation

The validation of the results obtained by the probabilistic calibration proposed in Subsection 3.3.4 can be performed by means of comparison with the sample of experimental outcomes. The validation should be performed with the same samples adopted for the statistical analysis and then differentiating between *new* and *existing* structures.

First of all, the following ratio should be addressed:

$$\mathcal{G}_m = \frac{f_{st,Experimental}}{f_{st,m}} \quad (3.29)$$

$$\mathcal{G}_k = \frac{f_{st,Experimental}}{f_{st,k}} \quad (3.30)$$

where $f_{st,Experimental}$ is the experimental outcome for lap or anchorage tensile strength from the experimental database (filtered according to the hypothesis of *new* or *existing* structures); $f_{st,m}$ is the associated mean value of ultimate lap or anchorage strength (i.e. Eq.(3.18a-b-c) with $p=0.5$ (m)); $f_{st,k}$ is the associated characteristic value of ultimate lap or anchorage strength (i.e. Eq.(3.18a-b-c) with $p=0.05$ (k)).

The reliability-based expressions proposed by Eq.(3.18a-b-c) can be considered as validated (i.e. consistent with the associated probability of under-exceedance) if the following conditional probabilities are fulfilled (differentiating between *new* and *existing* structures):

$$P[\mathcal{G}_m \leq 0 | new / existing structures] \approx 0.5 \quad (3.31)$$

$$P[\mathcal{G}_k \leq 0 | new / existing structures] \approx 0.05 \quad (3.32)$$

Concerning the case of *new* structures, Figure 3.24 shows that the Eq.(3.31) and Eq.(3.32) are fulfilled with good rate of accuracy.

In fact, the expression for mean value $f_{st,m}$ of laps and anchorage strength returns unsafe outcomes of the ratio \mathcal{G}_m in the 50.7% of the cases, whereas the expression for characteristic value $f_{st,k}$ returns unsafe results in the 4.6% of the cases.

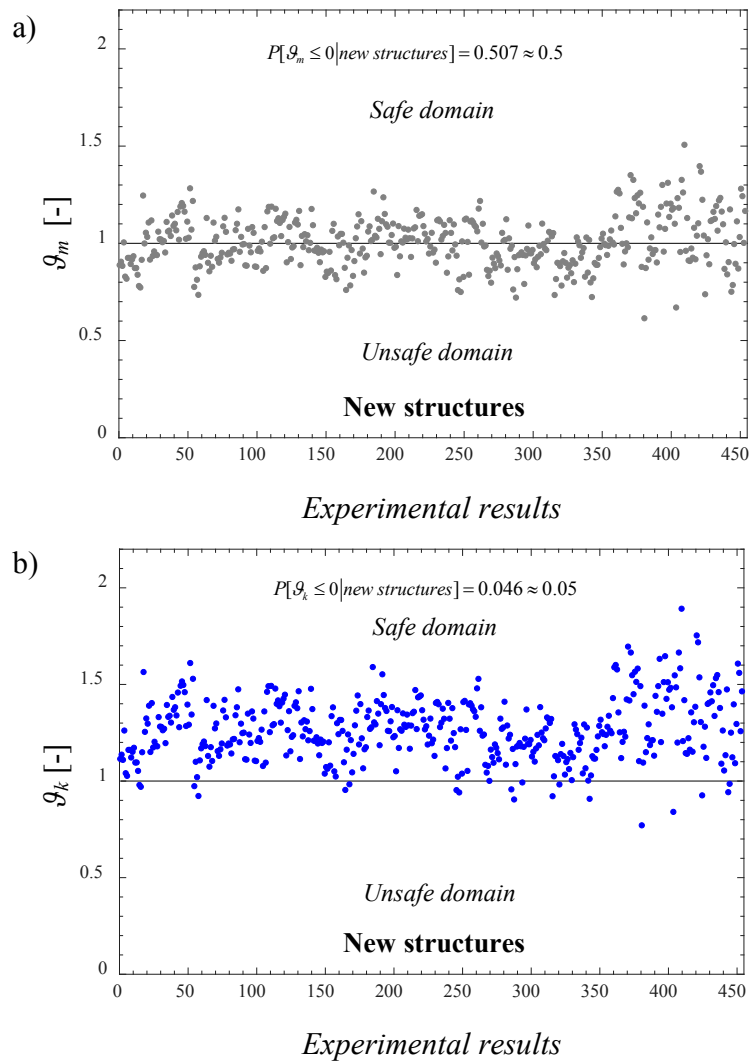


Figure 3.24: Experimental validation of the mean ($p=0.5$ (m)) (a) and of the characteristic ($p=0.05$ (k)) (b) expressions reported by Eq.(3.18a-b-c) concerning the sample for *new* structures.

Relating to the case of *existing* structures, Figure 3.25 leads to similar conclusions. In details, the expression for mean value $f_{st,m}$ of laps and anchorage strength returns unsafe outcomes of the ratio g_m in the 50.4% of the cases, whereas the expression for characteristic value $f_{st,k}$ returns unsafe results in the 5.2% of the cases.

In Table 3.14 are summarized the data necessary for the estimation of the conditional probabilities expressed by Eq.(3.31) and Eq.(3.32).

The number of samples collected in the filtered databases for new and existing structures are sufficient in order to validate the mean and the characteristic expressions. In fact, in order to estimate the probability of under-exceedance related to the characteristic value (i.e. 0.05) around 200 samples are sufficient.

On the contrary, the number of experimental results does not allow to validate the design expressions. In fact, to this purpose, a much higher number of experimental results is required (more than 1000, at minimum).

Table 3.14: Experimental samples and validation of the calibrated equations.

	New structures	Existing structures
N° results	454	677
N° results with $\vartheta_m \leq 0$	230	341
N° results with $\vartheta_k \leq 0$	21	35
$P[\vartheta_m \leq 0]$ [-]	0.507	0.504
$P[\vartheta_k \leq 0]$ [-]	0.046	0.052

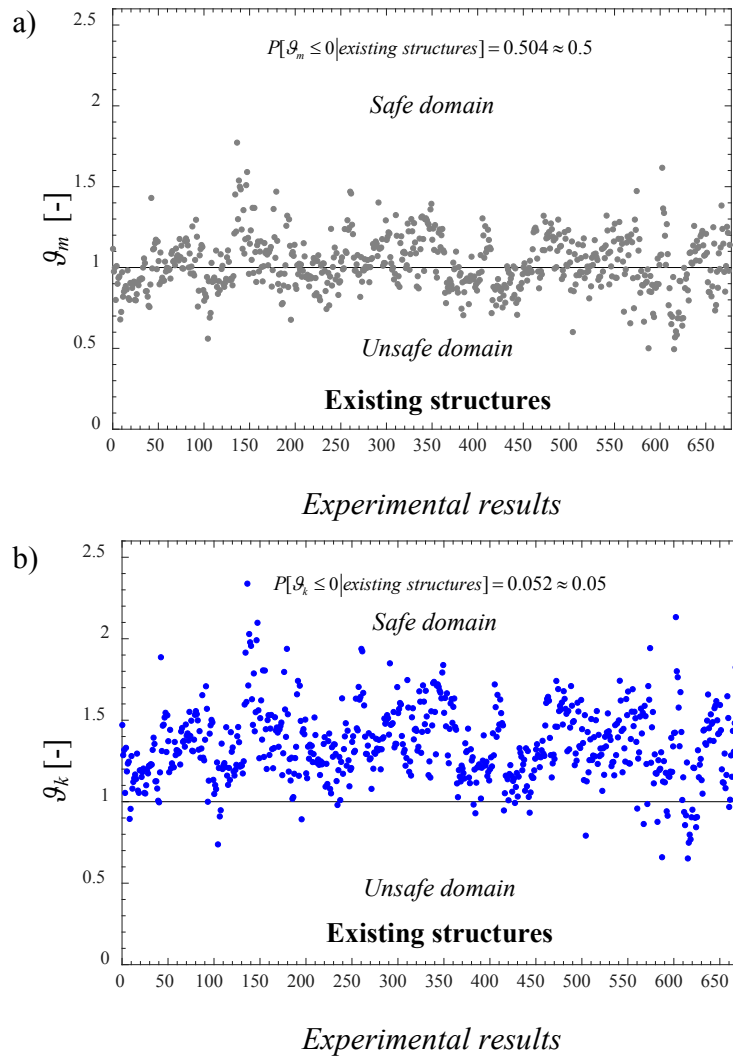


Figure 3.25: Experimental validation of the mean ($p=0.5$ (m)) (a) and of the characteristic ($p=0.05$ (k)) (b) expressions reported by Eq.(3.18a-b-c) concerning the sample for *existing* structures.

Then the experimental validation can be considered satisfied for Eq.(3.18a-b-c) for both the samples related to *new* and *existing* structures.

Comparison with theoretical approach

In the following, the comparison of the framework proposed in Section 3.2 with the calculation methodology proposed by *Taerwe, 1993* and furtherly applied by *König and Fischer, 1995* is proposed. It maintains its validity both for *new* and *existing* structures.

According to the probabilistic model described in Subsection 3.3.4, the resistance R turns out to be a lognormal random variable as ϑ and f_c are lognormally distributed random variables too.

Then, the application to Eq.(3.10) of the procedure reported *Taerwe, 1993* leads to the estimation of the quantiles of the *resistance random variable* R as follow

$$\begin{aligned} R_p &= \mu_R \cdot \exp(-h_p \cdot \sigma_{\ln R}) = \\ &= \mu_\vartheta \cdot f_{cm}^{0.25} \cdot g(a_j) \cdot \exp\left(-h_p \cdot \sqrt{\ln(V_\vartheta^2 + 1) + 0.0625 \cdot \ln(V_f^2 + 1)}\right) \end{aligned} \quad (3.33)$$

where $j = m, k, d$ with $m =$ mean value; $k =$ characteristic value (i.e. quantile 5%); $d =$ design value in function of a certain reliability index β ; μ_ϑ mean value and coefficient of variation V_ϑ of the resistance model uncertainty; $g(a_j)$ defined according to Eq.(3.13); $\sigma_{\ln R}$ standard deviation of the logarithm of the variable R .

The coefficients h_p defines the quantile of the variable R as: $h_m = 0$ for mean value; $h_k = 1.645$ for characteristic value; $h_d = \alpha_R \cdot \beta$ for design value, where the coefficient α_R is the FORM correction factor assumed equal to 0.8 for dominant resistance variables (*JCSS Probabilistic Model Code, 2001*) and β is the reliability index.

The global coefficient of variation V_R of lap strength taking into account the random variability of model uncertainties and concrete compressive strength may be evaluated with the following expression:

$$V_R = \sqrt{(V_\vartheta^2 + 1) \cdot (V_{f_c}^2 + 1)^{0.0625} - 1} \quad (3.34)$$

The quantile R_p is given in Eq.(3.33) in function of the mean value of concrete compressive strength f_{cm} , but codes provisions are usually expressed in function of the characteristic value f_{ck} . In compliance to the procedure proposed in previous sections and to structural codes, the introduction of f_{ck} in Eq.(3.33) should be done consistently with the hypothesis of lognormal distribution for cylinder concrete compressive strength as follows:

$$f_{ck} = f_{cm} \cdot \exp\left(-h_k \cdot \sqrt{\ln(V_{f_c}^2 + 1)}\right) \quad (3.35)$$

then:

$$f_{cm} = f_{ck} \cdot \exp\left(h_k \cdot \sqrt{\ln(V_{f_c}^2 + 1)}\right) \quad (3.36)$$

Next, the theoretical approach is proposed accounting for as representative value of concrete compressive strength the 5% characteristic one (f_{ck}). However, according to *Taerwe, 1993*, the derivation procedure can be easily extended to other representative values evaluating different quantiles of the lognormal distribution for concrete compressive strength from Eq.(3.35).

The general formulation of a quantile of R , in function of the concrete characteristic compressive strength f_{ck} , can be calculated substituting Eq.(3.36) in Eq.(3.33):

$$R_p = \mu_\theta \cdot f_{ck}^{0.25} \cdot g(a_j) \cdot \exp(a_1 - a_{2,p}) \quad (3.37)$$

with:

$$a_1 = 0.25 \cdot 1.645 \cdot \sqrt{\ln(V_{f_c}^2 + 1)} \quad (3.38)$$

and:

$$a_{2,p} = h_p \cdot \sqrt{\ln(V_\theta^2 + 1) + 0.0625 \cdot \ln(V_{f_c}^2 + 1)} \quad (3.39)$$

Finally, it is possible to define the probabilistic coefficient for lap strength $\zeta_p(f_{ck})$ as follows:

$$\zeta_p(f_{ck}) = \mu_\theta \cdot \exp(a_1 - a_{2,p}) \quad (3.40)$$

The exponential formulation reported by Eq.(3.40) is fully consistent with the result obtained by the results and the curve fitting proposed in Subsection 3.3.4, confirming the validity of the general framework proposed in Section 3.2 (that differently is valid also for probabilistic model different from the lognormal one).

Finally, according to Eq.(3.18b) the quantiles R_p of the *resistance random variable* R become:

$$R_p = f_{st,p} = \zeta_p(f_{ck}) \cdot 54 \text{ MPa} \cdot \left(\frac{f_{ck}}{25 \text{ MPa}}\right)^{0.25} \left(\frac{l_b}{\Phi}\right)^{0.55} \left(\frac{25 \text{ mm}}{\Phi}\right)^{0.2} \left[\left(\frac{c_{\min}}{\Phi}\right)^{0.25} \left(\frac{c_{\max}}{c_{\min}}\right)^{0.1} + k_m K_{tr} \right] \quad (3.41)$$

with $p = m, k, d$ for mean, 5% characteristic and design.

In Table 3.15 the comparison between the results of Eq.(3.40) and the ones obtained with Eq.(3.16b) and Eq.(3.17b) is proposed. The results of the general framework are consistent with the results of the theoretical approach (*Taerwe, 1993*).

Table 3.15: Comparison between the values of the probabilistic coefficients $\zeta_p(f_{ck})$ for the general framework of Sub-section 3.3.4 and the methodology of *Taerwe, 1993* for the case of *new* and *existing* structures.

Quantile	Probabilistic coefficient $\zeta_p(f_{ck})$ [-]			
	General framework (Subsection 3.3.4)		Taerwe, 1993 Eq.(3.40)	
	New structures Eq.(3.16b)	Existing Structures Eq.(3.17b)	New structures	Existing structures
$p=0.5$ (m)	1.03	1.07	1.04	1.07
$p=0.05$ (k)	0.83	0.80	0.83	0.80
$p=\Phi(-\alpha_R\beta);$ $\alpha_R=0.8, \beta=3.8$ (d)	0.69	0.63	0.69	0.63
$p=\Phi(-\alpha_R\beta);$ $\alpha_R=0.8, \beta=3.8$ (d)	0.65	0.59	0.66	0.59

The coefficient of variation of the *resistance random variable R* derived by Eq.(3.34) is also compared to the one of the *auxiliary random variable Z(f_c, ϑ ;f_{cm})* obtained with Eq.(3.15a) within Table 3.16. Again, the results are in agreement between the two approaches.

Table 3.16: Comparison between the coefficient of variation for resistance random variable R with general framework of Sub-section 3.3.4 and the methodology of *Taerwe, 1993* for the case of *new* and *existing* structures.

	General framework (Subsection 3.3.4 – $Z(f_c, \vartheta; f_{cm})$)		Taerwe, 1993 Eq.(3.34)	
	New structures	Existing Structures	New structures	Existing structures
Coefficient of variation of resistance random variable R V_R [-]	0.13	0.17	0.13	0.18

Laps and anchorages design: what level of reliability?

The choice of the level of reliability for design is one of the key choices drafting structural codes. In particular, the selection of the level of reliability to be adopted for laps and anchorages design for ordinary reinforced concrete structures is still strongly debated by researchers and practitioners. As discussed in Chapter 1, the target reliability levels that should be adopted in structural design of *new* and *existing* concrete structures are suggested in *ISO 2394, 2015*, *fib Model Code 2010*, *fib Bulletin 80* and *EN 1990*. Concerning ordinary structures with 50 years of service life, the accepted target reliability level is represented by $\beta = 3.8$, or $\beta = 4.3$, respectively in case of moderate or high consequences of structural failure.

Laboratory tests on lap splices and anchorages are commonly performed on four points bending tests with all bars lapped at the same section. Moreover, laps and anchorages are located in a constant bending moment region, therefore the positive effect of shear on lap strength (i.e. bending moment variability along the lap as described in *Souza, 2016*) is neglected. These common configuration leads, in general, to the worst case of *splitting* failure mode (see Subsection 3.3.1).

The conditions proposed in laboratory tests rarely occur in actual structures as the laps are almost never placed in the zones of maximum bending moment, not all the bars are, generally, lapped in the same section, concrete cover and shear reinforcements or links are sufficiently provided. Therefore, it is very difficult to find in literature (*Cairns and Eligehausen, 2014*) cases of structural collapse due to *splitting* bond failure, which may occur mainly because of wrong detailing and design.

Laps and anchorages are generally designed to transfer the design tensile stress σ_{sd} of the bar at ultimate limit state, but, if it is necessary to provide a certain level of ductility (e.g. non-redundant structural elements, such as the case of cantilever structures - as earth retaining walls), they should be designed to transfer the yielding strength f_{yd} of the bar, but not with a level of reliability higher than the one related to the whole structure (commonly designed according to $\beta = 3.8$ - moderate consequences of failure – in case of new structures with 50 years of service life). Then, structural redundancy and “good” construction practice and detailing (as laps staggering - *Cairns, 2014* -, their positioning in lowly stressed regions and minimum concrete cover requirements) suggest that, according to *ISO 2394, 2015*, *fib Model Code 2010*, *fib Bulletin 80* and *EN 1990*, a reliability index $\beta = 3.8$ should be considered for laps and anchorages design in the case of ordinary reinforced concrete structures with 50 years of service life and moderate consequences of failure.

Chapter 4

Advances in safety formats for NLFEAs of reinforced concrete structures

4.1 Introduction

The present Chapter deals with two important aspects concerning the application of NLFEA to design and assessment of reinforced concrete structures according to Section 2.3.

First of all, the *model uncertainty safety factor* γ_{Rd} for NLFEAs of reinforced concrete structures has been investigated. Various experimental tests concerning different typologies of structures with different behaviours and failure modes, i.e., walls, deep beams, panels, are simulated by means of appropriate two-dimensional finite elements structural models (i.e., plane stress configuration). Several NLFE structural models are defined to investigate the model uncertainty influence on the 2D NLFEAs of reinforced concrete structures in terms of global resistance, considering different modelling hypotheses (i.e., *epistemic* uncertainties). Then, a consistent treatment of the resistance model uncertainties is proposed following a Bayesian approach. After that, the mean value and the coefficient of variation characterizing the resistance model uncertainties are identified. Finally, the *model uncertainty safety factor* γ_{Rd} is evaluated according to the reliability differentiation defined by *fib Model Code 2010* (Section 1.3).

Secondly, the comparison of the different *safety formats* described in Section 2.3 for the estimation of the design strength of different reinforced concrete structures is performed. Specifically, non-linear finite element models are properly defined to reproduce different experimental tests. Successively, several non-linear finite element analyses are carried out in compliance with the different safety formats experimentally tested member in order to compare and discuss the results in terms of resistance and failure mode. In fact, the different safety formats are investigated to demonstrate if they are able to estimate the corresponding design global resistance capacities and to capture possible modifications in the *failure mode* for each structure. In order to apply non-probabilistic safety formats also in the critical cases due to their reduced computational effort, updated values of the aleatory uncertainty partial safety factor are proposed for the assessment of the design global resistance. Finally, a code format framework based on the levels of approximation approach *LoAs* is defined and commented.

4.2 Reliability-based evaluation of the resistance model uncertainty safety factor for NLFEAs

In general, the uncertainties related to the material properties (i.e. aleatory uncertainties) are well known and assessed is structural reliability and, specifically, within the methodologies proposed by the different safety formats for NLFEA.

Conversely, the level of uncertainty related to the definition of the resistance model (i.e. model uncertainty) adopting NLFE models turns out to be complex to be estimated and it is still object of discussion.

The numerical models commonly used for NLFEAS as well as the predicted response are merely estimations and approximations of the actual structural behavior of a structural member. In fact, the prediction of the actual structural response through NLFEAs is denoted by a certain level of uncertainty because any model that aims to describe the actual structural response of structural systems neglect, inevitably, some more or less important aspects as discussed in Section 1.2

In general, the definition of a structural model grounds on the basic principles of mechanics as equilibrium of forces, displacements compatibility and constitutive laws. Specifically, focusing on NLFEAs, the mentioned above basic principles are met by means iterative solution methods (e.g. Newton-Raphson algorithm, Arch-length algorithm) that leads, inevitably, to an approximation of the exact solution for the structural response. Furthermore, the different assumptions related to the equilibrium, kinematic compatibility and constitutive equations always leads to diverse solutions for the specific structural problem. Then, the multiplicity of choices that may be performed defining a NLFE model leads to a further degree of uncertainty having epistemic nature.

It implies that, consistently with the methodologies proposed by the safety formats for NLFEAs, the reliability-based calibration of the partial safety factor γ_{Rd} for the resistance modelling uncertainties (i.e. model uncertainty safety factor) is an important topic for future codes implementation.

4.2.1 Literature review related to resistance model uncertainties for NLFEA

The aspects related to the quantification of model uncertainties related to numerical resistance models has been faced by several literature references.

Shlune et al., 2016 numerically reproduced by means NLFEA different structural members which presented various failure modes: compression or bending failure (with under- and over-reinforced cross sections) and shear failure. The ratios between the resistances measured during experimental tests and the NLFE simulations showed a coefficient of variation within the range of 0.05 (in the case of flexural failure with under-reinforced cross-section) to 0.40 (in the case of shear failure due to crushing of concrete).

In compliance with *JCSS Probabilistic Model Code, 2001* concerning well validated numerical models, the hypothesis to have mean value and coefficient of variation equal to 1.00 and to 0.1, respectively, can be considered trustworthy in order to account for resistance model uncertainties in reliability analysis adopting NLFEA. The model uncertainty random variable is suggested to be modelled by means of a lognormal distribution.

Another important issue related to reinforced concrete structures is the validation of the NLFE model with respect to the actual failure mode. Always the *JCSS Probabilistic Model Code, 2001* proposes mean values and coefficients of variation for the resistance model uncertainty of 1.2 and 0.15 for bending failure modes and 1.4 and 0.25 concerning shear failure modes.

Nevertheless, the bending and shear failure modes are representative of ultimate behavior of beams and, considering more complex structural members, are not always discernible.

Kadlec and Červenka, 2016, proposed an efficient methodology for the assessment of model uncertainties in structural analysis by means NLFE models. The discussion focused on the dependence un modelling uncertainties from the failure mode with the proposal of a specific value for mean value and coefficient of variation for model uncertainties concerning the specific problem of punching in RC slabs.

Engen et al., 2017 reported the characterization of resistance model uncertainties for NLFEA performing the distinction between ductile and brittle failure modes. This has been carried out by reproducing with NLFE models the experimental outcomes reported in a benchmark database composed of 38 tests derived from several literature references. The results showed that the modelling uncertainty may be represented as a lognormal random variable with a mean value of 1.10 and a standard deviation of 0.12. However, in order to get to a comprehensive estimation of resistance model uncertainties for NLFEA of RC structures, a huge number of modelling hypotheses ad structural members should be investigated.

Concerning the value of the partial safety factor for the resistance model uncertainties γ_{Rd} limited information are given in literature. The *EN 1992* proposes to assume a value of γ_{Rd} equal to 1.06. However, to this value has been given an importance beyond the field in which it was introduced. In fact, this value has been suggested within the framework of non-linear analyses of reinforced concrete bridges and not generally for other structural members or systems (e.g. massive structures, walls, beams with variable geometry, panels etc.). Successively, the *fib Model Code 2010* proposed different values of γ_{Rd} depending on the level of validation of the structural model. The γ_{Rd} equal to 1 may be adopted for models without epistemic uncertainties (i.e. in case of presence of evidences of model validation in the actual design conditions). If low or a high level of epistemic uncertainties related to definition of the structural model are present (i.e., difficulties in the definition of actual structural conditions due to unknown design situations) the values, set equal to 1.06 and 1.1, are suggested. However all the

mentioned above values are not based on a straightforward calibration procedure and are not compliance with a predetermined level of reliability.

Therefore, an in-depth probabilistic characterization of the resistance model uncertainty random variable and of the related partial safety factor γ_{Rd} needs to be addressed in relation to the following aspects:

- the multiplicity of modelling hypotheses available to practitioners and engineers;
- the reliability differentiation between *new* and *existing* structures;
- the prescribed reliability level.

Next, the methodology for the derivation of the partial safety factor for resistance model uncertainties related to NLFEAs of RC structures is presented and discussed.

4.2.2 Proposed methodology for calibration of the model uncertainty safety factor γ_{Rd}

The quantification of the resistance model uncertainties, as already discussed in Section 1.3.1 should be performed in agreement with several aspects. In particular, concerning the specific topic of NLFE resistance models, these aspects should concern:

- the database of the experimental data, where should be provided all the parameters necessary for the numerical reproduction of the tests and for the definition of NLFE structural models;
- the variety of the failure modes and of the typology of structural members investigated;
- the probabilistic analysis of the observed sample of resistance model uncertainties that should be carried out in order to define the most likely probabilistic distribution with the associated parameters.

Very often, some information necessary for the definition on the NLFE model may be missing. The typical example is represented by material properties as the fracture energy of concrete or concrete tensile strength, that, in the practice, should be derived from the available experimental data (i.e. concrete compressive strength) adopting assumptions according to proven methodologies proposed by scientific literature and codes (e.g. *EN 1992* and *fib Model Code 2010*).

According to Section 1.3.1, the resistance model uncertainty, denoted as ϑ , can be expressed by a multiplicative law.

This latter relates the i -th actual global resistance (response) estimated from an experimental test $R_i(X, Y)$ to the i -th global resistance (or response) estimated by a NLFEA $R_{NLFEA,i}(X)$ and, may be expressed as follows:

$$R_i(X, Y) \approx \mathcal{G}_i R_{NLFEA,i}(X) \quad (4.1)$$

where X is the vector of basic variables included into the resistance model, Y is a vector of variables that may affect the resisting mechanism but are neglected in the model. As already stated in Section 1.3.1 the unknown effects of Y variables, if present, are indirectly incorporated and covered by the resistance model uncertainty random variable.

In order to perform the calibration of the resistance model uncertainty safety factor γ_{Rd} the following steps has been followed:

- 1) *Selection of the benchmark experimental tests*: the selection of the benchmark set of experimental results having different nature and different failure modes has been performed;
- 2) *Differentiation between modelling hypotheses*: the plausible *modelling hypotheses* able simulate specific reinforced concrete structure by means of NLFEAs should be involved in the calibration procedure. In fact, a comprehensive quantification of the resistance model uncertainties for NLFEAs requires to account for the different *modelling hypotheses* which may be selected by engineers.
- 3) *Probabilistic calibration (Bayesian approach)*: accounting for the differentiation between *modelling hypotheses*, it is necessary to define a probabilistic model able to characterise the resistance model uncertainty random variable \mathcal{G} estimating the mean value μ_g and the variance σ_g^2 . *JCSS Probabilistic Model Code, 2001*, suggests that the realizations of the random variable \mathcal{G} typically fits a lognormal probabilistic distribution. The treatment of the resistance model uncertainties can be developed following a *Bayesian approach*. Specifically, the mono-variate and unimodal lognormal *prior* distributions of the resistance model uncertainties related to the different *modelling hypotheses* can be evaluated. Then, each one of the *prior* distributions is updated on the basis of the data obtained from the other models in order to evaluate the *posterior* distributions. After that, the average statistical parameters of the posterior distributions related to the different structural models can be evaluated.

- 4) *Evaluation of the resistance model uncertainty safety factor γ_{Rd}* : grounds on the log-normality hypothesis, the partial safety factor representative of the resistance model uncertainties γ_{Rd} can be determined as follows:

$$\gamma_{Rd} = \frac{1}{\mu_g \exp(-\alpha_R \beta V_g)} \quad (4.2)$$

where μ_g is the mean value of the resistance model uncertainty random variable; V_g is the coefficient of variation of the resistance model uncertainty random variable calculated as σ_g/μ_g ; α_R is the first-order-reliability-method (FORM) sensitivity factor, assumed equal to 0.8 and 0.32 as suggested by *EN 1992-2 and fib Model Code 2010* for dominant and non-dominant resistance variables, respectively; β is the reliability index.

The study proposed in next Sections is devoted to the calibration of the *model uncertainty safety factor γ_{Rd}* related to plane stress (2D) NLFEMs of reinforced concrete structures subjected to static incremental loading.

Specifically, several experimental tests (performed under static incremental loading process), related to different structural systems that showed different failure modes, are considered and reproduced through plane stress (2D) NLFEMs. These simulations are performed considering different *modelling hypotheses* in order to estimate the resistance model uncertainties and calibrate the corresponding values of the partial safety factor in compliance with the described above approach.

4.2.3 Benchmark experimental tests

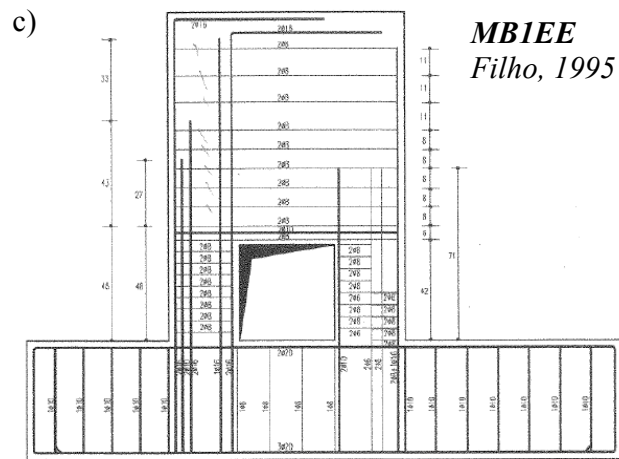
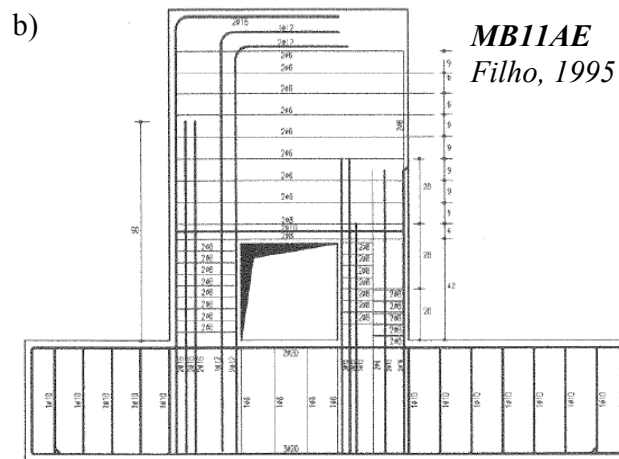
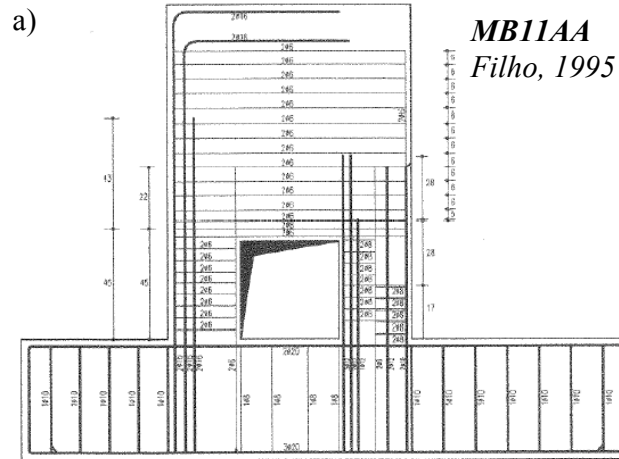
The benchmark experimental results presented in the scientific literature by *Filho,1995; Foster and Gilbert, 1998; Lefas and Kotsovos, 1990; Leonhardt and Walter, 1966; Vecchio and Collins, 1982; Pang and Hsu, 1995* are assumed. A total number of 25 structural members are selected for the investigation.

All the experimental tests, developed respectively on nine shear panels, on five deep beams and on eleven walls, have been performed through a monotonic incremental loading process up to failure as discussed by the original references. The structural members have been realized in laboratory and supported by statically determined configurations.

Subsequently, the short description of the different structural members is reported. However, more details may be acknowledged by the original references.

Filho,1995

The experimental tests described by *Filho,1995* concerns five reinforced concrete walls denoted respectively as MB11AA, MB11AE, MB1EE, MB1EE1 and MB4EE, with the following geometrical properties: 1.35 m high, 1 m wide, 0.12 m thick and stiffened by a 0.2 m thick and 0.5 m high lower beam.



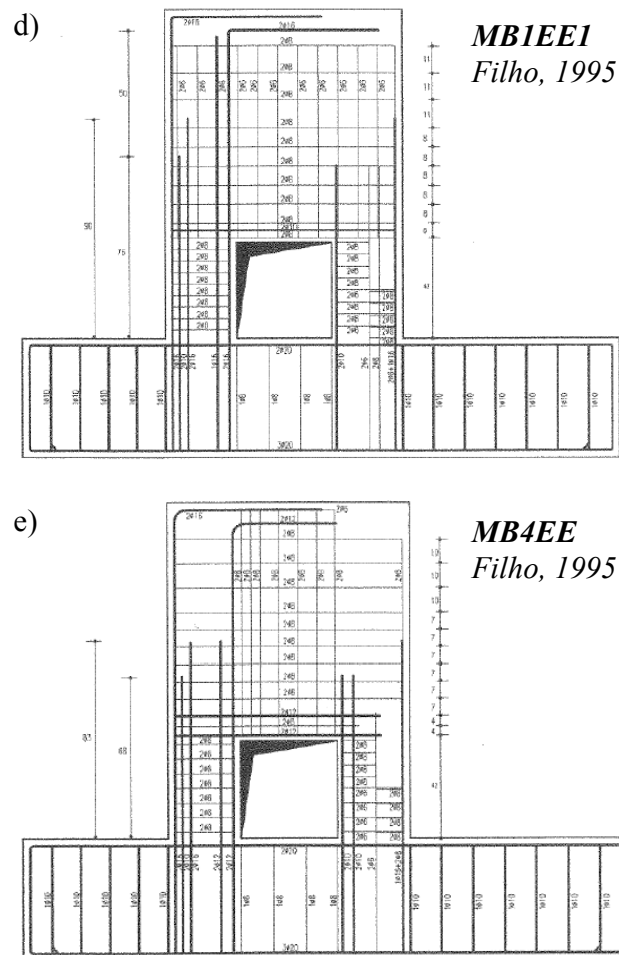


Figure 4.1: Detail of the walls tested by *Filho, 1999 (a-e)*.

The structures are characterized by a 0.4 m wide square opening, fully restrained at the base and loaded by a horizontal force at the top. The concrete compressive strength ranges from 39 to 42 MPa in the different tests, while the reinforcement amount varies significantly from one structure to the others, although keeping the general layout of the main reinforcements unchanged. The arrangement of the reinforcements and the main dimensions of the specimens are reported in Figure 4.1(a-e).

Foster and Gilbert, 1995

The experimental results of *Foster and Gilbert, 1995* are related to five 0.7 m deep and 0.125 m thick reinforced concrete beams denoted respectively as B2.0-1, B2.0-3, B3.0-1, B2.0A-4 and B3.0A-4, simply supported at the edges. The beams B2.0-1, B2.0-3 and B3.0-1 (Figure 4.2(a) - *Scheme a*) differ from the beams B2.0A-4 and B3.0A-4 (Figure 4.2(b) - *Scheme b*) concerning the load arrangement. The main tensile reinforcement consists of six $\phi 20$ longitudinal bars. The web reinforcement is made up of $\phi 6.3/75$ mm in the transverse direction and $\phi 6.3/135$ mm in the longitudinal direction. The concrete compressive strength varies in the range 78 - 88 MPa in the different tests.

Lefas and Kotsovos, 1990

The experimental test discussed by *Lefas and Kotsovos, 1990* focused on a reinforced concrete wall SW11 that is 1.2 m high, 0.75 m wide, 0.07 m thick and stiffened by 0.2 m thick upper and lower beams. The structural member is fully restrained at the base and loaded by a horizontal force at the top. The concrete compressive strength is 43 MPa, while the reinforcement consists of two $\phi 6.25/80$ mm horizontal bars and two $\phi 8/60$ mm vertical bars. The arrangement of the reinforcements and the main dimensions of the specimens are reported in Figure 4.3.

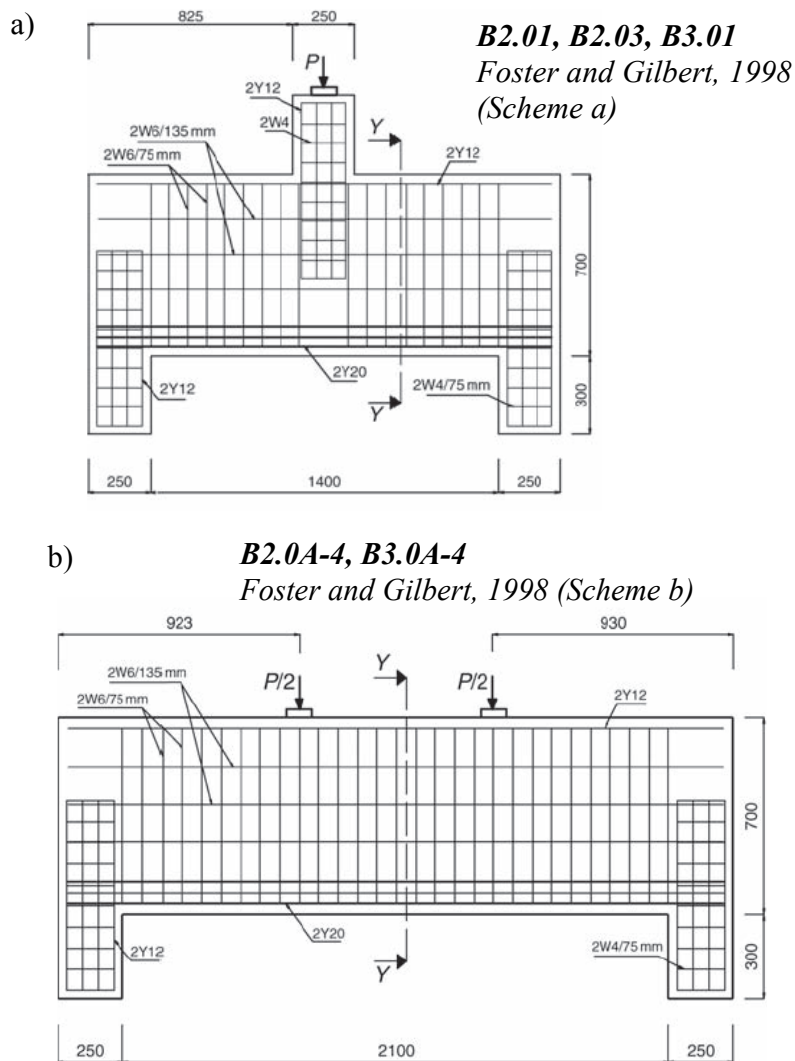


Figure 4.2: Detail of the deep beams tested by *Foster and Gilbert, 1998* (a-b).

SW11
Lefas and Kotsivos, 1990

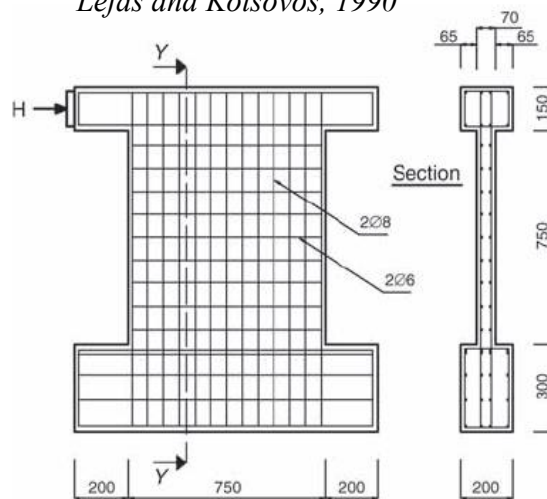
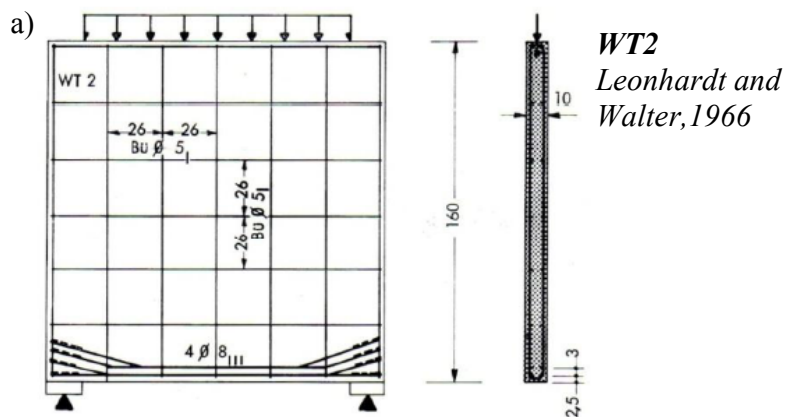


Figure 4. 3: Detail of the wall tested by *Lefas and Kotsivos, 1990*.

Leonhardt and Walther, 1966

The experimental results achieved by *Leonhardt and Walther, 1966*, analysed five deep beams denoted respectively as WT2, WT3, WT4, WT6 and WT7, which are 1.6 m wide and high. The beams present a uniform thickness of 0.1 m and have a simply supported static scheme. The reinforcement consists of horizontal and vertical stirrups and of additional bars in the bottom part of the structural elements. The concrete compressive strength varies between 26.7 and 28.7 MPa in the different tests, while the mechanical properties of the reinforcement depend on the diameter of the bars. The walls WT2, WT3, WT4 are loaded from the top and they differ in the amount of reinforcement in the bottom part of the structure (Figure 4.4(a-b) – *Scheme a*). The horizontal and vertical stirrups have diameter of 5 mm and spacing of 26 mm. The structures WT6 and WT7, differing for the distribution of the applied loads and for the reinforcement (Figure 4.4(c-d) – *Scheme b*), are loaded from the bottom.



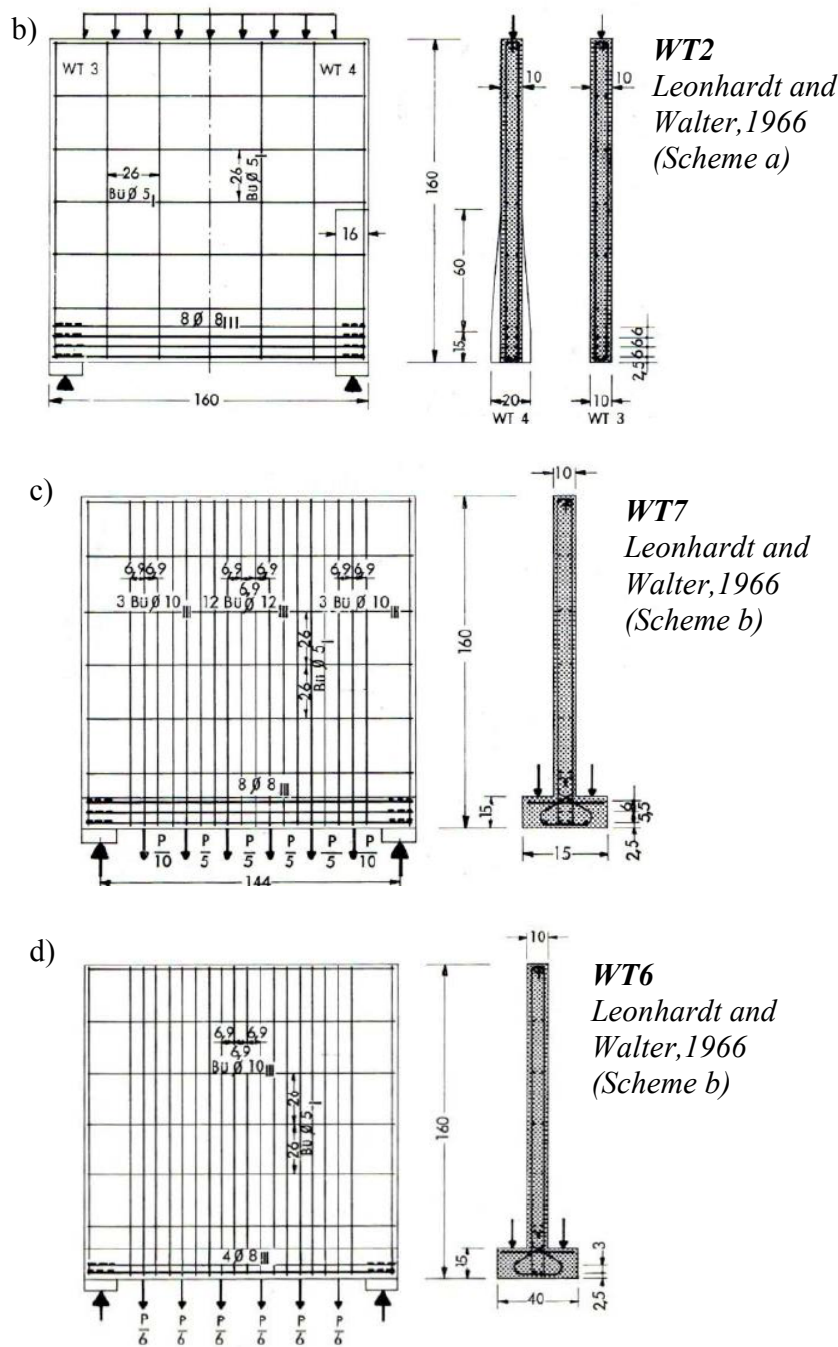


Figure 4. 4: Detail of the walls tested by *Leonhardt and Walter, 1966* (a-d).

Vecchio and Collins, 1982 and Pang and Hsu, 1995

The experimental tests carried out by *Vecchio and Collins, 1982* and *Pang and Hsu, 1995* are considered.

Particularly, four shear panels PV10, PV19, PV21 and PV22 were tested by *Vecchio and Collins, 1982* under monotonically increasing edge loads. The dimensions of each panel are 890 x 890 x 70 mm (Figure 4.5(a)). The actual concrete cylinder compressive strength varies between 14.6 and 19.6 MPa for the different tests. The reinforcement consists of a welded wire grid with the wires parallel to the edges of the panel. The reinforcement ratio in x and y directions varies from 1% to 1.79%. *Pang and Hsu, 1995* analyzed other five shear panels

A2, A4, B2, B5 and B6 loaded by compressive forces in the vertical direction and tensile forces in the horizontal direction. The dimensions of each panel are 1397 x 1397 x 178 mm (Figure 4.5(b)). The concrete compressive strength is about 42 MPa and the reinforcement grid is inclined at 45° with respect to the edges of the panels. The percentage of reinforcement along the inclined directions varies from 1.19% to 2.98%.

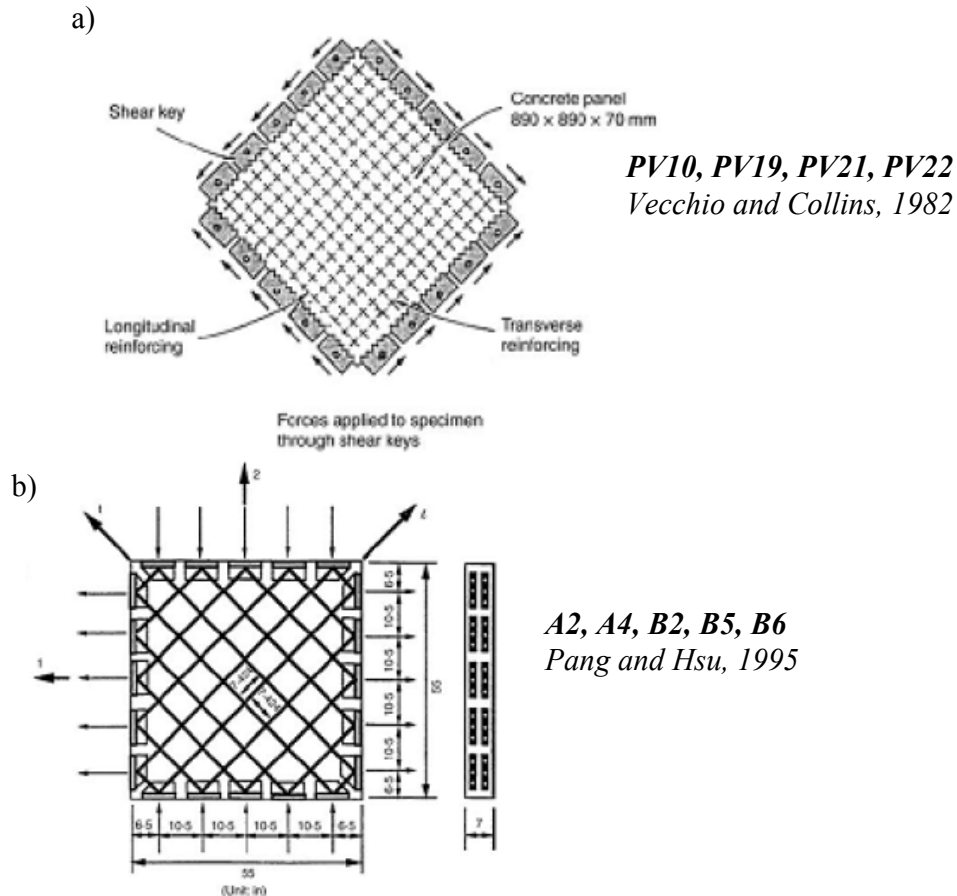


Figure 4.5: Detail of the panels tested by *Vecchio and Collins, 1982* (a) and by *Pang and Hsu, 1995* (b).

4.2.4 NLFEAs: modelling hypotheses and results

In the present Section, the detail of the plane stress (2D) NLFEAs performed in order to reproduce the experimental outcomes describe in Section 4.1.3 is reported.

First of all, the modelling hypotheses herein adopted are outlined and explained. Subsequently the results of the 2D NLFEAs are commented and compared to the experimental ones.

Note that, according to Section 2.1, all the numerical simulations have been performed after a sensitivity/calibration analysis. In fact, this is a crucial requirement for the proposal drawn by the results of the present investigation because leads to a reduction of the epistemic uncertainties. In other words, the designers/analysts involved in NLFEAs for the structural design or assessment process, should be confident with this approach.

Differentiation between modelling hypotheses

Several *modelling hypotheses* are available to perform plane stress (2D) NLFEAs of reinforced concrete structures. One *modelling hypothesis* can be identified by the series of assumption and methodologies adopted in order to fulfill equilibrium, kinematic compatibility and constitutive requirements. It implies that also the choice of a specific commercial NLFE software platform affects the characterization of certain *modelling hypothesis*.

In this investigation, three different types of software *Cervenka Consulting ATENA 2D*, *ADINA*, *TNO DIANA*, identified anonymously by *Software A*, *Software B* and *Software C* in order to avoid advertising for the different codes, are adopted with the aim to reproduce the outcomes of the set of experimental tests.

Furthermore, for each software, several choices about the hypotheses related to equilibrium, compatibility and constitutive laws can be performed.

In the details, in each software four-node quadrilateral iso-parametric plane stress finite elements, based on linear polynomial interpolation and 2x2 Gauss point's integration scheme, are used for the numerical simulations. The FE meshes has been properly defined after a mesh-sensitivity analysis. The non-linear system of equations is solved by means of the standard Newton-Raphson iterative procedure based on the hypothesis of linear approximation.

Concerning the constitutive models devoted to reproduce the actual non-linear materials behavior, for each software the following main characteristics for the FE models are also assumed:

- *Concrete*: the non-linear response of concrete in compression including softening with a reduction of the compression strength and shear stiffness (shear retention factor equal to 0.2) after cracking has been adopted (Section...., *Bertagnoli et al., 2015*). In detail, the mono-axial constitutive model for concrete proposed by *EN 1992-1-1*, the constitutive model described by *CEB-FIP Model Code 1990* and the constitutive model

described by *Thorenfeldt et al., 1987* have been selected in order to fit as much as possible the experimental results with each software (*Software A*, *Software B* and *Software C*). The smeared cracking with fixed crack direction model has been selected in order to reproduce the damaging of concrete;

- *Reinforcement*: a tri-linear σ - ε curve for the reinforcement steel has been adopted (*Bertagnoli et al., 2015*). The discrete and smeared models of the reinforcement, assuming a perfect bond between the reinforcement and the surrounding concrete, are considered;

All the material properties have been assumed according to the experimental ones. As usual, concerning missing information, as the concrete Young's modulus and the tensile concrete strength, they are derived as a function of the experimental available data (e.g. concrete compressive strength), according to *EN1991-1-1*.

Table 4.1: Assumptions related to the basic *modelling hypotheses* devoted to the definition of the non-linear FE numerical models.

	Software A	Software B	Software C
<i>Equilibrium</i>	<ul style="list-style-type: none"> - Standard Newton-Raphson based on the hypothesis of linear approximation; - Convergence criteria based on strain energy; - Load step sizes defined in compliance with the experimental procedure. 		
<i>Compatibility</i>	<p><i>Finite Elements</i></p> <ul style="list-style-type: none"> - Iso-parametric plane stress 4 nodes (2x2 Gauss points integration scheme with linear interpolation); - Discrete reinforcements; - Element size defined by means of an iterative process of numerical accuracy. 	<p><i>Finite Elements</i></p> <ul style="list-style-type: none"> - Iso-parametric plane stress 4 nodes (2x2 Gauss points integration scheme with linear interpolation); - Smeared reinforcements/discrete reinforcements; - Element size defined following an iterative process of numerical accuracy. 	
<i>Constitutive models</i>	<p style="text-align: center;"><i>CONCRETE</i></p> <ul style="list-style-type: none"> - Fixed crack model, smeared cracking, constant shear retention factor set equal to 0.2; - Mono-dimensional model extended to biaxial stress state; - Compression: non-linear with post peak linear softening branch; - Tension (differentiating between 3 modelling hypotheses): <ol style="list-style-type: none"> 1) Elastic - Brittle (BRITTLE); 2) Elastic with post peak linear tension softening (LTS); 3) Elastic - perfectly plastic (PLASTIC). <p style="text-align: center;"><i>REINFORCEMENT STEEL</i></p> <ul style="list-style-type: none"> - Tri-linear elastic – plastic. 		

The summary of the main hypotheses assumed in the definition of the simulations for 2D NLFEAs, adopting *Software A, B* and *C*, is listed in Table 4.1.

In addition to the differences inherent to the three types of software, another important differentiation in the definition of non-linear FE models has been considered related to the concrete tensile mechanical behavior. In fact, the local interaction between reinforcement and concrete between cracks gives rise to the “tension stiffening effect”. In numerical simulations, this effect may be taken into account through a modification of the constitutive tensile behavior of the concrete matrix (*Massicotte et al., 1990*). This modification refers to the definition of a tension softening law in the post peak concrete tensile behavior.

In the present investigation, three different constitutive laws for concrete in tension are considered in order to cover different hypotheses accounting for the tension stiffening effect: *elastic-brittle*, *elastic-plastic* and a *linear tension softening* as shown in Figure 4.6.

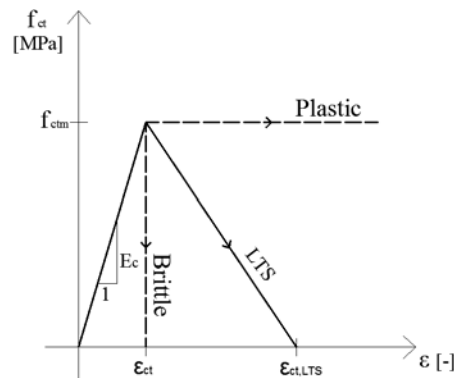


Figure 4.6: Different constitutive laws for concrete tensile behaviour.

These hypotheses has been adopted in order to cover the possible choices performed by engineers/analysts in order to model the influence of the “tension stiffening effect” on the structural behaviour.

The *elastic-brittle* and *elastic-plastic* constitutive laws are conceived as upper and lower limit (i.e. non-physical modelling hypotheses) approaches.

The constitutive law having a *linear tension softening* for the concrete tensile behavior represents the physical modelling hypothesis and has been calibrated by means of an iterative process for each software and each structural member with the aim to best fit each experimental result. Specifically, the slope of the softening branch has been modified in order to obtain the related numerical results in agreement (as much as possible) with the experimental response in terms of force-displacement or stress-strain. In this way, the fracture energy has been considered in absence of specific experimental tests and efficient provisions able to capture the large heterogeneity of the concrete properties of the different benchmark structural members. The iterative process devote to calibrate the *linear tension softening model* has been performed by setting the ultimate deformation in tension of concrete (i.e., $\epsilon_{ct,LTS}$ in Figure 4.6) as a function of the deformation at the tensile elastic limit (i.e., ϵ_{ct} in Figure 4.6). The explored range was between $2\epsilon_{ct}$ to $2\epsilon_{ct,LTS}$ without

evidences of significant dependence from the software and from the compressive strength.

Finally, each *modelling hypothesis* will be represented by the choice of a specific software (i.e. 3 software) and of behaviour of concrete in tension (i.e. 3 hypotheses). These *modelling hypotheses* belongs to the group of the epistemic uncertainties because each specific choice can lead to a reduction or increasing of the level of uncertainty (*Der Kiureghian and Ditlevsen, 2009*).

Altogether, 9 different *modelling hypotheses* (i.e *Model 1-9*) can be defined combining the different types of software with the different concrete tensile behaviours. A representation of the *modelling hypotheses* herein adopted are summarized in Figure 4.7.

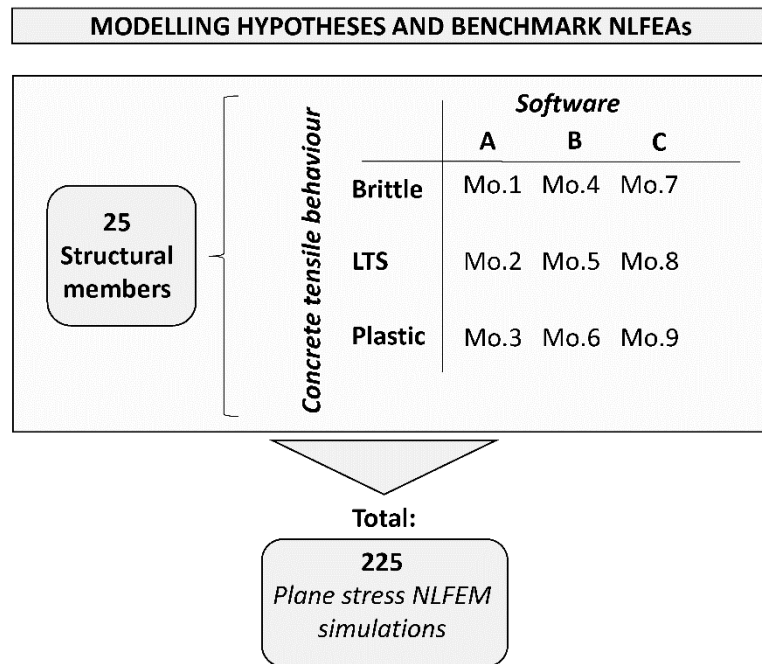


Figure 4.7: Distinction between the 9 *modelling hypotheses* (Mo.1-9) adopted for the resistance model uncertainty investigation and summary of the benchmark NLFEMs.

Finally, the quantification of the resistance model uncertainties can be performed for the different experimental tests of the 25 RC members, leading to a total number of benchmark NLFEMs equal to 225, as shown in Figure 4.7.

Results from NLFEAs of benchmark experimental tests

In the present section, the experimental results presented by the scientific references *Filho,1995; Foster and Gilbert, 1998; Lefas and Kotsovos, 1990; Leonhardt and Walter, 1966; Vecchio and Collins, 1982; Pang and Hsu, 1995* and the selected 25 different typologies of structural members are considered and assumed as benchmark test set for 2D NLFEAs.

The numerical models has been realized in according to the *modelling hypotheses* previously described and in compliance to the experimental tests configuration.

The experimental results, in terms of load vs displacement (*Filho,1995; Foster and Gilbert, 1998; Lefas and Kotsovos, 1990; Leonhardt and Walter, 1966*) or shear stress vs angular distortion diagrams (*Vecchio and Collins, 1982; Pang and Hsu, 1995*), are compared to the outcomes from the different 225 2D NLFEAs.

Note that *experimental systematic errors* (e.g., modifications in the geometry or in the constraints) can affect the experimental results and represent another source of uncertainties, as furtherly discussed comparing the results of the simulations.

Moreover, as specified by *Holický, 2016*, the *test uncertainty* can be ignored if the coefficient of variation of the test uncertainty is equal or lower than 0.05 (which is a common value for tests of non-deteriorated reinforced concrete members without experimental errors) and the coefficient of variation of NLFEA resistance model uncertainties is equal or higher than 0.10. As will be demonstrated in the next Section, the present investigation falls under this circumstance.

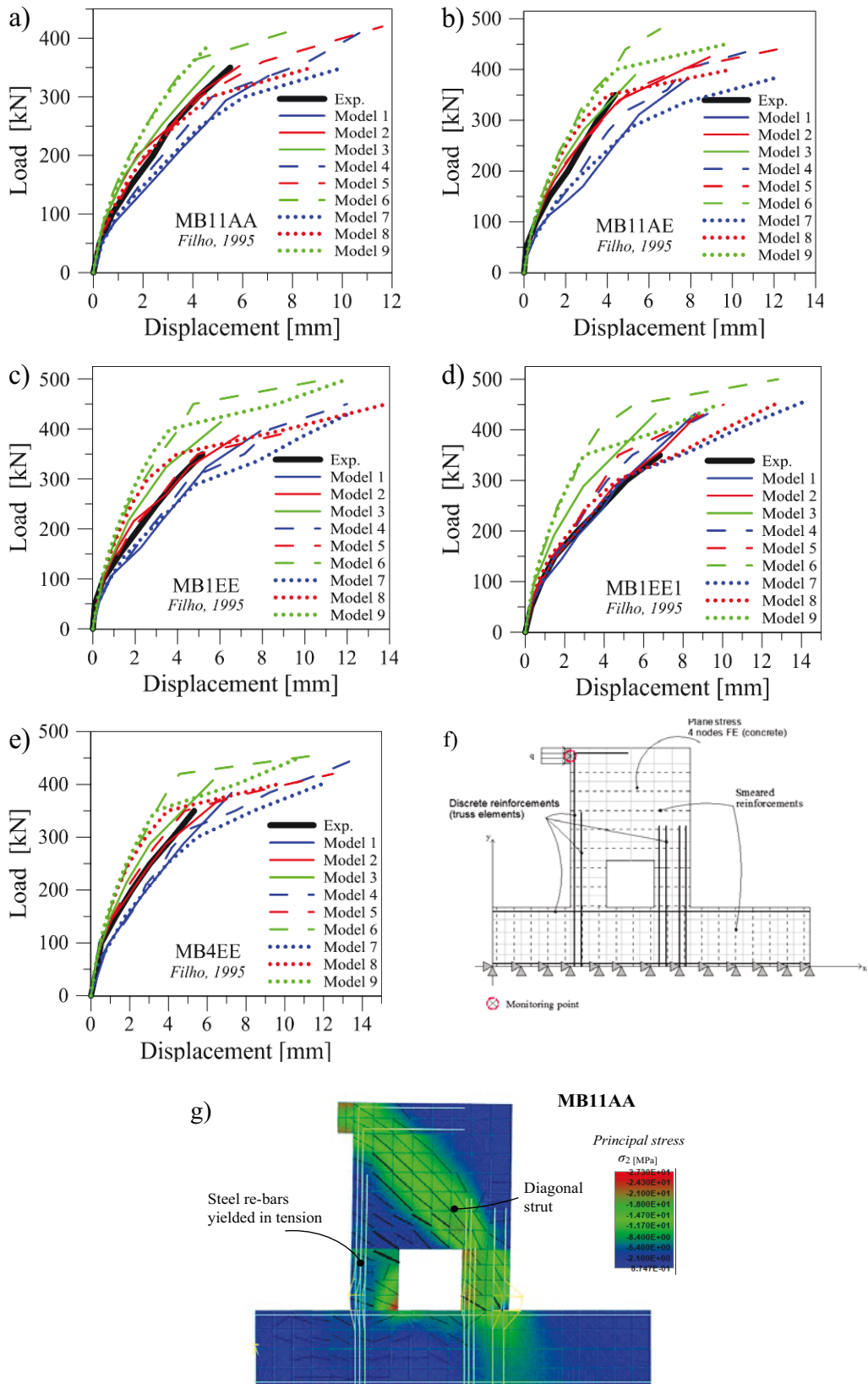
In the following the results of the NLFEAs having different modelling hypotheses are commented for each one of the benchmark experimental test sets.

- FILHO,1995

First of all, the results of the simulations performed on the walls MB11AA, MB11AE, MB1EE, MB1EE1 and MB4EE realized by *Filho, 1995* are discussed. The schematization of the non-linear FE model and the monitored points according to the experimental arrangement are illustrated in Figure 4.8(f). The numerical results in terms of global structural resistance of the simulations are listed in Table 4.2. The results from NLFEAs, plotted in Figure 4.8(a)-(e), adequately reproduce the experimental curve in terms of stiffness and resistance. The lowest results in terms of maximum load are achieved when the brittle constitutive law (models 1, 4, 7) is adopted for concrete tensile behavior, while the plastic constitutive law (models 3, 6, 9) always leads to an overestimation of the maximum load.

In general, all the simulations overestimate the ultimate displacement and then the structural ductility. The resisting mechanism occurs with the formation of a diagonal strut flowing from the loading device to the right side of the opening. The strut is equilibrated by the tensile steel reinforcements on the left side of the wall as shown in Figure 4.8(g). The failure mode occurs with the progressive yielding of the tensile reinforcements and concrete crushing in the column on the right side of the square opening, as illustrated in Figure 4.8(h). This failure is in compliance with

the experimental results. When the ultimate deformation for the concrete in compression is reached, all the simulations have been stopped due to the convergence loss of the numerical procedure.



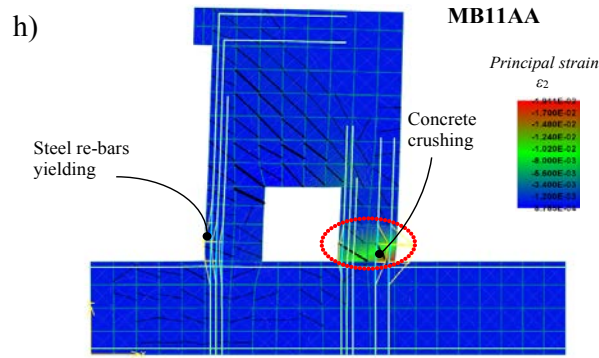


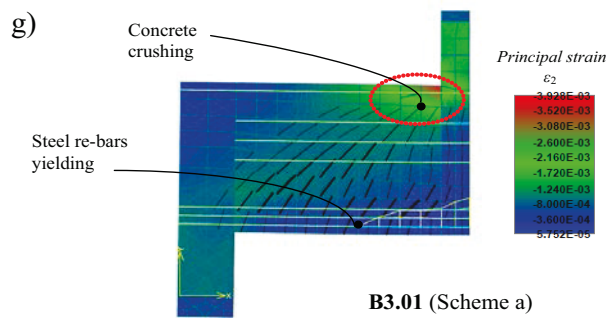
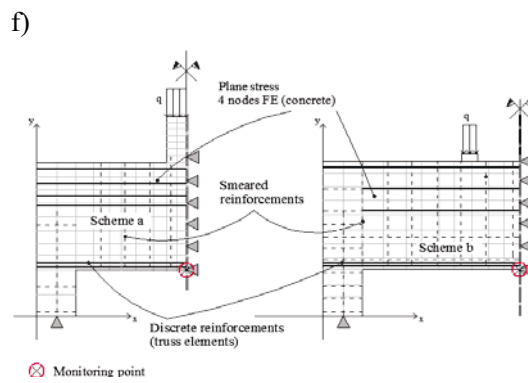
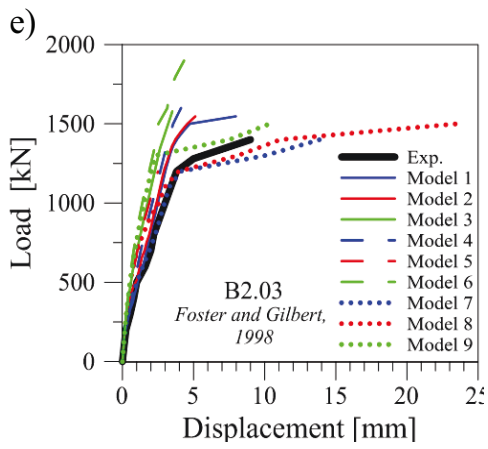
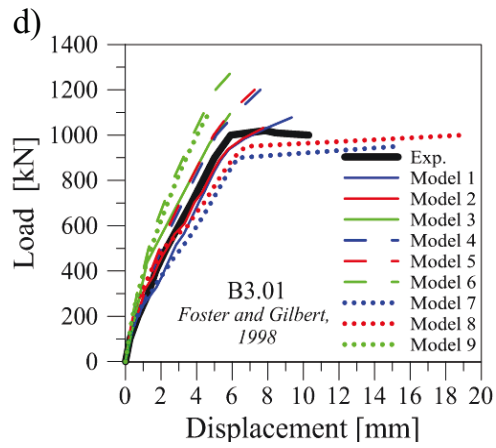
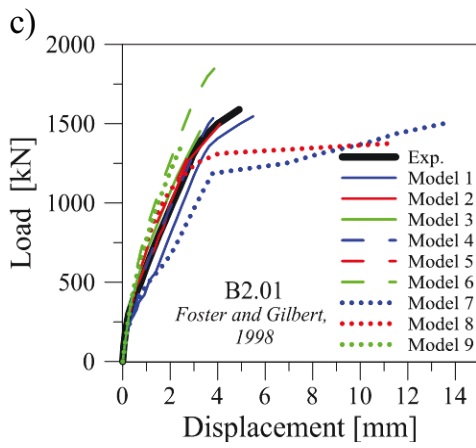
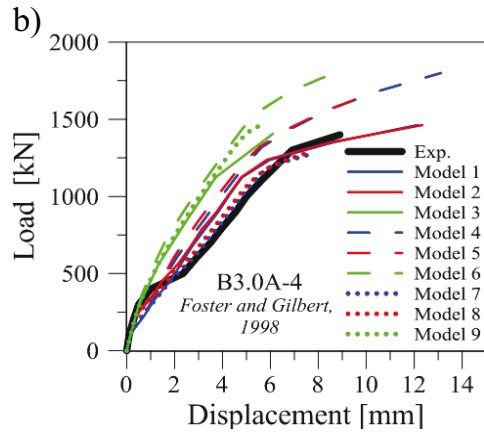
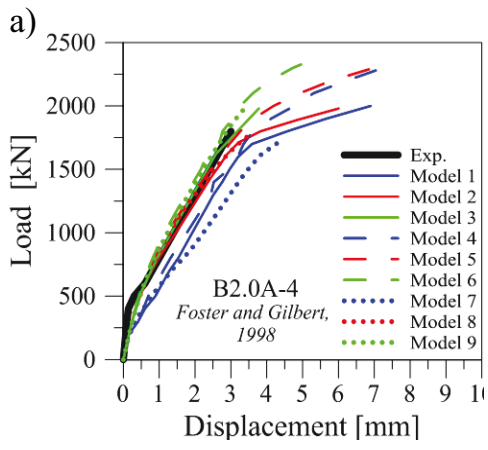
Figure 4.8: Load vs displacement diagrams from experimental tests of *Filho, 1995* and NLFEA results (a-e); numerical model schematization (f); crack patterns and σ_2 principal stress flow at first yielding (g) and principal strain ϵ_2 at failure (h) for MB11AA.

Table 4. 2: Results in terms of resistance from the experimental tests $R_{EXP,i}$ (*Filho, 1995*) and NLFEAs $R_{NLFEA,i}$ for the different structural models.

Exp. test	$R_{EXP,i}$ [kN]	$R_{NLFEA,i}$ [kN]								
		Mo. 1	Mo. 2	Mo. 3	Mo. 4	Mo. 5	Mo. 6	Mo. 7	Mo. 8	Mo. 9
MB1AA	350	336	353	353	420	420	420	350	350	384
MB1AE	407	382	425	389	440	440	480	384	400	450
MB1EE1	413	396	387	414	450	400	500	432	450	500
MB1EE1	416	432	432	432	450	450	500	459	450	450
MB4EE	400	384	372	408	455	420	455	400	400	450

- FOSTER AND GILBERT, 1998

The experimental results of *Foster and Gilbert, 1998* are related to five deep beams: B2.0-1, B2.0-3, B3.0-1, B2.0A-4 and B3.0A-4. The schematization of the non-linear FE model and the monitored points according to the experimental arrangement are illustrated in Figure 4.9(f). The numerical results in terms of global structural resistance of the simulations are listed in Table 4.3. Figures 4.9(a)-(e) show that models 3, 6, 8 related to elastic-plastic constitutive law for the concrete tensile behavior, always lead to an overestimation of the resistance. Models 1, 4, 7 (*elastic-brittle* in tension) do not always represent the lower bound, as in the case of the sample B3.0A-4. Concerning the beams having the *Scheme a* arrangement, the failure mode occurs with the progressive yielding of the tensile bottom reinforcements and concrete crushing at the top chord close to the column where the load is applied (Figure 4.9(g)). Whereas, the beams realized according to the *Scheme b*, have shown a progressive yielding of the bottom reinforcements with concrete crushing in the top chord between the loading devices, as plotted in Figure 4.9(h). All the simulations are able to reproduce the actual failure mode observed during the laboratory tests, exception for models 9 and 7 that showed a more ductile behavior (in particular for B2.01, B3.01 and B3.02 beams).



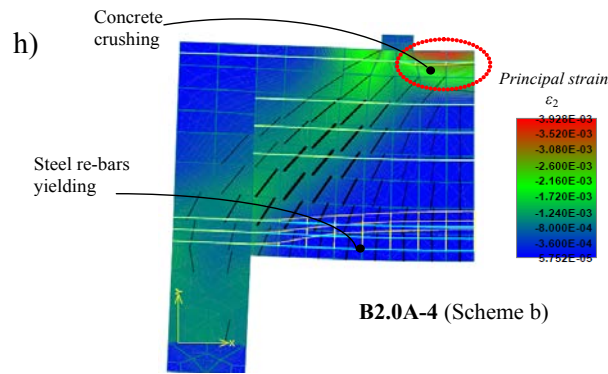


Figure 4.9: Load vs displacement diagrams from experimental tests of *Foster and Gilbert, 1998* and NLFEA results (a-e); numerical model schematization (f); crack patterns and principal strain ϵ_2 at failure for B3.01/ B2.0A-4 (g-h).

Table 4.3. Results in terms of resistance from the experimental tests *Foster and Gilbert, 1998* and NLFEAs $R_{NLFEA,i}$ for the different structural models.

Exp. test	$R_{EXP,i}$ [kN]	$R_{NLFEA,i}$ [kN]								
		Mo. 1	Mo. 2	Mo. 3	Mo. 4	Mo. 5	Mo. 6	Mo. 7	Mo. 8	Mo. 9
B2.0A-4	1800	2000	1980	1980	2300	2300	2400	1710	1800	1980
B3.0A-4	1400	1463	1463	1406	1800	1680	1800	1276	1276	1465
B2.0-1	1590	1547	1500	1453	1600	1700	1900	1500	1375	1375
B3.0-1	1000	1078	1031	1094	1200	1200	1300	950	1000	1100
B2.0-3	1400	1547	1547	1578	1600	1700	1900	1400	1500	1500

- LEFAS AND KOTSOVOS, 1990

The result by *Lefas and Kotsivos, 1990* considered for the investigation is the wall SW11. The schematization of the non-linear FE model as well as the monitored points according to the experimental arrangement are illustrated in Figure 4.10(b). The numerical results in terms of global structural resistance of the simulations are listed in Table 4.4. The NLFEA results, plotted in Figure 4.10(a), demonstrate that *Models 7, 8 and 9* significantly underestimate the ultimate failure load demonstrating the intrinsic dependence of the results on the software code selection (i.e., *Software C*), whereas *Models 3, 6, 9* overestimate the ductility of the structural member due to the choice of the plastic tensile behavior of the concrete in the inelastic phase.

Table 4.4: Results in terms of resistance from the experimental tests $R_{EXP,i}$ of *Lefas and Kotsivos, 1990* and NLFEAs $R_{NLFEA,i}$ for the different structural models.

Exp. test	$R_{EXP,i}$ [kN]	$R_{NLFEA,i}$ [kN]								
		Mo. 1	Mo. 2	Mo. 3	Mo. 4	Mo. 5	Mo. 6	Mo. 7	Mo. 8	Mo. 9
SW11	253	231	221	250	255	255	270	203	225	225

The actual failure mode is adequately reproduced by all the models, as shown in Figure 4.10(d) for SW11. Increasing the horizontal load applied to the top beam, a diagonal strut balanced by vertical external reinforcement develops inside the wall as illustrated in Figure 4.10(c). Progressively, the external reinforcements yield and the structural failure happens with concrete crushing in the right corner of the wall at the connection with the stiff foundation, as can be observed in Figure 4.10(d).

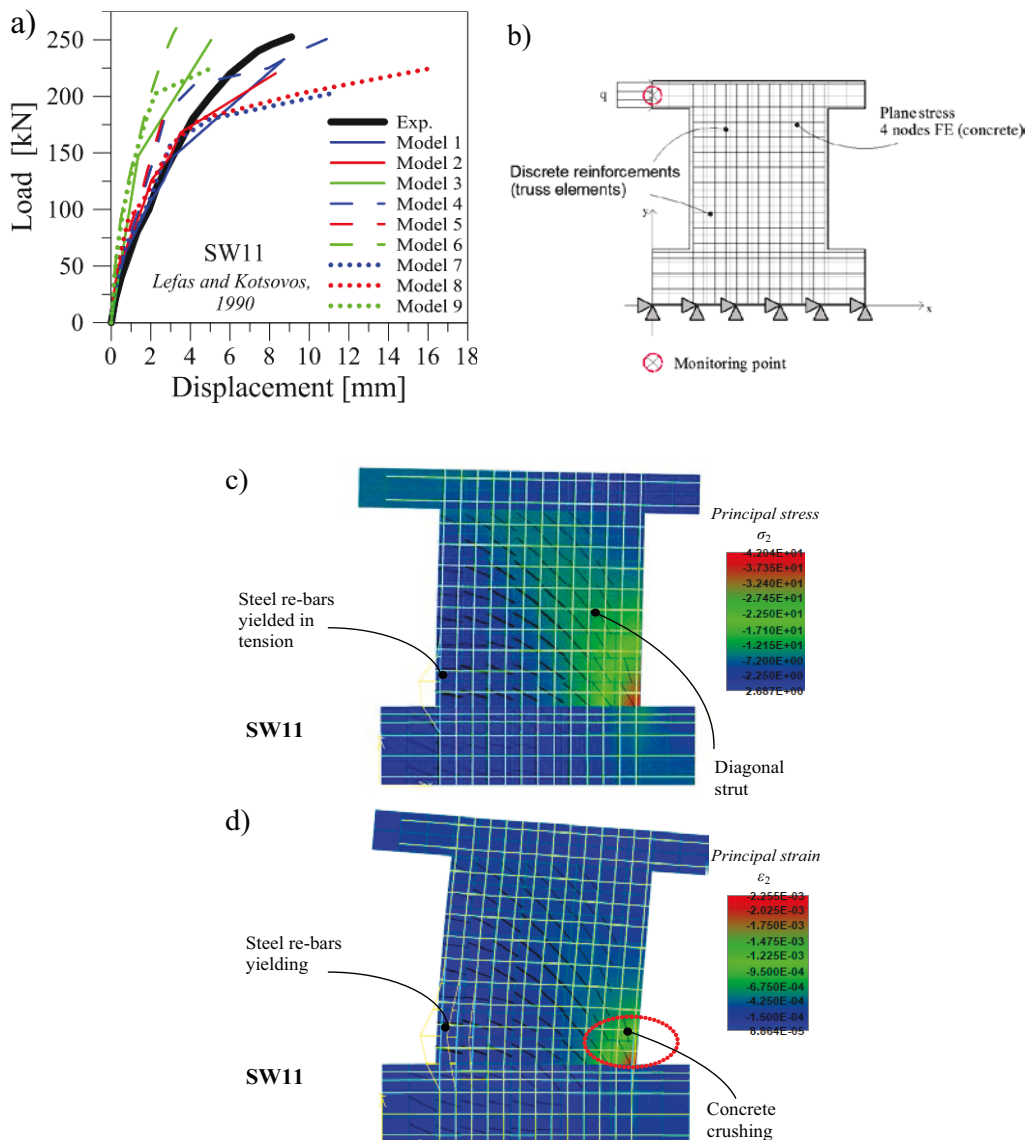


Figure 4.10: Load vs displacement diagrams from experimental tests of *Lefas and Kotsovos, 1990* and NLFEA results (a); numerical model schematization (b); crack patterns and σ_2 principal stress flow at first yielding (c) and principal strain ϵ_2 at failure for SW11 (d).

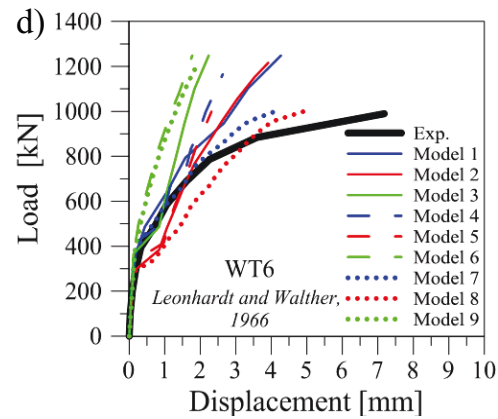
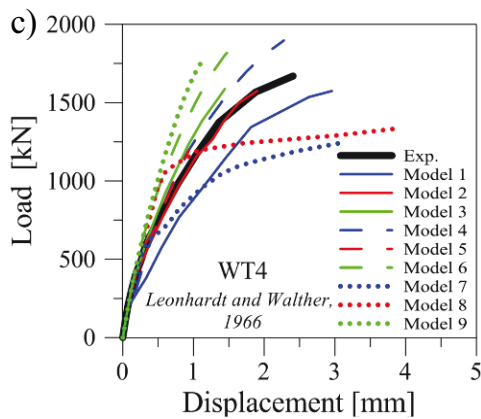
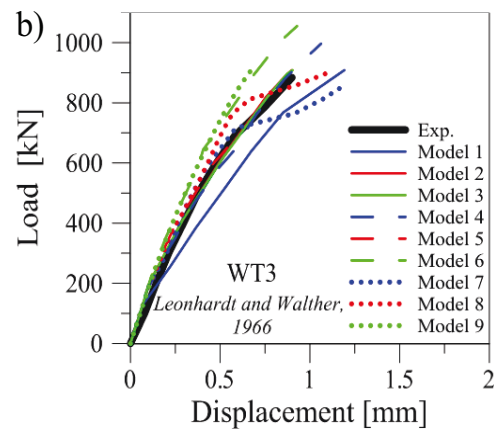
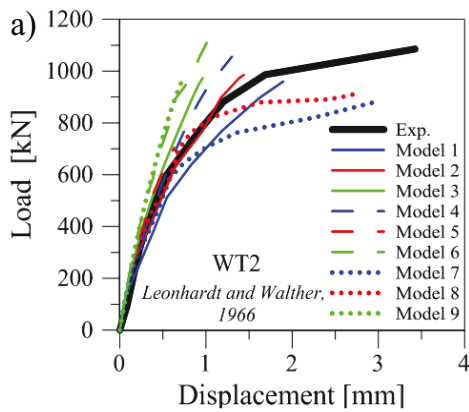
- LEONHARDT AND WALTER, 1966

The experimental results achieved by *Leonhardt and Walther, 1966* regarded five deep beams: WT2, WT3, WT4, WT6 and WT7. The numerical results in terms of global structural resistance of the simulations are reported in Table 4.5. Figure 4.11(a)-(e) illustrate that in most cases the ultimate load is overestimated, whereas the ductility of the structure is underestimated, especially when the plastic tensile behavior of the concrete in the inelastic phase (i.e., *Models 3, 6 and 9*) is considered. In fact, under the abovementioned assumption on the tensile behavior of the concrete, some incongruities are recognised in the identification of the actual failure mode. For example, WT2 beam (loading scheme: *Scheme a*) has shown experimentally a ductile behaviour with the bottom reinforcement yielding. Only *Models 7 and 8* were able to reproduce this failure mechanism (although underestimating the ultimate load). The other simulations on WT2 reached the failure load without bar yielding showing concrete crushing close to the supports,

as demonstrated in Figure 4.11(g). The actual failure mode has adequately been reproduced in the other cases, whereas with reference to the loading *Scheme b* (i.e., WT6 and WT7) the ultimate load is always overestimated. The latter one shows an arch-tie resisting mechanism with bar yielding during the simulations. Collapse occurred due to the concrete crushing near the support zone at the edge of the arch (Figure 4.11(h)).

Table 4.5: Results in terms of resistance from the experimental tests $R_{EXP,i}$ by Leonhardt and Walther, 1966 and NLFEAs $R_{NLFEA,i}$ for the different structural models.

Exp. test	$R_{EXP,i}$ [kN]	$R_{NLFEA,i}$ [kN]								
		Mo. 1	Mo. 2	Mo. 3	Mo. 4	Mo. 5	Mo. 6	Mo. 7	Mo. 8	Mo. 9
WT2	1085	960	986	973	1055	1055	1114	879	914	961
WT3	884	909	909	909	997	997	1055	860	908	908
WT4	1670	1574	1574	1587	1897	1897	1897	1242	1338	1767
WT6	990	1216	1248	1248	1165	1165	1248	1003	1003	1194
WT7	1151	1344	1395	1248	1331	1331	1331	1146	1146	1290



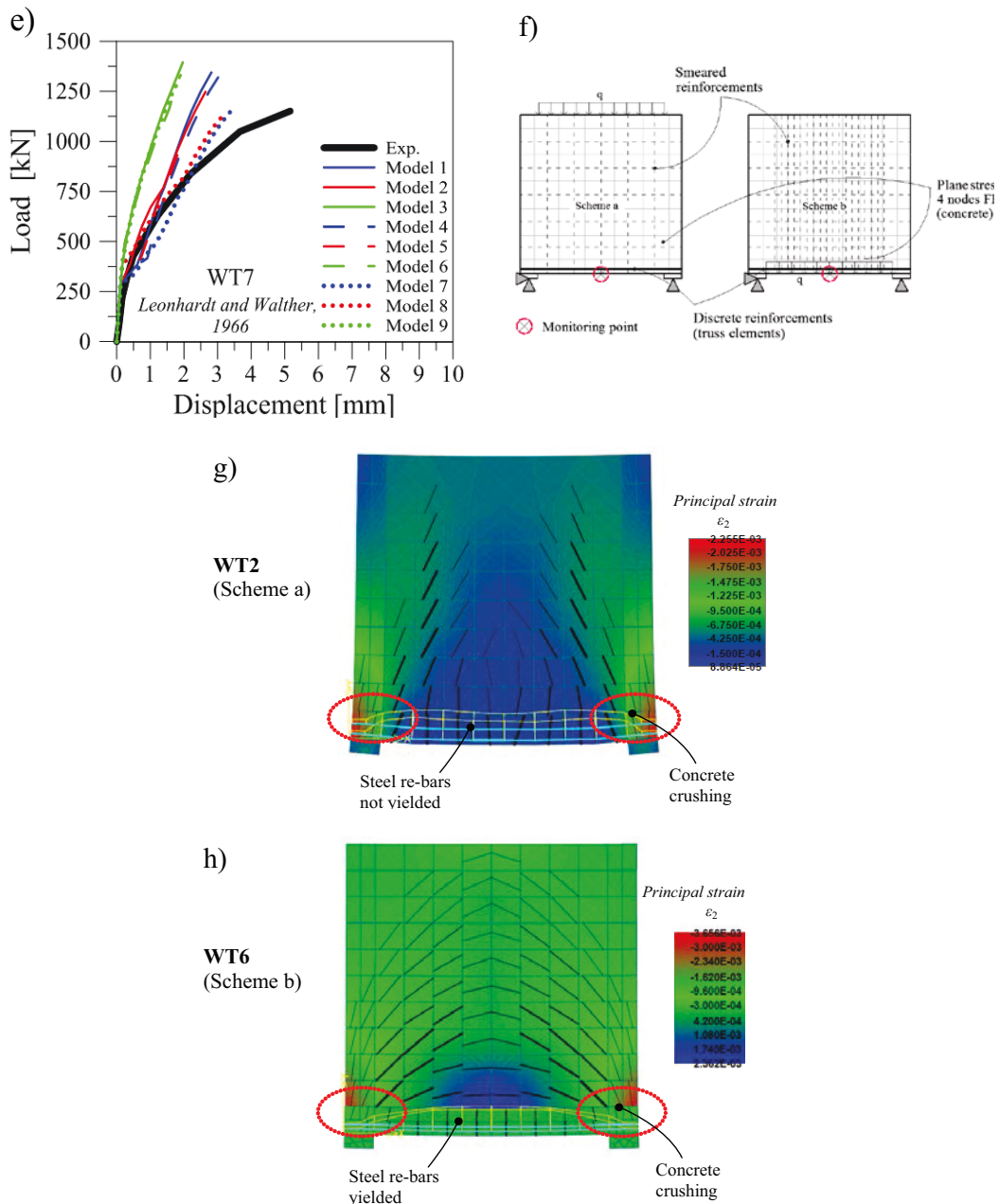
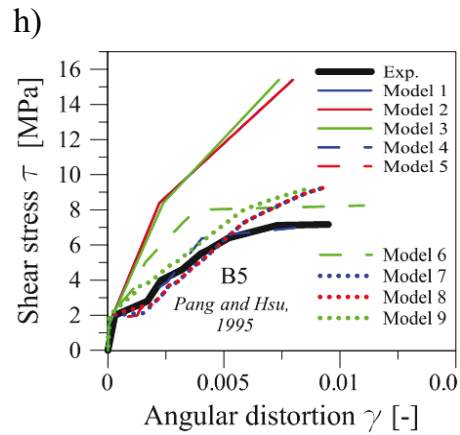
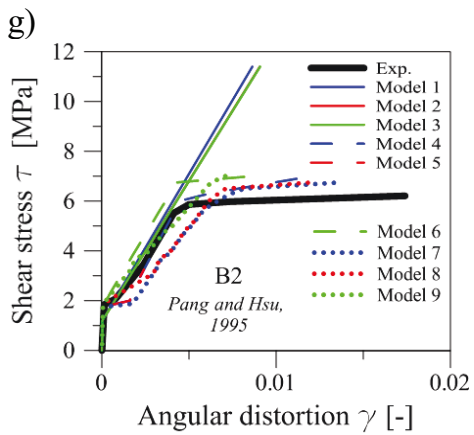
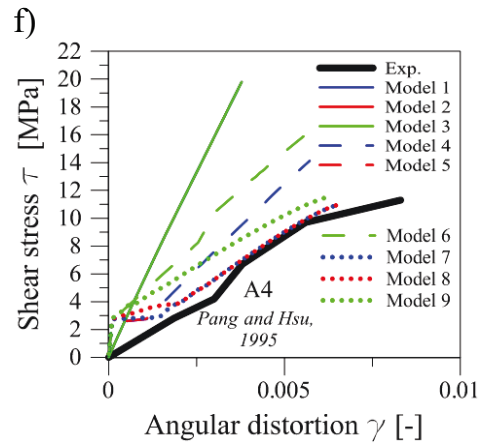
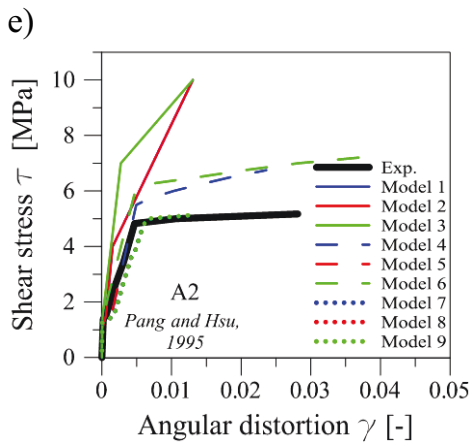
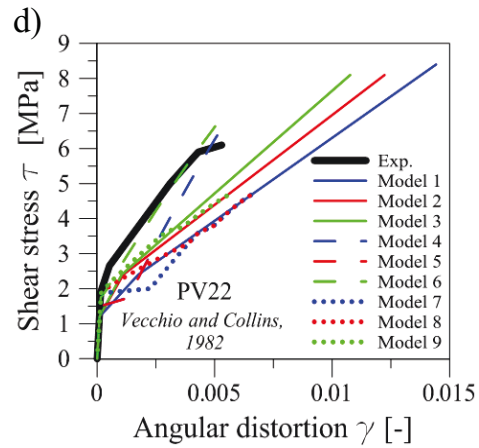
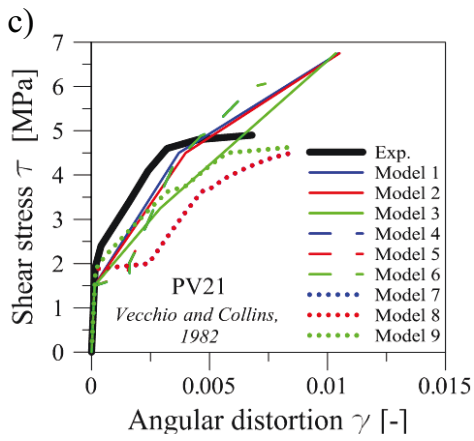
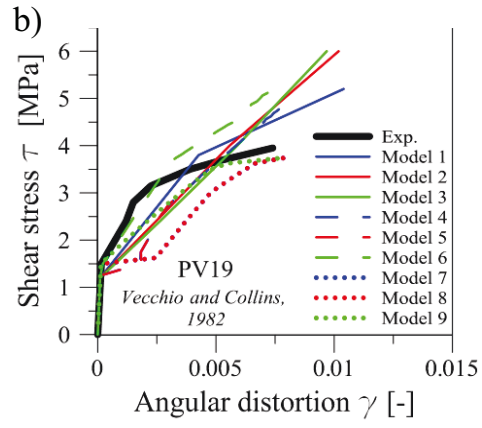
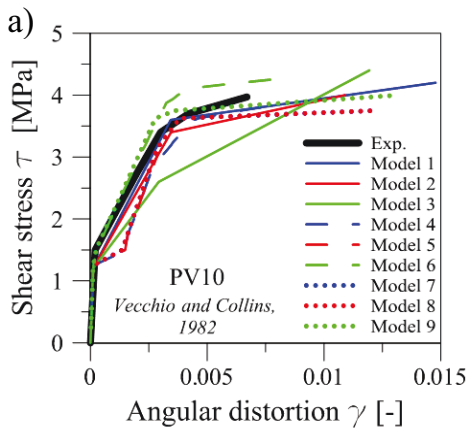


Figure 4.11: Load vs displacement diagrams from experimental tests of *Leonhardt and Walther, 1966* and NLFEA results (a-e); numerical model schematization (f); crack patterns and principal strain ϵ_2 at failure for WT2/WT6 (g-h).

- VECCHIO AND COLLINS, 1982; PANG AND HSU 2000

Finally, the experimental tests carried out by *Vecchio and Collins, 1982* (PV10, PV19, PV21 and PV22) and by *Pang and Hsu, 2000* (A2, A4, B2, B5 and B6) are considered and numerically reproduced.



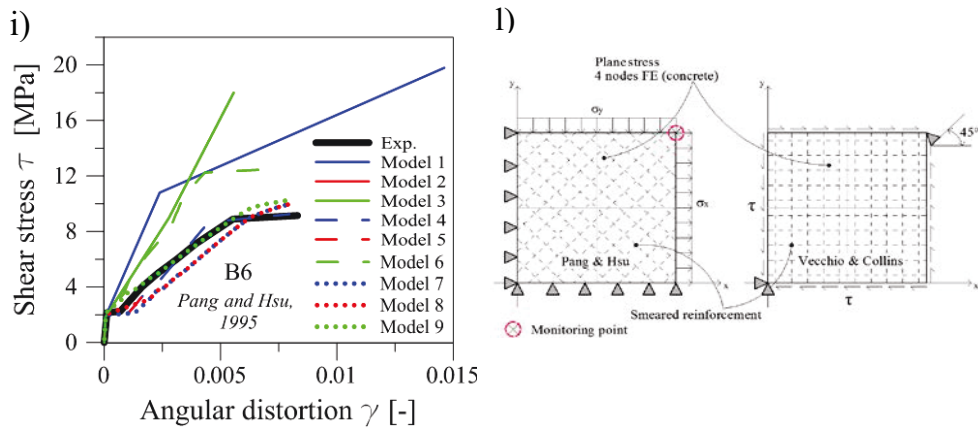


Figure 4.12: Shear stress τ vs angular distortion γ diagrams from experimental tests of *Vecchio and Collins, 1982* and *Pang and Hsu, 2000* and NLFEA results (a-i); numerical model schematization (l).

The schematization of the non-linear FE model and the monitored points according to the experimental arrangement are illustrated in Figure 4.12(l). The numerical results in terms of global structural resistance of the simulations are reported in Table 4.6.

Table 4. 6Results in terms of resistance from the experimental tests $R_{EXP,i}$ of *Vecchio and Collins, 1982* and *Pang and Hsu, 2000* and NLFEAs $R_{NLFEA,i}$ for the different structural models.

Exp. test	$R_{EXP,i}$ [MPa]	$R_{NLFEA,i}$ [MPa]								
		Mo. 1	Mo. 2	Mo. 3	Mo. 4	Mo. 5	Mo. 6	Mo. 7	Mo. 8	Mo. 9
PV10	3.97	4.20	4.00	4.40	3.81	4.00	4.25	3.75	3.75	4.00
PV19	3.95	5.20	6.00	6.00	4.87	4.88	5.18	3.75	3.75	3.75
PV21	4.90	6.75	6.75	6.75	6.00	5.94	6.06	4.50	4.50	4.63
PV22	6.10	8.40	8.10	8.10	6.75	6.75	6.75	4.75	4.75	4.75
A2	5.17	10.00	10.00	10.00	6.75	7.00	7.25	5.00	5.00	5.13
A4	11.30	19.80	19.80	19.80	14.13	14.13	16.25	11.00	11.00	11.50
B2	6.21	11.40	11.40	11.40	7.00	7.25	7.00	6.75	6.75	7.00
B5	7.17	15.40	15.40	15.40	7.13	7.25	8.25	9.25	9.25	9.25
B6	9.15	19.80	18.00	18.00	9.25	9.50	12.50	10.00	10.00	10.25

In contrast with the simple geometry of the panels, Figure 4.12(a)-(i) illustrate that it is very difficult to reproduce the actual behaviour. In fact, although some models are able to fit the experimental results (e.g., PV22), the majority provides an overestimation in terms of both the ultimate shear load and the ultimate shear distortion.

Furthermore, models with plastic and brittle concrete tensile behaviours, do not always represent the upper and the lower bound of the possible response, respectively. This very large difference between the numerical results and the experimental outcomes *Pang and Hsu, 2000* may probably depends on other uncertainties related to the perfect iso-static scheme during the experimental tests of the shear panels. Specifically, in this typology of test, the experimental instrumentations can be characterised by systematic errors leading to uncertainties in the geometry or in the constraints of the test and consequentially in the stress-strain configuration. These errors strictly related to the typology of the experimental test represent another source of uncertainties. This aspect will be considered in the

following within the probabilistic treatment for the proposal of the partial safety factor.

The results deriving from the mentioned above 225 non-linear FE simulations are adopted in the following in order to assess the resistance model uncertainties in 2D NLFEAs of reinforced concrete structures characterised by different failure modes. These results have also demonstrated the several difficulties, which commonly occur considering different types of software and constitutive laws, in reproducing the actual failure behaviour of structural members highlighting the need to calibrate appropriate values of the partial safety factor for the resistance model uncertainties.

4.2.5 Evaluation of the resistance model uncertainty safety factor for 2D NLFEAs of reinforced concrete structures

In the present section the statistic and probabilistic treatment of the outcomes reported in Section 4.1.4 is proposed in order to assess the *resistance model uncertainty safety factor* γ_{Rd} related to 2D NLFEAs of reinforced concrete structures. As already discussed, the numerical results differ significantly from one commercial software (i.e. *Software A, B and C*) to the others confirming that the choice of the software also induces a degree of uncertainty on the determination of the global structural response.

Next, after the quantification and probabilistic characterization of the resistance model uncertainty, the partial safety factor γ_{Rd} is estimated in compliance to a predetermined level of reliability.

Quantification of the resistance model uncertainty

The resistance model uncertainty ϑ_i can be assessed according to Section 1.3.1 investigating the ratio between experimental and numerical results. This can be performed without distinguishing between the failure modes related to reinforcement yielding and/or to concrete crushing, as the aim of the study is to propose a partial safety factor for the global analysis and reliability evaluation of reinforced concrete structures.

In Table 4.7 the results in terms of ϑ_i are reported for each structural member and for each *modelling hypothesis*. The results in Table 4.7 shows that the *elastic-brittle* and *elastic-plastic* behaviour of concrete in tension do not necessarily bound the experimental failure load. The results also demonstrate the effectiveness of the different assumptions on the behaviour of concrete in tension during the inelastic global response of the structural member to capture its actual failure mode. In fact, in the case the numerical model provides wrong predictions related to the failure mode, values of ϑ_i much different from unity are recognised.

Table 4.7: Results of the investigation: ratios $\mathcal{G}_i = R_{EXP,i}/R_{NLFEA,i}$ for the different *modelling hypotheses* (Mo.1-9).

Ref. [*]	Exp. test	Model Uncertainty \mathcal{G}_i [-]								
		Mo. 1	Mo. 2	Mo. 3	Mo. 4	Mo. 5	Mo. 6	Mo. 7	Mo. 8	Mo. 9
<i>Fihlo, 1995</i>	MB1AA	0.90	0.91	0.91	0.78	0.78	0.75	1.05	1.00	0.91
	MB1AE	0.96	0.96	1.00	0.78	0.83	0.78	1.10	1.10	0.96
	MB1EE ₁	1.03	1.06	1.09	0.99	0.94	0.84	1.06	1.16	1.16
	MB1EE ₁	0.93	0.97	0.91	0.83	0.83	0.77	1.05	1.00	0.91
	MB4EE	0.90	0.90	0.89	0.88	0.82	0.74	1.00	0.93	0.93
<i>Fosters ad Gilbert, 1998</i>	B2.0A-4	1.04	0.99	0.99	0.83	0.83	0.83	1.00	1.00	0.91
	B3.0A-4	1.07	0.96	1.05	0.93	0.93	0.85	1.06	1.02	0.90
	B2.0-1	1.04	1.07	1.00	0.92	1.03	0.83	0.96	0.92	0.83
	B3.0-1	0.96	0.96	0.96	0.92	0.92	0.83	0.91	0.92	0.92
	B2.0-3	1.04	1.08	0.98	0.88	0.95	0.88	1.00	1.00	0.89
<i>Lefas and Kotsovos, 1990</i>	SW11	1.10	1.14	1.01	0.99	0.99	0.94	1.25	1.12	1.12
<i>Leonhardt and Walther, 1966</i>	WT2	1.13	1.10	1.12	1.03	1.03	0.97	1.23	1.19	1.13
	WT3	0.97	0.97	0.97	0.89	0.89	0.84	1.03	0.97	0.97
	WT4	1.06	1.06	1.05	0.88	0.88	0.88	1.34	1.25	0.95
	WT6	0.81	0.79	0.79	0.85	0.85	0.79	0.99	0.99	0.83
	WT7	0.86	0.83	0.92	0.86	0.86	0.86	1.00	1.00	0.89
<i>Vecchio and Collins, 1982</i>	PV10	0.95	0.99	0.90	1.04	0.99	0.93	1.06	1.06	0.99
	PV19	0.76	0.66	0.66	0.81	0.81	0.76	1.05	1.05	1.05
	PV21	0.73	0.73	0.73	0.82	0.82	0.81	1.09	1.09	1.06
	PV22	0.73	0.75	0.75	0.90	0.90	0.90	1.28	1.28	1.28
<i>Pang and Hsu, 2000</i>	A2	0.52	0.52	0.52	0.77	0.74	0.71	1.03	1.03	1.01
	A4	0.57	0.57	0.57	0.80	0.80	0.70	1.03	1.03	0.98
	B2	0.54	0.54	0.54	0.89	0.86	0.89	0.92	0.92	0.89
	B5	0.47	0.47	0.47	1.01	0.99	0.87	0.78	0.78	0.78
	B6	0.46	0.51	0.51	0.99	0.96	0.73	0.92	0.92	0.89

It is also possible to observe that the difference detected between the actual and the predicted failure loads may be significantly high. Specifically, unsafe ratios \mathcal{G}_i up to 0.46 with the highest dispersion values are achieved in the case of the shear panels tested by *Pang and Hsu, 2000*, as previously highlighted. It means that the NLFE numerical models have not always been able to describe the actual structural response. Moreover, *modelling hypotheses* herein adopted generally overestimate the failure resistances of the structures under investigation. Therefore, the predicted values of the failure load, in general, are not on the safe side. This aspect is crucial with respect to the safety verification with the consequence that a particular care is necessary to the calibration of the resistance model uncertainties partial safety factor for NLFEAs of reinforced concrete structures.

The very low values of \mathcal{G}_i for the shear panels of *Pang and Hsu, 2000* are possibly due to the experimental difficulties to realize a perfect iso-static scheme during the experimental test leading to additive uncertainties (i.e. *experimental uncertainties*) related to the actual mechanical behaviour, as previously

commented. This observation suggests to perform the probabilistic analysis estimating the model uncertainties \mathcal{G}_i , on the one hand, accounting for all the results and, on the other hand, excluding the shear panels results of *Pang and Hsu, 2000* in order to compare the results.

Statistical analysis of the resistance model uncertainty

Next, the probabilistic models adopted in order to describe the resistance model uncertainty are discussed and validated.

The graphical analysis of the ratios $\mathcal{G}_i=R_{EXP,i}/R_{NLFEA,i}$ related to the *Model 6* is defined by means of the frequency histogram (Figure 4.13(a)) and the probability plot (Figure 4.13(b)) under the assumption of log-normality (the case excluding *Pang and Hsu, 2000* is reported). The frequency histogram and the probability plot show that the sample data follow a unimodal lognormal distribution. Similar results are achieved for the other models.

The probability paper and the frequency histogram demonstrate that the lognormal distribution can be assumed for the resistance model uncertainties according to *JCSS Probabilistic Model Code, 2001*. Moreover, the *Chi-square test* has also been performed for each structural model (*Models 1-9*, both considering and non-considering the results *Pang and Hsu, 2000*) conforming the assumption of *unimodal lognormal distributions* with significance levels set equal to 0.05.

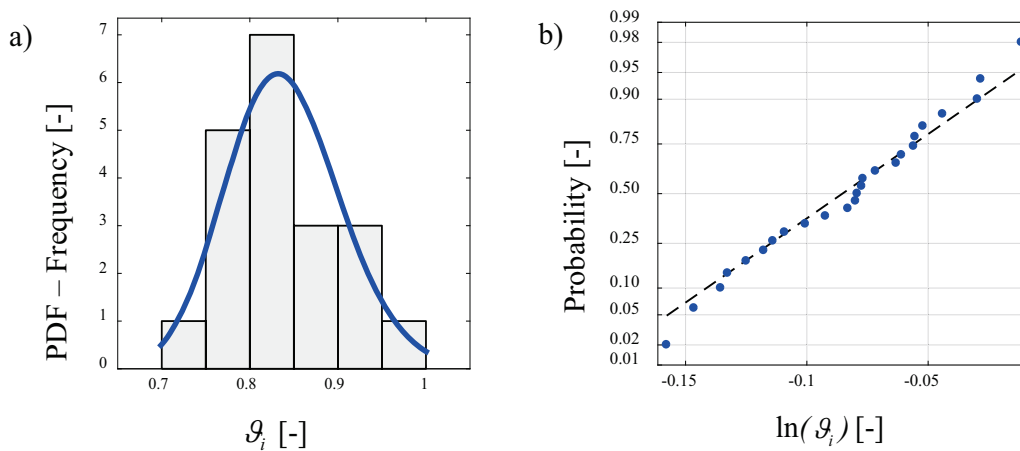


Figure 4.13: Histogram and lognormal probability density function of the ratio \mathcal{G}_i for the Model 6 (a); Probability plot of $\ln(\mathcal{G}_i)$ for the Model 6 (b); excluding *Pang and Hsu, 2000* results.

Similarly, the *Chi-square test* and the graphical analysis of the ratios $\mathcal{G}_i=R_{EXP,i}/R_{NLFEA,i}$ related to all the models are also defined confirming the assumption of *unimodal lognormal distribution*. The Figure 4.14(a) and the Figure 4.14(b) illustrates, respectively, the frequency histogram and the probability plot of all the models excluding *Pang and Hsu, 2000* results.

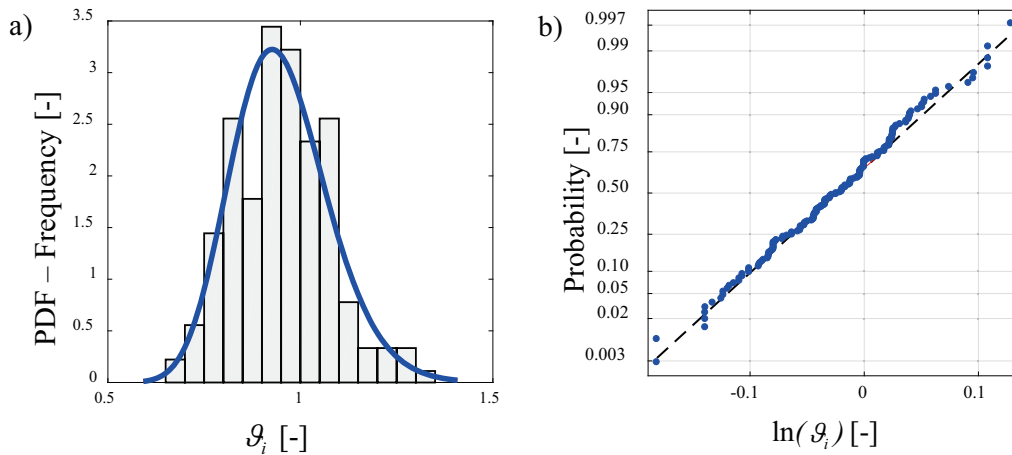


Figure 4.14: Histogram and lognormal probability density function of the ratio g_i for all the models excluding Pang and Hsu [6] results (a); Probability plot of $\ln(g_i)$ for all the models excluding *Pang and Hsu, 2000* results (b).

Probabilistic analysis of the resistance model uncertainty: Bayesian approach

The probabilistic analysis of the resistance model uncertainty for NLFEAs is assessed by means of a Bayesian approach, which allows the updating of the prior data through new information (Figure 4.15).

The *prior* information is represented by the resistance model uncertainty values conditional to the use of a specific *modelling hypothesis* (i.e., software code choice combined to the assumption on concrete tensile behaviour), whereas the *new* information, which makes it possible to update the *prior* results, is different for each *modelling hypothesis* and consists of the numerical outcomes (see Table 4.7) related to the other eight models. Precisely, the *prior* information for each *modelling hypothesis* is updated on the basis of the data obtained from the other models to evaluate the *posterior* distributions. Since the purpose of this study is the development of a comprehensive probabilistic model, the resistance model uncertainty after the Bayesian updating has to be averaged over all the different plausible structural models that can be used by engineers.

As discussed in the previous subsection, a *lognormal* probability density function (PDF) $f(g|M_j)$ of the resistance model uncertainty can be defined conditional to the structural model M_j evaluating the distribution parameters (i.e., mean value and variance). For each one of the 25 (20 excluding *Pang and Hsu, 2000* results) experimental tests, 9 models are considered (three commercial software codes and three laws for concrete behaviour in tension, see Table 4.1 and Figure 4.7) for a total of 225 (180 excluding *Pang and Hsu, 2000* results) NLFEAs. By means of the Bayesian updating, the assessment of the resistance model uncertainties consists of the following steps:

- assessment of the *marginal* distribution $F(M_j)$, $j=1, \dots, 9$, considering the different models equiprobable;
- assessment of the *prior* distribution functions for the resistance model uncertainties $F(g|M_j)$ for each structural model M_j , which represent the prior

data;

- for each structural model M_j , assessment of the statistical parameters, that are assumed deterministic and summarized into the vector z , of the distribution function $F_{M_j}(\mathcal{G}|z)$ averaging the statistical parameters of the other models; in this way, nine $F_{M_j}(\mathcal{G}|z)$, $j=1, \dots, 9$, are estimated and each one represents the *new* information, deriving from the results of the other eight models, for the structural model M_j ;
- assessment of the *posterior* distribution functions $F(\mathcal{G} | M_j, z)$ for each structural model M_j , which represent the posterior data;
- assessment of the *average posterior* distribution function $F(\mathcal{G} | Z)$ with the estimation of the distribution parameters, which are assumed deterministic and summarized into the vector Z , averaging the statistical parameters of the posterior distributions of the different structural models.

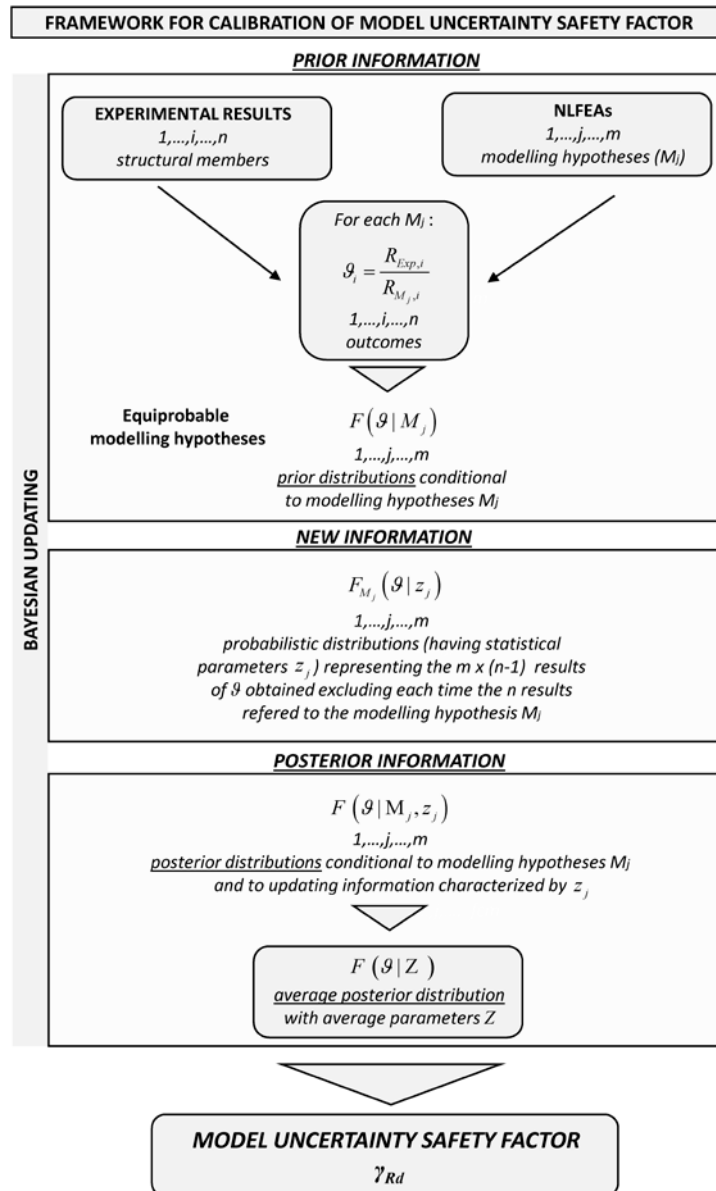


Figure 4.15: Framework for the Bayesian updating and assessment of the partial safety factor for resistance model uncertainty in 2D NLFEAs of reinforced concrete structures; in the present investigation $m=9$ and $n=20-25$.

As demonstrated in previous subsection and according to *JCSS Probabilistic Model Code, 2001*, the resistance model uncertainties for reinforced concrete structures are modelled by unimodal lognormal distributions $F(\mathcal{G}|M_j)$. As a result of the Bayesian procedure, the mean value and coefficient of variation of the *posterior* density functions $F(\mathcal{G}|M_j, z)$ are reported in Tables 4.8 and 4.9 together with the statistical parameters of the *prior* distributions $F(\mathcal{G}|M_j)$ and of the distributions representing the *new* information $F_{M_j}(\mathcal{G}|z)$. The statistical parameters of the lognormal distributions in Tables 4.8 and 4.9 have been evaluated by means of the *maximum likelihood* technique (i.e. maximum likelihood estimators – MLE). It should be noticed that, considering all the results, the coefficient of variation of the *posterior* distributions $F(\mathcal{G}|M_j, z)$ on the resistance model uncertainties for each structural model is not negligible and it ranges from 0.11 to 0.17 (Table 4.8).

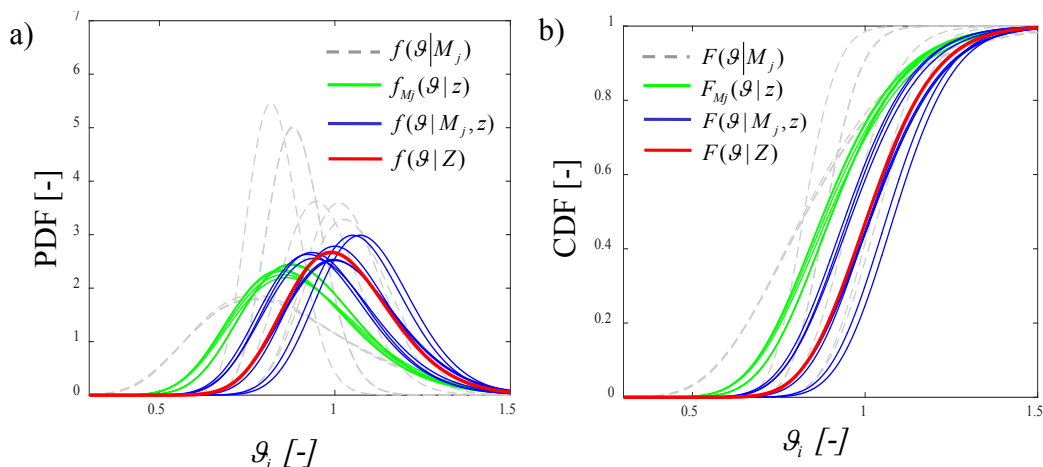


Figure 4.16: Prior and posterior and new information PDFs (a) and CDFs (b); (all results).

Table 4.8: Mean values and coefficients of variation of the prior/posterior and new information distribution functions (all results) with the statistical uncertainty.

Structural Model	Prior distributions (Lognormal) $F(\mathcal{G} M_j)$		Statistical uncertainty		New information (Lognormal) $F_{M_j}(\mathcal{G} z)$		Statistical uncertainty		Posterior distributions (Lognormal) $F(\mathcal{G} M_j, z)$	
	$\mu_{\mathcal{G}}$ [-]	$V_{\mathcal{G}}$ [-]	$C(1,1)$	$C(2,2)$	$\mu_{\mathcal{G}}$ [-]	$V_{\mathcal{G}}$ [-]	$C(1,1)$	$C(2,2)$	$\mu_{\mathcal{G}}$ [-]	$V_{\mathcal{G}}$ [-]
1	0.83	0.34	0.0031	0.0017	0.91	0.20	0.0002	0.00008	1.02	0.15
2	0.83	0.33	0.0030	0.0016	0.91	0.20	0.0002	0.00008	1.02	0.15
3	0.82	0.32	0.0029	0.0015	0.91	0.20	0.0002	0.00009	1.02	0.15
4	0.89	0.10	0.0003	0.0002	0.90	0.23	0.0002	0.0001	0.96	0.17
5	0.89	0.10	0.0003	0.0002	0.91	0.20	0.0002	0.00006	0.96	0.16
6	0.82	0.11	0.0003	0.0002	0.91	0.20	0.0002	0.00006	0.95	0.17
7	1.04	0.11	0.0005	0.0003	0.88	0.22	0.0002	0.0001	1.09	0.11
8	1.02	0.11	0.0005	0.0002	0.88	0.23	0.0002	0.0001	1.07	0.12
9	0.96	0.12	0.0005	0.0003	0.89	0.23	0.0002	0.0001	1.02	0.14
Average statistical parameters									Posterior distribution (Lognormal) $F(\mathcal{G} Z)$	
									$\mu_{\mathcal{G}}$ [-]	$V_{\mathcal{G}}$ [-]
									1.01	0.15

Instead, excluding the experimental results of *Pang and Hsu, 2000*, the coefficient of variation of the *posterior* distributions drops to values ranging from 0.10 to 0.15 (Table 4.9).

In addition, the *statistical uncertainty* associated with the estimates of the distribution parameters for the prior distributions and for each distribution representative of the new information can be expressed by the covariance matrices C for the parameters estimates and may be determined through the inverse of the *Fischer information matrices* (Faber, 2012).

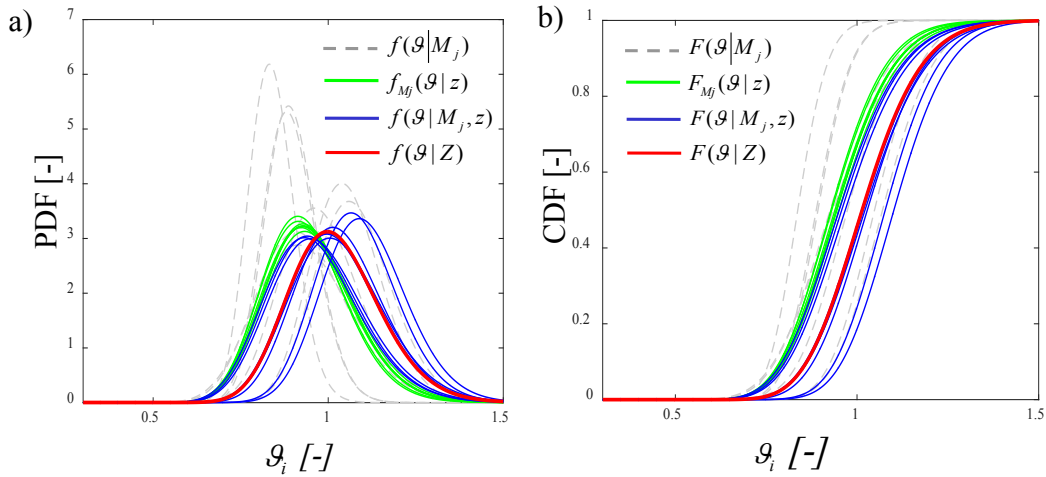


Figure 4.17: Prior and posterior and new information PDFs (a) and CDFs (b); (excluding *Pang and Hsu, 2000* results).

Table 4.9: Mean values and coefficients of variation of the prior/posterior and new information distribution functions (excluding *Pang and Hsu, 2000* results) with the inherent statistical uncertainty.

Structural Model	Prior distributions (Lognormal) $F(\mathcal{G} M_j)$		Statistical uncertainty		New information (Lognormal) $F_{M_j}(\mathcal{G} z)$		Statistical uncertainty		Posterior distributions (Lognormal) $F(\mathcal{G} M_j, z)$	
	$\mu_{\mathcal{G}}$ [-]	$V_{\mathcal{G}}$ [-]	$C(1,1)$	$C(2,2)$	$\mu_{\mathcal{G}}$ [-]	$V_{\mathcal{G}}$ [-]	$C(1,1)$	$C(2,2)$	$\mu_{\mathcal{G}}$ [-]	$V_{\mathcal{G}}$ [-]
1	0.94	0.14	0.0009	0.0005	0.94	0.14	0.0001	0.00005	1.02	0.12
2	0.93	0.16	0.0011	0.0006	0.94	0.14	0.0001	0.00005	1.02	0.13
3	0.93	0.15	0.0010	0.0005	0.94	0.14	0.0001	0.00005	1.01	0.13
4	0.89	0.10	0.0004	0.0002	0.95	0.14	0.0001	0.00006	0.97	0.14
5	0.89	0.09	0.0003	0.0002	0.94	0.14	0.0001	0.00005	0.96	0.14
6	0.84	0.09	0.0003	0.0002	0.94	0.14	0.0001	0.00006	0.95	0.15
7	1.07	0.09	0.0006	0.0003	0.93	0.14	0.0001	0.00005	1.10	0.10
8	1.05	0.09	0.0004	0.0002	0.93	0.14	0.0001	0.00005	1.08	0.10
9	0.97	0.12	0.0007	0.0004	0.94	0.14	0.0001	0.00006	1.03	0.12
Average statistical parameters									Posterior distribution (Lognormal) $F(\mathcal{G} Z)$	
									$\mu_{\mathcal{G}}$ [-]	$V_{\mathcal{G}}$ [-]
									1.01	0.12

In Tables 4.8 and 4.9, the terms of the main diagonal of the abovementioned *Fischer information matrices* (i.e., $C(1,1)$ and $C(2,2)$ representative of the variance of the parameters μ_{θ} and σ_{θ} , respectively) are also reported for each *prior* distribution and for each distribution representative of the *new* information, respectively, related to each structural model.

The mean values of the *posterior* distributions are slightly higher than the corresponding prior values due to the distributions related to the new information $F_{M_j}(\theta|z)$. Regardless of the software selected for the analysis, after the Bayesian updating, *Models 3, 6, 9* (plastic behavior for concrete in tension) have shown the largest coefficient of variation. This is due to the fact that they have always presented the lowest mean value μ_{θ} (i.e. unsafe bias corresponding to an overestimation of the actual strength) and the highest coefficient of variation for the model uncertainties.

The *prior* and *posterior* probability density and cumulative distribution functions (i.e. PDFs-CDFs) of the resistance model uncertainty together with the distributions related to the *new* information are plotted respectively in Figure 4.16(a) - 4.16(b) considering all the results and in Figure 4.17(a) - 4.17(b) excluding the results of *Pang and Hsu, 2000*. The mean value and the coefficient of variation of the resistance model uncertainties are respectively equal to 1.01 and 0.15 as listed in Table 4.8 considering all the results, and to 1.01 and 0.12 as reported in Table 4.9 excluding *Pang and Hsu, 2000* results.

As the *Pang and Hsu, 2000* results led to higher level of epistemic uncertainty related, mainly, to uncertain experimental tests, the calibration of the partial safety factor is performed considering only the set of results derived excluding such experimental outcomes.

Resistance model uncertainty safety factor γ_{Rd}

The results of the statistical and probabilistic analysis proposed in previous subsections allow to perform the calibration of the partial factor γ_{Rd} related to the resistance model uncertainties for 2D NLFEMs of reinforced concrete structures. The *resistance model uncertainty safety factor* γ_{Rd} can be derived as a function of the required reliability level taking into account the reliability differentiation proposed by structural Codes (e.g. *fib Model Code 2010*; *EN1990*). The target levels of reliability for the ULS design and assessment of new and existing reinforced concrete structures are suggested, respectively, by *fib Model Code 2010*; *EN1990*; *ISO 2394, 2015*; *fib Bulletin 80, 2016*.

fib Model Code 2010 differentiates the target values of the reliability index β as a function of the consequences of failure and of the reference service life of the structure. Concerning new structures with 50 years of service life, the value of β may be assumed equal to 3.1, 3.8 and 4.3 respectively for low, moderate and high consequences of structural failure. As for existing structures, the level of reliability is identified as a function of the residual service life as well as a range of β is suggested depending on the costs necessary for the safety measures. For a residual service life

of 50 years, the value of β may be adopted in the range 3.1-3.8; for residual service life of 15 years, β can be selected in the range 3.4-4.1; for residual service life of 1 year, the values of β are suggested varying in the range of 4.1-4.7. In the hypothesis of lognormal distributions for the resistance model uncertainties ϑ and adopting the statistical parameters reported in Table 4.9 (i.e., $\mu_\vartheta = 1.01$, $V_\vartheta = 0.12$ excluding Pang and Hsu, 2000 results), the partial safety factor γ_{Rd} can be calculated in compliance with Eq.(4.2) for the different levels of reliability suggested by *fib Model Code 2010*, as listed in Tables 4.10 and 4.11.

Table 4.10: Values of the partial safety factor γ_{Rd} for the model uncertainties in 2D NLFEAs of reinforced concrete structures according to *fib Model Code 2010* (hypothesis of *non-dominant* resistance variable).

	Service life	Consequences of failure	Reliability index β	FORM factor α_R	Partial safety factor γ_{Rd}
					Excluding results Pang and Hsu,2000
New structures	[Years]	[-]	[-]	[-]	[-]
	50	Low	3.1	Non-dominant 0.32	1.12
	50	Moderate	3.8		1.15
	50	High	4.3		1.17
Existing structures	Residual service life		Reliability index β	FORM factor α_R	Partial safety factor γ_{Rd}
			Excluding results Pang and Hsu,2000		
	[Years]		[-]	[-]	[-]
	50		3.1 - 3.8	Non-dominant 0.32	1.12- 1.15
	15		3.4 - 4.1		1.13- 1.16
1		4.1 - 4.7	1.16 - 1.19		

Table 4.11: Values of the partial safety factor γ_{Rd} for the model uncertainties in 2D NLFEAs of reinforced concrete structures according to *fib Model Code 2010* (hypothesis of *dominant* resistance variable).

	Service life	Consequences of failure	Reliability index β	FORM factor α_R	Partial safety factor γ_{Rd}
					Excluding results Pang and Hsu,2000
New structures	[Years]	[-]	[-]	[-]	[-]
	50	Low	3.1	Dominant 0.8	1.34
	50	Moderate	3.8		1.44
	50	High	4.3		1.52
Existing structures	Residual service life		Reliability index β	FORM factor α_R	Partial safety factor γ_{Rd}
			Excluding results Pang and Hsu,2000		
	[Years]		[-]	[-]	[-]
	50		3.1 - 3.8	Dominant 0.8	1.34 - 1.44
	15		3.4 - 4.1		1.39 - 1.49
1		4.1 - 4.7	1.49 - 1.58		

Table 4.10 reports the values of γ_{Rd} estimated in the hypothesis of non-dominant resistance variable according to *fib Model Code 2010* and *EN1990* and assuming the FORM sensitivity factor α_R equal to 0.32 (i.e., multiplying the coefficient, assumed for dominant resistance variable $\alpha_R = 0.8$, by 0.4). Note that, as suggested by *fib Model Code 2010* in a common reliability analysis, the random variability of the concrete mechanical properties may be described by a lognormal distribution with a coefficient of variation equal to 0.15, whereas the random variability of steel properties may be defined by a lognormal distribution with coefficient of variation ranging from 0.05 to 0.08. The value of the coefficient of variation for the resistance model uncertainties estimated in the present investigation excluding the results *Pang and Hsu, 2000* (i.e., $V_g=0.12$) is lower than the one commonly assumed for the probabilistic modelling of concrete compressive strength. It means that in case of a reliability assessment through NLFEAs, the uncertainty on the resistance side should be dominated by the aleatory uncertainties related to material resistances instead of the model uncertainty. Under this circumstance, the assumption of the model uncertainty as a non-dominating variable, according to *fib Model Code 2010* and *EN1990*, is valid with the consequence that the value of the partial safety factor γ_{Rd} would be lower than the one under the hypothesis of dominant resistance variable associated to the model uncertainties.

In this case of *non-dominant* resistance variable, considering structures with an ordinary service life of 50 years and moderate consequences of structural failure ($\beta=3.8$), the value of γ_{Rd} can be set to 1.15. For existing structures, γ_{Rd} vary between 1.12 and 1.19 for the different residual service lives and reliability indices. In Table 4.11, the values of the partial safety factor γ_{Rd} , evaluated in the hypothesis of dominant resistance variable for the model uncertainties (i.e., $\alpha_R=0.8$) in the definition of resistance models within 2D NLFEAs, are also reported. This assumption leads to values of the partial safety factor γ_{Rd} higher than 30% respect to the ones estimated according to *fib Model Code 2010* and *EN1990* in case of non-dominant random variable. It is also worth to underline that the hypothesis of dominant resistance variable for the model uncertainties refers to the epistemic uncertainties for the global behaviour of the structure and does not influence the other uncertainties (i.e., aleatory ones) within the safety formats for NLFEAs of r.c. structures.

The range of the values for the partial safety factor γ_{Rd} suitable for existing structures is also proposed in Tables 4.10 and 4.11 with the same hypotheses, depending on the residual service life and on the costs for an upgrading of the structure. Otherwise, considering all the results of Table 4.8, the partial safety factors have also computed and are slightly higher (about 5%) than the ones proposed in Tables 4.10 and 4.11.

This Section, has been devoted to the estimation of the influence of *epistemic* uncertainties within safety verifications by means NLFEA. In the following Section, the comparison of different safety formats is proposed taking into account the influence of the *aleatory* uncertainties.

4.3 Comparison between safety formats for NLFEAs

The present Section aims to compare the different *safety formats* introduced in Section 2.3 (i.e. *Partial Factor Method* (PFM), *Global Resistance Methods* (GRMs) and *Probabilistic Method* (PM)) in order to estimate the global design strength of different reinforced concrete members by means NLFEAs.

Specifically, non-linear finite element models are properly defined to reproduce different experimental tests. Successively, several non-linear finite element analyses are carried out in compliance with the different safety formats for each reinforced concrete structure experimentally tested in order to compare and critically discuss the results in terms of resistance and failure mode.

As introduced in Chapter 1 the *fib Model Code 2010* define the *Levels of Approximation* approach (i.e LoAs) as methodological approach for multi-level evaluation of the structural safety. According to this principle, lower *LoAs* imply the use of simplified, and almost safer, resistance models with lower time spending required to assess the structural safety. Conversely, the highest levels of approximation suggested by makes it possible to adopt refined numerical methods (such as the non-linear finite element method (NLFE)) in order to assess the structural reliability. Nevertheless, facing the draft on new *fib Model Codes*, the possibility to apply the *LoAs* in order to classify the different *safety formats* is seriously analyzed by responsible scientific committees.

For this reason, in the present, the different *safety formats* are investigated and compared to demonstrate if they are able to estimate the corresponding global design resistance capacities and to capture any possible modification in the *failure mode* for each structure (and then perform “safe” predictions). In the details, the term *failure mode* will represent: “*global structural collapse due to a specific material failure occurred in a specific location within the structural member*”. Moreover, the suitability of the safety formats to be classified according to *LoAs* approach is also discussed.

The following *safety formats*, described in Section 2.3, has been compared and discussed:

1. Partial Factor Method (PFM) (*fib Model Code 2010*);
2. Global Resistance Methods (GRMs)
 - Method of estimating the coefficient of variation of the structural resistance (ECOV) (*fib Model Code 2010*);
 - Global Resistance Factor (GRF) (*fib Model Code 2010*);
 - Global Safety Format (GSF) (*Allaix et. Al, 2013*);
3. Probabilistic Method (PM) (*fib Model Code 2010*).

The detailed description of the methodologies is proposed in Section 2.3. In the following, the study cases adopted in order to compare the different *safety formats* are described.

4.3.1 Case studies and NLFE modelling

The following reference RC structures have been assumed: four simply supported beams with web openings having experimental results known from the literature (*Aykac et al., 2013*) and one simply supported “T” beam designed according to *EN 1992-1-1* and checked also with *fib Model Code 2010*.

In the first subsection, the description of the structural members with the loading configuration is reported and, subsequently, the NLFE models are calibrated according to the experimental evidences. In this process of definition and calibration of the NLFE models, the actual values of the material properties coming from the experimental measurements are considered as mean values.

Description of the structural members and of the actual structural behavior

Firstly, the beams with web openings realized and tested by *Aykac et al., 2013* are described. Four beams with a 150 x 400 mm rectangular section and with a span length of 3900 mm have been selected from the original experimental campaign. The first three beams are characterized by n°12 200x200 mm square openings and are casted with growing reinforcement ratios (e.g., SL, SM, SH where S=square openings, L=low reinforcement ratio, M=medium reinforcement ratio, H=high reinforcement ratio). The fourth beam has n°12 circular openings with a diameter of 200 mm and crossing diagonal reinforcements between the openings. The characteristics of the beams from *Aykac et al., 2013* selected for the present investigation are reported in Tables 4.12 and 4.13 with the mechanical properties of the materials.

Table 4.12: Beams selected with the geometric details of longitudinal reinforcements and with properties of concrete.

Ref.	Beam	Opening	Tensile reinforcement		Compression reinf.	Diagonal reinf.	f _c [MPa]
			Amount [-]	Ratio [-]			
<i>Aykac et al., 2013</i>	SL	Square	2Φ8 and 2Φ10	0.0045	2Φ8	-	22
	SM	Square	2Φ8 and 4Φ10	0.0070	2Φ8	-	20
	SH	Square	2Φ8 and 7Φ10	0.0111	2Φ8	-	21
	CLX	Circular	2Φ8 and 7Φ10	0.0045	2Φ8	2Φ10	22
-	T-Beam	No openings	3Φ24	0.0123	4Φ14	-	28

Table 4. 13: Properties of the reinforcements.

Ref.	Diameter [mm]	f_y [MPa]	E_s [MPa]
<i>Aykac et al., 2013</i>	$\Phi 8 - \Phi 10 - \Phi 12$	480	200000
	$\Phi 4 - \Phi 6$	520	200000
T-Beam	$\Phi 8 - \Phi 14 - \Phi 24$	495	200000

The geometric scheme with the reinforcement arrangement for each beam from *Aykac et al., 2013* is depicted in Figure 4.18(a)-(d). The experimental tests were conducted by means of a 200 kN capacity steel frame.

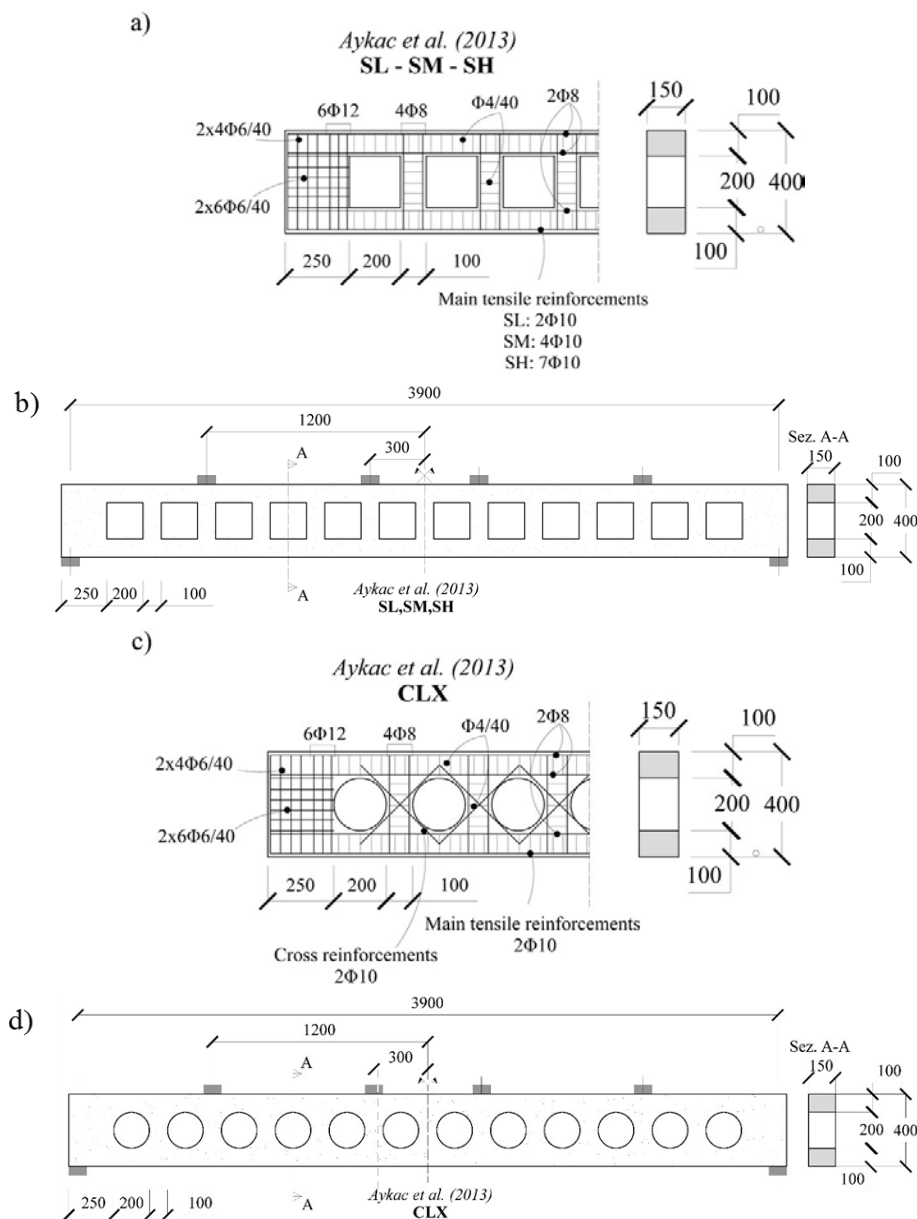


Figure 4.18: Reinforcements arrangement for beams with square openings SL, SM, SH (a) and CLX (c); representation of the tests set and loading configuration (b) and (d) (modified from *Aykac et al., 2013*). (Dimensions in [mm]).

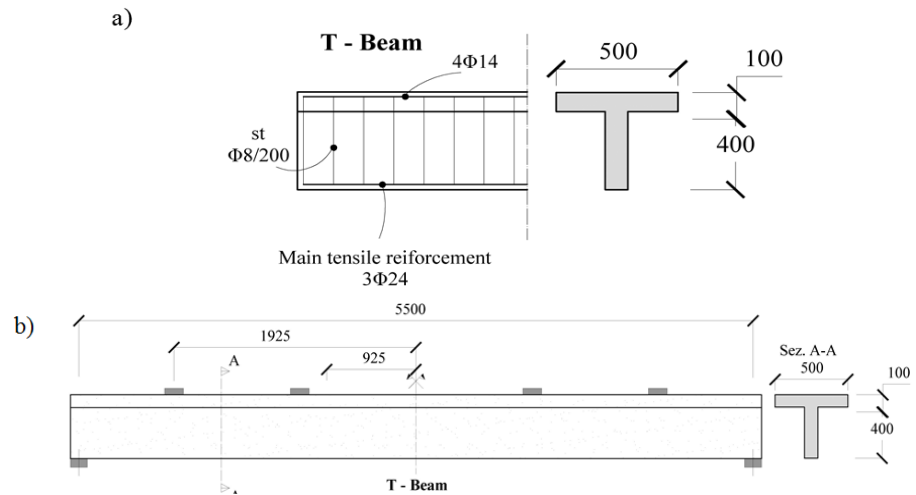


Figure 4.19: Reinforcements arrangement for the T-Beam (a) and representation of the static scheme and loading configuration (b). (Dimensions in [mm]).

Specimens were simply supported and symmetrically loaded at four points with the loading points located at 0.3 m and 1.2 m on either side of the midspan. The load from a hydraulic cylinder was equally distributed to the four loading points by means of a main and of two secondary steel spreading beams. Six-point bending condition (two support and four loading points) was adopted (Figure 4.18(b) and (d)).

The last beam considered for the investigation has been designed from the authors according to *EN 1992-1-1* in order to fail in bending for a total design load of 335 kN. The structural verifications, performed also in compliance with *fib Model Code 2010*, are fully satisfied. The beam has a “T” shaped cross section with total height of 500 mm, top flange width of 500 mm and web width of 150 mm. The top flange thickness is 100 mm. The details of reinforcements and of material properties are, respectively, reported in Tables 4.12 and 4.13 and represented in Figure 4.19(a). The beam is supposed to be loaded with a six point bending scheme (Figure 4.19(b)).

Definition, calibration and validation of the NLFE models

The finite element models of the Beams SL, SM, SH, CLX and of the T-Beam have been performed adopting the software *ATENA 2D*, using four-node quadrilateral iso-parametric plane stress finite elements, which are based on a linear polynomial interpolation and 2x2 Gauss point’s integration scheme. The FE meshes have properly been defined after an appropriate sensitivity analysis. The non-linear system of equations is solved by means of the standard Newton-Raphson iterative procedure based on the hypothesis of a linear approximation.

Concerning the material models, non-linear behavior of concrete in compression has been modelled with the SBeta Model available in the *ATENA 2D* platform. This model allows to consider compression softening behavior with a

reduction of the compression strength and shear stiffness (shear retention factor equal to 0.2) after cracking.

The tensile concrete behavior has been modelled with a linear tension softening law to take into account the “tension stiffening effect”, as widely discussed in Section 2.2 and 4.2. Concerning the beams of *Aykac et al., 2013*, the inclination of the softening branch has been modified by means of an iterative process to best fit the experimental response in terms of force-displacement or stress-strain as also carried out in Section 4.2. Whereas, for the T-Beam designed according to *EN1992-1-1* the ultimate strain in tension has been assumed as ten times the elastic strain at the peak tensile strength. In this way, the fracture energy has been again accounted for, in absence of specific experimental tests and provisions.

The two-dimensional failure criteria defined by *Kupfer and Gerstle, 1973* has been adopted in order to model the plane-stress failure mode of concrete matrix and the cracking process has been reproduced using the smeared cracking with fixed crack direction model.

Concerning the reinforcement steel, the bi-linear constitutive law in tension and in compression (assuming a hardening behavior with an increase of strength at the ultimate deformation of 7% equal to 15% of the yielding strength) has been adopted. The reinforcement has been modelled with discrete bar elements assuming a perfect bond with the surrounding concrete.

The finite element models have been defined considering half beam due to the perfect symmetry. In agreement with the experiments performed by *Aykac et al., 2013* and with the loading configuration selected for T-Beam, the following loading history has been considered to perform the NLFEMs:

- Dead weight;
- Incremental loading applied according to the test set configuration up to failure.

The Young modulus of the materials and the concrete tensile strength have been calculated starting from the actual values of the parameters given from the experiments (i.e., assumed as mean values) in compliance with *JCSS Probabilistic Model Code 2001* and *fib Model Code 2010*. Table 4.14 describes and summarizes the *modelling hypotheses* performed concerning the equilibrium, the compatibility and constitutive law within the definition of the NLFEM models.

In the following, for all the RC beams, the structural resistance is represented in terms of the ultimate global loads reached during the incremental loading processes according to the experimental tests as reported in Table 4.15 with a description of the *failure modes*, also shown in Figure 4.20.

As introduced before, the *failure mode* identifies a specific resisting mechanism developed with the crisis of a specific material in a certain region of the structural member.

Table 4.14: Basic *modelling hypotheses* assumed in the definition of NLFE numerical models.

	Software: ATENA 2D
<i>Equilibrium</i>	<ul style="list-style-type: none"> - Standard Newton-Raphson based on the hypothesis of linear approximation <li style="padding-left: 20px;">- Convergence criteria based on strain energy - Load step sizes defined in compliance with the experimental procedure
<i>Compatibility</i>	<p style="text-align: center;"><i>FINITE ELEMENTS</i></p> <ul style="list-style-type: none"> - Iso-parametric plane stress 4 nodes (2x2 Gauss points integration scheme with linear interpolation) <li style="padding-left: 20px;">- Discrete reinforcements - Element size defined by means of an iterative process of numerical accuracy
<i>Constitutive laws</i>	<p style="text-align: center;"><i>CONCRETE</i></p> <ul style="list-style-type: none"> - Fixed crack model, smeared cracking, constant shear retention factor = 0.2 <li style="padding-left: 20px;">- Mono-dimensional model extended to biaxial stress state - Compression: Non-linear with post peak linear softening branch - Tension: Elastic with post peak linear tension softening (LTS) <p style="text-align: center;"><i>REINFORCEMENT STEEL</i></p> <ul style="list-style-type: none"> - bi-linear constitutive law for the reinforcement in tension and in compression

Table 4.15: Comparison between the NLFEAs results and the experimental outcomes.

Ref.	Beam	Experimental ultimate load R_{Exp} [kN]	Actual failure mode	Material properties used for NLFEA	Ultimate load from NLFEA R_m [kN]	NLFEA failure mode
<i>Aykac et al, 2013</i>	SL	92.2	<i>Bending</i>	<i>Mean</i>	85.1	<i>Bending</i>
	SM	117.0	<i>Vierendeel</i>	<i>Mean</i>	100.7	<i>Vierendeel</i>
	SH	123.0	<i>Vierendeel</i>	<i>Mean</i>	109.9	<i>Vierendeel</i>
	CLX	116.0	<i>Bending</i>	<i>Mean</i>	94.2	<i>Bending</i>
-	T-Beam	435.4	<i>Bending</i>	<i>Mean</i>	458.6	<i>Bending</i>

The beams with square opening present ultimate loads that increase as the reinforcement ratio increases (i.e., SL, SM and SH) with different failure modes. In fact, the beam with a low reinforcement ratio is characterised by a bending failure mode as illustrated in Figure 4.20 (a), whereas Beams SM and SH present a Vierendeel failure mode as shown in Figure 4.20(c-e), respectively. The failure mode of the Beam CLX is a bending mechanism (Figure 4.20(g)).

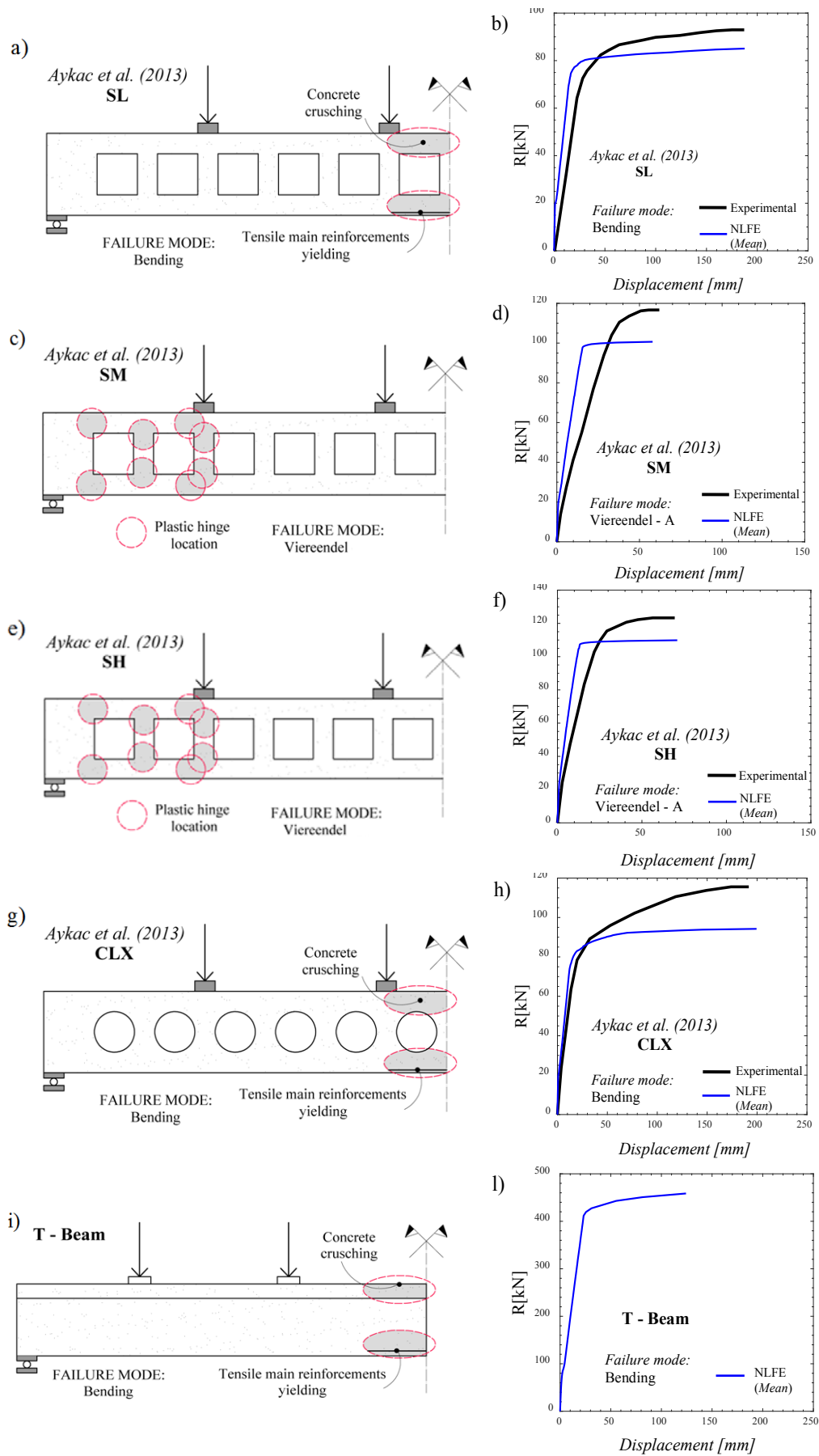


Figure 4.20: Failure modes recognised from NLFEAs with numerical and experimental load-displacement curves.

Finally, the T-Beam is characterised by a bending failure mode according to the design purposes *EN1992-1-1* (Figure 4.20(i)). Table 4.15 reports in place of the experimental ultimate load the ultimate load evaluated according to *EN1992-1-1* using mean values of material properties.

Note that the failure modes of the beams with openings are in agreement with the experimental evidences. In Figures 4.13(b),(d),(f),(h),(l), the load-displacement curves for each RC beam are shown and compared to the experimental outcomes regarding the beams with openings. In addition, the differences in terms of the global resistance between the numerical results and the experimental ones are mainly due to the modelling uncertainties of these complex structures and this lack of knowledge, in practice and for a comprehensive evaluation of structural reliability, is covered by the corresponding *resistance model uncertainty safety factor* γ_{Rd} as discussed in Section 4.1.

4.3.2 Results from NLFEAs

The results of NLFEAs required for the application of the different safety formats are reported and commented separately for PFM and global resistance methods, ECOV, GRF and methods that requires probabilistic modelling as PM and GSF.

NLFEAs results according to PFM, ECOV and GRF

Next, the comparison between the following *safety formats* is reported, considering each one of the five RC beams:

- *Partial factor method (PFM) (fib Model Code 2010)*: is based on using the design values of the material resistances;

- *Estimation of the coefficient of variation (ECOV) (fib Model Code 2010)*: is based on using the mean values and the characteristic values of the material properties;

- *Global resistance factor (GRF) (fib Model Code 2010, EN1992-2)*: is based on using the f_{cmd} value for concrete and the f_{ym} value (set equal to the experimental value) for reinforcement.

Beam SL Aykac et al, 2013	Ultimate Load [kN]	Failure mode
NLFE - $R_{NLFEA}(f_d)$	65.1	Bending
NLFE - $R_{NLFEA}(f_m)$	85.1	
NLFE - $R_{NLFEA}(f_k)$	77.1	
NLFE - $R_{rep}(f_{cmd}, f_{ym})$	79.9	

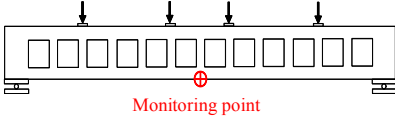
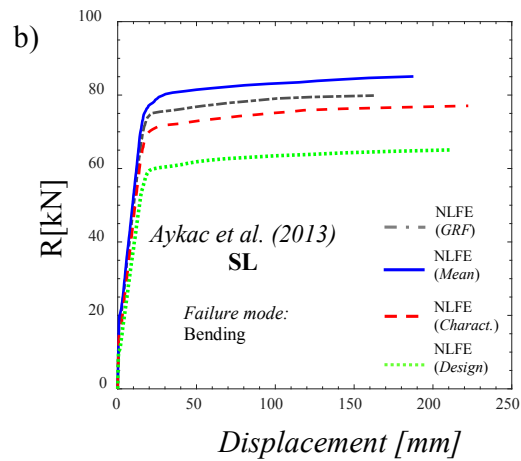



Figure 4.21: Beam SL Aykac et al, 2013: Failure mode recognised for simulations performed with NLFEAs (a); results in terms of ultimate global resistance R for the NLFE simulations in agreement with the PFM, ECOV and GRF methods (b).

Figures 4.21 - 4.25 illustrates the load-displacement curves evaluated with the characteristic, design and mean values together with the the load-displacement curve defined using f_{cmd} and f_{ym} in compliance with the three *safety formats* for the five reinforced concrete beams, respectively. In addition, a description of the corresponding *failure mode* is also indicated. As obvious, the numerical curves present the peak resistance values when the mean values of the material properties are considered. With reference to the *failure mode*, for each RC beam the resistance mechanism is the same identified in the previous section. Specifically, Beam SL, Beam CLX and T-Beam present bending failure modes, whereas Beam SM and Beam SH are characterised by a Vierendeel failure mode, herein identified as “Vierendeel - A” mechanism, equal to the one shown in Figures 4.20(c) and (e).

It is worthy to observe that the resistance, estimated using the f_{cmd} and f_{ym} values, tends to the resistance achieved with the mean values if the bending failure mode occurs due to the relevant contribution of the steel re-bars. Instead, the curve tends to the resistance achieved with the characteristic values if the Vierendeel failure mode occurs due to the dominant role of the concrete.

Beam SM Aykac et al, 2013	Ultimate Load [kN]	Failure mode
NLFE - $R_{NLFEA}(f_d)$	73.1	Vierendeel - A
NLFE - $R_{NLFEA}(f_m)$	100.7	
NLFE - $R_{NLFEA}(f_k)$	85.5	
NLFE - $R_{rep}(f_{cmd}, f_{ym})$	84.3	

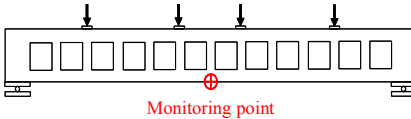
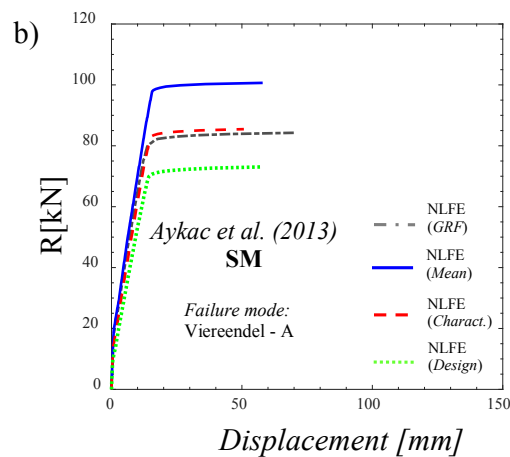



Figure 4. 22: Beam SM Aykac et al, 2013: Failure mode recognised for simulations performed with NLFEAs (a); results in terms of ultimate global resistance R for the NLFE simulations in agreement with the PFM, ECOV and GRF methods (b).

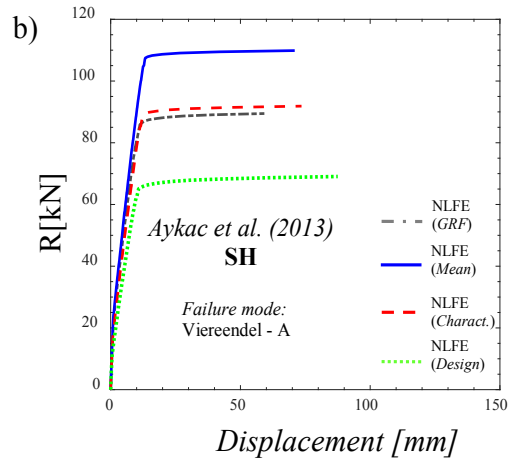
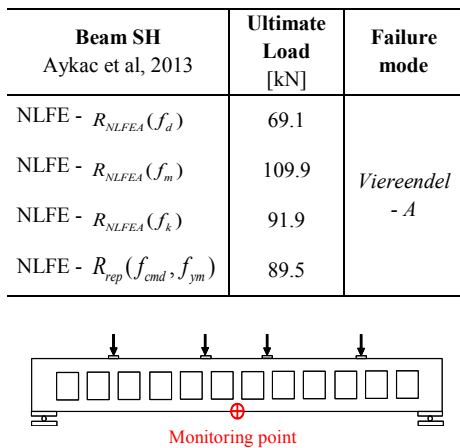


Figure 4.23: Beam SH Aykac et al, 2013: Failure mode recognised for simulations performed with NLFEAs (a); results in terms of ultimate global resistance R for the NLFE simulations in agreement with the PFM, ECOV and GRF methods (b).

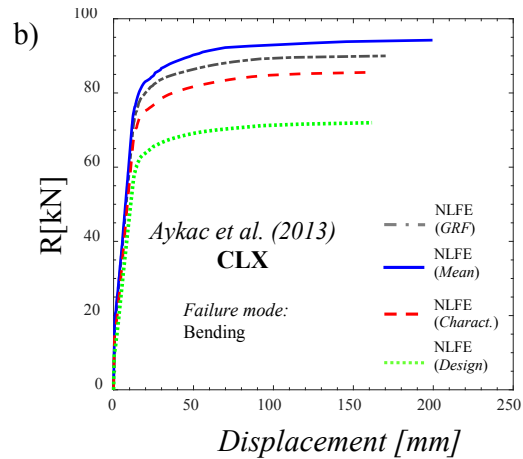
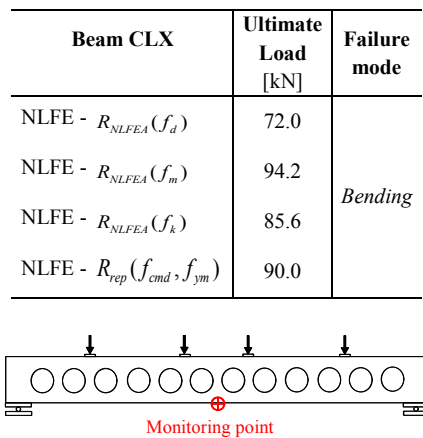


Figure 4.24: Beam CLX Aykac et al, 2013: Failure mode recognised for simulations performed with NLFEAs (a); results in terms of ultimate global resistance R for the NLFE simulations in agreement with the PFM, ECOV and GRF methods (b).

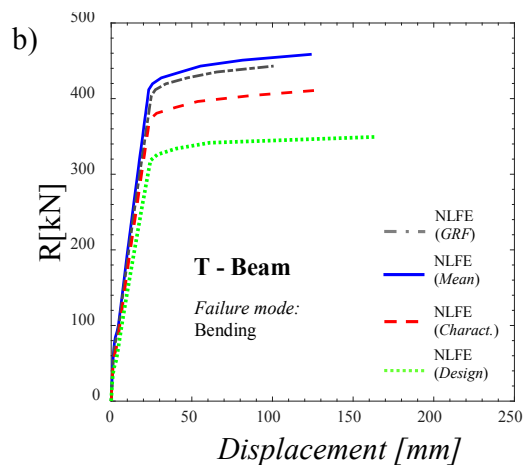
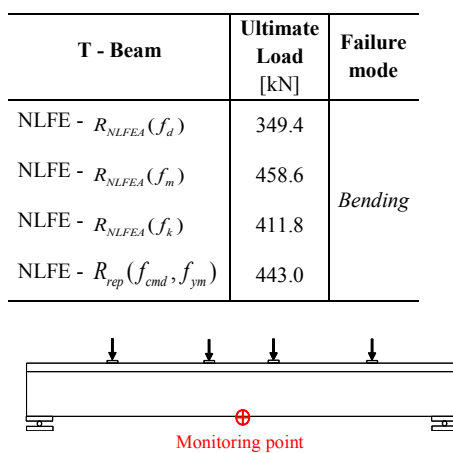


Figure 4.25: T-Beam: Failure mode recognised for simulations performed with NLFEAs (a); results in terms of ultimate global resistance R for the NLFE simulations in agreement with the PFM, ECOV and GRF methods (b).

The abovementioned mechanical observation highlights the influence of the *failure mode* in estimating the global structural response, leading to a different order of the load levels achieved from these three *safety formats* for the analysed beams.

NLFEAs results according to GSF nad PM

In the following the applications of the “probabilistic” *safety formats* on each one of the five reinforced concrete beams is reported:

- *Global safety format (GSF) (Allaix et al., 2013)*: is based on using the mean values of the material properties and on a reduced probabilistic analysis to estimate the coefficient of variation of the global structural resistance;

- *Probabilistic method (PM) (fib Model Code 2010)*: is based on a reduced probabilistic analysis to estimate the probabilistic distribution of the global structural resistance and the related design quantile.

In the both abovementioned *safety formats*, a reduced probabilistic analysis is performed adopting the *Latin Hypercube Sampling (LHS) method (McKey et al., 1979; Olsson et al., 2003)* as the preferred technique to define 30 sampled NLFE models.

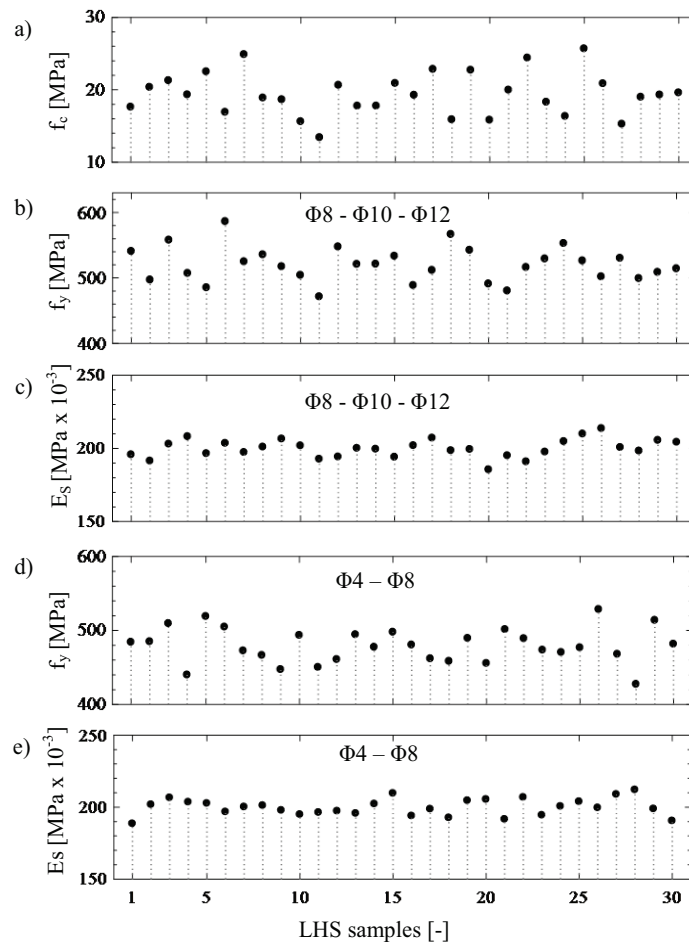


Figure 4.26: Beam SL (Aykac et al., 2013): sampled values of the relevant random variables of the 30 NLFE models.

Specifically, the structural properties assumed as independent random variables relevant to the problem with the corresponding probabilistic distributions are reported in Table 4.16.

If other aleatory uncertainties (e.g., geometrical properties) are relevant to the problem, they can be considered following the similar approach according to the LHS technique.

The concrete tensile strength f_{ct} as well as the concrete Young modulus E_c have been assumed as random variables dependent on the concrete compressive strength f_c random variable according to *JCSS Probabilistic Model Code, 2001*. Moreover, note that regarding the reinforced concrete beams tested by *Aykac et al., 2013*, the mechanical properties of the various reinforcements are different (Table 4.12), so the number of random independent variables to consider increases

In fact, with reference to Beam SL, as example, Figure 4.26 shows the sampled values of each one of the five independent random variables employed to define the 30 NLFE models. In fact, for each sample, it is possible to read the five sampled values of the five random variables combined by the ones of the LHS method. Similar process has been followed to define the 30 NLFE models of the other four reinforced concrete beams.

Table 4. 16: Probabilistic models (*JCSS Probabilistic Model Code, 2001*) for the main independent random variables affecting the structural behaviour.

Random variable	Probabilistic distribution	Mean value*	Coefficient of variation
Concrete cylinder compressive strength f_c [MPa]	<i>log-normal</i>	f_{cm}	0.15
Reinforcement steel yielding strength f_y [MPa]	<i>log-normal</i>	f_{ym}	0.05
Reinforcement steel Young modulus E_s [MPa]	<i>log-normal</i>	200000	0.03

*Mean value = experimental value for reference *Aykac et al., 2013*[21]

The results from the 30 NLFEAs carried out for each reinforced concrete beam are, respectively, depicted in Figures 4.27 - 4.31, illustrating all the failure modes that occur as well as the results in terms of the global structural resistance (Figure 4.27(b), Figure 4.28(c), Figure 4.29(b), Figure 4.30(b), Figure 4.31(c)).

These figures also illustrate the lognormal probability density functions (PDFs) with the mean value, the coefficient of variation (CoV), estimated by means of the *maximum likelihood technique* (i.e., ML), and the p-value after Anderson-Darling test confirm the log-normality assumption (Figure 4.27(c), Figure 4.28(d), Figure 4.29(c), Figure 4.30(c), Figure 4.31(d)).

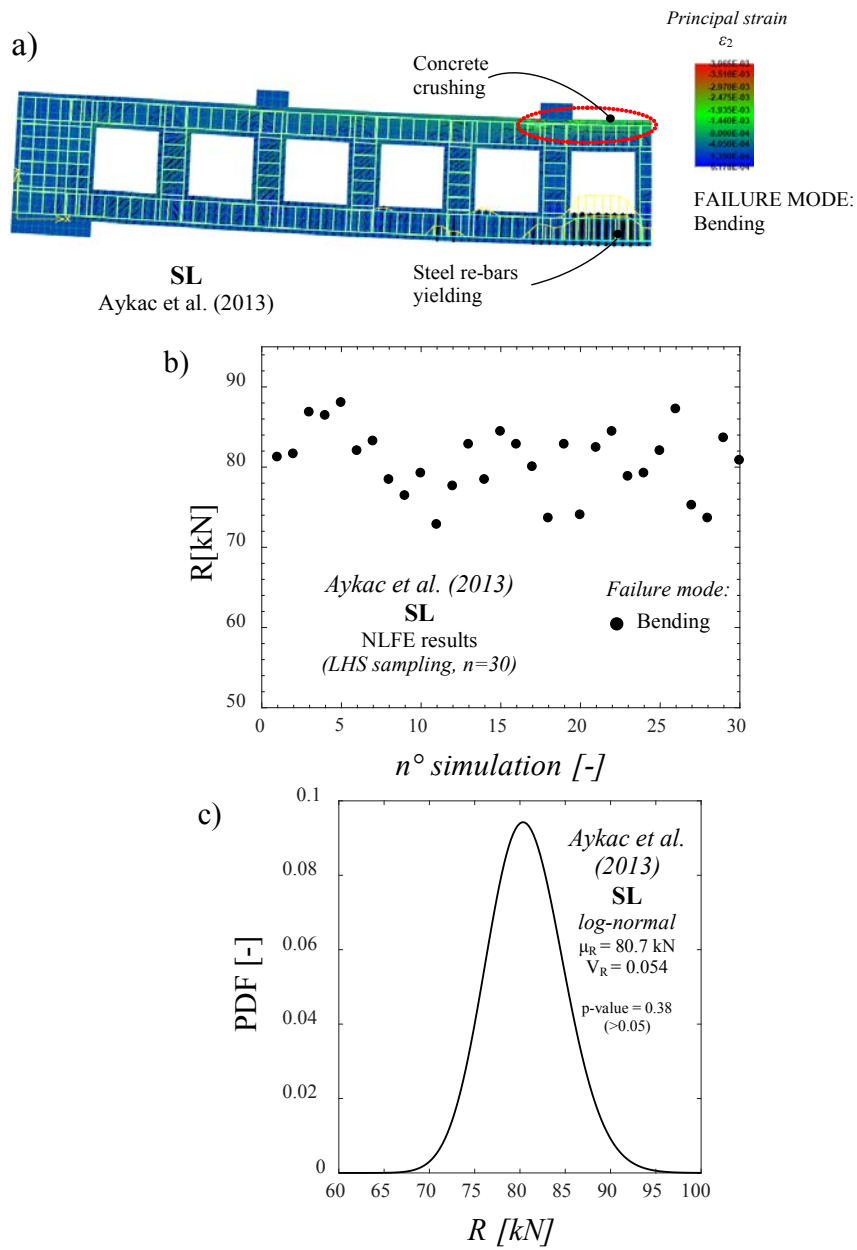


Figure 4.27: Beam SL (Aykac et al., 2013): Failure mode recognised for simulations performed with NLFEAs (a); results in terms of ultimate global resistance R for the NLFE simulations coming from $n=30$ LHS samples (b); lognormal probabilistic distribution for the global resistance R (c).

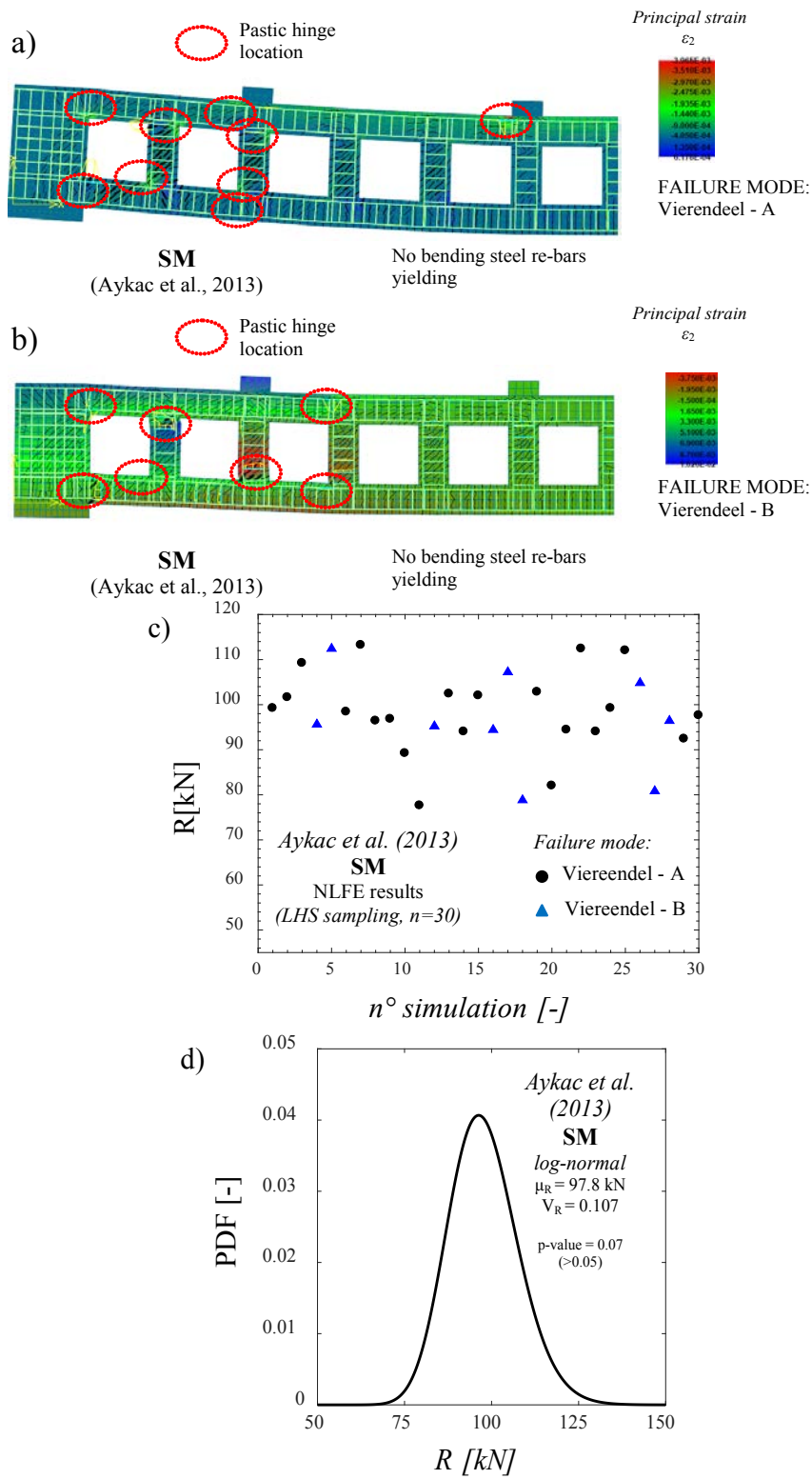


Figure 4.28: Beam SM (Aykac et al., 2013): Failure modes recognised for simulations performed with NLFEAs (a)-(b); results in terms of ultimate global resistance R for the NLFE simulations coming from $n=30$ LHS samples (c); lognormal probabilistic distribution for the global resistance R (d).

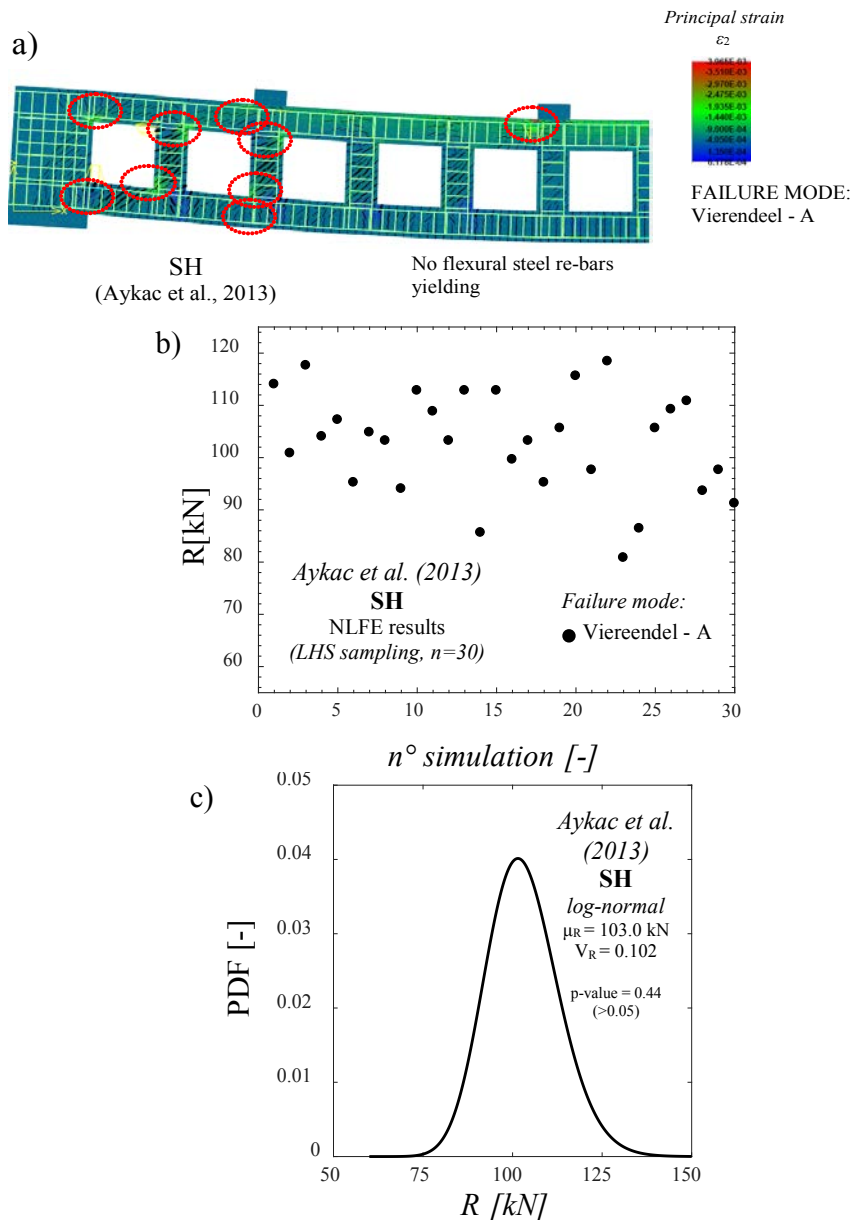


Figure 4.29: Beam SH (Aykac et al., 2013): Failure mode recognised for simulations performed with NLFEAs (a); results in terms of ultimate global resistance R for the NLFE simulations coming from $n=30$ LHS samples (b); lognormal probabilistic distribution for the global resistance R (c).

From the observation of the all 30 numerical results related to each RC structure, it derives that:

- Beam SL is always characterized by only one failure mode having a bending mechanism with concrete crushing and yielding of the steel re-bars (Figure 4.27(a)-(b));
- Beam SM presents two failure modes with a Vierendeel mechanism characterized by local failures in different structural regions (Vierendeel-A; Vierendeel-B) (Figure 4.28(a)-(c));

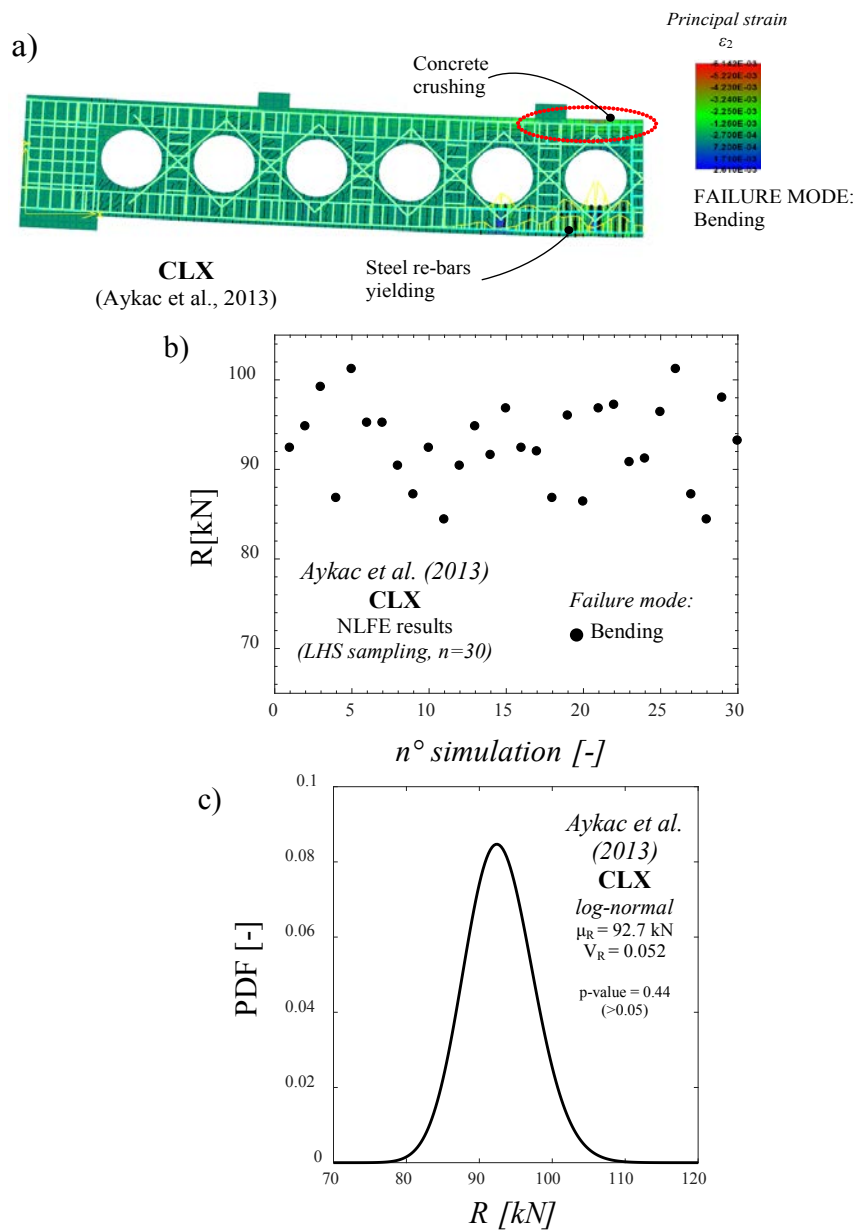


Figure 4.30: Beam CLX (Aykac et al., 2013): Failure mode recognised for simulations performed with NLFEAs (a); results in terms of ultimate global resistance R for the NLFE simulations coming from $n=30$ LHS samples (b); lognormal probabilistic distribution for the global resistance R (c).

- Beam SH is always characterized by only one failure mode having a Viereendel-A mechanism (Figure 4.29(a)-(b));

- Beam CLX is always characterized by only one failure mode having a bending mechanism with concrete crushing and yielding of the steel re-bars (Figure 4.30(a)-(b));

- T-Beam presents two failure modes having, respectively, a bending mechanism with concrete crushing and yielding of the steel re-bars and a shear mechanism with concrete crushing (Figure 4.31(a)-(b)).

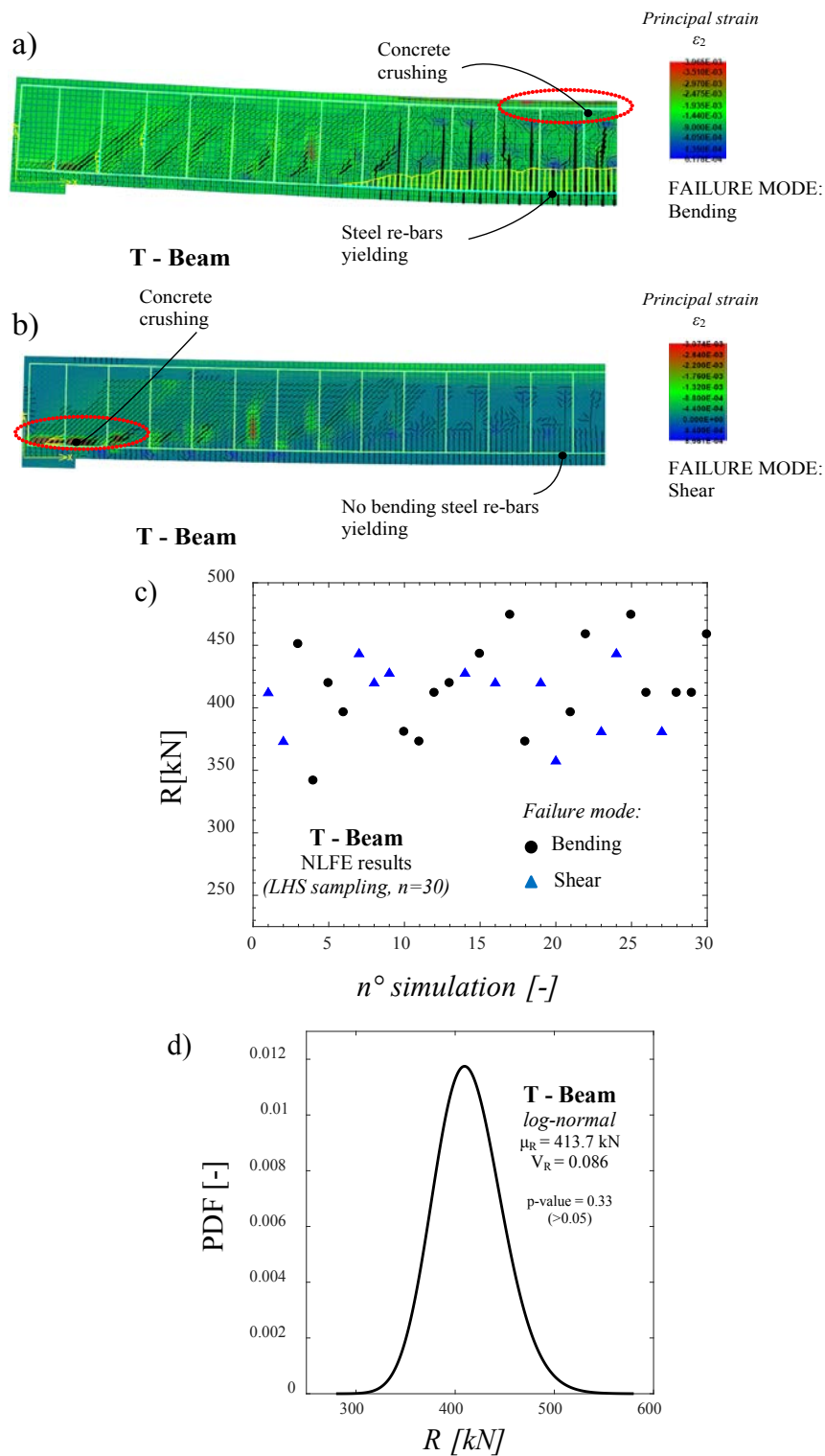


Figure 4.31: Beam designed according to *fib* Model Code 2010 and to EC2 (T-Beam): Failure modes recognised for simulations performed with NLFEAs (a)-(b); results in terms of ultimate global resistance R for the NLFE simulations coming from $n=30$ LHS samples (c); lognormal probabilistic distribution for the global resistance R (d).

Table 4.17: Results from the LH sampling and ML estimates of the parameters.

Ref.	Beam	N° of LH samples [-]	Probabilistic distribution [-]	ML estimates		
				μ_R [kN]	σ_R [kN]	V_R [-]
<i>Aykac et al, 2013</i>	SL	30	<i>lognormal</i>	80.7	4.4	0.054
	SM			97.8	10.4	0.107
	SH			103.0	10.5	0.102
	CLX			92.8	4.8	0.052
-	T-Beam			413.7	35.6	0.086

These results, summarized in Table 4.17, demonstrate that the *failure mode* strongly depends from the values of the material properties assumed in order to perform the NLFEM simulations for the assessment of the structural reliability.

4.3.3 Comparison between outcomes of safety formats

In this section, the global structural resistances in terms of design ultimate load of the five RC beams are evaluated in compliance with each *safety format*, according to Section 2.3 .

As previously explained, the design ultimate loads have been computed assuming a value of the *resistance model uncertainty factor* γ_{Rd} equal to 1.00 as well as a reliability index β equal to 3.8 for ordinary structures with moderate consequences in the case of failure with a lifetime of 50 years. In addition, the FORM sensitivity factor α_R is considered equal to 0.8 in the hypothesis of dominant resistance variable.

In Table 4.18, all the main results for each beam and safety format are reported: the ultimate loads achieved from the NLFEMs, the *failure modes*, the statistical parameters if necessary and, finally, the design ultimate loads.

In Figure 4.32 in semi-logarithmic scale, for the reinforced concrete beams, the cumulative distribution functions (CDFs) evaluated according to the results related to PM safety format in the previous section, are shown and are assumed as reference probability functions since they account for the effect of the possible modifications of the failure mode. On these reference CDFs all the design ultimate loads of the different safety formats are reported and compared. On the vertical axis on the right side of each figure, the corresponding values of the reliability index β are also reported. Note that the reliability levels shown in Figure 4.32 do not represent the actual safety level of the different reinforced concrete members because they are evaluated in absence of the model uncertainty random variable, according to the hypothesis of use a unitary value for γ_{Rd} .

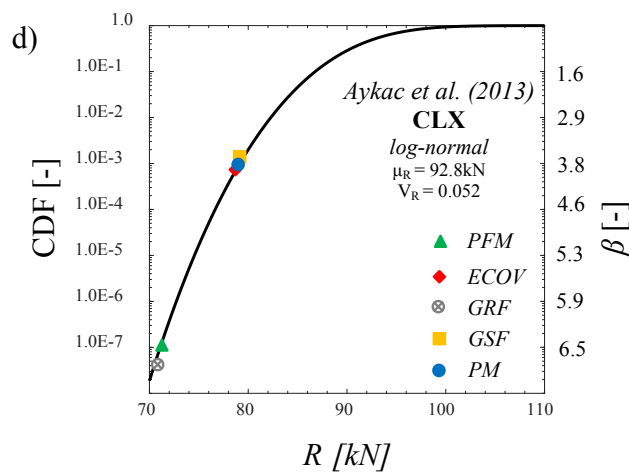
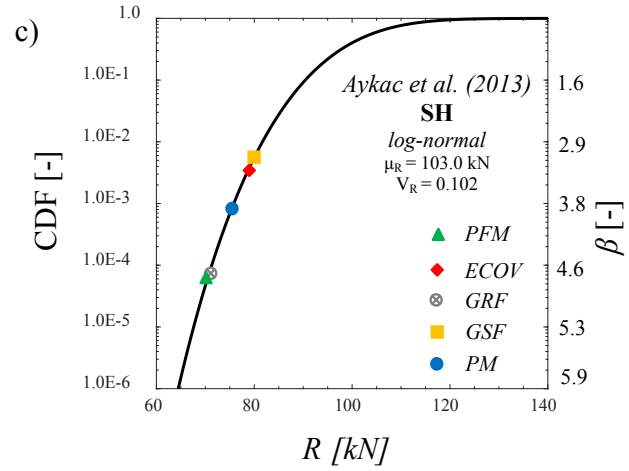
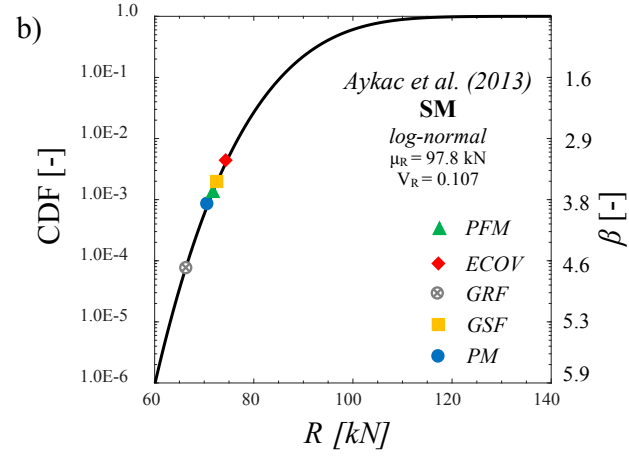
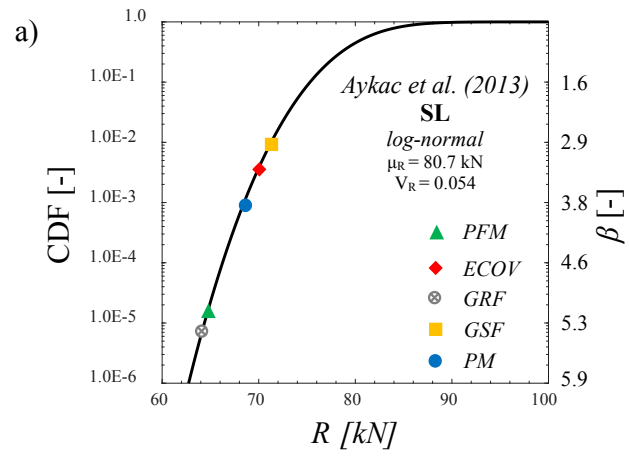
Analyzing the results, it is possible to state that for the Beam SL, Beam SH and Beam CLX the *failure mode* does not present any modification and the GRF and PFM safety formats always provide design ultimate loads lower the one evaluated with the PM (Figure 4.25(a),(c),(d)).

Table 4.18: Results in terms of design ultimate load from different safety formats.

Safety format	Ultimate load R [kN]	Failure mode	V_R	γ_R	Design ultimate load R_d [kN]
Beam SL (Aykac et al., 2013)					
PFM	65.1	<i>Bending</i>	-	-	65.1
ECOV*	85.1 - 77.1	<i>Bending</i>	0.060	1.20	70.9
GRF	79.9	<i>Bending</i>	-	1.27	62.8
GSF	30 results	<i>Bending</i>	0.054	1.18	72.2
PM	30 results	<i>Bending</i>	0.054	1.24	68.5
Beam SM (Aykac et al., 2013)					
PFM	73.1	<i>Vierendeel - A</i>	-	-	73.1
ECOV*	100.7 - 85.5	<i>Vierendeel - A</i>	0.099	1.35	74.5
GRF	84.3	<i>Vierendeel - A</i>	-	1.27	66.4
GSF	30 results	<i>Vierendeel - A and B</i>	0.107	1.38	72.8
PM	30 results	<i>Vierendeel - A and B</i>	0.107	1.42	70.7
Beam SH (Aykac et al., 2013)					
PFM	69.1	<i>Vierendeel - A</i>	-	-	69.1
ECOV*	109.9 - 91.9	<i>Vierendeel - A</i>	0.108	1.39	79.0
GRF	89.5	<i>Vierendeel - A</i>	-	1.27	70.5
GSF	30 results	<i>Vierendeel - A</i>	0.102	1.37	80.5
PM	30 results	<i>Vierendeel - A</i>	0.102	1.46	75.4
Beam CLX (Aykac et al., 2013)					
PFM	72.0	<i>Bending</i>	-	-	72.0
ECOV*	94.2 - 85.6	<i>Bending</i>	0.058	1.19	79.0
GRF	90.0	<i>Bending</i>	-	1.27	70.9
GSF	30 results	<i>Bending</i>	0.052	1.17	80.5
PM	30 results	<i>Bending</i>	0.052	1.19	79.1
T-Beam					
PFM	349.4	<i>Bending</i>	-	-	349.4
ECOV*	458.6 - 411.8	<i>Bending</i>	0.065	1.22	376.1
GRF	443.0	<i>Bending</i>	-	1.27	348.9
GSF	30 results	<i>Bending; Shear</i>	0.086	1.30	352.9
PM	30 results	<i>Bending; Shear</i>	0.086	1.44	318.3

*For ECOV method, the two values of the ultimate load correspond, respectively, to $R(f_m)$ and $R(f_k)$

Moreover, for the Beam CLX, the ECOV safety format also provides a design ultimate load lower than the estimation of the PM (Figure 4.32(d)).



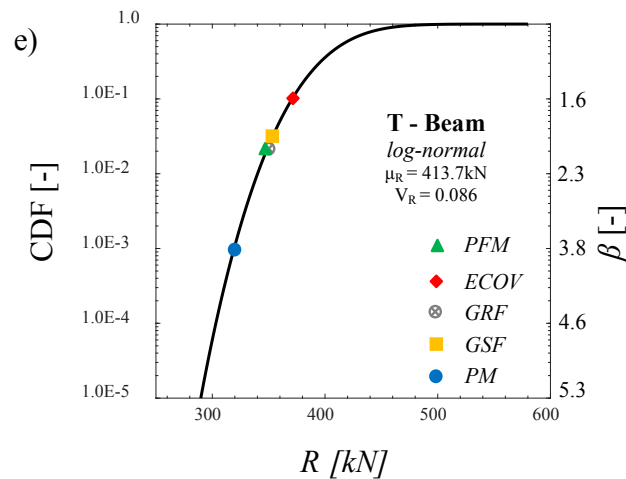


Figure 4.32: Probability plot of the design ultimate loads related to the different *safety formats*: Beam SL(a); Beam SM(b); Beam SH(c); Bema CLX(d); T-Beam (e). ($\gamma_{Rd} = 1.00$; $\beta = 3.8$; $\alpha_R = 0.8$).

Instead, for the Beam SM and T-Beam the failure modes are characterized by modifications, especially regarding the T-Beam. In fact, for the Beam SM, only the GRF safety format provides a design ultimate load lower than the one of the PM (Figure 4.32(b)); for the T-Beam all the PFM and GRMs (i.e. ECOV, GRF and GSF) safety formats estimate design ultimate loads higher than the one of the PM with lower reliability levels because they are not able to capture the modifications of the *failure mode* as shown in Figure 4.32(e).

The differences in design ultimate loads of the different safety formats in the T-Beam are so large because the modifications in the failure modes affect both the materials and the location where failure occurs: the bending mechanism involves both materials at the midspan, whereas the shear mechanism involves only the concrete near to the restraint. Regarding the Beam SM the modifications in the failure modes are due to the differences in the locations of the local mechanisms.

This analysis implies that when the design ultimate resistance is estimated by means of a safety format, which does not take into account the actual probabilistic distribution of the structural resistance as a function of the possible failure modes, the predetermined safety level is not adequately guaranteed.

In fact, although the ECOV and GSF safety formats take into account a statistical parameter within the design resistance assessment, they do not actually account for the modification of the *failure mode* due to the following reasons: the coefficient of variation in the ECOV safety format is evaluated by means of a simplified approach which, obviously, does not consider any possible modification in the *failure mode*; whereas, the GSF safety format fails due to the assumption to assess the mean value of the distribution of the global structural resistance equal to the value achieved from a NLFEA by employing the mean values of the material properties.

4.3.4 Discussion and proposals

The results reported in Section 4.2.3 indicates that a methodology able to capture the mechanical behavior of the structure depending on the values assumed for material properties is necessary (i.e., *failure mode sensitivity*). At the same time, the methodology should be easy and with limited required computational effort. For this reason, the first subsection proposes a framework based on two preliminary NLFEMs to discern the applicability, or not, of the PFM and GRMs (i.e. non-probabilistic safety formats) in comparison with the PM. If PFM and GRMs can not be applied, a new safety factor is proposed in the second subsection to cover the effects of the aleatory uncertainty and inherent simplification of non-probabilistic safety formats on the prediction of global structural response. In the third subsection, a further *safety format* based on a safe “a priori” hypothesis related to the coefficient of variation of global resistance is proposed according to the results of Section 4.2.3. Finally, the possible implementation of a methodology based on the *levels of approximation approach* (LoAs) is discussed.

Preliminary NLFEM simulations

The present subsection proposes a proposal for a preliminary evaluation of the *failure mode sensitivity* by means of two *preliminary* NLFEMs in order to verify the applicability of the PFM and GRMs (i.e. ECOV, GRF and GSF) in comparison with the PM. The two *preliminary analyses* consist of:

- 1) one NLFEM simulation using the *mean* values for the concrete properties and the *design* values for the reinforcement properties;
- 2) one NLFEM simulation using the *design* values for the concrete properties and the *mean* values for the reinforcement properties.

A simplified graphical representation of the meaning of the two *preliminary analyses* is reported in Figure 4.33.

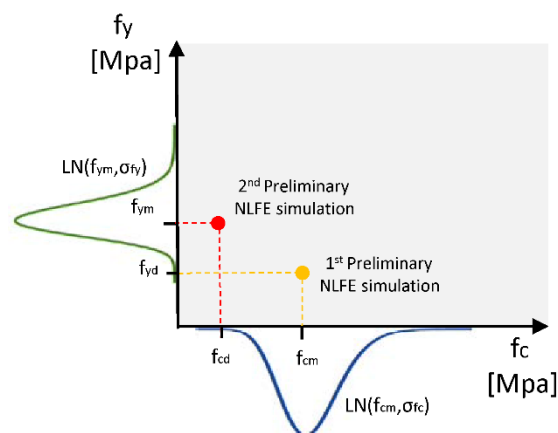


Figure 4.33: Graphical representation of the two preliminary NLFEM analyses assuming as variables the reinforcement yielding strength f_y and the concrete compressive strength f_c .

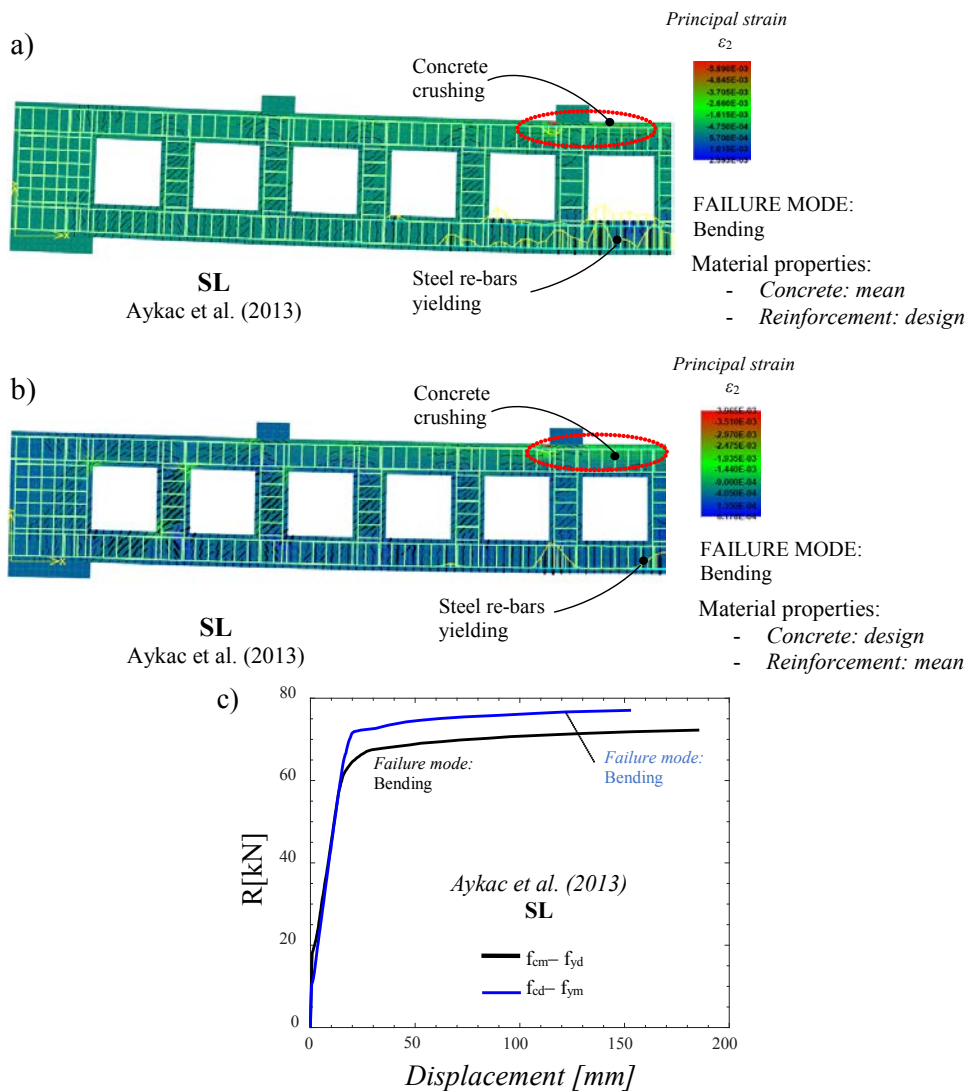


Figure 4.34: Beam SM (Aykac et al., 2013): *failure modes* recognised for the two *preliminary* simulations (a)-(b); load-displacement curves (c).

If the *failure modes* from these two *preliminary analyses* are the same, it follows that one between PFM and the GRMs (specifically GRF, ECOV, GSF methods) as well as the PM can be adopted to estimate the design ultimate load, whereas if the *failure modes* are different, an in-depth discussion for the selection the *safety format* to be used for the safety verification is required.

With reference to all the reinforced concrete beams considered in the previous sections, the results of the preliminary analyses are reported in Table 4.19 and confirm that, for both Beam SM and T-Beam, the failure mode changes when a material (i.e., concrete/steel) is assumed stronger or weaker than the other one. In Figures 4.34 and 4.35, the *failure modes* recognized for the two *preliminary* NLFE simulations related to Beam SL and to T-Beam are illustrated as well as the corresponding load-displacement curves.

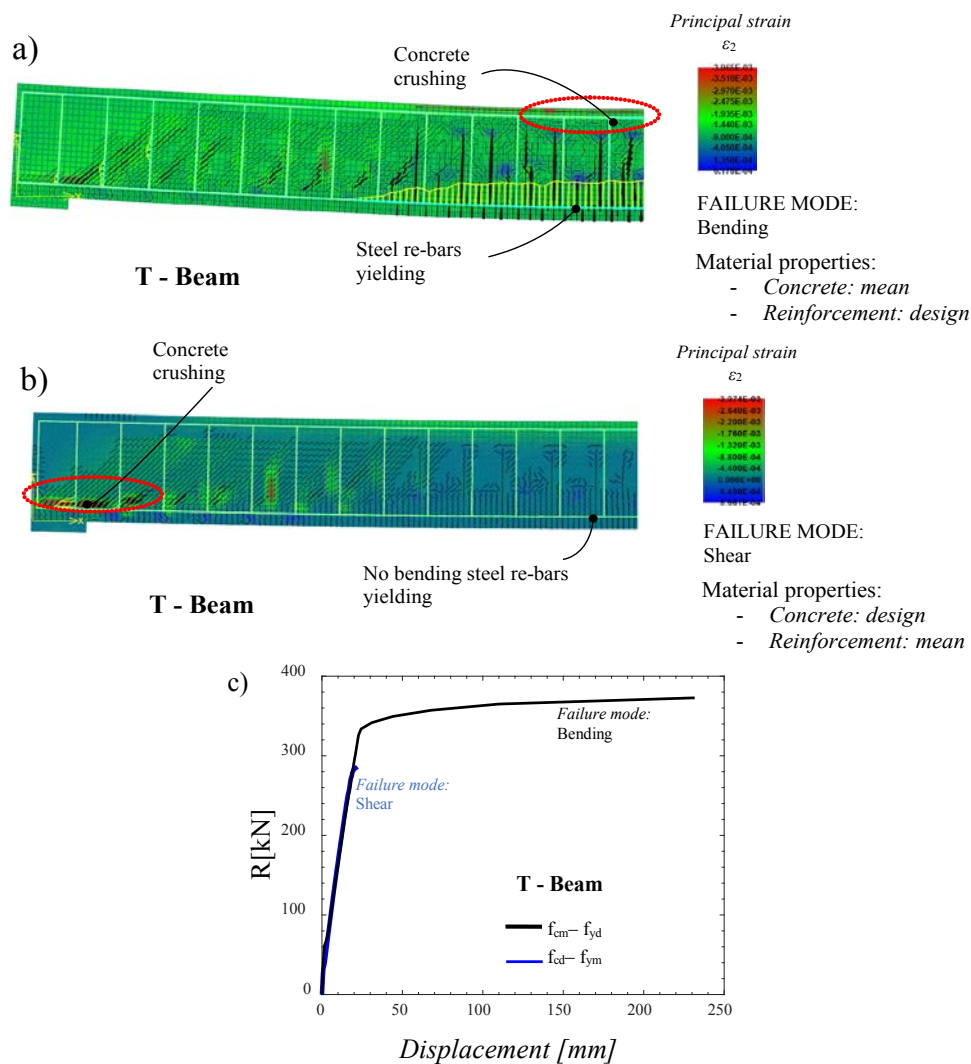


Figure 4.35: Beam designed according to *fib* Model Code 2010 and to EN 1992-1-1 (T-Beam): *failure modes* recognised for the two *preliminary* simulations (a)-(b); load-displacement curves (c).

The Figure 4.34 confirms that the *failure mode* does not change and a more ductile response when the design value is adopted for the reinforcement steel. The Figure 4.35 clearly highlights the difference in the two *failure modes* for the T-Beam: ductile and brittle *failure modes*.

As discussed in Subsection 4.2.3, with reference to Beam SL, all the design ultimate loads reported in Table 4.18 are valid; regarding the T-Beam, only the design ultimate load achieved by the PM is acceptable (Figure 4.32(e)).

However, for practical applications and facing to the LoAs approach, the PM requires an high computational effort and in the next section a new proposal is described in order to apply the PFM and GRMs (without performing probabilistic analyses) also in the case the modification of the *failure mode* occur.

Table 4.19: Results from the *preliminary analyses*.

Preliminary NLFEAs	Material properties		Ultimate load R [kN]	Failure mode
	Concrete f_c [MPa]	Reinforcement f_y [MPa]		
SL (Aykac et al., 2013)				
1	<i>Mean</i>	<i>Design</i>	72.3	<i>Bending</i>
2	<i>Design</i>	<i>Mean</i>	77.1	
SM (Aykac et al., 2013)				
1	<i>Mean</i>	<i>Design</i>	92.7	<i>Vierendeel - B</i>
2	<i>Design</i>	<i>Mean</i>	71.2	<i>Vierendeel - A</i>
SH (Aykac et al., 2013)				
1	<i>Mean</i>	<i>Design</i>	89.5	<i>Vierendeel - A</i>
2	<i>Design</i>	<i>Mean</i>	80.6	
CLX (Aykac et al., 2013)				
1	<i>Mean</i>	<i>Design</i>	85.6	<i>Bending</i>
2	<i>Design</i>	<i>Mean</i>	82.8	
T-Beam				
1	<i>Mean</i>	<i>Design</i>	358.8	<i>Bending</i>
2	<i>Design</i>	<i>Mean</i>	286.2	<i>Shear</i>

Failure-mode based safety factor γ_{FM}

In order to apply PFM and GRMs due to their reduced computational effort also in the critical cases, updated values of the aleatory uncertainty global safety factor are herein proposed for the assessment of the design global resistance. In Table 4.20 are reported the values of the global resistance factors γ_R for the different safety formats according to the literature (*Allaix et al., 2013; fib Model Code 2010*). On the base of the results of the present work, an additional *failure mode-based safety factor* denoted as γ_{FM} is proposed (Table 4.20). The γ_{FM} safety factor is defined in order to cover the uncertainties related to the inherent simplifications performed within the definition of the PFM and GRMs (i.e. non-probabilistic methods) and their influence on the prediction of the actual *failure mode* due to the *failure mode sensitivity* of the structure induced by *aleatory* uncertainties.

In agreement with Table 4.20, the assessment of the design global resistance R_d can be performed, according to the selected safety format, as follows:

$$R_d = \frac{R_{rep}}{\gamma_R \cdot \gamma_{FM} \cdot \gamma_{Rd}} \quad (4.3)$$

The *failure mode-based safety format factor* γ_{FM} has been calibrated in order to get the results, in terms of design global resistance R_d evaluated with the PFM and GRMs (i.e. GSF, ECOV, GRF) reported in Table 4.18, in compliance with the design global resistance R_d estimated with the probabilistic method (PM).

Table 4.20: Summary of the global resistance factors γ_R , of the failure mode factors γ_{FM} and of the model uncertainty factor γ_{Rd} for the different safety formats.

Safety format	Results from preliminary simulations			Model uncertainty safety factor γ_{Rd} [-]
	Same failure modes	Different failure modes		
	Global resistance safety factor γ_R [-]	Global resistance safety factor γ_R [-]	Failure mode-based safety factor γ_{FM} [-]	
PM	$\exp(\alpha_R \cdot \beta \cdot V_R)$	$\exp(\alpha_R \cdot \beta \cdot V_R)$	1.00	1.15 See Section 4.1
GSF			1.15	
ECOV				
GRF	1.27	1.27		
PFM	1.00	1.00		

This assessment leads to values of γ_{FM} varying in the range about 1.00-1.18. Therefore, the value of γ_{FM} set equal to 1.15 is herein suggested. In Table 4.20, in sake of completeness, is also reported the suggested value for the *resistance model uncertainty safety factor* γ_{Rd} set equal to 1.15 according to Section 4.1.

The herein proposed general framework for the use of NLFEAs to assess the design global structural resistance (for the design/assessment of new/existing structures) according to the different safety formats is depicted in Figure 4.36.

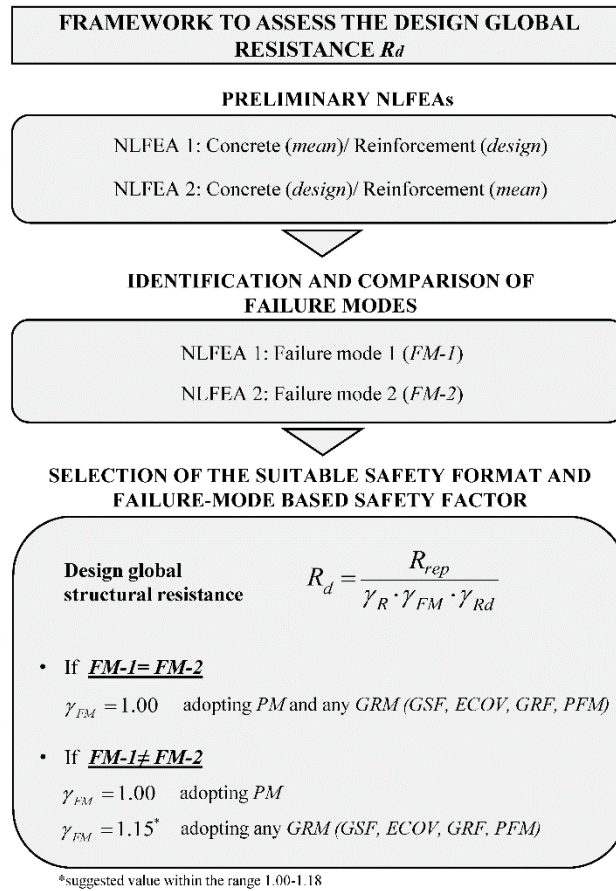


Figure 4. 36: Flowchart of the proposed methodology for the assessment of design global resistance R_d by means of NLFEAs.

New simplified safety format and applicability of the levels of approximation approach

In this last subsection, the proposal for a new simplified safety format pertaining to the GRMs is discussed together to the possibility of application of the principles of the *LoAs* approach to the safety formats for NLFEAs.

First of all, the results reported in Table 4.18 shows that the coefficient of variation V_R of the global structural resistance vary between 0.054 and 0.107 concerning reinforced concrete members having different *failure modes*. This result highlight that even if the global collapse is due to failure of concrete (supposed to have a coefficient of variation for compressive strength equal to 0.15 according to *fib Model Code 2010*), the coefficient of variation V_R of the global resistance is still influenced by the coefficient of variation of the reinforcement yielding strength (supposed to be 0.05 according to *fib Model Code 2010*).

In fact, Figure 4.37 shows that the coefficient of variation of the five structural members investigated in previous subsections are bounded by the coefficient of variation of concrete compressive strength equal to 0.15 (failure mode characterized by pure concrete failure) and the coefficient of variation of the reinforcement yielding strength set equal to 0.05 (failure mode characterized by pure yielding of reinforcements).

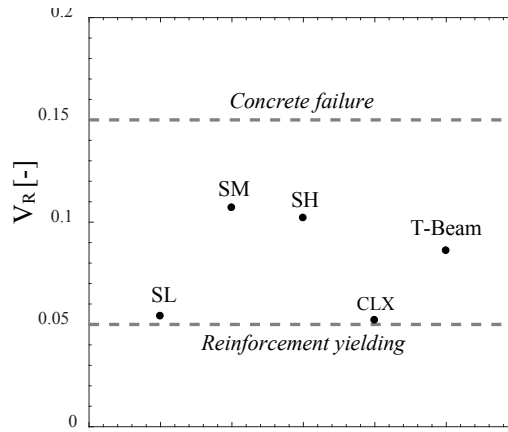


Figure 4.37: Bounds for coefficient of variation showed by global resistance.

These results suggest that to assume the coefficient of variation of the global structural response set equal to the one commonly adopted for concrete compressive strength (i.e. $V_R = 0.15$) is a safe hypothesis. Then the safety verification may be performed, in extremely simplified manner, only adopting one NLFE simulation defined using mean values of material properties (i.e. $R(f_m)$) and setting the *global resistance factor* γ_R equal to:

$$\gamma_R = \exp(\alpha_R \cdot \beta \cdot 0.15) \quad (4.4)$$

according to the assumption of lognormality for the probabilistic distribution of global structural resistance.

Then, in case of ordinary structures of new construction having 50 years of service life with moderate consequences of failure (i.e. $\beta = 3.8$ with $\alpha_R = 0.8$, *fib Model Code 2010*), the *global resistance factor* γ_R can be set equal to 1.58.

Finally, the safety verification can be performed according to:

$$R_d = \frac{R_{NLFEA}(f_m)}{\gamma_R \cdot \gamma_{FM} \cdot \gamma_{Rd}} \quad (4.5)$$

This approach can be denoted as “*Simplified Mean Value Method*” (SMVM) as it is based on mean values of material properties and on an “a priori” simplified assumption about the coefficient of variation of the global structural resistance. Furthermore, the *failure mode-based safety factor* γ_{FM} can always be assumed as equal to 1.00 without perform any *preliminary* simulation, as the high coefficient of variation assumed for global structural response already cover the uncertainties related failure mode sensitivity and presence of brittle *failure modes*.

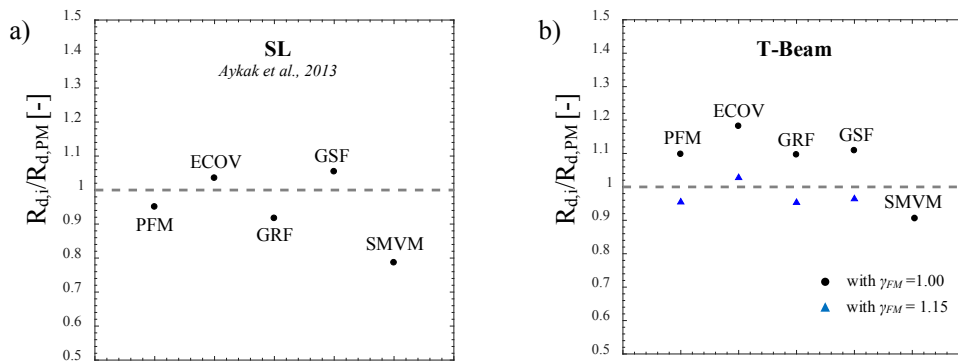


Figure 4.38: Ratio between the design resistances obtained with the different safety formats (i.e. PFM, ECOV, GRF, GSF and SMVM) and the PM for the beams SL (*Aykac et al., 2013*) and T-Beam.

In Figure 4.38(a-b) are shown the ratio between the design resistance obtained by means the different *safety formats* PFM, ECOV, GRF, GSF and SMVM and the PM. Specifically, in Figure 4.38(a) are reported the ratio for the SL beam of *Aykac et al., 2013* the failed in *bending* for both the *preliminary* simulations. In this case the prediction of the different safety formats are closer or safer respect to the solution obtained with the PM and justifies the assumption of *failure mode-based safety factor* γ_{FM} set equal to 1.00, as discussed in previous subsection.

Figure 4.38(b) reports the ratio for the T-Beam that presented *bending* and *shear failure modes* within the two *preliminary* simulations. In this case, the PFM, ECOV, GRF and GSF all overestimate the global design resistance with respect to the PM solution without considering the *failure mode-based safety factor* γ_{FM} set equal to 1.15. The application of the $\gamma_{FM} = 1.15$ leads to global design resistances in agreement with the one obtained with PM. It should be noticed that, also in the case of the T-Beam, the result obtained with the SMVM methodology does not require

the γ_{FM} correction as the associated design global resistance is already safer than the one obtained with PM.

Finally, the results of the present dissertation indicate that the *LoAs* approach may be applied also to safety verifications by means of NLFEMs. In fact, the global structural response may be determined with different levels of accuracy and with different time spending in order to perform simulations and to apply the different safety formats.

In next Section, the possible implementation of the *LoAs* approach is proposed in the light of the observations and the results obtained in Section 4.2 and 4.3.

4.4 Levels of approximation format for design and assessments of reinforced concrete structures by means NLFEA

According to the levels of approximation approach (LoAs) defined by *fib Model Code 2010*, a framework suitable for implementation in future codes (as by *fib Model Code 2020*) can be defined according to the results of the present dissertation. In the details, three *LoAs* can be defined complying to the following fundamental criteria:

- definition of a *general notation* able to include parameters representing the global structural behavior that may differ from the global resistance referred to a specified external load, as for example displacements, accelerations, imposed deformations, etc... ;

- all the levels of approximation (*LoAs*) should be referred to a specific level of reliability identified by the *target reliability index* β ;

- *LoA I*, requires limited number of NLFE simulations with “a priori” assumptions related to the coefficient of variation of global structural response;

- *LoA II*, requires limited number of NLFE simulations with a simplified method for the estimation of the coefficient of variation of global structural response;

- *LoA III*, requires the definition of simplified or full probabilistic models in order to perform the reliability analysis.

4.4.1 General

In compliance with the limit states design approach, the basic requirement can be considered as satisfied if the following inequality is met:

$$GECP_d \geq GEDP_d \quad (4.6)$$

where $GECP_d$ is the design *Global Engineering Capacity Parameter*, which may be represented by the ultimate value, in a specific loading situation, of external loads, displacements, accelerations, internal forces, imposed displacements and all the other possible parameters able to reflect the global structural response; $GEDP_d$ is the design *Global Engineering Demand Parameter* defined according to the $GECP_d$ in compliance to codes provisions for the actions related to the specific limit state.

The methods for structural verification and assessment (i.e. safety formats) according to a predefined level of reliability can be classified complying to the levels of approximation approach as:

- *LoA I* :
 - i. Partial Factor Method (*PFM*)
 - ii. Simplified Mean Value Method (*SMVM*)

- *LoA II* :
 - i. Method of estimation of coefficient of variation (*ECOV*)

- *LoA III* :
 - i. Simplified Probabilistic Method (*SPM*)
 - ii. Full Probabilistic Method (*FPM*)

All the safety formats are based on the basic principles characterizing the global resistance format (*GRF*). The levels of approximation *LoA I* (only for *PFM*) and *LoA II* requires to perform two *preliminary simulations* crossing material properties of concrete and reinforcement (i.e. mean/design and vice-versa) in order to be applied properly. The *LoA III* requires the definition of appropriate probabilistic models for the main involved variables (i.e. resistances and actions).

In the mentioned above safety formats three different safety factors are adopted with the following meaning:

- γ_R , *global engineering capacity safety factor* which accounts for the aleatory uncertainty related to the basic variables that may influence the structural behaviour (e.g. materials properties);

- γ_{Rd} , *resistance model uncertainty safety factor* which accounts for the epistemic uncertainty related to the non-linear model definition;

- γ_{FM} , *failure mode-based safety factor* which accounts for the additional uncertainty related to the simplifications performed in the definition of the safety format and their influence on the prediction of the actual failure mode at the design level.

In Table 4.21 are reported the mentioned above safety factors suggested for ordinary reinforced concrete structures of new construction having moderate consequences of failure and 50 years of service life.

Table 4.21: Partial factors involved by the different safety formats according to ordinary structures of new construction having moderate consequences of failure with 50 years of service life (i.e. $\beta = 3.8$, $\alpha_R = 0.8$).

Level of approximation	Safety format	Global engineering capacity safety factor γ_R [-]	Model uncertainty safety factor γ_{Rd} [-]	Failure mode-based safety format factor γ_{FM} [-]	
				Result from preliminary simulations	
				Same failure modes	Different failure modes
LoA I	SMVM	1.58	1.15	1.00	
	PFM	1.00		1.00	1.15
LoA II	ECOV	see Sec. 4.4.3			
LoA III	SPM	see Sec. 4.4.4			
	FPM	-			

4.4.2 Level of approximation I (LoA I)

The level of approximation I methods related to the reliability-based structural verification and assessment of reinforced concrete structures by means non-linear analysis are identified by:

- the *Simplified Mean Value Method (SMVM)*;
- the *Partial Factor Method (PFM)*.

Simplified Mean Value Method (SMVM)

The evaluation of design *Global Engineering Capacity Parameter* - $GECP_d$ - can be performed by means non-linear analysis according to:

$$GECP_d = \frac{GECP(x_m)}{\gamma_R \cdot \gamma_{FM} \cdot \gamma_{Rd}} \quad (4.7)$$

where x_m is the vector of basic variables identified by their mean values (or measured values concerning existing structures).

The *global engineering capacity safety factor* γ_R can be set equal to 1.58 concerning ordinary structures of new construction having 50 years of service life. This value is derived according to the hypothesis of lognormal distribution of the $GECP$, assuming a coefficient of variation V_{GECP} equal to 0.15 as commonly done for the concrete compressive strength and setting the reliability index $\beta = 3.8$ with $\alpha_R = 0.8$ (i.e. dominant variable). Values related to different levels of reliability (i.e. β and α_R) and can be derived from Eq.(4.8):

$$\gamma_R = \exp(\alpha_R \cdot \beta \cdot 0.15) \quad (4.8)$$

The *model uncertainty safety factor* γ_{Rd} can be set equal to 1.15 concerning ordinary structures of new construction having 50 years of service life.

Values related to different levels of reliability (i.e. β and α_R) can be derived from Eq.(4.9):

$$\gamma_{Rd} = \frac{1}{1.01} \exp(\alpha_R \cdot \beta \cdot 0.12) \quad (4.9)$$

where 1.01 and 0.12 are, respectively, the mean value and the coefficient of variation of resistance model uncertainty.

The *failure-mode based safety factor* γ_{FM} can be set equal to 1.00 without any *preliminary simulation*. In fact, the choice of a fixed value of coefficient of variation V_{GECp} equal to the coefficient of variation usually adopted for concrete compressive strength (i.e. 0.15) already cover the possibility of a brittle failure mode.

Partial Factor Method (PFM)

The evaluation of design *Global Engineering Capacity Parameter* - $GECP_d$ - can be performed according to:

$$GECP_d = \frac{GECP(x_d)}{\gamma_{FM} \cdot \gamma_{Rd}} \quad (4.10)$$

where x_d is the vector of basic variables identified by their design values according to codes provisions for different levels of reliability (i.e. *fib Model Code 2010*, *EN 1990*, *fib Bulletin 80*).

The *model uncertainty safety factor* γ_{Rd} can be set equal to 1.15 concerning ordinary structures of new construction having 50 years of service life. Values related to different levels of reliability (i.e. β and α_R) can be derived from Eq.(4.11):

$$\gamma_{Rd} = \frac{1}{1.01} \exp(\alpha_R \cdot \beta \cdot 0.12) \quad (4.11)$$

where 1.01 and 0.12 are, respectively, the mean value and the coefficient of variation of resistance model uncertainty.

The *failure-mode based safety factor* γ_{FM} can be defined base on the results of the two *preliminary analyses*. The $\gamma_{FM}=1.15$ should be adopted if different failure modes are recognized within the *preliminary analyses* or if the *preliminary analyses* are not performed, while, the $\gamma_{FM} = 1.00$ can be adopted if the same failure mode is evidenced.

4.4.3 Level of approximation II (LoA II)

The level of approximation II method related to the reliability-based structural verification and assessment of reinforced concrete structures by means non-linear analysis is identified by:

- *Method of estimation of coefficient of variation (ECOV)*

Method of estimation of coefficient of variation (ECOV)

The evaluation of design *Global Engineering Capacity Parameter - GECP_d* can be performed by means non-linear analysis according to:

$$GECP_d = \frac{GECP(x_m)}{\gamma_R \cdot \gamma_{FM} \cdot \gamma_{Rd}} \quad (4.12)$$

where x_m is the vector of basic variables identified by their mean values (or measured values concerning existing structures). The GECP is assumed as a lognormal distributed variable.

The *global engineering capacity safety factor* γ_R can be evaluated as:

$$\gamma_R = \exp(\alpha_R \cdot \beta \cdot V_{GECP}) \quad (4.13)$$

where α_R and β are the FORM sensitivity factor and the target reliability index, respectively. The value of α_R can be assumed as be equal to 0.8 in the hypothesis of dominant variable and the value of β can be set equal to 3.8 in case of ordinary structures with 50 years of service life.

According to the lognormality hypothesis, the coefficient of variation of the global engineering capacity parameter V_{GECP} can be estimated as:

$$V_{GECP} = \frac{1}{1.65} \cdot \ln \left(\frac{GECP(x_m)}{GECP(x_k)} \right) \quad (4.14)$$

where $GECP(x_m)$ and $GECP(x_k)$ are the results of non-linear analyses performed with mean values x_m and characteristic values x_k of main involved variables.

The *model uncertainty safety factor* γ_{Rd} can be set equal to 1.15 concerning ordinary structures of new construction having 50 years of service life. Values related to different levels of reliability (i.e. β and α_R) can be derived from Eq.(4.15):

$$\gamma_{Rd} = \frac{1}{1.01} \exp(\alpha_R \cdot \beta \cdot 0.12) \quad (4.15)$$

where 1.01 and 0.12 are, respectively, the mean value and the coefficient of variation of resistance model uncertainty.

The *failure-mode based safety factor* γ_{FM} can be defined base on the results of the two *preliminary analyses*. The $\gamma_{FM} = 1.15$ should be adopted if different failure

modes are recognized within the *preliminary analyses* or if the *preliminary analyses* are not performed, while, the $\gamma_{FM} = 1.00$ can be adopted if the same failure mode is evidenced.

4.4.4 Level of approximation III (LoA III)

The level of approximation III methods related to the reliability-based structural verification and assessment of reinforced concrete structures by means non-linear analysis are identified by:

- *Simplified Probabilistic Method (SPM)*;
- *Full Probabilistic Method (FPM)*.

Simplified Probabilistic Method (SPM)

The evaluation of design *Global Engineering Capacity Parameter - GECP_d* - can be performed according to:

$$GECP_d = \frac{GECP_m}{\gamma_R \cdot \gamma_{Rd}} \quad (4.16)$$

where $GECP_m$ is the mean value of the probabilistic distribution of global engineering capacity parameter $GECP$.

The *global engineering capacity safety factor* γ_R can be defined as:

$$\gamma_R = \exp(\alpha_R \cdot \beta \cdot V_{GECP}) \quad (4.17)$$

where α_R and β are the FORM sensitivity factor and the target reliability index, respectively. The value of α_R can be assumed as be equal to 0.8 in the hypothesis of dominant variable and the value of β can be set equal to 3.8 in case of ordinary structures with 50 years of service life.

The mean value $GECP_m$ and coefficient of variation V_{GECP} of the *global engineering capacity parameter* $GECP$ can be evaluated performing non-linear analyses adopting a simplified probabilistic model for concrete and reinforcements properties according to Table 4.22.

Table 4.22: Simplified probabilistic model for SPM.

	Distribution	Mean value	Coefficient of variation
Concrete cylinder compressive strength	<i>lognormal</i>	f_{cm}	0.15
Reinforcement yielding strength	<i>lognormal</i>	$f_{ym} = 1.1 f_{yk}$	0.05

A reduced Monte Carlo simulation by means Latin Hypercube Sampling LHS with at least 30 samples should be accomplished. The $GECP$ variable is modelled by means of a lognormal distribution.

All the other properties related to the definition of the non-linear model should be derived starting from concrete cylinder compressive strength and reinforcement yielding strength according to current specifications (e.g. *EN 1992, 2004* and *fib Model Code 2010*).

The *model uncertainty safety factor* γ_{Rd} can be set equal to 1.15 concerning ordinary structures of new construction having 50 years of service life. Values related to different levels of reliability (i.e. β and α_R) can be derived from Eq.(4.18):

$$\gamma_{Rd} = \frac{1}{1.01} \exp(\alpha_R \cdot \beta \cdot 0.12) \quad (4.18)$$

where 1.01 and 0.12 are, respectively, the mean value and the coefficient of variation of resistance model uncertainty.

Full Probabilistic Method (FPM)

The assessment of the structural reliability is performed in the performance domain estimating the probability of failure under the relevant design situation and comparing the result with the target probability. The full probabilistic method requires the definition of a complete probabilistic model related both to material resistances, geometry, actions and related model uncertainties.

Then, the following inequality should be met:

$$P[\mathcal{G}_R \cdot GECP(X_i) - \mathcal{G}_A \cdot GEDP(Y_j) \leq 0] \leq p_T \quad (4.19)$$

where $GECP(X_i)$ is the global engineering capacity parameter evaluated in function of the main random variables X_i characterizing the structural behavior (e.g. resistances, geometry); $GEDP(Y_j)$ is the global engineering demand parameter evaluated in function of the main random variables Y_j representing the external actions; \mathcal{G}_R and \mathcal{G}_A are the model uncertainty random variables related to non-linear analysis and actions, respectively; p_T is the target probability.

Information related to probabilistic modelling or material resistances, geometry and actions with associated model uncertainties can be derived from literature (e.g. *JCSS Probabilistic Model Code 2001*).

The *model uncertainty* \mathcal{G}_R related to the characterization of the global engineering capacity parameter by means of non-linear analysis can be identified by means of a lognormal distribution having mean value set equal to 1.01 and coefficient of variation set equal to 0.12.

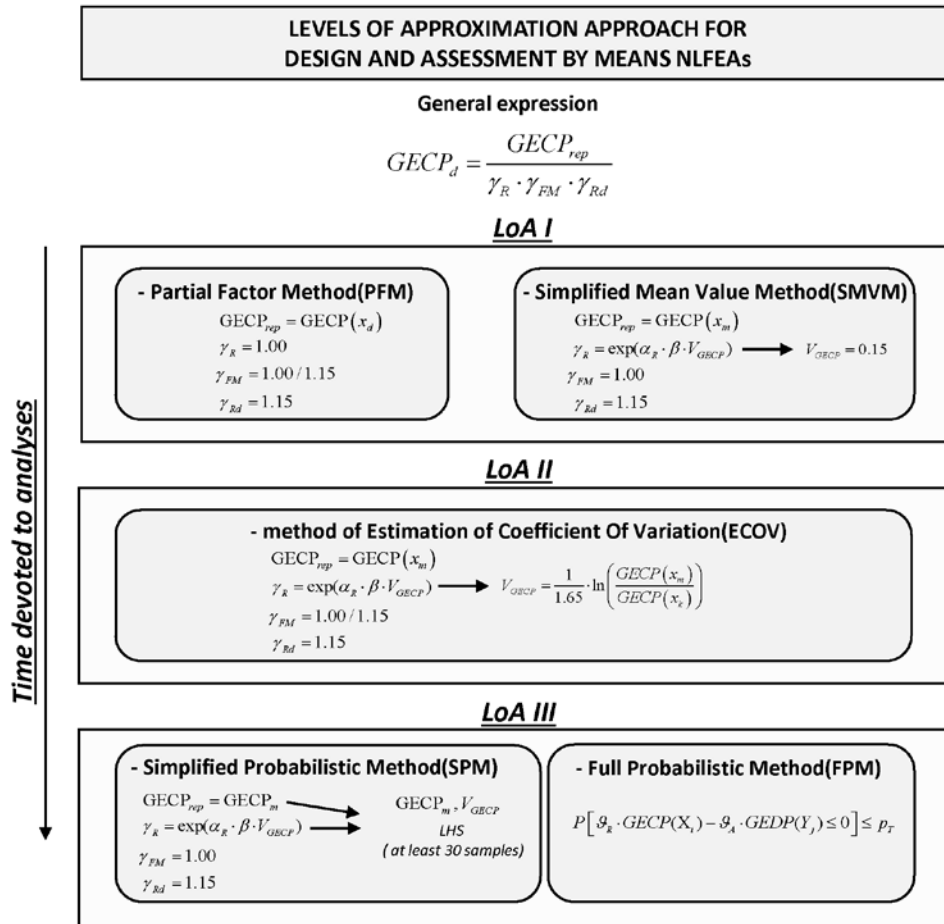


Figure 4.39: Summary of the proposed code format based on the levels of approximation approach.

The Figure 4.39 summarize the proposed framework based on the *LoAs* approach for design and assessment of reinforced concrete structures by means of NLFEAs. The time devoted to perform the safety verification increase passing from *LoA I* to *LoA III* also with the complexity of implementation of the probability theory.

Chapter 5

Conclusions

The present dissertation report advances concerning structural reliability analysis related to two important topics:

- the probabilistic calibration of empirical and semi-empirical resistance models;
- the use of non-linear finite elements software for *design* and *assessment* of *new* and *existing* reinforced concrete structures.

Specifically, a framework based on the Monte Carlo method for the derivation of design equations from empirical or semi-empirical resistance models has been proposed. The procedure allows to account for of the influence of both *aleatory* and resistance model uncertainties (i.e. *epistemic*) in the reliability-based calibration of the mentioned above resistance models.

This result can be obtained by means of the definition of multiplicative probabilistic coefficients ζ_p , which are related to a specific probability of under-exceedance p . The design coefficient ζ_d is directly related to a certain value of the reliability index β (i.e. probability of failure). Then, the final design equation can be derived as a function of the level of reliability required by the codes for *new* and *existing* structures. The proposed procedure is very general as it is independent from the probabilistic model defined for the main random variables. Furtherly, it is suitable for the calibration of design formulations corresponding to both serviceability (SLE) and ultimate limit states (ULS).

The methodology herein developed has been applied to the probabilistic calibration of the semi-empirical model proposed by *fib Model Code 2010* for laps and anchorages tensile strength evaluation. The calibration of model uncertainty for the mentioned above semi-empirical model has been performed on the basis of an extended experimental database distinguishing between *new* and *existing* structures. Then, the semi-empirical model for tensed lapped joints and anchorages strength calculation probabilistically calibrated. The reliability-based design expression for laps and anchorage strength has been defined depending on the selected level of reliability according to codes prescriptions. The derived formulation has been adopted in order to define the expression for ultimate bond strength suitable for laps and anchorage design.

Finally, the outcomes of the procedure has been validated according to experimental results and to a simplified analytic procedure.

The second part of the dissertation focused on the use of NLFEAs for structural design and assessment.

First of all, the *model uncertainty safety factor* γ_{Rd} (i.e., *epistemic* uncertainties) concerning the global structural resistance for 2D non-linear finite element method analyses of reinforced concrete structures has been defined. Several experimental tests concerning different typologies of structures with different behaviours and failure modes (i.e., walls, deep beams, panels), have been numerically simulated by means of appropriate 225 NLFEAs considering different software and three different constitutive laws for the behaviour of concrete in tension. From the comparison with the experimental outcomes, the FE results have demonstrated the many difficulties, which commonly occur employing different types of software and constitutive laws, in reproducing the actual failure behaviour and the actual failure load of the structural members herein considered. The resistance model uncertainty have been computed and characterised by appropriate lognormal distributions. Subsequently, a consistent treatment has been proposed following a Bayesian approach to define the mean value and the coefficient of variation characterizing the distribution functions of the resistance model uncertainties. Specifically, the mean value and the coefficient of variation of the resistance model uncertainties are respectively equal to 1.01 and 0.15 considering all the results, and to 1.01 and 0.12 excluding the tests affected by another source of uncertainties related to the experimental static configurations. Successively, in agreement with safety formats for NLFEAs, the values of the *model uncertainty safety factor* γ_{Rd} have been evaluated and proposed as a function of the target reliability levels corresponding to *new* or *existing* structures, of the failure consequences and of the hypothesis of dominant or non-dominant resistance variable. Specifically, excluding the results assumed as tests affected by uncertainties on the experimental static configurations, the *model uncertainty safety factor* γ_{Rd} presents a range of variation for *new* or *existing* structures between around 1.3 and 1.6 in the hypothesis of dominant resistance variable and between around 1.1 and 1.2 in the hypothesis of non-dominant resistance variable. Instead, accounting for all the results, the partial safety factors related to the resistance model uncertainties are slightly higher (about 5%). Finally, for both *new* and *existing* ordinary structures, in the hypotheses of non-dominant resistance variable, of moderate consequences of structural failure and for a service life of 50 years, a *model uncertainty safety factor* γ_{Rd} for 2D NLFEAs of reinforced concrete structures equal to 1.15 is suggested.

Secondly, the comparison between different *safety formats* within the *Global Resistance Format* (GRF) for the estimation of the global design strength of different reinforced concrete structures has been proposed. Specifically, NLFE models are properly defined to reproduce the experimental tests and, successively, to perform several NLFEAs in compliance with the different *safety formats* for each reinforced concrete beam. The different *safety formats* are investigated to demonstrate if they are able to estimate the corresponding design global resistance

capacities capturing any modification in the failure mode of the reinforced concrete structure. The PM is obviously assumed as the reference safety format.

From the analysis of the results, it is possible to state that for some beams (i.e., Beam SL, Beam SH and Beam CLX) the failure mode does not present any modification and the GRF and PFM safety formats always provide design ultimate loads lower than the one evaluated with the PM. Moreover, for the Beam CLX, the ECOV safety format also provides a design ultimate load lower than the estimation of the PM. Instead, for the other beams (i.e., Beam SM and T-Beam) the failure modes are characterized by some modifications. In fact, for the Beam SM, only the GRF safety format provides a design ultimate load lower than the one of the PM; for the T-Beam, the PFM and all the GRMs safety formats (i.e. ECOV, GRF and GSF) estimate design ultimate loads higher than the one of the PM with lower reliability levels because they are not able to capture the modifications in the failure mode. This analysis highlights that when the design ultimate resistance is estimated by a *safety format*, which does not take into account the actual distribution of the structural resistance as a function of the possible modifications in the failure mode, the safety level is not adequately guaranteed. The structural safety assessment should be always based on the assessment of the mechanical response of a structure. It follows that the capability to capture any possible modification in the failure mode for the different *safety formats* is a fundamental safety requirement.

According to the outcomes of the mentioned above comparison, a preliminary evaluation, composed of two *preliminary NLFEAs* under the hypothesis of one material (i.e., concrete/steel) stronger than the other one and vice versa, is proposed to verify the applicability of the simplified *safety formats*. In fact, if the *failure mode* does not change in the two preliminary analyses it follows that PFM and GRMs (specifically GRF, ECOV, GSF methods) can be adopted to estimate the design ultimate load, whereas if the resistance mechanism are different, the PM is suggested as the unique *safety format* able to perform a reliable estimation of the design ultimate load within the reliability assessment. In order to apply simplified *safety formats* also in the critical cases due to their reduced computational effort, a *failure mode-based safety factor* γ_{FM} related to the inherent simplifications of non-probabilistic safety formats is proposed for the assessment of the design global resistance in case the structure is sensitive to change its *failure mode*. The suggested value for the *failure mode-based safety factor* γ_{FM} results to be 1.15. However deeper investigations are necessary.

Finally, the applicability of the *Levels of Approximation approach (LoAs)* to safety formats for NLFEAs of reinforced concrete structures has been discussed. A *LoA I* safety format denoted as “*Simplified Mean Value Method*” (*SMVM*) has been proposed and validated according to the hypothesis of coefficient of variation of global resistance equal to 0.15, which is generally assumed to model the variability of concrete compressive resistance. Then, a comprehensive code format framework based on three *Levels of Approximation approach (LoAs)* has been defined.

References

- ACI 408 bond database, 2001.
- ADINA R & D. Inc.. 71 Elton Avenue Watertown. MA 02472. USA. 2014.
- Allaix DL, Carbone VI, Mancini G. Global safety format for non-linear analysis of reinforced concrete structures. *Structural Concrete* 2013; 14(1): 29-42.
- Aykac B, Kalkan I, Aykac S, Egriboz EM. Flexural behaviour of RC beams with regular square or circular web openings, *Engineering Structures*, 56, pp. 2165-2174, 2013.
- ATENA 2D v5. Cervenka Consulting s.r.o. . Prague. Czech Republic. 2014.
- Bertagnoli G., Mancini G. 2009. “ Failure analysis of hollow core slabs tested in shear.” *Structural Concrete* 10(3):139-152.
- Bertagnoli G, La Mazza D, Mancini G. Effect of concrete tensile strength in non – linear analysis of 2D structures: a comparison between three commercial finite element softwares. 3rd International Conference on Advances in Civil, Structural and Construction Engineering – CSCE 2015. Rome. 104-111. 10-11 December 2015.
- Burkhardt, C. J.: Zum Tragverhalten von Übergreifungsstößen in hochfestem Beton (Behavior of lapped splices in high strength concrete), Dissertation, RWTH Aachen, 2000.
- Canbay, E. and Frosch, R. J.: Bond strength of lap-spliced bars, *ACI Structural Journal*, 102 (4), pp.605–614, 2005.
- CEB-FIP Model Code for Concrete Structures 1990, CEB-FIP, Lausanne, 1990
- CEN: EN 1992-1-1: Eurocode 2 – Design of concrete structures. Part 1-1: general rules and rules for buildings. CEN, Brussels, 2004.
- CEN EN 1992-2 Eurocode 2 - Design of concrete structures, Part 2: concrete bridges. CEN 2005. Brussels.
- CEN EN 1990 Eurocode. 2002. “Basis of structural design.” Brussels.
- Cervenka, V. (1985) - Constitutive Model for Cracked Reinforced Concrete, *Journal ACI, Proc.* V.82, Nov-Dec., No.6, pp.877-882.
- Colsson A, Sandberg G, Dahlblom O. On latin hypercube sampling for structural reliability analysis , *Structural Safety*, 25(1), pp. 47-68, 2003.
- Cornell, C. A. 1967. “Bounds on the reliability of structural systems.” *J. Struct. Div.*, 931, 171–200.
- Cornell, C.A., A probability-based structural code, *ACI Journal*, Vol.66, pp 974-1985.
- Crisfield, M.A., Wills, J. (1989)- The Analysis of Reinforced Concrete Panels Using Different Concrete Models, *Jour. of Engng. Mech.*, ASCE, Vol 115, No 3, March, pp.578-597.
- Darwin, D., Pecknold, D.A.W. (1974) - Inelastic Model for Cyclic Biaxial Loading of Reinforced Concrete, *Civil Engineering Studies*, University of Illinois, July.

- R. De Borst and P. Nauta, "Non-orthogonal cracks in a smeared finite element model", *Engineering Computations* 2, pp. 35-46, 1985
- DIANA FEA BV. Delftechpark 19a 2628 XJ Delft. The Netherlands. 2017.
- Ditlevsen, O. 1979. "Narrow reliability bounds for structural systems." *J. Struct. Mech.*, 74, 453–472.
- Eligehausen, R.: 'Übergreifungsstöße zugbeanspruchter Rippenstäbe mit geraden Stabenden' (Lapped splices of tensioned deformed bars with straight ends). *Deutscher Ausschuss für Stahlbeton*, 301, Berlin: Ernst & Sohn, 1979.
- Engen M, Hendriks MAN, Köhler J, Øverli JA, Åldtstedt E. A quantification of modelling uncertainty for non-linear finite element analysis of large concrete structures. *Structural Safety* 2017; 64: 1-8.
- Faber, Michael : *Statistics and Probability Theory*, Springer, 2012.
- fib. 2013. "*fib Model Code for Concrete Structures 2010*." International Federation for Structural Concrete (fib), Lausanne, Switzerland.
- fib Bulletin N°72. 2015. "Bond and anchorages of embedded reinforcements – Background to the fib Model Code for Concrete Structures." Lausanne.
- fib TG 4.5 bond tests database, 2005.
- fib Bulletin N°45. Practitioner's guide to finite element modelling of reinforced concrete structures – State of the art report. Lausanne; 2008.
- fib Bulletin N°80: Partial factor methods for existing concrete structures, Lausanne, 2016.
- Filho JB. Dimensionamento e comportamento do betao estrutural em zonas com discontinuidades. PhD thesis. Universidade Tecnica de Lisboa 1995.
- Foster SJ, Gilbert J. Experimental studies on high strength concrete deep beams. *ACI Structural Journal* 1998; 95: 382-390.
- Gelman, A., Carlin, J. B., Stern, H. S. and Dunson, D.B.: *Bayesian data analysis*, 3rd Edition CRC Press, 2014.
- Goto, Y. 1971. Cracks Formed in Concrete Around Deformed Tension Bars. *ACI*
- Haldar, A. and Mahadevan, S.: *Probability, Reliability and Statistical Methods in Engineering Design*, John Wiley and Sons Inc., 2000.
- Hasofer A., Lindt N, An exact and invariant first order reliability format, *Proc. ASCE, J. Eng. Mech. Div.*, 1974, pp 111-121.
- Holický M, Retief JV, Sikora M. Assessment of model uncertainties for structural resistance. *Probabilistic Engineering Mechanics* 2016; 45: 188-197.
- Jakubovskis, R. and Juknys, M. Finite element modelling of bond in reinforced concrete elements. *Mokslas - Lietuvos Ateitis science -future of Lithuania* 2016; 8(5): 504-508. <http://dx.doi.org/10.3846/mla.2016.969>.
- JCSS. *JCSS Probabilistic Model Code*, 2006.
- Kadlec L, Červenka V. Model Uncertainties of FEM Nonlinear Analyses of Concrete Structures. *Solid State Phenomena* 2016; 249: 197-202.
- Kalos, M.H. and P.A. Whitlock; *Monte Carlo Methods, Volume 1: Basics*, John Wiley & Sons, 1986
- Kiureghian AD, Ditlevsen O. Aleatory or epistemic? Does it matter?. *Structural Safety* 2009; 31: 105-112.
- Kupfer, H. B. and Gerstle, H. K. (1973). Behavior of Concrete under Biaxial

- Stresses. *Journal Engineering Mechanics Division* 99(4).
- Köenig, G. and Fischer, J.: Model uncertainties concerning design equations for the shear capacity of concrete members without shear reinforcement, *CEB Bulletin d'Information N°224*, pp. 49-94, 1995.
- König G., Hosser D., The simplified level II method and its application on the derivation of safety elements for level I, *CEB Bulletin no.147*, February 1962.
- ISO 2394:2015: General principles on reliability for structures, Genève, 2015.
- Lefas ID, Kotsovos MD. Behaviour of reinforced concrete structural walls: strength, deformation characteristics and failure mechanism. *ACI Structural Journal* 1990; 87: 23-31.
- Lemnitzer, L., Schroder, S., Lindorf, A., Cutbach, M. Bond behaviour between reinforcing steel and concrete under multiaxial loading conditions in concrete containments. 20th International Conference on Structural Mechanics in Reactor Technology (SMiRT 20), Espoo, Finland, August 9-14, 2009.
- Leonhardt F, Walther R. Wandartige Träger. Deutscher Ausschuss für Stahlbeton. Heft 178. Ernst & Sons. Berlin. Germany.1966.
- Lettow, S.: Ein Verbundelement für nichtlineare Finite Element Analysen – Anwendung auf Übergreifungsstöße (Bond element for nonlinear finite element analysis — application to lapped splices), Dissertation, University of Stuttgart, 2006.n
- Massicotte B, Elwi AE, MacGregor JG. Tension-stiffening models for planar reinforced concrete members. *Journal of Structural Engineering* 1990; 116(11): 3039-3058.
- Mckey MD, Conover WJ, Beckman RJ. A comparison of three methods for selecting values of input variables in the analysis from a computer code. *Technometrics*, 1979; 21:239-45.
- Muttoni A., Ruiz M.F. 2008. “ Shear strength of members without transverse reinforcements as function of critical shear crack width.” *ACI Structural Journal* 219:163-172.
- Muttoni A, Ruiz MF. Levels-of-approximation approach in codes of practice. *Struct Eng Int J Int Assoc Bridge Struct Eng.* 2012;22(2):190-4.
- Pang XBD, Hsu TTC. Behaviour of reinforced concrete membrane elements in shear. *ACI Structural Journal* 1995; 92: 665-679.
- Riggs HR, Powell GH. Rough crack model for analysis of concrete. *J. Eng. Mech. Div. ASCE* 1986; 112(5): 448-464.
- Riks, E., 1972. The application of Newton's method to the problem of elastic stability. *Journal of Applied Mechanics*, 39:1060-1065.
- Riks, E., 1979. An incremental approach to the solution of snapping and buckling problems. *International Journal of Solids and Structures*, 15:529-551.
- Rots, J. G. Computational Modelling of Concrete Fracture, PhD thesis, Delft University of Technology, 1988
- Shlune H, Gylltoft K, Plos M. Safety format for non-linear analysis of concrete structures. *Magazine of Concrete Research* 2012; 64(7): 563-574.

- Sikora M, Holicky M, Prieto M, Tanner P. Uncertainties in resistance models for sound and corrosion-damaged RC structures according to EN 1992-1-1. *Materials and structures* 2014; 48: 3415-3430.
- Souza, M. H.: The influence of loading arrangements in non-staggered lap splices in RC beams, Interim report, University of Southampton, 2016.
- Taerwe, R.L.: Toward a consistent treatment of model uncertainties in reliability formats for concrete structures, CEB Bulletin d'Information N° 105-S17, pp. 5-34, 1993.
- Taerwe, R.L.: Toward a consistent treatment of model uncertainties in reliability formats for concrete structures, CEB Bulletin d'Information N° 105-S17, pp. 5-34, 1993.
- Tepfers, R. 1973. A Theory of Bond Applied to Overlapped Tensile Reinforcement Splices for Deformed Bars. PhD-Thesis. Chalmers University of Technology. Göteborg, Sweden. 328 p.
- Thorenfeldt E, Tomaszewicz A and Jesen J, 1987 "Mechanical properties of high-strength concrete and applications in design", Proc. Symp. Utiliz. of High-Strength Concrete, 149-159.
- Vecchio FJ, Collins MP. The response of reinforced concrete to in-plane and normal stresses. Department of Civil Engineering. University of Toronto. Canada. 1982.
- Vecchio, F.J., Collins, M.P (1986)- Modified Compression-Field Theory for Reinforced Concrete Beams Subjected to Shear, *ACI Journal*, Proc. V.83, No.2, Mar-Apr., pp 219-231.